Holographic Entanglement Entropy: RG Flows and Singular Surfaces

by

Ajay Singh

A thesis
presented to the University of Waterloo
in fulfillment of the
thesis requirement for the degree of
Doctor of Philosophy
in
Physics

Waterloo, Ontario, Canada, 2012

I hereby declare that I am the sole author of this thesis. This is a true copy of the thesis, including any required final revisions, as accepted by my examiners.

I understand that my thesis may be made electronically available to the public.

Abstract

Over the past decade, the AdS/CFT correspondence has proven to be a remarkable tool to study various properties of strongly coupled field theories. In the context of the holography, Ryu and Takayanagi have proposed an elegant method to calculate entanglement entropy for these field theories. In this thesis, we use this holographic entanglement entropy to study a candidate c-theorem and entanglement entropy for singular surfaces.

We use holographic entanglement entropy for strip geometry and construct a candidate c-function in arbitrary dimensions. For holographic theories dual to Einstein gravity, this c-function is shown to decrease monotonically along RG flows. A sufficient condition required for this monotonic flow is that the stress tensor of the matter fields driving the holographic RG flow must satisfy the null energy condition over the holographic surface used to calculate the entanglement entropy. In the case where the bulk theory is described by Gauss-Bonnet gravity, the latter condition alone is not sufficient to establish the monotonic flow of the c-function. We also observe that for certain holographic RG flows, the entanglement entropy undergoes a 'phase transition' as the size of the system grows and as a result, evolution of the c-function may exhibit a discontinuous drop.

Then, we turn towards studying the holographic entanglement entropy for regions with a singular boundary in higher dimensions. Here, we find that various singularities make new universal contributions. When the boundary CFT has an even spacetime dimension, we find that the entanglement entropy of a conical surface contains a term quadratic in the logarithm of the UV cut-off. In four dimensions, the coefficient of this contribution is proportional to the central charge c. A conical singularity in an odd number of spacetime dimensions contributes a term proportional to the logarithm of the UV cut-off. We also study the entanglement entropy for various boundary surfaces with extended singularities. In these cases, extended singularities contribute through new linear or quadratic terms in logarithm only when the locus of the singularity is even dimensional and curved.

Acknowledgements

It gives me immense pleasure to thank my supervisor, Robert C. Myers, for his constant support and patient guidance throughout my Ph.D. Through countless discussions, he has expanded my knowledge, pointed me to interesting projects and guided me through them. For sure, I am in a lifelong debt to him for the learning that took place in his company in or outside physics.

I would also like to thank Aninda Sinha, Subir Sachdev, Luis Lehner, Jorge Escobedo and Sayeh Rajabi for collaboration in various finished and unfinished research projects. I have greatly benefited from conversations and discussions I had with Janet Hung, Misha Smolkin and various other researchers at Perimeter Institute. Janet Hung and Prarit Agarwal took the responsibility of reading some of the sections of the thesis, which is deeply appreciated.

I also thank Prof. Tapobrata Sarkar, (late) Prof. S. D. Joglekar and various other professors for helping me learn physics during my days at IIT Kanpur. When it comes to learning, it doesn't go without mentioning the torture I gave (and received in equal proportion) in long discussions with Ramalingam Loganayagam. However, conversations with Udit Singh and Saurabh Madaan were lighter during which they used to reveal new business plans.

It has been a privilege to be a resident at the Perimeter Institute for Theoretical Physics (PI) throughout my graduate studies. Apart from providing financial support and a stimulating learning environment, I am being helped in crucial visa related issues. For that, I thank Sheri Keffer and the Human Resources department of PI. Research at Perimeter Institute is supported by the Government of Canada through Industry Canada and by the Province of Ontario through the Ministry of Research & Innovation.

I have a really long list of friends here in Waterloo and in other parts of the world who have helped me at various stages of undergraduate and graduate studies. I take this opportunity to express my gratitude for all I have received from them.

Further, I deeply thank my family and in-laws for their endless love, support and encouragement. I was fortunate to find my mother as a source of inspiration from an early stage, who is an extremely humble, hard working and dedicated lady. To say the least, I owe my family pretty much what I am today!

Finally, last three years flew by so quickly particularly because of Swati. Whether physics worked or not, her limitless love, care and artistic ingenuity has made each day of these years as vibrant and colourful as her paintings. Like on every front in life, she deserves half the credit for this thesis!

Dedication

To my parents, Swati and everybody I have learned something from, including
Srinivasa Ramanujan (1887–1920)
and
Swami Vivekananda (1863–1902).

Table of Contents

List of Tables

List of Figures

Chapter 1

Introduction

The Standard Model of particle physics describes three of the four fundamental forces of the nature. Since its development in 1960's and 1970's, the standard model has been tested extensively at particle accelerators over the succeeding period. Although the Standard Model falls short of being a complete theory of all the fundamental forces, the successful predictions of this theory, especially in precision tests carried out at the LEP and SLC facilities, has firmly established it as the low-energy limit of any unified theory, that may also include gravity [1].

The theoretical structure of the standard model mainly consists two disjoint theories: quantum chromodynamics (QCD) that describes strong interactions and the Glashow-Salam-Weinberg (GSW) electroweak theory that describes electromagnetic and weak interactions [2, 3, 4]. At the energy scales above 100 Gev, both electromagnetic and weak interactions are unified in a single theory with $SU(2) \times U(1)$ symmetry. At this unification scale, the matter content (fermions) and force mediators of the theory are massless. As a result of the spontaneous symmetry breaking of $SU(2) \times U(1)$, the scalar takes the non-zero vacuum expectation value and the fermions, gauge vector bosons and Higgs boson gain mass. Finally in the low energy effective theory, we get electromagnetic force mediated by the massless photon and weak force is mediated by the massive W^+, W^- and Z bosons.

Although the standard model has been the most successful model in explaining the fundamental physics, there are several fronts where it seems incomplete. For example, the standard model doesn't explain the neutrino oscillations and a finite Higgs mass gives rise to puzzles like the hierarchy problem and the problem of small cosmological constant. More importantly, the underlying mathematical structure for the standard model is inadequate to describe the gravity. As the gravity couples with every bit of the stress energy

tensor, one requires infinite counter terms to renormalize the theory. In other words, now we know that the quantum mechanical version of the Einstein's classical gravity, or its immediate modifications are not renormalizable. Now given these difficulties, there is strong motivation to find the correct theory of quantum gravity and we mention two particular scenarios where quantum nature of gravity is important. First, at the early stage of the universe, the spacetime was highly curved and to explain the big-bang, we will definitely need the quantum gravity. Second, now there are stronger astronomical evidence that black holes do exist in our universe [5], and we need a quantum mechanical theory of gravity to understand these exotic objects.

One of the most intriguing puzzles about the black holes is the information paradox. In 1970's, Hawking used the semiclassical arguments to show that a black hole is not completely black and it radiates [6]. The radiation takes place because of the spontaneous creation of a particle anti-particle pair and as a result, mass of the black hole reduces. If this process continues long enough, it is expected that eventually the black hole will disappear. Now if all that comes out of the black hole is the thermal radiation, all the information about the matter dumped in the black hole will be lost after it evaporates. This loss of information actually threatens the fundamental quantum determinism which says that information about a quantum system evolved under the unitary operators is always conserved. In this context, the idea of black hole entropy is introduced, which says that the black hole entropy is proportional to the area of the black hole horizon [7]. As the inside regime of any black hole is inaccessible, it is expected that the information about the degrees of freedom of the black hole is stored on its horizon at a scale of the Planck length. This interpretation led to the beautiful idea of holography in field theories, which means that all the degrees of freedom of any region lies on the boundary that surrounds it. Now simultaneously, in slightly different developments, it is noted that the von Neuman entanglement entropy in field theories also follows the area law [8, 9]. This interesting similarity in the black hole entropy and entanglement entropy has received much attention and there is an open question if the black hole entropy is entanglement entropy [8, 9, 10, 11]. Hence, a deeper understanding of the black holes and the information paradox might not only demand a theory of quantum gravity, but also we need to understand the nature of the entanglement entropy.

Now let us return to the problem of quantizing the Einstein's gravity. The key reason that gravity is non-renormalizable is that we had assumed the fundamental particles to be point particles. As a result, the loop diagrams are divergent and we need infinite parameters to renormalize the theory. One of the possible solution of this problem can be that the fundamental particles are not precisely the point particles but there is an internal length scale associated with them. This simple idea is at the core of the string theory and

one assumes that all the fundamental particles are nothing but the various excitations of a single string. Now because of this internal length scale, as shown in figure 1.1, the loop-diagrams in string theory will smear out rendering a renormalizable theory of quantum gravity. Apart from that, string theory has also been a great source of remarkable ideas which have enhanced our understanding of fundamental physics. Among all, one of the most intriguing is the AdS/CFT conjecture, which has been studied extensively in the last decade. This conjecture has been vigorously used to study various properties of the specific class of strongly coupled field theories. As entanglement entropy plays a crucial role in quantum field theories (QFT's), it is natural to utilize the AdS/CFT correspondence to understand it. Hence, in this chapter, we review basic idea of string theory, gauge-gravity duality and entanglement entropy to lay the foundation for later chapters, where we use holographic techniques to uncover some interesting properties of entanglement entropy.

This chapter is organized as follows: in section 1.1, we first give a brief review of string theory which is aimed for the discussion of the AdS/CFT correspondence. For more complete review, the interested reader may consult to [12, 13, 14, 15]. In section 1.2, we discuss basic properties of the AdS geometry and introduce the AdS/CFT correspondence. Then in section 1.3, we discuss RG flow and c-theorems in quantum field theories and then explain how they are implemented in the AdS/CFT correspondence. In this section, we also review the basic properties of the entanglement entropy in field theories and the proposal by Ryu and Takayanagi [16] to calculate it using the holography. Finally in section 1.4, we briefly explain how rest of the thesis is organised.

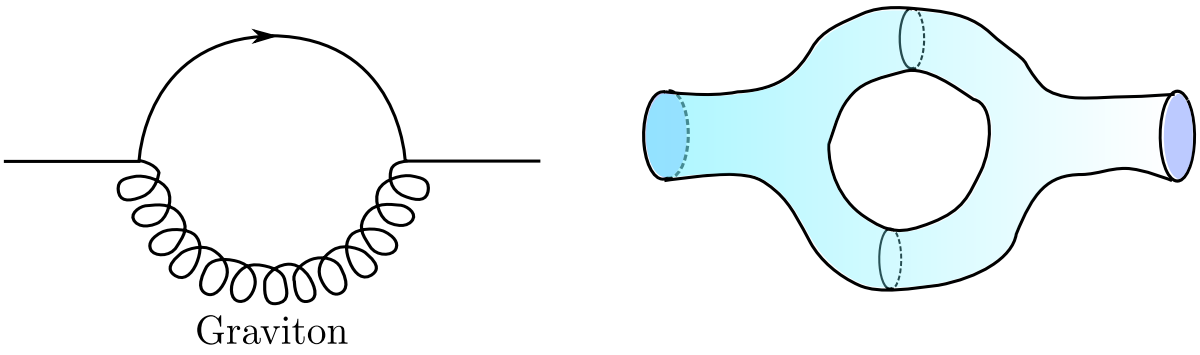

(a) (b)

Figure 1.1: (Color Online) Panel (a) is a self-energy diagram for a fermion containing a graviton in the loop. Panel (b) show how the vertices in this event will smear out removing the UV divergences if we consider strings.

1.1 Overview of string theory

The simplest model of string theory is the bosonic string model in the flat background, which also plays the role of a useful tool in understanding its more complicated versions. The idea is to assume a one dimensional object, the string, propagating in the D-dimensional space time. Then it will trace a two dimensional worldsheet and the action for the string is naturally given by the area of the worldsheet. However, such an action is hard to quantize and the equivalent but convenient action for bosonic string theory is the Polyakov action [17]:

$$I_\sigma \;=\; -\frac{1}{4\pi\alpha'}\int d^2\sigma\sqrt{-h}\,h^{\alpha\beta}\partial_\alpha X^\mu\partial_\beta X^\nu\eta_{\mu\nu}\,. \tag{1.1}$$

This action simply treats the spacetime coordinates as D free scalar fields on the two dimensional worldsheet. Here $\sigma^\alpha=(\tau,\sigma)$ are the coordinates on the worldsheet and $h_{\alpha\beta}$ is the worldsheet metric, which is an independent dynamical variable. Further, X^μ are the scalar fields from the worldsheet point of view and describe the embedding of worldsheet in the D-dimensional Minkowski target space with metric $\eta_{\mu\nu}$. Finally, α' is the Regge slope and it is related to the string tension T and string length scale ℓ_s by

$$T \;=\; \frac{1}{2\pi\alpha'} \;=\; \frac{1}{2\pi\ell_s^2}\,. \tag{1.2}$$

We further note that there are two local worldsheet symmetries of the Polyakov action, namely the reparameterization invariance of coordinates (τ,σ), and the Weyl (or conformal) invariance $h_{\alpha\beta}\to e^{2w(\tau,\sigma)}h_{\alpha\beta}$. Now the quantization of the worldsheet theory gives rise to various interesting phenomenon. First, one finds that for open string, *i.e.,* string with end-points, one can impose Dirichlet or Neumann boundary conditions on the boundary of the worldsheet. For closed strings, the worldsheet does not have any boundary and fields satisfy the (anti)periodicity conditions. Further, the preservation of conformal invariance and the Lorentz symmetry implies that the spacetime has to be 26 dimensional. With this 26-dimensional target space, one finds that the lightest modes of open and closed strings are tachyonic. These tachyonic modes can be ignored in the further discussion of the bosonic strings. As we will point out later, in the more realistic models of string theory where we also have fermions, tachyons can be removed by truncating the theory in a sensible way. The next high energy excitations of both open and closed strings are massless and remarkably, some closed string modes turn out to be graviton in the 26-dimensional target space. Now, similar to quantum field theories, we expect the strings to interact. The description of the interaction between the strings is only breaking and fusing into each

other by a local interaction of the worldsheet as shown in figure 1.2. Further, using the operator-state correspondence of the two-dimensional conformal field theory on the string worldsheet, one can find a local vertex operator in the worldsheet theory corresponding to each asymptotic state of the string. Now similar to field theories, one can use these vertex operators in the path integral to calculate the string scattering amplitudes. In the perturbative framework, similar to Feynman diagrams, one needs to sum over all the worldsheet topologies with all vertex operators of incoming and outgoing string states. In the end, using the conformal symmetry of the worldsheet, the calculation of the string scattering amplitudes boils down to finite dimensional integrals over the 'moduli space' of the worldsheet.

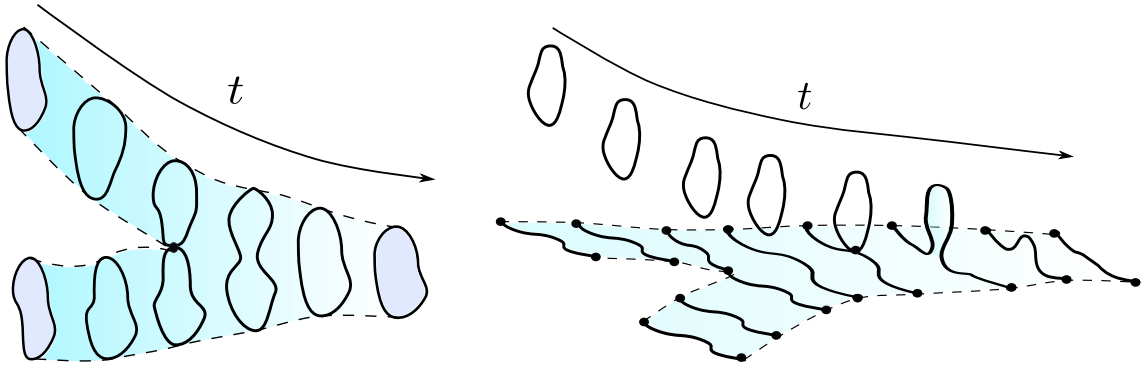

Figure 1.2: (Color Online) This figure shows examples of string interactions. In panel (a), two closed strings fuse to make one closed string. In panel (b), first two open string combine into one open string and then a closed string breaks and joins with the open string.

We can further consider the strings in curved D-dimensional background spacetime. Then in (1.1), we need to replace $\eta_{\mu\nu}$ with the curved metric $G_{\mu\nu}$ in the target space. As graviton is one of the states of the string, we can say that in some sense, spacetime is a coherent background of string states. Now if gravity background makes its appearance in the worldsheet action, it makes sense to include the backgrounds of other massless string states too. So using the form of the vertex operators for various massless closed string excitations, with Euclidean signature on the worldsheet metric, one can generalise the action for bosonic strings (1.1) to [18, 19]

$$I_\sigma = \frac{1}{4\pi\alpha'}\int d^2\sigma\sqrt{h}\left[\left(h^{\alpha\beta}G_{\mu\nu}(X)+i\epsilon^{\alpha\beta}B_{\mu\nu}(X)\right)\partial_\alpha X^\mu\partial_\beta X^\nu+\alpha' R\Phi(X)\right]. \tag{1.3}$$

Here X^μ are spacetime coordinates, R is the worldsheet Ricci scalar and $G^{\mu\nu}$ is the metric in the target space. Further $B_{\mu\nu}$ is the two-form Kalb-Ramond field and Φ is the dilaton. These are the massless excitations of a closed oriented string which we are considering. Further, $\epsilon^{\alpha\beta}$ is antisymmetric tensor on two-dimensional worldsheet and it is normalized such that $\epsilon^{\tau\sigma} = 1/\sqrt{h}$. Note that here we are focusing only on the low energy excitations. In this limit, we assume that the gravity is weakly curved and if background curvature is controlled by the distance scale L, then the dimensionless coupling $\ell_s/L \ll 1$, where ℓ_s is the string length. In this regime, perturbative theory is a useful tool and we can ignore the high energy states of the strings in (1.3). While all this happens in the two dimensional worldsheet theory, one can find the low energy effective action for strings in target space and it turns out to be

$$I = \frac{1}{2\kappa_0^2}\int d^{26}X\sqrt{-G}\,e^{-2\Phi}\left(\mathcal{R} - \frac{1}{12}H_{\mu\nu\lambda}H^{\mu\nu\lambda} + 4\,\partial_\mu\Phi\partial^\mu\Phi\right). \tag{1.4}$$

Where $\mathcal{R}$ is the Ricci scalar in the target space, $H_{\mu\nu\lambda} = \partial_\mu B_{\nu\rho} + \partial_\nu B_{\rho\mu} + \partial_\rho B_{\mu\nu}$ and κ_0 is the coupling constant of order $\kappa_0 \sim g_s\ell_s^{12}$, where g_s is the string coupling and ℓ_s is the string length. Note that here κ_0 is not fixed by the field equations and can be changed by the field redefinition of Φ. Now remarkably, the first few terms in effective action (1.4) gives the Einstein's gravity in $D = 26$ dimensional spacetime. It can be further seen through the scattering diagrams of strings that dilaton Φ is related to the string coupling by $g_s = e^{\langle\Phi\rangle}$, where $\langle\Phi\rangle$ is the background (or expectation) value of the dilaton. So in string theory, different backgrounds will have different string coupling and in this sense, string coupling is a dynamical variable which is fixed by the theory itself. Further, our one dimensional objects, the strings, are charged under two-form field $B_{\mu\nu}$. We will soon see that in superstring theory, there are even higher form fields and that will give rise to higher dimensional charged objects, namely the Dirichlet branes. Finally, we wrap up this discussion of bosonic strings by reminding the reader that the effective action (1.4) in target space is recovered under two approximations: First, all the background fields vary slowly on the string length scale, *e.g.,* $\ell_s\nabla\Phi/\Phi \ll 1$, and hence at leading order, strings are treated as point particles. So the length of the string is one of the parameters in the perturbative expansion of quantum corrections. Second, we expect that the background values of the fields and string coupling are also small and the stringy corrections are also treated perturbatively. Finally, we emphasize the importance of the conformal symmetry of the worldsheet theory by mentioning that the equations of motion for fields in target space can also be recovered from the trace anomalies of the worldsheet CFT. In this way, the equations of motion for various fields in action (1.4) are nothing but the beta function for the various couplings in the worldsheet theory. So in recovering the Einstein's gravity in 26 dimensions from the simplest model of string theory, the diffeomorphism and Weyl

scaling of worldsheet play a crucial role.

To introduce spacetime fermions in the spectrum of the string theory, we need to introduce fermions in the worldsheet theory. Now there are two main formalisms to introduce fermions in supersymmetric worldsheet theory: the Ramond-Neveu-Schwarz (RNS) formalism and the Green-Schwarz (GS) formalism. Although we find five different, consistent superstring theories through different formalisms, various dualities among these string theories suggest that they are all various limits of a single M-theory. Here, we will discuss some details about the RNS formalism of superstring theory because they result in type IIA and IIB string theories, which are more relevant to our discussion of gauge-gravity duality.

In RNS formalism, the two dimensional worldsheet theory contains as many Majorana spinors $\psi^A(\tau, \sigma)$ as the dimension of the target space. Here A runs over the target space dimensions D. Now similar to scalar fields on worldsheet of open strings, we need to impose the boundary condition on the edges. For closed strings, the boundary condition will take the form of the periodicity condition. In both cases, Lorentz invariance allows two types of boundary or periodicity conditions on the spinor fields. One can either have $\psi(\tau, 0) = \psi(\tau, \sigma_0)$ or $\psi(\tau, 0) = -\psi(\tau, \sigma_0)$. Here $\sigma_0 = \pi$ for open string worldsheet and $\sigma_0 = 2\pi$ for closed string worldsheet. These two boundary conditions will give rise to two types of independent oscillators, namely the Ramond sector and the Neveu-Schwarz sector of the oscillators. As a results of these periodicity or anti-periodicity conditions, the fermionic oscillators in Ramond sector, *i.e.,* for $\psi = \psi$, will have integer frequencies and in Neveu-Schwarz sector, *i.e.,* for $\psi = -\psi$, will have half integer frequencies.

In an open string, the right and left moving modes are not independent and hence, a particular fermion can be either a Ramond or a Neveu-Schwarz mode. After quantization, the spectrum of the worldsheet fermions in Ramond sector contains the zero modes, which actually do not contribute in the energy, and hence the ground state is degenerate. Interestingly, these degenerate ground states in the Ramond sector are organized into a spacetime spinor in the target space. On the other hand, the Neveu-Schwarz sector of the fermions in an open string does not have any zero modes in the spectrum. The situation is more interesting in the closed strings. In this case, the left and right moving oscillators are independent and hence a closed string contains the following mixed sectors: R-R, R-NS, NS-R or NS-NS. Further, the preservation of the conformal invariance in the quantized worldsheet theory implies that now the target space is 10-dimensional. However, the spectrum of NS-NS sector in this theory contains the tachyons, which is indeed a problem with this formalism. To further construct a consistent theory, one needs to utilize Gliozzi-Scherk-Olive (GSO) projection of states [20], which eliminates half of the states and also ensures the spacetime supersymmetry in the target space.

The idea behind the GSO projection is to use the chirality and the number of fermions in consecutively Ramond and Neveu-Schwarz sectors to find a consistent truncation of the theory. In Neveu-Schwarz sector, after projecting the states under a 'fermion number operator', only the states with odd numbers of fermionic oscillator excitations survive. As tachyonic state in NS sector has zero fermion number, this state is removed. Similarly in Ramond sector, one projects the states under a 'chirality' operator. In this case, the choice of positive or negative chirality is just a matter of choice for open strings. However in closed strings, there are two independent modes and one can perform the GSO projection on both right and left moving modes independently. Now if we take the opposite GSO projection on the Ramond sectors of left and right moving modes, the spinors have the opposite chirality and it is called type IIA theory. Also, we can take the same GSO projection on the left and right moving modes of closed strings and now spinors have the same chirality. This is called the type IIB theory. Note that as a result of GSO projection, type IIA is a non-chiral spacetime theory and type IIB is a chiral spacetime theory.

In both type IIA and IIB string theories, the massless bosonic content comes from the R-R and NS-NS sectors. In the NS-NS sector, we find the usual dilaton, graviton and the two-form Kalb-Ramond field for both type IIA and IIB theories. However, the content in R-R sector will depend on the chirality of the theory and it will be different for type IIA and IIB. In both theories, the R-R sector can be decomposed into representations of $SO(9,1)$ which are antisymmetric form field potentials with n indices. In type IIA, we have $n = 1, 3, 5, 7, 9$ and in type IIB theory we have $n = 0, 2, 4, 6, 8$. This implies that in 10-dimensional IIA and IIB theories, there are consequently odd and even form potentials. In case of bosonic string theory, we discussed that open strings (one dimensional objects) were charged under a two-form field, namely the B-field. Similarly, we find that there are extended objects in the superstring theory, namely the $(p+1)$-dimensional Dirichlet branes (Dp-branes), which are charged under these new R-R forms. In IIA theory, there are form potentials with $1, 3, 5, 7$ and 9 indices and hence theory contains Dp-branes with $p = 0, 2, 4, 6$ and 8. Similarly, IIB has form potentials with $0, 2, 4, 6, 8$ indices and contains Dp-branes with $p = 1, 3, 5, 7$ and 9.

The support for the existence of the higher dimensional extended objects also comes from the black hole radiation, that we discussed earlier. The Hawking radiation will result in the reduction of the mass of the black holes and it will eventually reach to extremal limit. In this limit, the black hole has the minimal mass compatible with the charges and there is no Hawking radiation. Further, the supergravities have black hole and black brane solutions which have R-R charges. As Hawking radiation carries away only mass but not charge, the remnant will also carry R-R charge. Hence, it is expected that the full quantum theory of gravity must carry the objects which will source the R-R fields and can

describe the complete process of the black hole evaporation. One remarkable result in this direction is the black hole state counting using the D-branes for a specific class of black holes [21]. The idea is to begin with a supersymmetric black hole, which will be equivalent to strongly coupled D-branes when the entropy is evaluated using the Bekenstein-Hawking formula. Now at weak coupling, the D-branes can be viewed as bound states of minimally charged BPS solitons, and one can topologically count the degeneracy of these states. As the number of states will not change from going back to strong coupling, this result for number of states also applies to the black hole. Remarkable, the state counting using this idea is found to match with the Bekenstein-Hawking entropy which follows the area law.

Apart from that, the D-branes arise naturally in the discussion of the open strings. We can have open strings states whose ends satisfy the Dirichlet boundary conditions along the directions orthogonal to a Dp-branes and Neumann boundary condition in rest of the directions. Then the end of the open string can only move along the Dp-brane and various open string excitations will determine the location and shape of this Dp-brane. It is more explicit in this picture that the D-branes are charged dynamical objects and similar to the strings, D-branes respond to the background fields. The dynamics of the D-branes can be described by the world-volume action which involve the background fields acting as the generalized field dependent couplings. In bosonic string theory, the only surviving fields in the low energy limit are the massless open string states. For this case, the Dirac-Born-Infeld (DBI) action describing a Dp-brane moving in the background created by the massless closed string modes $G_{\mu\nu}, B_{\mu\nu}$ and Φ is given by

$$S_p \;=\; -T_p \int d^{p+1}\xi\, e^{-\Phi} \sqrt{-\det(\gamma_{ab} + 2\pi\alpha' F_{ab} + B_{ab})}\,, \tag{1.5}$$

where T_p is the tension and ξ^a are the coordinates describing the Dp-brane. Further, γ_{ab} and B_{ab} are the pull-back of the spacetime metric on the worldvolume and the two-form field $B_{\mu\nu}$ in spacetime:

$$\gamma_{ab} \;=\; G_{\mu\nu} \frac{\partial X^\mu}{\partial \xi^a} \frac{\partial X^\nu}{\partial \xi^b} \quad \text{and} \quad B_{ab} \;=\; B_{\mu\nu} \frac{\partial X^\mu}{\partial \xi^a} \frac{\partial X^\nu}{\partial \xi^b}\,. \tag{1.6}$$

Finally, $F_{ab} = \partial_a A_b - \partial_b A_a$ is the field strength for the gauge field A_a, which is one of the massless open string excitations and lives on the Dp-brane. There are other massless open string excitations which are fluctuations of the D-brane in the orthogonal directions, *e.g.,* ϕ^I in eq. (1.7). In (1.5), dilaton appears because all physics arise at the open string tree-level processes and dilaton governs the coupling between them. Further, other fields appear as a combination of $2\pi\alpha' F_{ab} + B_{ab}$, which preserve the spacetime gauge invariance.

The situation becomes much more interesting when we have a stack of N overlapping Dp-branes and want to understand their dynamics. We find that the low energy limit of a stack of Dp-branes is a super $U(N)$ Yang-Mills theory. Note that we can label the end points of the open strings by the Chan-Paton factors which are the boundary terms in the worldsheet action and do not contribute to the energy. However, these Chan-Paton factors keep track of the information of which Dp-brane the string is ending on and using these, the massless fields on the brane could be naturally combined into $N \times N$ Hermitian matrices. Then the gauge symmetry takes the form of $U(N)$ symmetry from a stack of N overlapping Dp-branes. Now the leading two-derivative bosonic part of the low-energy action describing a stack of N Dp-brane takes the following form

$$I_N \;=\; -(2\pi\alpha')^2 T_p \int d^{p+1}\xi \,\mathrm{Tr}\left(\frac{1}{4}F_{ab}F^{ab} + \frac{1}{2}\mathcal{D}_a\phi^I\mathcal{D}^a\phi^I - \frac{1}{4}\sum_{I\neq J}[\phi^I,\phi^J]^2\right), \tag{1.7}$$

where gauge field $(A_a)^m{}_n$ have extra indices for $U(N)$ and $F_{ab} = \partial_a A_b - \partial_b A_a + i[A_a, A_b]$. Further, $\mathcal{D}_a\phi^I = \partial_a\phi^I + i[A_a, \phi^I]$, where ϕ^I is in the adjoint representation of the gauge group and the over all coefficient in front of the Yang-Mills term is coupling $1/g^2_{\mathrm{YM}}$. Further, the complete action for the dynamics of a stack of N Dp-branes will take the form of a supersymmetric $U(N)$ Yang-Mills theory. This remarkable result is at the foundation of the gauge-gravity duality and we will discuss it in some detail in the next subsection.

1.2 The AdS/CFT correspondence

After a quick stroll through the superstring theory, we turn towards the bold conjecture by Maldacena [22]. In its original form, the conjecture says that the $\mathcal{N} = 4$ super Yang-Mills theory is equivalent to the type IIB string theory on $\mathrm{AdS}_5\times\mathrm{S}^5$. The motivation for the conjecture come from the dynamics of a stack of D-branes in different limits which we will discuss in detail. However, here we take a brief detour to review some basic properties of the AdS space which are crucial to the gauge-gravity duality.

1.2.1 The AdS space

The Anti-de Sitter (AdS) space is a maximally symmetric space with negative curvature. It is the simplest solution of the Einstein-Hilbert action for gravity with a negative cosmological constant. For this gravity, we can write the following action in $(d+1)$-dimensional

spacetime:

$$I \;=\; \frac{1}{16\pi G_d}\int d^{d+1}x\sqrt{-g}\left(R+\frac{d(d-1)}{L^2}\right)\,, \tag{1.8}$$

where G_d is the gravitational constant in $(d+1)$ dimensions and we follow the convention that metric has 'mostly positive' signature. Also, we have normalized the cosmological constant term such that the length scale L will be AdS radius. The AdS space is the simplest solution of the vacuum Einstein equations

$$R_{\mu\nu}+\frac{d}{L^2}g_{\mu\nu} \;=\; 0\,. \tag{1.9}$$

As AdS space is maximally symmetric, we also have

$$R_{\mu\nu\sigma\rho} \;=\; -\frac{1}{L^2}\left(g_{\mu\sigma}g_{\nu\rho}-g_{\mu\rho}g_{\nu\sigma}\right)\,. \tag{1.10}$$

Further to describe the $(d+1)$-dimensional AdS space, we can consider its embedding into a pseudo-Euclidean $(d+2)$-dimensional space with coordinate y^a and metric $\eta_{ab} = \mathrm{diag}(-,+,\ldots,+,-)$, where $a = 0,1,\ldots,d+1$. In this space, the line element is invariant under the Lorentz-like group $SO(2,d)$. Now we can define the AdS space by

$$(y^0)^2-\sum_{i=1}^{d}(y^i)^2+(y^{d+1})^2 \;=\; L^2\,, \tag{1.11}$$

which is both homogeneous and isotropic and has the isometry group $SO(2,d)$. The global coordinates (τ,ρ,Ω_i), which cover the hyperboloid (1.11) once, are defined by

$$y_0 \;=\; L\cosh(\rho)\cos(\tau)\,, \qquad y_{d+1} \;=\; L\cosh(\rho)\sin(\tau)\,, \tag{1.12}$$

$$y_i \;=\; L\sinh(\rho)\,\Omega_i \qquad \left(i=1,\ldots,d;\sum_i\Omega_i^2 \;=\; 1\right)\,, \tag{1.13}$$

where $\rho \geq 0$ and $\tau \in [0,2\pi)$. The metric for $(d+1)$-dimensional AdS space is the metric induced on the surface (1.11) and in global coordinates, it becomes

$$ds^2 \;=\; L^2\left(-\cosh^2(\rho)d\tau^2+d\rho^2+\sinh^2(\rho)\,d\Omega_{d-1}^2\right)\,, \tag{1.14}$$

where $d\Omega_{d-1}^2$ represents the line element on unit $(d-1)$-sphere. The isometry group $SO(2,d)$ of AdS has the maximal compact subgroup $SO(2)\times SO(d)$. It is apparent from the above metric that the $SO(2)$ part represents the translation along the τ direction and $SO(d)$

gives rotation of S^{d-1}. So in principle, these are closed time-like curves along τ direction, as it has a topology of S^1. Now to obtain a causal spacetime, we can unwrap the S^1 by taking $\tau \in (-\infty, \infty)$. This will give us the universal covering of the hyperboloid and it will be referred by AdS_{d+1} in our discussion of the AdS/CFT correspondence. Further, there is an another useful set of coordinates $(u, t, \vec{x})$ which are defined as

$$\begin{aligned} y_0 &= \frac{1}{2u}\left(1 + u^2(L^2 + \vec{x}^2 - t^2)\right), \qquad y_{d+1} = L\,u\,t\,, \\ y^i &= L\,u\,x^i \quad (i = 1, \ldots, d-1)\,, \\ y^d &= \frac{1}{2u}\left(1 - u^2(L^2 - \vec{x}^2 + t^2)\right), \end{aligned} \tag{1.15}$$

where $u > 0$ and $\vec{x} \in \mathbb{R}^{d-1}$. With these coordinates, the metric takes the following form

$$ds^2 = L^2\left(\frac{du^2}{u^2} + u^2(-dt^2 + d\vec{x}^2)\right). \tag{1.16}$$

In this form of the metric, the subgroups $ISO(1, d-1)$ and $SO(1,1)$ of isometry $SO(2,d)$ are apparent. Here, $ISO(1,d-1)$ is the Poincare transformation on $(t, \vec{x})$ and $SO(1,1)$ is

$$(t, \vec{x}, u) \to (\lambda t, \lambda \vec{x}, u/\lambda)\,, \quad \lambda > 0\,. \tag{1.17}$$

As we will see below, this scaling is identified with the dilatation in the conformal symmetry group of $\mathbb{R}^{1,d-1}$ in the AdS/CFT correspondence. Further, the coordinates $(u, t, \vec{x})$ are called the Poincare patch and they actually cover only one half of the hyperboloid (1.11). One way to see it from (1.15) is that now we only cover the range $y_0 \geq -y_{d+1}^2/2uL^2$. To understand it further, we use the Penrose diagram of AdS_{d+1}. In the metric (1.14), we introduce the coordinate θ related to ρ by $\tan(\theta) = \sinh(\rho)$, where $0 \leq \theta < \pi/2$. Then, the metric takes the following form

$$ds^2 = \frac{L^2}{\cos^2\theta}\left(-d\tau^2 + d\theta^2 + \sin^2(\theta)\sum_i d\Omega_i^2\right). \tag{1.18}$$

Now we can ignore the conformal factor in front of the metric and find that the geometry is conformally mapped to $R \times S^d$. Note that we have $0 \leq \theta < \pi/2$, so only half of the sphere of S^d is part of the AdS. We have drawn this geometry in 1.3 where $\theta = 0$ is the north pole of S^d and $\theta = \pi/2$ is equator. In figure 1.4, we have also shown the Poincare patch, which only covers part of the hyperboloid.

Now we briefly discuss the particles and fields in the AdS_{d+1} space. We can learn some simple properties of the AdS space by studying its causal structure using the Penrose

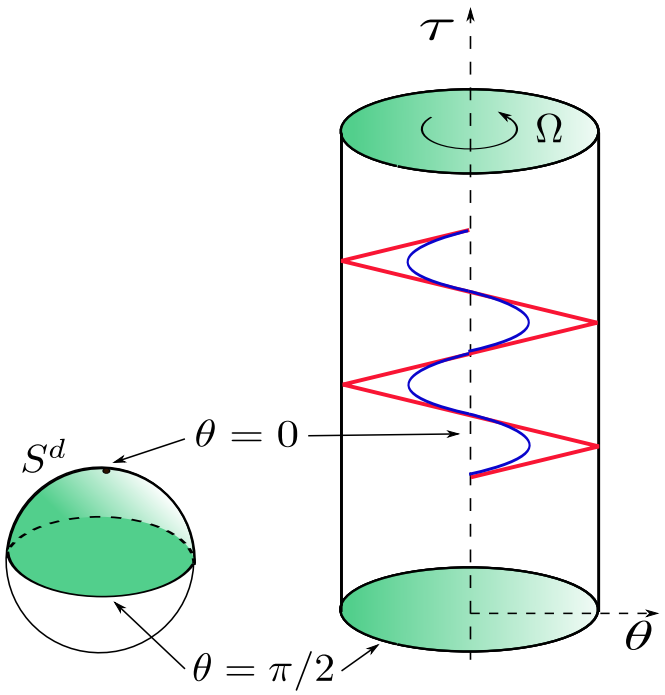

Figure 1.3: (Color online) This figure shows the Penrose diagram for AdS_{d+1}, which is mapped on one-half of $R \times S^d$. As $0 \leq \theta \leq \pi/2$, only half of the sphere is mapped. In the cylinder, the axes is mapped to $\theta = 0$ and surface is mapped to $\theta = \pi/2$. We have also shown the geodesics of a massive (blue) and massless (red) particles. A massive particle never reach the boundary and oscillates around $\theta = 0$. However, a massless particle can reach the boundary is finite time and bounce back if proper boundary condition is set. Note that for both massless and massive particles, the time period of oscillation is same.

diagram 1.3. The AdS_{d+1} can be conformally mapped to $R \times S^d$ and in this geometry, a massive particle moving along the geodesic never reaches the boundary of the AdS. In fact, it performs an oscillatory motion around $\theta = 0 = \rho$ as shown in figure 1.3. Note that the Penrose diagram of AdS space is a cylinder. Hence, with respect to an observer moving along its geodesic, a massless particles can go to the boundary and bounce back in finite time if proper boundary conditions are set.

Further, in our discussions below, we will be particularly interested in gravity coupled to a scalar field. In this case, if the critical points of the scalar potential yield a negative cosmological constant, the background geometry will be AdS for each such stationary point. The stability of the system demands that the conserved energy functional of the

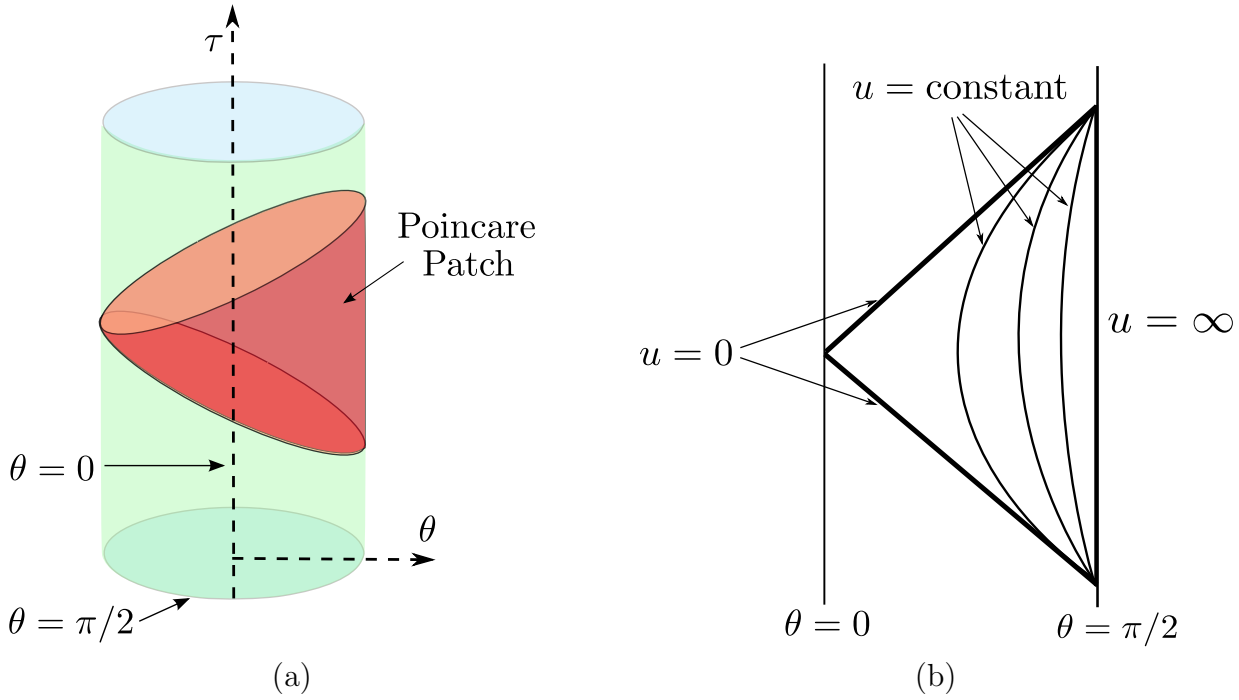

Figure 1.4: (Color Online) Panel (a) shows the Poincare patch in Penrose diagram of the AdS_{d+1}. As shown in figure 1.3, AdS_{d+1} can be conformally mapped on $R \times S^d$ and cross section of the cylinder is half of the sphere S^d. The region of the cylinder in red color is the Poincare patch and it only covers part of the AdS_{d+1}. In panel (b), we again show the Penrose diagram of AdS_{d+1} where now every point represents a unit S^{d-1}. Here, the triangle is the Poincare patch.

field theory is positive for a suitable space of fluctuations, namely for those the energy integral converges. When this stability condition is translated to condition on the mass of the scalar, it requires that the scalar mass squared may be tachyonic but the value is bounded below [23, 24, 25]. This stability condition is known as the Breitenlohner-Freedman (BF) bound on the mass of the scalar and is given by

$$m^2 \geq -\frac{d^2}{4L^2}\,. \tag{1.19}$$

In the context of the AdS/CFT correspondence, this condition will be related to the dimension of the operator on the CFT side and we will return to it when we will discuss the RG flows in holography.

1.2.2 The gauge-gravity duality

After a brief discussion of the properties of the AdS space, now we will discuss the basics of the gauge-gravity duality and set up the AdS/CFT dictionary. Before we make some general statements about this duality, it will be interesting to discuss the specific case for field theories in four spacetime dimensions. Here our review is very brief and interested readers can find many more details in [26, 27].

To begin with, let us consider the type IIB string theory in flat ten-dimensional Minkowski space with a stack of N coincident D3-branes. The D3-branes will extend in a $(3+1)$-dimensional hyperplane in the full $(9+1)$-dimensional space. In this system, there are two types of excitations: Closed string excitations in the empty space around the D3-branes and the open string excitations of the D3-branes. At the energy scales lower than the string scale $1/\ell_s$, we can integrate out the massive excitations and only massless modes for open and closed strings will survive in the effective field theory. As discussed in the section 1.1, the massless open string excitations in low energy limit will be described by a $U(N)$ gauge theory and in particular for D3-branes, it will be $\mathcal{N}=4$ supersymmetric $U(N)$ Yang-Mills. So the effective action for this system will be following:

$$S \;=\; S_{close} + S_{open} + S_{interaction}\,, \tag{1.20}$$

where S_{close} describe the massless closed string modes which is the ten dimensional type IIB supergravity. Note that in general, we also have additional higher derivative corrections in this action but these will be dropped in the low energy limit. The second term S_{open} describes the D3-branes dynamics and it is defined on the $(3+1)$-dimensional worldvolume. It contains the $\mathcal{N}=4$ super-Yang-Mills lagrangian and the higher derivative corrections in string length ℓ_s. Finally, $S_{interaction}$ describes the interaction between the closed string modes in the bulk and D-branes, and the coupling between these is proportional to $g_s\alpha'^2$, where $\alpha' = \ell_s^2$. So in the low energy limit, *e.g.*, $\ell_s \to 0$, these massless open and closed string modes decouple.

Now we can take the low energy limit by keeping all the dimensionless parameters, string coupling g_s and N fixed, and sending the string length $\ell_s \to 0$. In this limit, we can see that the interaction lagrangian between the bulk and the brane excitations will drop out and the long distance (low energy) modes of gravity will become free. Simultaneously, all the higher derivative corrections to brane action will vanish and we will be left with the pure $\mathcal{N}=4$ SYM in four spacetime dimensions, which is known to have conformal symmetry. So in the low energy limit, we have two decoupled systems: A free supergravity in ten dimensions and four dimensional superconformal field theory. Now, we can further take

the strong coupling limit by increasing g_s. Then, we get a strongly coupled superconformal theory with large 't Hooft coupling, *i.e.,* $\lambda_t = g_s N \gg 1$.

We can also consider this system from a different point of view. As the D-branes are massive charged objects, they can act as source for various supergravity fields. So a closed string moving beside a stack of N D3-branes can interact as shown in the figure 1.5. For this interaction, the effective coupling is $g_s N$, where N comes from the fact that open string can end on any of the N D-branes. Here, we assume that g_s is small and we can work in the perturbative framework. However, if N become very large such that $N \gg 1/g_s$, the effective coupling becomes large and perturbative treatment is insufficient. So we integrate out the D-brane contribution and then are left with the full non-linear supergravity fields around D-brane. Effectively, now the closed strings propagate in the ten dimensional curved spacetime and as g_s is still small, they can be treated perturbatively.

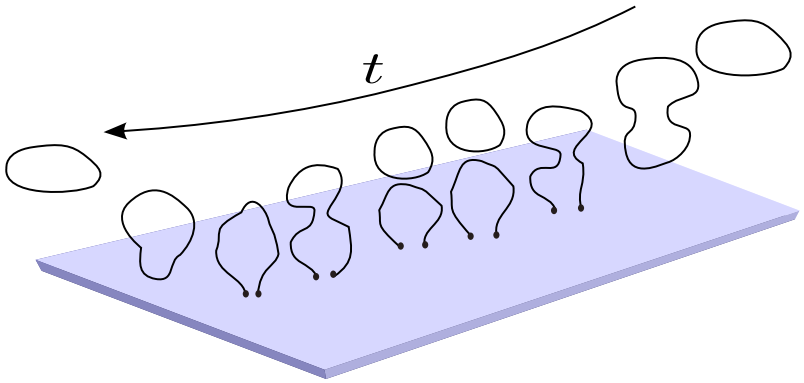

Figure 1.5: This diagram shows how a closed string passing beside a stack of N D-branes interacts with it. The Chan-Paton factor at the tip of the open strings keep track of the information on which D-brane they are ending.

By integrating out the contribution of N D3-branes, we get a specific supergravity solution. We assume that the world volume is described by the coordinates $x^\mu = (t, x^1, x^2, x^3)$ and the transverse directions are y^i with $i = 1, \ldots, 6$ and $\sum_i (y^i)^2 = r^2$. If the D3-branes

are put at the origin of the transverse space, the supergravity solution is given by

$$\begin{aligned} ds^2 &= \frac{1}{\sqrt{f(r)}}\left(-dt^2+dx_1^2+dx_2^2+dx_3^2\right)+\sqrt{f(r)}(dy^i)^2\,, \\ F_5 &= (1+*)dt\,dx_1\,dx_2\,dx_3\,df^{-1}\,, \\ f &= 1+\frac{L^4}{r^4}\,, \qquad L^4 = 4\pi g_s\ell_s^4 N\,, \end{aligned} \tag{1.21}$$

where F_5 is the five-form flux and $*$ represents the Hodge dual. Also, $(dy^i)^2 = dr^2 + r^2 d\Omega_5^2$ and $d\Omega_5^2$ is metric over unit S^5. In this solution, as g_{tt} depends on r, the energy of an object E measured by an observer at a fixed r will be red-shifted with respect to the energy E_∞ measured by an observer at infinity. The relation between E and E_∞ is:

$$E_\infty = \frac{E}{(f)^{1/4}}\,, \tag{1.22}$$

which means that any object near $r = 0$ will appear to have a very low energy for the observer at infinity. Now we take the low energy limit in the background described by (1.21). From the point of view of the observer at infinity, there are now two types of low energy excitations. First, we have the massless excitations propagating in the asymptotically flat region which will have very large wavelength. Second, all kind of excitations can be taken very close to the horizon $r = 0$ and for an observer at infinity, they will appear massless. Now again, the first type of excitations with very large wavelength will decouple from the second type of excitations when the wavelength becomes much larger than the brane throat. So in the low energy limit, once again we are left with two decoupled systems: one is the free bulk supergravity and second is type IIB closed strings in the near horizon region of the geometry.

To take the low energy limit, we keep all the dimensionful quantities fixed and take $\ell_s \to 0$. We want to have the arbitrary excited string states in the throat region (near $r = 0$). So we keep the energy of these excitations in terms of string units fixed and that will mean that $E\ell_s \sim$ constant. In the field theories, the energy is measured by the observer at the infinity. From (1.22), the energy of the excitations in the throat geometry for the observer at infinity becomes $E_\infty \sim Er/\ell_s$. If we also want to keep it fixed, we need to take the limit $r \to 0$ in (1.21) keeping r/ℓ_s^2 fixed. This will imply that $r \ll L$ and we find that the throat geometry becomes

$$ds^2 = \frac{r^2}{L^2}\left(-dt^2+(dx^1)^2+(dx^2)^2+(dx^3)^2\right)+L^2\frac{dr^2}{r^2}+L^2 d\Omega_5^2\,, \tag{1.23}$$

that is $AdS_5 \times S^5$.

Remarkably, both in first and second approach of taking the low energy and large N limits for the stack of D3-branes, we recover two decoupled systems. In first case, we get a free ten-dimensional supergravity and $\mathcal{N}=4$ super Yang-Mills theory. In second case, we recover the same ten-dimensional supergravity and the classical $AdS_5 \times S^5$ geometry. Now the Maldacena conjecture is that we can drop the supergravity from both of the cases and in the large N limit, the $\mathcal{N}=4$ SYM is equivalent to the $AdS_5 \times S^5$ geometry. In fact, in the strongest form of the conjecture, which we assume here, it says that $\mathcal{N}=4$ $U(N)$ SYM in $(3+1)$ dimensions is equivalent to a type IIB superstring theory in $AdS_5 \times S^5$ for all values of N and $g_{\rm YM}$.

Schematically, we can summarize the above discussion in the following flow chart:

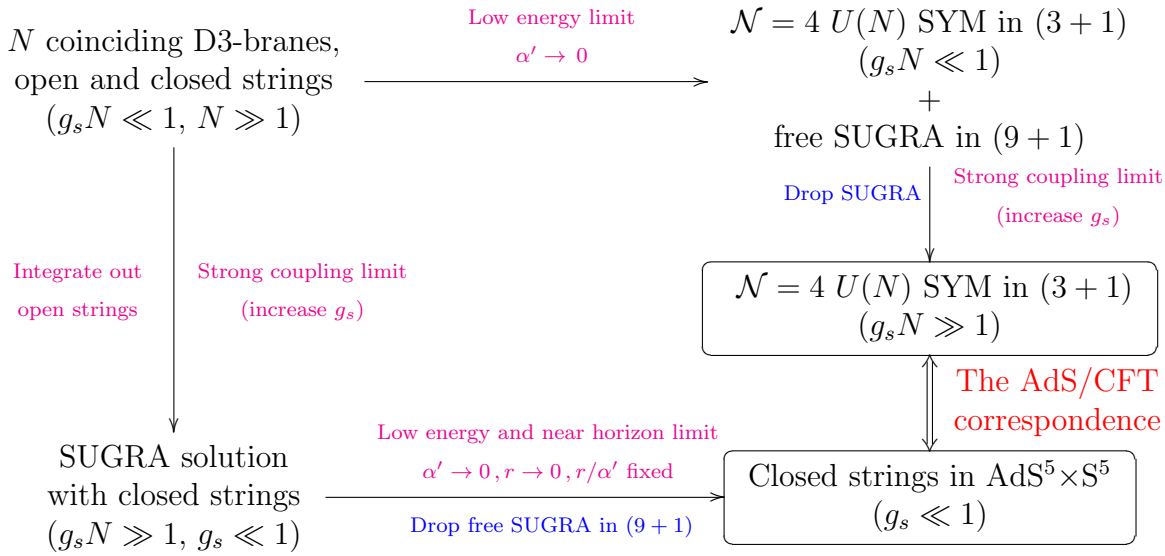

Now having discussed the proposal for the conjecture, we will make the AdS/CFT dictionary more concrete. Here we will begin with the symmetries of the both of the theories. Essentially, the $U(N)$ group is equivalent to the free $U(1)$ vector multiplet times an $SU(N)$ gauge group. In case of D-branes, the $U(1)$ part is related to their centre of mass motion and in the supergravity solution, it is related to the massless modes which live between the region connecting the bulk and the throat. Hence the $r \to 0$ region will only be describing the $SU(N)$ part of the group. Explicitly, the number of the color charges N on the field theory side is related to the flux of the five form Ramond-Ramond field strength on the S^5,

$$N = \int_{S^5} F_5 \,. \tag{1.24}$$

Further, the AdS space has $SO(4,2)$ group of isometries. On the field theory side, we have the same symmetry from the conformal group in $(3+1)$ spacetime. So the fact that the field theory is conformal translates to the idea that the dual gravity is AdS. On field theory side, we have superconformal group and hence, we have twice the usual number of supersymmetry generators. Equivalently on the gravity side, the number of the supersymmetries is twice that of the full solution (1.21) containing the asymptotic region. Further, the $SU(4)$ R-symmetry group of the field theory is related to the rotation along S^5, that has $SO(6)$ symmetry.

Now we can also relate various parameters on the both sides of the duality. From the D-brane dynamics, we recover that the Yang-Mills coupling in the field theory, $g_{\rm YM}$ is related to the string coupling g_s by $g_s = g_{\rm YM}^2$. Note that in the field theory, $g_{\rm YM}$ can be small. However, from the 't Hooft counting, it can be seen that the effective coupling in the field theory is 't Hooft coupling $\lambda_t = g_{\rm YM}^2 N$. Further, the string length ℓ_s is not an independent parameter in the theory. Here the relevant parameter is its ratio with the AdS radius L, which is related to the 't Hooft coupling by $L^4/\ell_s^4 = 4\pi\lambda_t$. This relation can further be extended to include ten-dimensional Newton's constant $G^{(10)} = 8\pi^6 \ell_s^8 g_s^2$ [1]. We can also see that the perturbative description of the field theory is reliable when $\lambda_t \sim L^4/\ell_s^4 \ll 1$ and the classical description of gravity is reliable when AdS radius L is very large compared to the string scale ℓ_s, *i.e.,* $\lambda_t \sim L^4/\ell_s^4 \gg 1$. The gauge gravity duality is a strong-weak duality in the sense that strongly coupled field theory is dual to a classical gravity and weakly coupled field theory is dual to a strongly coupled string theory.

Further, the duality between the AdS spaces and CFT's is conjectured to extend to certain other dimensions as well. There are supergravity constructions which will generate AdS_{d+1} geometries with $d = 2, 3$ and 6 and these are proposed to be dual to d-dimensional CFT's (for example see [26] and references there in). Further, we can go beyond the empty AdS vacuum space, and we can have all kinds of processes and topologies in asymptotically AdS spaces which will be dual to various deformations of the boundary CFT. These ideas actually expand the applicability of the AdS/CFT correspondence to a much wider class of field theories and particularly allow us to construct RG flows. On the boundary, a larger scale will be related to the larger depth in the bulk gravity. We can view this, for example, for the geodesics which begin from the boundary and then bounce back. Then for wider scale, which is the distance between the beginning and ending points, these geodesics will probe deeper regions of the dual gravity. In this sense the ultraviolet regime of the gravity, which is the region near $r = 0$, is dual to the infrared degrees of freedom of the field theory. Similarly, the asymptotic region of the AdS space will correspond to the UV fixed point

[1] For a setup where the ten-dimensional bulk geometry is $\mathrm{AdS}_5 \times S^5$, five-dimensional Newton's constant $G^{(5)}$ in AdS_5 is related to 10-dimensional Newton's constant by $G^{(5)} = G^{(10)}/\mathrm{Volume}(S^5) = G^{(10)}/\pi^3 L^5$.

of the field theory. Hence, the extra radial dimension in the dual gravity is considered the energy scale of the boundary field theory and in particular, can be used as the direction of the RG flow. Now we can place a scalar potential along the radial direction of the gravity and if the mass of the scalar is tachyonic in the asymptotic region, it will give us a RG flow triggered by a relevant operator. We will discuss these issues in more detail below.

Further, all the fields in the gravity are dual to some operators in the field theory. We can place the boundary field theory at some IR cut-off $r = r_c$ of the gravity, where r is the radial direction of the AdS. Then the value of the bulk fields at this IR cut-off of the gravity will source various dual operators in the field theory. For example, we can consider a scalar field ϕ in the bulk gravity and it has a value ϕ_0 at a cut-off $r = r_c$. Then ϕ_0 will source the dual operator $\mathcal{O}$ in the boundary field theory which is at some UV scale. The magic of the AdS/CFT conjecture comes in the play in calculating the correlation functions of such operators. The idea is that, the partition function for the CFT is dual to the partition function of the string theory in the bulk. So we have

$$\langle e^{-\int \phi_0 \mathcal{O}} \rangle_{CFT} \; = \; Z_{string}(\phi, \phi_0)\,, \tag{1.25}$$

where ϕ is a solution of the equation of motion for the scalar field in gravity with the boundary condition $\phi(r_c) = \phi_0$. Now in the large N and 't Hooft coupling limit, the gravity becomes classical and we can make the saddle point approximation for the gravity action. Then we recover that the generating functional of the CFT is dual to the classical gravity action in the bulk with large N and 't Hooft coupling corrections:

$$W_{CFT} = -\log\langle e^{-\int \phi_0 \mathcal{O}} \rangle_{CFT} \; = \; S_{\text{classical gravity}} + \mathcal{O}\left(\frac{1}{N^2}\right) + \mathcal{O}\left(\frac{1}{\lambda_t}\right)\,. \tag{1.26}$$

Using this generating functional, one can calculate various correlation functions for the dual field theories. More interestingly, these ideas can be used to study various real-time phenomenon and transport properties of the strongly coupled field theories which are otherwise inaccessible by the existing theoretical tools.

At this point, we close the discussion of the AdS/CFT correspondence and discuss some other ideas like the RG flows, c-theorems and entanglement entropy. In the next section, we will also explain in some detail how these ideas are implemented in the AdS/CFT correspondence.

1.3 RG flows, c-theorems and Entanglement entropy in QFT

The renormalization group (RG) is a remarkable framework to study quantum field theories. In the Wilsonian approach to RG flow, we get the effective field theory at a particular energy scale by integrating out the high energy degrees of freedom. The effect of integrating out these degrees of freedom is taken into account by the couplings of the field theory and hence they flow with the energy scale. So in the parameter space of the coupling constants, every point will describe the field theory for a specific energy scale. Further, in the space of couplings, we can have stationary points under the renormalization group flow, *i.e.,* derivative of the couplings with respect to the energy scale (namely the beta functions) vanish. These are known as the fixed points of the theory and because of the vanishing beta functions, corresponding theories will have conformal symmetry.

Further, we can categorize different operators according to their behavior along the RG flow. Depending on their scaling behaviour along the flow, an operator can be relevant, irrelevant and marginal. If the theory flows under a RG flow, then the magnitude of the observable related to an operator can either be always increasing, decreasing or a mixed behavior. In case the magnitude of an operator increases, this observable will be needed to describe the IR theory and hence it is a relevant operator. However, if the observable decrease along the RG flow, in the IR regime, this operator will be insignificant for the macroscopic behavior of the theory. Hence it will be called an irrelevant operator. For marginal operators, the coupling constant is independent of energy scale and hence their behaviour can fall in both of the categories along the flow.

Now, the field theories we are actually interested in resemble with the QCD and they are conformal field theories at very high energy. In other words, we have a UV fixed point in the theory. If the UV theory is perturbed by a relevant operator, the RG flow will drive the theory to a new IR fixed point. For a long time, intuitively it is known that such RG flows are irreversible. Note that in the Wilsonian approach to the renormalization group, as we flow to the IR theory, the higher energy degrees of freedoms are integrated out. So clearly we expect that there should be some measure to count these degrees of freedom which will also constrain the direction of the flow. Mathematically this idea goes by the name of the c-theorem by which we mean: In the coupling space of a field theory, one can define a c-function such that it decreases monotonically along the RG flow from a UV to an IR fixed point. So far we have found consistent c-theorems in $d = 2$ and 4 dimensional field theories which we will discuss in the section 1.3.2. However in the next subsection, we discuss how RG flows are implemented in the AdS/CFT correspondence, which are

extensively used to get insight into c-theorem in various dimensions.

1.3.1 Holographic RG flows

In the AdS/CFT correspondence, a field theory is dual to a gravity theory in a background with one extra dimension. The extra spatial dimension is interpreted as the energy scale related to the RG flow of the boundary field theory. In this case, the region of the gravity theory deep in the interior of the AdS space is dual to the IR regime of the field theory. Similarly, the far asymptotic region of AdS is dual to the UV regime of the field theory. To realize the RG flow in the AdS/CFT correspondence, let us consider a CFT on the d-dimensional boundary. Let us assume that it is perturbed by a relevant operator $\mathcal{O}$ and the RG flow drives it to an IR fixed point. To realize this situation in the AdS/CFT correspondence, we consider the simplest example where operator $\mathcal{O}$ is dual to the scalar field ϕ in the dual gravity. We can further simplify the system and assume that this scalar is minimally coupled to the gravity and has a scalar potential. Such a system will permit consistent solutions for the scalar field in the gravity which will only depend on the radial direction of the bulk geometry. Now these radial solutions will actually represent the RG flows of the CFT triggered by the operator $\mathcal{O}$. The bulk geometry at a fixed radial coordinate will be dual to the boundary field theory at a particular point along the RG flow and the fixed points of the flow will be at the stationary points of the scalar potential.

To study RG flow solutions in more detail, let us consider the following action for the bulk gravity:

$$I = \frac{1}{2\ell_{\rm P}^{d-1}} \int d^{d+1}x\sqrt{-g}\left[R - \frac{1}{2}\left(\partial\phi\right)^2 - V(\phi)\right], \tag{1.27}$$

where R is the Ricci scalar for the $(d+1)$-dimensional gravity and $V(\phi)$ is the scalar potential. In the action (1.27), the cosmological constant term has been absorbed into the scalar potential and we assume that $V(\phi)$ has various critical points where the potential energy is negative, *i.e.,*

$$V(\phi_i) \;=\; -\frac{d(d-1)}{L^2}\alpha_i^2 \qquad \text{where} \qquad \left.\frac{\partial V}{\partial \phi}\right|_{\phi=\phi_i} \;=\; 0\,. \tag{1.28}$$

Here L is some convenient scale while the dimensionless parameters α_i distinguish the different fixed points of the boundary theory. Now, with an appropriate choice of the bulk potential, $\mathcal{O}$ will be a relevant operator at that UV fixed point and an RG flow can be triggered by perturbing the UV CFT with this operator. So in holography, the non-trivial radial profile of the scalar, which will connect two of the critical points, will describe this

RG flow. Note that at fixed points (1.28), the gravity vacuum is simply AdS_{d+1} with curvature scale given by $\tilde{L}^2 = L^2/\alpha_i^2$.

Further, to consider solutions describing holographic RG flows, we begin by writing the scalar and gravitational equations of motion as

$$\nabla^2\phi - \frac{\delta V}{\delta\phi} = 0\,, \tag{1.29}$$

$$R_{ab} - \frac{1}{2}R g_{ab} = T_{ab}\,. \tag{1.30}$$

Also, the stress tensor for the scalar field is given by

$$T_{ab} = \frac{1}{2}\partial_a\phi\,\partial_b\phi - \frac{1}{2}\,g_{ab}\left(\frac{1}{2}\,(\partial\phi)^2 + V(\phi)\right)\,. \tag{1.31}$$

Now we make the ansatz that the bulk geometry describing the RG flows will be of the following form:

$$ds^2 = e^{2A(r)}\,\eta_{ij}\,dx^i dx^j + dr^2\,, \tag{1.32}$$

where radial evolution of the geometry is entirely captured by the conformal factor $A(r)$. At a fixed points where the geometry is AdS_{d+1}, the conformal factor is simply $A(r) = r\alpha_i/L$ where L/α_i is the AdS curvature scale. Implicitly, we will assume that asymptotic UV boundary is at $r \to \infty$ while the IR part of the solution corresponds to $r \to -\infty$. Hence for an RG flow between two fixed points as described above, the metric (1.32) approaches that of AdS_{d+1} in both of these limits. For nontrivial RG flows, we also include a simple ansatz for the scalar: $\phi = \phi(r)$. In particular then, this ansatz maintains Lorentz invariance in the boundary directions. Now with above metric and scalar ansatz, there are two nontrivial components of the gravitational equations (1.30):

$$d(d-1)A'^2 = 2\,T_r{}^r\,, \tag{1.33}$$

$$2\,(d-1)A'' + d(d-1)A'^2 = 2\,T_t{}^t\,. \tag{1.34}$$

Here prime denotes a derivative with respect to r. Using eq. (1.31), we find the following components of stress-energy tensor

$$T_r{}^r = \frac{1}{4}(\phi')^2 - \frac{1}{2}V(\phi)\,, \tag{1.35}$$

$$T_i{}^j = -\,\delta_i{}^j\left(\frac{1}{4}(\phi')^2 + \frac{1}{2}V(\phi)\right)\,. \tag{1.36}$$

With the present ansatz, the equation of motion for the bulk scalar (1.29) becomes

$$\phi'' + d\, A'\, \phi' - \frac{\delta V}{\delta \phi} \;=\; 0\,. \tag{1.37}$$

Here, the three equations of motion above are not all independent. For example, one can derive eq. (1.34) by differentiating eq. (1.33) and then substituting in eqs. (1.33) and (1.37). Taking the difference of eqs. (1.33) and (1.34), we find that the null energy condition becomes

$$T_t^{\,t} - T_r^{\,r} \;=\; (d-1)A'' \;\leq\; 0\,. \tag{1.38}$$

Now for equations (1.33–1.37), a simple set of explicit solutions can be constructed by using the approach developed for brane-world phenomenology in [28, 29]. The key idea is to consider a special class of scalar potentials that can be defined in terms of a 'superpotential' and then express the solution in terms of this superpotential. First, we write the scalar potential in terms of a superpotential $W(\phi)$ as follows:

$$V(\phi) = 2\,(d-1)^2 \left(\frac{\delta W}{\delta \phi}\right)^2 - d(d-1)W^2\,. \tag{1.39}$$

With a potential of this form, the equations of motion above can be re-expressed as first order equations:

$$\begin{aligned} \phi' \;&=\; -2\,(d-1)\frac{\delta W}{\delta \phi}\,, \\ A' \;&=\; W\,. \end{aligned} \tag{1.40}$$

Given these first order equations, we may now solve for the metric (1.32) and the scalar profile in quadratures.

As we pointed out earlier, it will depend on the scalar potential if the operator $\mathcal{O}$ is either relevant or irrelevant in the UV. The dimension of an operator in the CFT is related to the mass of the scalar field around the critical point describing the asymptotic AdS geometry and hence by changing $V(\phi)$, we can make the operator relevant. For a minimally coupled massive scalar field, *i.e.,* $V(\phi) = -m^2\phi^2/2$, if we assume that the solution near the boundary $r \to \infty$ is given by

$$\phi \simeq e^{-\Delta\, r/L_{UV}}\,, \tag{1.41}$$

then we find following two values of Δ from equations of motion [30]

$$\Delta_\pm \;=\; \frac{d}{2} \pm \sqrt{\left(\frac{d}{2}\right)^2 + m^2 L_{UV}^2}\,. \tag{1.42}$$

Here L_{UV} is the AdS radius of the bulk metric in the asymptotic limit, *i.e.,* $A(r) = r/L_{UV}$ asymptotically. Now we will expect that the solution near the boundary is of the form $\phi \simeq \phi^{(+)}e^{-\Delta_+ r/L_{UV}} + \phi^{(-)}e^{-\Delta_- r/L_{UV}}$. Now if $m^2 > 0$, we have $\Delta_- < 0$ and this mode grows asymptotically. In the AdS/CFT correspondence, the coefficient of the 'slowly decaying' part of the solution, *i.e.,* the coefficient of $e^{-\Delta_- r/L_{UV}}$ for $m^2 > 0$, will behave as a source on the boundary. In (1.26), this mode is used to calculate the two point function of operator $\mathcal{O}$. Also for $m^2 > 0$, the dimension of the operator will be Δ_+ and the other piece, *i.e.,* the coefficient $\phi^{(+)}$ will be related to the expectation value $\langle\mathcal{O}\rangle$.

Now a relevant operator in the boundary theory will be of dimension $\Delta < d$. For $m^2 > 0$, the dimension of the operator $\Delta_+ > d$. So to have a relevant operator on the boundary theory, we need to allow the scalar mass to be tachyonic. In AdS space, the negative mass squared is allowed but it is bounded below by the Breitenlohner-Freedman (BF) bound $m^2 \geq -d^2/4L_{UV}^2$, as discussed in section 1.2.1. With this lower bound on the scalar mass, we find that the allowed dimensions of the operator is $\Delta_+ > d/2$. However, the unitarity condition in CFT bounds the dimension of the operator from below by $\Delta > (d-2)/2$. On the gravity side, this bound is achieved by allowing the alternative quantization in the following range [31]

$$-\frac{d^2}{4} \leq m^2 \leq -\frac{d^2}{4} + 1\,. \tag{1.43}$$

In this range, both of the solutions with scaling dimension of the operator $\Delta = \Delta_\pm$ are valid and there are two different quantization of the scalar field in AdS, related to two admissible boundary conditions [23, 24, 25]. For range (1.43), the bulk gravity is dual to two different CFT's. In one of them the corresponding operator has the dimension Δ_+ and in another Δ_-. Now in range (1.43), we have $(d-2)/2 \leq \Delta_- \leq d/2$ and in this way, we achieve the allowed bound on the dimension of the operator in the CFT.

By tuning the scalar potential, we can change the mass of the scalar field in the UV. As the scalar mass is related to the dimension of the dual operator, we make it relevant or irrelevant by controlling the scalar potential. In the UV, the mass of the scalar is given by

$$m^2 = -\frac{\partial^2 V}{\partial\phi^2}\Big|_{r\to\infty}\,, \tag{1.44}$$

and for $m^2 > 0$, the dimension of the dual operator is $\Delta_+ > d$. In this case, the operator is irrelevant. However for tachyonic mass squared, $m^2 < 0$ and we find that both $\Delta_\pm < d$. Hence, for this range the operator $\mathcal{O}$ is a relevant operator. Clearly, we can tune the mass of scalar potential to construct the desired RG flows.

1.3.2 C-theorems

In this section, we briefly review the ideas of the c-theorems in field theories. As discussed earlier, let us assume that we have a theory with a UV fixed point and if perturbed with a relevant operator, the theory flows to a new IR fixed point. In the Wilsonian approach to the RG flow, this will correspond to integrating out the high-energy degrees of freedom and we expect that this loss of degrees of freedom will make the RG flow irreversible. This complete scheme is manifested in the idea of a c-theorem, which says that there is a certain c-function made out of the couplings of the theory, which will decrease monotonically along the RG flow from the UV to the IR fixed point.

In constructing such a c-function in even dimensions, the conformal anomalies have played a vital role. It has been long know that when an even dimensional conformal field theory is placed in a curved background, the trace of the stress-energy tensor does not vanish and we get trace anomalies [32, 33, 34]. For a CFT in even d-dimensional spacetime, the trace anomaly is given by

$$\langle T^{\mu}_{\mu} \rangle = \sum_{n} B_n I_n - 2(-)^{d/2} A E_d \,, \tag{1.45}$$

which defines the central charges A and B_n. Here I_n and E_d are Weyl invariant curvature terms, which are constructed from the background geometry. In particular, E_d is the Eular density in d dimensions and I_n can be written in terms of Weyl tensors. Note that in (1.45), we have ignored a scheme dependant conformal invariant total derivative. For $d = 2, 4$ and 6, we find that trace anomalies will define one, two and four central charges.

In [35], Zamolodchikov proved that there exists a positive definite function c_2, which decreases monotonically along the RG flows. At the fixed points of the RG flow, this function is stationary and coincides with the central charge c of the Virasoro algebra of the associated CFT. A direct consequence for any RG flow connecting two such fixed points is then that

$$[\, c \,]_{\rm UV} \geq [\, c \,]_{\rm IR} \,. \tag{1.46}$$

In deriving this result, Zamolodchikov only used simple properties like renormalizability, unitarity and existence of translational and rotational symmetries in the theory. As a generalization to higher dimensions, Cardy proposed that the central charge associated with A-type trace anomaly, *i.e.,* the coefficient A in eq. (1.45), should decrease monotonically along RG flows for QFT's in any even number of dimensions [36]. This proposal coincides with the c-theorem in $d = 2$ as the central charge c is related to the our expression for trace anomaly (1.45) by $c = 12A$. Cardy's conjecture was extensively studied in $d = 4$

and a great deal of support was found with nontrivial examples. In [37], Osborn derived Cardy's conjecture for a perturbative fixed points. There, dimensional regularization was used on the non-linear sigma model to define the renormalized composite operators and this approach generalized the Zamolodchikov's proof to $d = 4$ perturbative fixed points. Further, Cardy's conjecture was also found to be true in some non-perturbative cases, in particular in supersymmetric gauge theories [38, 39, 40, 41]. In [38, 39], an exact expression for the flow of central charge A between two conformal fixed points was derived in $\mathcal{N} = 1$ supersymmetric theories in the conformal window. These calculation explicitly showed that central charge a does satisfy the c-theorem and we have $a_{\rm UV} \geq a_{\rm IR}$. Also, counter examples were found where the other central charge c is such that $c_{\rm UV} \leq c_{\rm IR}$, showing that there is no c-theorem for the central charge c.

Recently, a remarkable new proof of this c-theorem was presented for any four-dimensional RG flow connecting two conformal fixed points [42, 43]. This result draws on earlier work involving the spontaneous breaking of conformal symmetry [44] and bounds on couplings in effective actions [45]. It remains to determine, however, how much more of the structure of two-dimensional RG flows carries over to higher dimensions.

Further, it remains to be understood if the c-theorems also extend to odd dimensions and higher even dimensions. Recently, there have been strong indications that entanglement entropy might be a useful tool in identifying the relevant central charges of the CFT which will satisfy consistent c-theorems. We will discuss these ideas in greater detail in chapter 2 but in next section, we review some basics of entanglement entropy and how holography can be used to calculate it.

1.3.3 Entanglement entropy

Entanglement is a quantum mechanical phenomenon in which the quantum states of two or more objects have to be described with reference to each other, even though the individual objects may be spatially separated. Thus it is possible to prepare a bipartite system in a pure state such that the observations performed on one part of the system are correlated to the observations on the other part, in spite of the fact that both subsystems are causaly disconnected. One of the measures of the quantum entanglement is the entanglement entropy, which is given by the von Neumann entropy of a density matrix describing a subsystem. To define entanglement entropy, let us consider a spin lattice at zero temperature. This system will be described by the pure ground state $|\Psi\rangle$, if the ground state is not degenerate. For this case, the density matrix is given by $\rho = |\Psi\rangle\langle\Psi|$. Now, we bipartition the system into two subsystems A and its complement B. To calculate entanglement entropy of the

subsystem A, we find the reduced density matrix ρ_A by tracing out the degrees of freedom in subsystem B:

$$\rho_A \;=\; \mathrm{tr}_B(\rho)\,. \tag{1.47}$$

Now, the entanglement entropy (EE) for subsystem A is defined as

$$S_A \;=\; -\mathrm{tr}_A(\rho_A \log \rho_A)\,. \tag{1.48}$$

Here, we note that if the density matrix is a function of time, entanglement entropy is defined at a fixed time. Also, if we calculate EE for a complete system in a pure state, *i.e.,* $\rho = \rho_A$, we find that $S_A = 0$. Note that generalization of EE to quantum mechanical systems at finite temperature only requires the use of the thermal density matrix $\rho \sim e^{-H/T}$, where T is the temperature and H is the total Hamiltonian.

In a quantum field theory (QFT) on d-dimensional spacetime, we can define a subsystem by partitioning the space into V and its compliment $\bar{V}$ on a constant time slice. As shown in the figure 1.6, both of these regions are separated by the entangling surface ∂V. Now similar to (1.47), we can find the density matrix for the region V, namely ρ_V, by integrating out the degrees of freedom in region $\bar{V}$. In terms of ρ_V then, the von Neumann entropy becomes

$$S_V \;=\; -\mathrm{tr}_V(\rho_V \log \rho_V)\,. \tag{1.49}$$

It is important to note that von Neumann entropy is divergent in continuum theories. Hence, we regulate the entanglement entropy (EE) by using a length scale δ, which acts as a UV regulator. Then, typically the leading order term in EE is proportional to the area of the entangling surface ∂V:

$$S_V \;=\; \gamma\,\frac{\mathrm{Area}\,[\partial V]}{\delta^{d-1}} + \text{subleading terms}\,. \tag{1.50}$$

Here γ is a dimensionless constant and it depends on the field theory under consideration. As the entanglement entropy depends on the geometry of the entangling surface, it is also called the geometric entropy. Further, EE satisfies the strong subadditivity condition which says that, if we have two subsystems V_1 and V_2

$$S_{V_1} + S_{V_2} \geq S_{V_1 \cap V_2} + S_{V_1 \cup V_2}\,. \tag{1.51}$$

Note that because of this condition, the entanglement entropy of a composite system can be less than the summation of EE of its parts.

In general, the calculation of EE in quantum field theories is a tedious task. However, these calculations are significantly simplified by using the so called replica trick [11]. In this

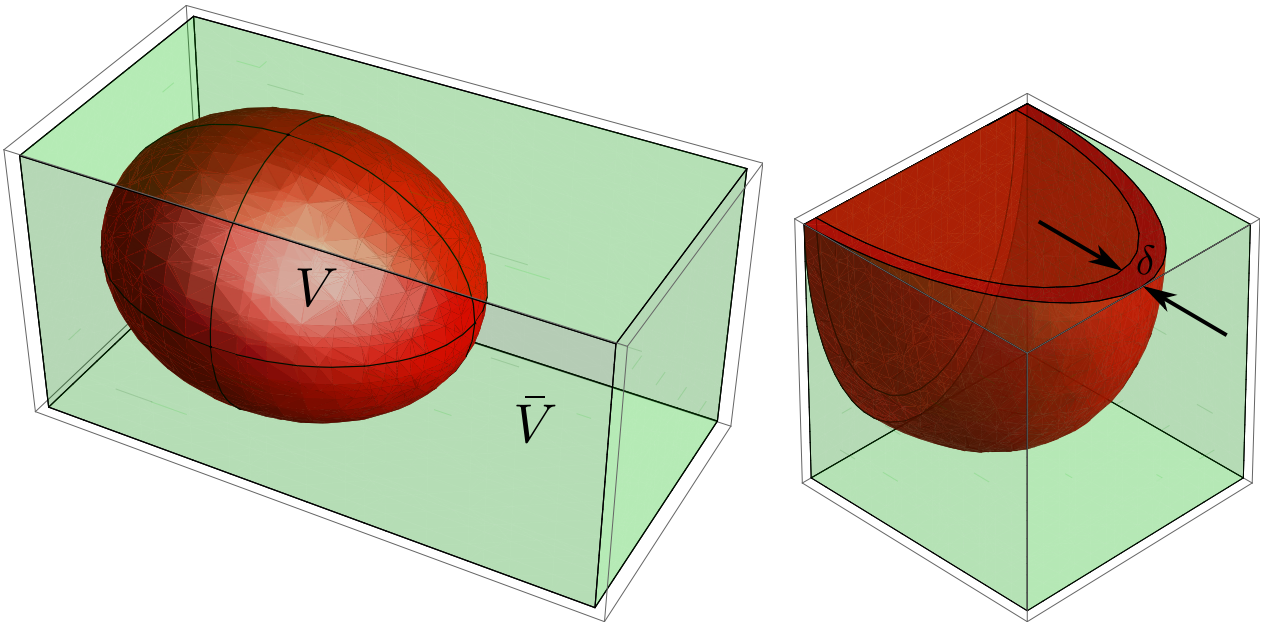

(a) (b)

Figure 1.6: (Color Online) Panel (a) shows how the field theory background is bipartitioned into regions V and $\bar{V}$. Panel (b) shows how can we introduce a UV cut-off to regulate the entanglement entropy.

approach, one considers n copies of the background geometries. Then, the entangling region V is removed from these copies by cutting the background geometry on the entangling surface ∂V. Further, the edges of these n copies along the cut on the entangling surface ∂V are sewed cyclically to make a single n-fold cover of the background, which excludes the entangling region V. Now the trace of the n^{th}-power of density matrix $\text{tr}_V(\rho_V^n)$ for the region V can be found by using the path integral over this n-fold geometry. For that, one needs to glue the fields analytically when they pass from one sheet to another and this geometry contains a conical singularity with angular excess $2\pi(n-1)$ at the entangling surface ∂V. Now $\text{tr}_V(\rho_V^n)$ can be used in

$$S_V \;=\; -\frac{\partial}{\partial n}\text{tr}_V(\rho_V^n)\big|_{n=1} \;=\; -\frac{\partial}{\partial n}\log \text{tr}_V(\rho_V^n)\big|_{n=1}\,, \tag{1.52}$$

to calculate the EE. Note that we have normalised ρ_V such that $\text{tr}_V(\rho_V) = 1$, for which the above expression is true.

For entanglement entropy of region surrounded by smooth entangling surface, it can be

seen that in general the structure of divergence is following

$$S = \frac{p_{d-2}}{\delta^{d-2}} + \frac{p_{d-4}}{\delta^{d-4}} + \ldots + \begin{cases} \frac{p_1}{\delta} + p_0 + \mathcal{O}(\delta) & \text{for odd } d\,, \\ \frac{p_2}{\delta^2} + p_0 \log\left(\frac{\ell}{\delta}\right) + \mathcal{O}(1) & \text{for even } d\,. \end{cases} \tag{1.53}$$

In this expression, the terms which depend on the UV cut-off are proposed to have a geometric structure and they are expected to depend on various contractions of the curvatures of the entangling surface [46, 47]. For example, p_{d-2} is typically proportional to the area of entangling surface ∂V. As the cut-off dependant contribution comes from small wavelength degrees of freedoms, it is expected that such terms will only depend on the geometry of the entangling surface. Now we can consider a specific class of entangling surfaces, which can be scaled by a single macroscopic length scale ℓ. Then in (1.53), we should have $p_i \sim \ell^i$ to match the dimensions for all the UV divergent terms. Note that in general, quantum field theories can have various dimensionful coupling constants and we can construct dimensionless quantities by combining them with length scale ℓ. Now there is a bold proposal [46] that for such scalable surfaces, if we write $p_i = c_i \ell^i$, c_i's are independent of ℓ in (1.53). So the dimensionless coefficients c_i's do not depend on the dimensionless terms build out of dimensionful couplings of the field theory and ℓ. In this sense, along the RG flow, the terms $c_i = p_i/\ell^i$ for such specific surfaces will depend only on the UV theory. We can further note that in (1.53), p_0 is the cut-off independent universal term. What it means is that if we change the cut-off $\delta \to x\delta'$, the term p_0 will not get any contribution from x. Being independent of UV cut-off, this term is of significant physical importance. As we will later see that our discussions will be focused on studying the properties of this term.

Further, in even dimensional conformal field theories, the logarithmic contribution can be considered to arise from the gravitational trace anomalies. It is seen from both the heat kernel method and the holographic studies that contribution of entangling surface to gravitational trace anomalies will fix the coefficient of the logarithmic divergence. If we focus on specific class of entangling surfaces, for which the subspace orthogonal to the entangling surface has an axial symmetry, this contribution can be calculated exactly [48]. For such specific entangling surfaces with single length scale ℓ, the extrinsic curvature is zero. Then as proposed in [49, 50], we can take derivative of the trace anomaly (1.45) for region V with respect to the Riemann tensor $R_{\mu\nu\rho\sigma}$ to find the logarithmic term in EE:

$$S_{\log} = \log(\ell/\delta) \int_{\partial V} d^{d-2}x\sqrt{h}\left[2\pi\epsilon^{ij}\epsilon_{kl}\sum_n B_n \frac{\partial I_n}{\partial R^{ij}{}_{kl}} - 2(-)^{d/2} A\, E_{d-2}\right]. \tag{1.54}$$

Here integration is over the $d-2$ dimensional entangling surface ∂V and ϵ_{ij} are the two dimensional volume form in the space transverse to ∂V. Now the above expression is not

complete for the most general entangling surfaces. What is missing in this expression are the extrinsic curvature dependent terms and some other intrinsic curvature terms for $d > 4$, both of which are set to zero by the axial symmetry of the entangling surface. In $d = 4$ dimensional CFT's these terms have been found using the conformal symmetry and the holographic entanglement entropy and they are given by [51]

$$S_{\log} = \log(\ell/\delta)\frac{1}{4\pi}\int_{\partial V} d^2x\sqrt{h}\left[c\left(C^{ijkl}\epsilon_{ij}\epsilon_{kl} - K_a^{\hat{\imath}\,b}K_b^{\hat{\imath}\,a} + \frac{1}{2}K_a^{\hat{\imath}\,a}K_b^{\hat{\imath}\,b}\right) - 2\,a\,\mathcal{R}\right] . \quad (1.55)$$

Here C^{ijkl} is the Weyl tensor and h is the induced metric on the surface ∂V. Further a and c are the central charges of the CFT and $\mathcal{R}$ is the Ricci scalar for the intrinsic geometry on ∂V. $K_b^{\hat{\imath}\,a}$ is the extrinsic curvature of the embedding related to the orthogonal vector $n^{\hat{\imath}a}$. As there are two orthogonal vectors for this surface, $\hat{\imath} = 1, 2$.

We have pointed out that calculation of EE is a tedious task in general. However, there is a very elegant proposal in the context of the AdS/CFT correspondence which allow us to calculate EE for strongly coupled field theories. In the next section, we review this proposal by Ryu and Takayanagi [16] in some detail.

1.3.4 Holographic entanglement entropy

In [16, 52], Ryu and Takayanagi conjectured a simple method of calculating EE in the boundary field theory using the AdS/CFT correspondence. They proposed that EE for a region V in the boundary CFT is given by the area of the minimal area surface v, which extends in the bulk gravity and coincides with the entangling surface ∂V at the AdS boundary

$$S(V) = \frac{2\pi}{\ell_{\rm P}^{d-1}}\min_{v\sim V}[\,A(v)\,] . \quad (1.56)$$

Here $A(v)$ is the area of the surface v and $v \sim V$ means that surface v is homologous to V as shown in figure 1.7. The symbol 'min' indicates that one should extremize the area functional over all such surfaces v and evaluate it for the surface yielding the minimum area. Note that this procedure minimizes the area of the surface when we are working with Euclidean signature of the metric. In Minkowski signature of the metric, one can find other 'saddle points' and although this area is extrema, it need not to be minimum. Also, above equation is for EE at a fixed time and assumes that the bulk physics is described by (classical) Einstein gravity and we have adopted the convention $\ell_{\rm P}^{d-1} = 8\pi G_N$. Hence the functional which is extremized on the right-hand side of eq. (1.56) matches the standard

expression for the horizon entropy of a black hole. So for region V in d dimensional CFT, eq. (1.56) reduce to

$$S(V) = \frac{2\pi}{\ell_{\rm P}^{d-1}} \int_v d^{d-1}x \sqrt{h}\,, \tag{1.57}$$

where integration is over the surface v and h_{ab} is the induced metric on this surface. Note that we have cut the surface v somewhere close to the boundary and this will appear as the UV cut-off in the dual theory. So the UV cut-off will appear in the limits of the integrations in (1.57).

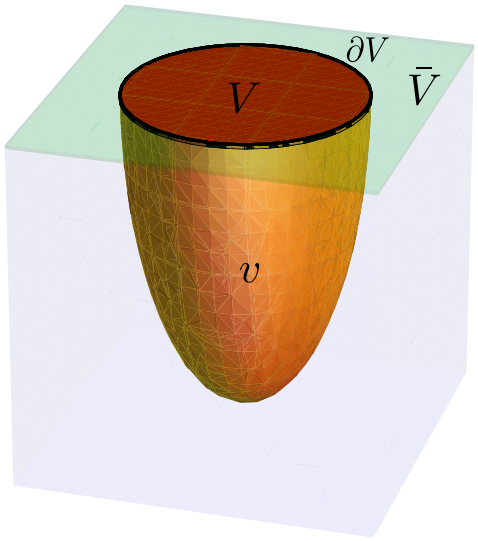

Figure 1.7: The boundary field theory is bipartitioned into regions V and $\bar{V}$. The EE for region V is given by the area of homologous minimal area surface v which extends in the bulk gravity.

This remarkably simple proposal has passed extensive consistency tests. The EE (1.56) was shown to satisfy the strong subadditivity condition (1.51) with a very elegant proof given by Headrick and Takayanagi [53] (also see [54] for initial study). Further, the leading order term in EE (1.56) follows the well known area law with

$$S(V) \simeq \frac{L^{d-1}}{G_N} \frac{A(\partial V)}{\delta^{d-2}} + \dots\,, \tag{1.58}$$

where $A(\partial V)$ is the area of the $d-2$ dimensional entangling surface ∂V measured in the background metric of the CFT. Also, here δ is a UV regulator that we get by stopping the

surface v in the asymptotic limit along the radial direction of AdS. The holographic EE (1.56) also recovers the known results for $d = 2$ CFT's on a circle. In [55] (and references therein), the EE for a two-dimensional critical system has been studied and it is found that for CFT on a system of finite size L_0

$$S(\ell) = \frac{c}{3} \log \left(\frac{L_0}{\pi \delta} \sin \left(\frac{\pi \ell}{L_0} \right) \right) , \tag{1.59}$$

where c is the central charge and ℓ is the subsystem for which the EE is being calculated. If this CFT is perturbed by a relevant operator then RG flow will drive it to a gapped fixed point in the IR. At this fixed point, in the large ℓ limit, the EE is given by

$$S_\ell = \frac{c}{6} \log \left(\frac{\xi}{\delta} \right) , \tag{1.60}$$

where ξ is the correlation length in the IR theory [56]. Remarkably, all of these results can be derived by the holographic EE (1.56) in proper gravitational dual [16]. Further, as we saw in (1.54), the logarithmic contribution for entanglement entropy in even dimensional CFT's contain various central charges of the theory. The calculation of EE (1.56) for various geometries on the boundary theory has shown precise consistency with eq. (1.54) and (1.55). Finally, there has been attempts for explicitly proving the holographic entanglement entropy. In [57], an explicit proof of (1.56) was attempted using the replica trick. As pointed out around (1.52), in this method the n-fold geometry will have a conical singularity. Now without the knowledge of the full string theory in the bulk gravity, it is hard to work with it in a controlled way [58]. So in [59], a different approach is being used to prove the holographic formula for EE for spherical geometry. There the boundary CFT was mapped to a hyperbolic geometry using a conformal mapping, which also maps the vacuum state of former to a thermal state in later geometry. In this hyperbolic geometry, the thermal entropy (that is now the black hole entropy in AdS/CFT) is evaluated using the AdS/CFT and found to match with holographic formula (1.56).

All the above consistency checks put the Ryu-Takayanagi prescription for holographic EE on the strong footing and it can be confidently used to study strongly coupled field theories. However, the above formula (1.56) is for CFT's dual to Einstein gravity. For these theories, all the central charges are same since there are no extra parameters in the gravity theory. So one needs to expand the parameter space of the couplings by introducing higher derivative corrections in the action and in that case, the central charges will begin to be distinguished. The simplest set of higher derivative terms arise in the Lovelock gravity where various Euler densities appear as higher derivative interactions in the gravity theory [60, 61]. In [48, 62], authors have generalized the definition of holographic EE (1.56) to the

Lovelock gravities. Here we focus on adding only the four derivative Gauss-Bonnet term in the gravity action and in $d+1$ dimensions, it is given by

$$I = \frac{1}{2\ell_{\rm P}^{d-1}} \int d^{d+1}x\sqrt{-g}\left[\frac{d(d-1)}{L^2} + R + \frac{\lambda L^2}{(d-2)(d-3)}\mathcal{X}_4\right], \tag{1.61}$$

where

$$\mathcal{X}_4 = R_{abcd}R^{abcd} - 4R_{ab}R^{ab} + R^2\,. \tag{1.62}$$

For this action, one can try to guess the expression for EE and it turns out that it is not just the Wald entropy [63, 64, 65]. The consistency checks in this case, on which Wald entropy fails, are that it does not produce the precise dependence of universal term on the central charges expected for a CFT. Note that for EE in four dimensional CFT's, we already know the universal term (1.55). However, the correct formula for EE comes from the black hole entropy in Lovelock gravity, which was proposed in [66]. Now the entanglement entropy functional, which will be minimized, is given by

$$\begin{aligned} S &= \frac{2\pi}{\ell_{\rm P}^{d-1}} \int_v d^{d-1}x\,\sqrt{h}\left[1 + \frac{2\,\lambda L^2}{(d-2)(d-3)}\mathcal{R}\right] \\ &\quad + \frac{4\pi}{\ell_{\rm P}^{d-1}} \int_{\partial v} d^{d-2}x \frac{2\,\lambda L^2}{(d-2)(d-3)}\sqrt{\tilde{h}}\,\mathcal{K}\,. \end{aligned} \tag{1.63}$$

As shown in figure 1.7, this will give the entanglement entropy for region V and the integrations are over the surface v and at its boundary ∂v. Note that to impose the UV cut-off, we need to stop the surface v somewhere near the asymptotic boundary and this process introduces the boundary ∂v. Further, h is the induced metric over the surface v and $\mathcal{R}$ is the Ricci scalar for the induced metric and $\mathcal{K}$ is the extrinsic curvature at the boundary ∂v. Finally, $\tilde{h}$ is the induced metric at the boundary ∂v. In eq. (1.63), the second term, which is a boundary term, is the Gibbons-Hawking term in the functional to make the variational principle consistent. By considering various entangling geometries, it has been verified that holographic EE (1.63) produce the correct dependence on the central charges of the theory [48], consistent with eq. (1.54). We will see in later sections that EE for Gauss-Bonnet gravity is an extremely useful tool in our investigations.

1.4 Outline

The entanglement entropy, that we discussed in previous section, has emerged as an interesting theoretical quantity for studies of quantum matter. For example, it allows one

to distinguish new topological phases or different critical points [67, 68, 55, 69]. In the context of the AdS/CFT correspondence, it is also used in characterizing new properties of holographic field theories [70, 71, 72, 73], where it has been suggested that entanglement entropy may play a fundamental role in the quantum structure of spacetime, *e.g.,* [74, 75, 76, 77]. So given the huge importance of entanglement entropy, in this thesis, we will take small steps towards answering following two major questions related to entanglement entropy:

- Entanglement entropy is a non-local quantity that depends on various correlations in QFT's. Does this quantity contain information about the degrees of freedom of field theory along the RG flows in Wilsonian sense?
- The physically relevant information about a QFT is hidden in the universal terms of the entanglement entropy. So what are these universal terms for most general entangling surfaces and in particular for singular entangling surfaces?

As discussed in section 1.3.2, c-theorems are extremely important mathematical ideas which constraint the direction of the RG flows. However, our knowledge of the existence of consistent c-theorems is restricted only to selected even dimensional field theories. Note that although there is a proposal that the central charge A defined by the gravitational trace anomalies (1.45) satisfies a consistent c-theorem, it has been proven only in $d = 2$ and 4-dimensional field theories. The natural hurdle in extension of the c-theorems to odd dimensions is that there are no gravitational trace anomalies and hence there is no standard method to identify the central charge which might satisfy a c-theorem.

Guided by previous work on holographic c-theorems, which we review in section 2.1, in chapter 2 we use the entanglement entropy to construct a sensible candidate c-function in arbitrary dimensions and study it under holographic RG flows. Our proposed c-function is constructed from the EE for a strip or a slab geometry in arbitrary dimensions. It is UV regulator independent and found to flow monotonically along the RG flows in field theories dual to Einstein gravity, if the matter field satisfies the null energy condition in the bulk gravity. By studying the explicit examples, we also discover a very interesting behaviour of the EE. We find that for a strip in arbitrary dimensions, EE goes through a 'first order phase transition' in specific RG flows when the width of the strip, which is also the IR scale in the system, is varied. In some sense, these phase transitions signify a discontinuous change in the correlations of the field theory when energy scale is varied in certain smooth RG flows. Now, we know that for Einstein gravity, the central charges of the dual CFT are same. Hence, a better check of our c-theorem will be to study it in the settings where

central charges of the CFT can be distinguished. So this c-function is further studied in the Gauss-Bonnet gravity and we find that now, the null energy condition is not a sufficient condition for the monotonic flow of the c-function.

Over the years, EE for quantum field theories has been studied extensively for the regions bounded by smooth entangling surfaces. This has helped us identify certain universal terms in EE and understand their geometric structure. For some cases, it is also known how these universal terms encode the field theory data, *e.g.,* the central charges of even dimensional CFT's. However, very little is known about the EE for surfaces with conical or other kind of singularities. Chapter 3 will be aimed at understanding the EE for regions bounded by a singular entangling surface. The EE for a kink in $d = 3$ dimensional field theory is known to contain a logarithmic divergence [78, 79]. We extend this result to conical singularities in arbitrary dimensions. For a cone in even dimensional field theories, the universal term is now quadratic in logarithmic divergence. However, for a cone in odd dimensional field theories, the universal term is linear in logarithm. We further study the EE for singular surfaces for CFT's dual to Gauss-Bonnet gravity. The idea is to understand the structure of the universal contribution in terms of the central charges of the CFT. For four-dimensional field theories, we find that the conical singularity contributes in the universal term through the central charge c, which is defined by the gravitational trace anomalies. We also study the EE for surfaces, which contain a singularity that is extended on a certain set of points, namely on the locus of the singularity. Through various examples, we conclude that such extended singularities contribute in universal term of EE with new linear or quadratic logarithmic terms only when the locus of the singularity is even dimensional and curved.

Finally in chapter 4, we summarise our results and discuss future directions. Chapter 2 has a (marginally) successful attempt to construct a c-theorem using the holographic entanglement entropy and chapter 3 is a study of the EE for various singular surfaces. Both of these projects are just the tip of the icebergs and various interesting questions still remains to be answered.

Published material

The research presented in this thesis has either been published or submitted or going to be submitted to scientific journals. These papers have been a collaborative effort of author with his supervisor and the author has contributed in all aspects of the research and publication.

Chapter 2 has appeared as the following research article:

- R. C. Myers and A. Singh, "Comments on Holographic Entanglement Entropy and RG Flows," JHEP **1204**, 122 (2012) [arXiv:1202.2068 [hep-th]].

Chapter 3 appears as:

- R. C. Myers and A. Singh, "Entanglement Entropy for Singular Surfaces," arXiv:1206.5225 [hep-th].

On a side note, there are three other research projects by the author during his Ph.D., which do not appear in this thesis. Two of the projects, which are published articles, are:

- A. Singh and A. Sinha, "Quantum corrections to screening at strong coupling," Nucl. Phys. B **864**, 167 (2012) [arXiv:1204.1817 [hep-th]].
- R. C. Myers, S. Sachdev and A. Singh, "Holographic Quantum Critical Transport without Self-Duality," Phys. Rev. D **83**, 066017 (2011) [arXiv:1010.0443 [hep-th]].

and one remains as an unpublished note:

- J. Escobedo and A. Singh, "Phase Transition in Melvinized Solutions".

Chapter 2

Holographic entanglement entropy and RG flows

As discussed in section 1.3.2, Zamolodchikov [35] showed that renormalization group (RG) flows of two-dimensional quantum field theories were governed by a remarkable underlying structure. There exists a positive definite function c_2, which decreases monotonically along the RG flows connecting two fixed points and

$$\big[\, c \,\big]_{\text{UV}} \geq \big[\, c \,\big]_{\text{IR}} \,. \tag{2.1}$$

More recently, Casini and Huerta [80, 81] developed an elegant reformulation of Zamolodchikov's c-theorem in terms of entanglement entropy in two dimensions. In their construction, the c-function was defined as

$$c_2 \;=\; 3\,\ell\,\frac{dS(\ell)}{d\ell}\,, \tag{2.2}$$

where $S(\ell)$ denotes the entanglement entropy for an interval of length ℓ. Then it follows that $dc_2/d\ell \leq 0$ from the strong subadditivity property of entanglement entropy, as well as the Lorentz symmetry and unitarity of the underlying QFT. Therefore, as the QFT is probed at longer distance scales, *i.e.,* one increases ℓ, this c-function (2.2) decreases monotonically. Further, for a two-dimensional CFT, the entanglement entropy is given by [55, 82, 83]

$$S_{\text{CFT}} = \frac{c}{3}\,\log(\,\ell/\delta) + c'\,, \tag{2.3}$$

where c is the central charge, δ is a short-distance regulator and c' is a non-universal constant (independent of ℓ). Hence $c_2 = c$ at RG fixed points.

Further, Cardy [36] generalized the two-dimensional c-theorem with a conjecture that the central charge associated with A-type trace anomaly – see eq. (1.45) – should decrease monotonically along RG flows for QFT's in any even number of dimensions. As we will review below, support for Cardy's generalized c-theorem was also established using the AdS/CFT correspondence [84, 85, 86, 87, 88]. One of the advantages of the investigating RG flows in a such holographic framework is that the results are readily extended to arbitrary dimensions. In particular then, the analysis of holographic RG flows identified a certain quantity satisfying an inequality analogous to eq. (2.1) for *any dimension*, that is, for both odd and even numbers of spacetime dimensions. Since the trace anomaly is only nonvanishing for even d, a new interpretation was required for odd d. Ref. [87, 88] identified the relevant quantity as the coefficient of a universal contribution to the entanglement entropy for a particular geometry in both odd and even d. These holographic results then motivated a generalized conjecture for a c-theorem for RG flows of odd- and even-dimensional QFT's. For even d, this new central charge was shown to precisely match the coefficient of the A-type trace anomaly [87, 88] and so this conjecture coincides with Cardy's proposal. For odd d, it was shown that this effective charge could also be identified by evaluating the partition function on a d-dimensional sphere [59] and so the conjecture is connected to the newly proposed F-theorem [89, 90, 91, 92].

The above developments motivated the work in this chapter, which examines the connections between entanglement entropy and RG flows in a holographic framework. Earlier work in this direction can be found in [62, 47, 93]. Here, we make a simple generalization of the c-function in eq. (2.2) to higher dimensions and then use a holographic framework to examine its behaviour in RG flows. We are able to show that subject to specific conditions, the flow of the c-function is monotonic for boundary theories dual to Einstein gravity. In examining specific flow geometries, we also find that the entanglement entropy undergoes a 'first order phase transition' as the size of the entangling geometry passes through a critical value. That is, in our holographic calculation, there are competing saddle points and the dominant contribution shifts from one saddle point to another at the critical size.

An overview of this chapter is as follows: In section 2.1, we review the standard derivation of holographic c-theorems with both Einstein gravity and Gauss-Bonnet gravity in the bulk. We stress that in either case, the monotonic flow of the c-function requires that the matter fields driving the holographic RG flow must satisfy the null energy condition. In section 2.2, we discuss the holographic entanglement entropy for the 'strip' or 'slab' geometry and construct a c-function which naturally generalizes eq. (2.2) to higher dimensions. In section 2.3, we show that for an arbitrary RG flow solution in Einstein gravity, this c-functions decreases monotonically if the bulk matter fields satisfy the null energy condition. Section 2.4 considers explicit examples of holographic RG flows and demon-

strates that in certain cases, the entanglement entropy undergoes a 'phase transition.' As a result, the c-function exhibits a discontinuous drop along these RG flows. In section 2.5, we examine holographic RG flows with Gauss-Bonnet gravity and there, we find that the null energy condition is insufficient to constrain the flow of our c-function to be monotonic. We conclude with a brief discussion of our results and future directions in section 2.6. In section 2.7, we provide additional details about calculations and results in this chapter. Section 2.7.1 presents certain technical details related to the discussion in section 2.3. In the section 2.7.2, we discuss holographic RG flow solutions in Gauss-Bonnet gravity. Finally, section 2.7.3 describes the construction of a bulk theory for which the holographic flow geometries examined in section 2.4 would be solutions of the equations of motion.

2.1 Review of holographic c-theorems

Here we begin with a review of the holographic c-theorem as originally studied by [84, 85, 86] for Einstein gravity. These references begin by constructing a holographic description of RG flows, which we discussed in detail in section 1.3.1. The simplest case to consider is $(d+1)$-dimensional Einstein gravity coupled to a scalar field described by the action (1.27). We also assume that similar to (1.28), the potential $V(\phi)$ has various critical points where the potential energy is negative. At these critical points, the geometry is AdS_{d+1} and their curvature scale is given by $\tilde{L}^2 = L^2/\alpha_i^2$.

Now in the context of the AdS/CFT correspondence, the bulk scalar above is dual to some operator $\mathcal{O}$ and the fixed points (1.28) of the scalar potential represent the critical points of the boundary theory. In particular then, with an appropriate choice of the bulk potential, $\mathcal{O}$ will be a relevant operator for a certain fixed point and so an RG flow will be triggered by perturbing the corresponding critical theory by this operator in the UV. Of course, the holographic description of this RG flow is that the scalar field acquires a nontrivial radial profile which connects two of the critical points in eq. (1.28). The bulk geometry for this solution can be described with a metric of the following form [84, 85, 86]

$$ds^2 = e^{2A(r)}\,\eta_{ij}\,dx^i dx^j + dr^2\,. \tag{2.4}$$

Here, the radial evolution of the geometry is entirely encoded in the conformal factor $A(r)$. At a fixed point where the geometry is AdS_{d+1}, the conformal factor is simply $A(r) = r/\tilde{L}$ where again $\tilde{L}$ is the AdS curvature scale. Implicitly, we will assume that asymptotic UV boundary is at $r \to \infty$ while the IR part of the solution corresponds to $r \to -\infty$. Hence for an RG flow between two fixed points as described above, the metric (2.4) approaches that of AdS_{d+1} in both of these limits.

Now following [84, 85, 86], we define:

$$a_d(r) \equiv \frac{\pi^{d/2}}{\Gamma(d/2)\ (\ell_{\rm P} A'(r))^{d-1}}\,, \tag{2.5}$$

where 'prime' denotes a derivative with respect to r. Then for general solutions of the form (2.4), one finds

$$\begin{aligned} a_d'(r) &= -\frac{(d-1)\pi^{d/2}}{\Gamma(d/2)\,\ell_{\rm P}^{d-1} A'(r)^d}\, A''(r) \\ &= -\frac{\pi^{d/2}}{\Gamma(d/2)\,\ell_{\rm P}^{d-1} A'(r)^d}\, \left(T^t{}_t - T^r{}_r\right) \geq 0\,. \end{aligned} \tag{2.6}$$

Above in the second equality, Einstein's equations were used to eliminate $A''(r)$ in favour of components of the stress tensor.[1] The final inequality assumes that the matter fields obey the null energy condition [94]. Now given the usual connection between r and energy scale in the CFT, eq. (2.6) indicates that $a(r)$ is always increasing as we move from low energies to higher energy scales. Further, if the flow function (2.5) is evaluated for an AdS background, one finds a constant:

$$a_d^* = a_d(r)\big|_{\rm AdS} = \frac{\pi^{d/2}}{\Gamma(d/2)}\,\frac{\tilde{L}^{d-1}}{\ell_{\rm P}^{d-1}}\,. \tag{2.7}$$

Hence if we compare this constant for the UV and IR fixed points of the holographic RG flow, we find the holographic c-theorem:

$$\left[\,a_d^*\,\right]_{\rm UV} \;\geq\; \left[\,a_d^*\,\right]_{\rm IR}\,. \tag{2.8}$$

To make closer contact with the dual CFT, we recall the trace anomaly (1.45)

$$\langle\, T^i{}_i \,\rangle = \sum_n B_n\, I_n - 2\,(-)^{d/2} A\, E_d\,, \tag{2.9}$$

which defines the central charges for a CFT in an even number of spacetime dimensions. Each term on the right-hand side is a Weyl invariant constructed from the background geometry. In particular, E_d is the Euler density in d dimensions while the I_n are naturally written in terms of the Weyl tensor (as well as its covariant derivatives), *e.g.*, see [95, 96].

[1] Note that for the scalar field theory in eq. (1.27), we have $T^t{}_t - T^r{}_r = -(\phi')^2/2 \leq 0$.

Note that in eq. (2.9), we have ignored the possible appearance of a conformally invariant but also scheme-dependent total derivative.

A holographic description of the trace anomaly was developed [97, 98] and can be applied to the AdS_{d+1} stationary points in the present case (for even d). These calculations show that a_d^*, the value of the flow function at the fixed points, precisely matches the A-type central charge in eq. (2.9), *i.e.,* $a_d^* = A$ for even d [87, 88]. Hence with the assumption that the matter fields obey the null energy condition, the holographic CFT's dual to Einstein gravity satisfy Cardy's conjecture of a c-theorem for quantum field theories in higher dimensions [36]. Of course, one must add the caveat that for these holographic CFT's, *i.e.,* those dual to Einstein gravity, all of the central charges in eq. (2.9) are equal to one another [97, 98]. Hence the holographic models (1.27) considered above can not distinguish between the behaviour of A and B_n in RG flows.

It has long been known that to construct a holographic model where the various central charges are distinct from one another, the gravity action must include higher curvature interactions [99, 100]. In part, this motivated the recent holographic studies of Gauss-Bonnet (GB) gravity [60, 61] — for example, see [101, 102, 103, 104, 105, 106, 107, 108, 109]. In section 2.5, we will extend our discussion of holographic RG flows to GB gravity with the following action

$$I = \frac{1}{2\ell_{\mathrm{P}}^{d-1}} \int d^{d+1}x\sqrt{-g}\left(R + \frac{\lambda L^2}{(d-2)(d-3)}\mathcal{X}_4 - \frac{1}{2}(\partial\phi)^2 - V(\phi)\right) , \tag{2.10}$$

where

$$\mathcal{X}_4 = R_{abcd}R^{abcd} - 4R_{ab}R^{ab} + R^2 . \tag{2.11}$$

As before, we again assume the scalar potential has various stationary points as in eq. (1.28), where the energy density is negative. Note that for convenience, we are using the same canonical scale L which appears for the critical points in eq. (1.28) in the coefficient of the curvature-squared interaction in eq. (2.10). Hence the strength of this GB term is controlled by the dimensionless coupling constant, λ. We write the curvature scale $\tilde{L}$ of the AdS vacuum as $\tilde{L}^2 = L^2/f_\infty$ where the constant f_∞ satisfies [87, 88]

$$\alpha_i^2 - f_\infty + \lambda f_\infty^2 = 0 . \tag{2.12}$$

In general, eq. (2.12) has two solutions but we only consider the smallest positive root

$$f_\infty = \frac{1 - \sqrt{1 - 4\lambda\,\alpha_i^2}}{2\lambda} , \tag{2.13}$$

with which, in the limit $\lambda \to 0$, we recover $f_\infty = \alpha_i^2$ and $\tilde{L}^2 = L^2/\alpha_i^2$, as discussed above for Einstein gravity. One would find that graviton fluctuations about the AdS solution corresponding to the second root are ghosts [110, 111, 112] and hence the boundary CFT would not be unitary. The theory (2.10) is further constrained by demanding that the dual boundary theory respects micro-causality or alternatively, that it does not produce negative energy fluxes [101, 102, 103, 104, 105, 106, 107, 108, 109, 113].

For our present purposes, the most important feature of GB gravity (2.10) is that the dual boundary theory will have two distinct central charges. To facilitate our discussion for arbitrary $d \geq 4$, we would like to define two central charges that appear in any CFT for any d – including odd d – and hence for our purposes, the trace anomaly is not a useful definition of the central charges. Following [113, 87, 88], we consider:

$$C_{\rm T} = \frac{\pi^{d/2}}{\Gamma(d/2)} \left(\frac{\tilde{L}}{\ell_{\rm P}}\right)^{d-1} [1 - 2\lambda f_\infty] \,, \tag{2.14}$$

$$a_d^* = \frac{\pi^{d/2}}{\Gamma(d/2)} \left(\frac{\tilde{L}}{\ell_{\rm P}}\right)^{d-1} \left[1 - 2\frac{d-1}{d-3}\lambda f_\infty\right] . \tag{2.15}$$

The first charge $C_{\rm T}$ is that controlling the leading singularity of the two-point function of the stress tensor.[2] The second central charge a_d^* can be determined by calculating the entanglement entropy across a spherical entangling surface [87, 88]. Using the results of [115, 116], it was further shown [87, 88] that a_d^* is the central charge appearing in the A-type trace anomaly in even dimensions, *i.e.*, $a_d^* = A$ in eq. (2.9). In terms of these central charges, the micro-causality constraints, referred to previously, are conveniently written as [113]

$$\frac{d(d-3)}{d(d-2)-2} \leq \frac{C_{\rm T}}{a_d^*} \leq \frac{d}{2} \,. \tag{2.16}$$

Now assuming the existence of bulk solutions describing holographic RG flows for the GB theory (2.10),[3] we can establish a holographic c-theorem following the analysis of [87, 88]. We begin by constructing two flow functions [87, 88]:

$$\widehat{C}_{\rm T}(r) \equiv \frac{\pi^{d/2}}{\Gamma(d/2)} \frac{1}{(\ell_{\rm P}\, A'(r))^{d-1}} \left(1 - 2\lambda\, L^2\, A'(r)^2\right) , \tag{2.17}$$

$$a_d(r) \equiv \frac{\pi^{d/2}}{\Gamma(d/2)} \frac{1}{(\ell_{\rm P}\, A'(r))^{d-1}} \left(1 - 2\frac{d-1}{d-3}\lambda\, L^2 A'(r)^2\right) . \tag{2.18}$$

[2] Here, as in [114], we have normalized $C_{\rm T}$ so that in the limit $\lambda \to 0$, $C_{\rm T} = a_d^*$. This choice is slightly different from that originally presented in [113], *i.e.*, $C_{\rm T}|_{[113]} = \frac{d+1}{d-1}\frac{\Gamma(d+1)}{\pi^d}\, C_{\rm T}|_{\rm here}$.

[3] Section 2.7.2 includes a discussion of one approach to constructing such solutions.

These expressions were chosen as the simplest extensions of eq. (2.5) which yield the two central charges above at the fixed points, *i.e.*, $a_d(r)|_{AdS} = a_d^*$ and $\widehat{C}_{\rm T}(r)|_{AdS} = C_{\rm T}$ — recall that $A(r) = r/\tilde{L}$ for the AdS vacua. Now let us examine the radial evolution of $a_d(r)$ in a holographic RG flow:

$$\begin{aligned} a_d'(r) &= -\frac{(d-1)\,\pi^{d/2}}{\Gamma\left(d/2\right)\ell_{\rm P}^{d-1}A'(r)^d}\,A''(r)\left(1-2\lambda\,L^2\,A'(r)^2\right) \\ &= -\frac{\pi^{d/2}}{\Gamma\left(d/2\right)\ell_{\rm P}^{d-1}A'(r)^d}\left(T^t{}_t - T^r{}_r\right) \geq 0\,. \end{aligned} \tag{2.19}$$

Here, the equations of motion for GB gravity (see eq. (2.143)) have been used to trade the expression in the first line for the components of the stress tensor appearing in the second line. As before with Einstein gravity, we assume the null energy condition applies for the matter fields for the final inequality to hold. In eq. (2.10), the matter contribution is still a conventional scalar field action and so just as before $T_t{}^t - T_r{}^r = -(\phi')^2/2 \leq 0$. With this assumption, it then follows[4] that $a_d(r)$ evolves monotonically along the holographic RG flows and we can conclude that the central charge a_d^* is always larger at the UV fixed point than at the IR fixed point. Hence we recover precisely the same holographic c-theorem found previously with Einstein gravity, namely,

$$\left[a_d^*\right]_{\rm UV} \;\geq\; \left[a_d^*\right]_{\rm IR} \tag{2.20}$$

One can also consider the behaviour of $\widehat{C}_{\rm T}$ along RG flows

$$\widehat{C}_{\rm T}{}'(r) = -\frac{(d-1)\,\pi^{d/2}}{\Gamma\left(d/2\right)\ell_{\rm P}^{d-1}A'(r)^d}\,A''(r)\left(1-2\frac{d-3}{d-1}\,\lambda\,L^2\,A'(r)^2\right) \tag{2.21}$$

but there is no clear way to establish that $\widehat{C}_{\rm T}{}'(r)$ has a definite sign. Hence this holographic model (2.10) seems to single out a_d^* as the central charge which satisfies a c-theorem. This result has also been extended to holographic models with more complex gravitational theories in the bulk:[5] quasi-topological gravity [87, 88], general Lovelock theories [118, 119], higher curvature theories with cubic interactions constructed with the Weyl tensor [87, 88] and $f(R)$ gravity [118]. The result is also established for holographic models where the RG flow is induced by a double-trace deformation of the boundary CFT [120]. Given the relation $a_d^* = A$ in even dimensions, these holographic results support Cardy's proposal

[4] We note that some additional arguments are needed to ensure that there are no problems with $A'(r) < 0$ for odd d [87, 88].

[5] Similar results were also found to apply in the context of cosmological solutions [117].

[36] that the central charge A (rather than any other central charge) evolves monotonically along RG flows. However, it is even more interesting that these results suggest that a similar behaviour also occurs for the central charge a_d^* in odd dimensions. Further while the original field theory definition of a_d^* involved a calculation of entanglement entropy [87, 88], it was shown that the same charge can also be identified by evaluating the partition function on S^d [59]. Hence the exciting new field theoretic results of [89, 90, 91, 92] provide further evidence for the same c-theorem in odd dimensions.

In any event, a key requirement for the holographic c-theorem to hold for Einstein gravity (2.8) or for GB gravity (2.20) is that the matter fields obey the null energy condition. Of course, this holds when these gravitational theories are coupled to a simple scalar field, as in eqs. (1.27) and (2.10), this constraint is trivially satisfied. However, phrasing the constraint in terms of the null energy condition allows for more general scenarios for the matter fields driving the holographic RG flow. We should add that the same constraint also ensures the holographic c-theorem holds for all of the extensions of the bulk gravity theory mentioned above. We might mention that violations of the null energy condition quite generally lead to instabilities [121, 122] and so it is a natural constraint to define a reasonable holographic model. In the following, we will also see that the same constraint can be related to the monotonic flow of a holographic c-function defined in terms of entanglement entropy.

2.2 Holographic entanglement entropy and a c-function

Before beginning our holographic analysis, we must first identify a candidate c-function using entanglement entropy for $d \geq 3$. Recall that [80, 81] identifies such a c-function for two-dimensional quantum field theories as

$$c_2 = 3\,\ell\,\frac{\partial S}{\partial \ell} \tag{2.22}$$

where S is the entanglement entropy for an interval of length ℓ on an infinite line. As described above, using the result (2.3) for the entanglement entropy of $d = 2$ CFT's, one finds $c_2 = c$ at any fixed points of the RG flows, *i.e.,* eq. (2.22) yields the central charge of the underlying CFT at the fixed points. We would like to emulate this construction in higher dimensions. However, one should recall that in general the entanglement entropy for field theories in higher dimensions will contain many (non-universal) power law divergences depending on the geometry of the entangling surface, *e.g.,* see eq. (1.53). Hence we expect a simple derivative with respect to some scale characteristic of the entangling surface will

typically yield a result which depends on the cut-off. While there may be various strategies to avoid this outcome – see further discussion in section 2.6 – here we take the following simple approach: First we note that, at the fixed points, the power law divergences are geometric in origin and all but the leading area-law terms vanish if the geometries of the background and the entangling surface are both flat. Hence we consider a 'strip' or 'slab' geometry, where the entangling surface consists of two parallel flat (d–2)-dimensional planes separated by a distance ℓ in a flat background spacetime. The entanglement entropy (of a CFT) then takes the simple form [16, 52]

$$S_{\rm CFT} = \alpha_d \frac{H^{d-2}}{\delta^{d-2}} - \frac{1}{(d-2)\beta_d}\, \mathcal{C}_d\, \frac{H^{d-2}}{\ell^{d-2}}\,, \tag{2.23}$$

where α_d and β_d are dimensionless numerical factors and H is a(n infrared) regulator distance along the entangling surface – we assume that $H \gg \ell$. That is, H^{d-1} is the area for each of the planes comprising the entangling surface and so the first contribution in eq. (2.23) is simply the usual area law term. The coefficient of the second finite term is proportional to a central charge in the underlying d-dimensional CFT, which we denote $\mathcal{C}_d$. Hence we can isolate this central charge by writing

$$\mathcal{C}_d = \beta_d\, \frac{\ell^{d-1}}{H^{d-2}}\, \frac{\partial S_{\rm CFT}}{\partial \ell}\,. \tag{2.24}$$

Hence we are naturally lead to consider the quantity

$$c_d = \beta_d\, \frac{\ell^{d-1}}{H^{d-2}}\, \frac{\partial S}{\partial \ell} \tag{2.25}$$

as a candidate for a c-function along the RG flows, so that $c_d = \mathcal{C}_d$ at the fixed points of the flow. We will identify the precise value of the coefficient β_d with our holographic calculations below — see eq. (2.30). Comparing eqs. (2.22) and (2.25), we can view the latter expression as the simplest generalization of the two-dimensional c-function (2.22) to higher dimensions. At the outset, we wish to say that we will find below that will only be able to prove that this candidate c-function actually decreases monotonically along RG flows for holographic models with Einstein gravity in the bulk. However, another goal in the following analysis is to connect the behaviour of this c-function defined using holographic entanglement entropy with the standard discussions of holographic c-theorems [84, 85, 86, 87, 88]. We should also mention that eq. (2.25) was previously suggested as a c-function in [52].

2.2.1 Holographic entanglement entropy on an interval

In this section, we derive some of useful results to evaluate eq. (2.25) for holographic RG flows in following sections. The holographic models in sections 2.3 and 2.4 will be described by Einstein gravity in the bulk, while we will consider GB gravity [60, 61] in section 2.5.

The seminal work of Ryu and Takayanagi [16, 52] provided a holographic construction to calculate entanglement entropy which we discussed in detail in section 1.3.4. In the d-dimensional boundary field theory, the entanglement entropy between a spatial region V and its complement $\bar{V}$ is given by (1.56) in the $(d+1)$-dimensional bulk spacetime. In [62, 48], the expression (1.56) was extended to holographic theories dual to GB gravity (2.10) in the bulk. The new prescription still extremizes over bulk surfaces v which connect to the entangling surface at the asymptotic boundary, however, the entropy functional to be extremized becomes (1.63). Note that now expression of EE contains the Ricci scalar of the induced geometry over the surface v and the extrinsic curvature of the boundary ∂v at the asymptotic cut-off surface. We apply this expression only for $d \geq 4$ since it is only for these dimensions that the GB interaction (2.11) contributes to the gravitational equations of motion.

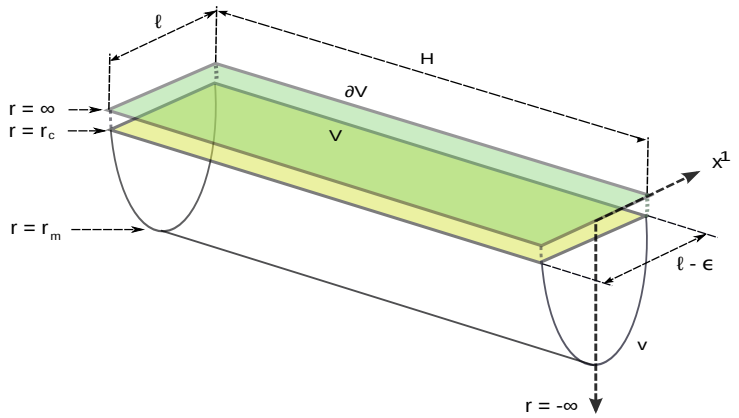

Figure 2.1: (Colour Online) The strip V in the asymptotic boundary, with the minimal surface v in the bulk ending on ∂V. The entangling surface ∂V consists of two flat (hyper)planes positioned at $x^1 = \ell/2$ and $x^1 = -\ell/2$. A regulator length H is introduced to limit the extent of these planes along the remaining directions.

Now let us begin to consider evaluating the holographic entanglement entropy for a general RG flow. As in the previous section, we assume the bulk metric takes the form

given in eq. (2.4). Then the boundary geometry is simply flat space and we define the entangling surfaces as follows: First recall that the entangling surface divides a Cauchy surface (*e.g.,* the constant time slice, $x^0 = t = 0$) into two regions. As described above, we wish to consider an interval of length ℓ and so we introduce two flat (hyper)planes at $x^1 = \ell/2$ and $x^1 = -\ell/2$, as shown in figure 2.1. We also introduce a regulator length H to limit the size of the two planes along the $x^{2,3,\cdots,d-1}$ directions, *e.g.,* we can imagine the boundary is periodic in these directions with length $H \gg \ell$. Hence the area of either plane is H^{d-1}, as described at eq. (2.23). In calculating the holographic entanglement entropy, we consider bulk surfaces that end on the entangling surface as $r \to \infty$, as shown in figure 2.1. With the 'slab' geometry described here, the radial profile of these surfaces will only be a function of the coordinate $x = x^1$. We will write the profile as $r = r(x, w = \ell)$ where w indicates the width of the interval which sets the boundary condition, *i.e.,* in the present case, $x \to \ell/2$ as $r \to \infty$. Of course, the holographic calculations are only well-defined if we introduce an asymptotic cut-off surface as some $r = r_c$. The position of this surface is related to a short distance cut-off in the boundary theory, *i.e.,* $r_c = \tilde{L}\,\log(\tilde{L}/\delta)$. The radial profile will define another useful UV scale ϵ with $r_c = r(x = (\ell - \epsilon)/2, w = \ell)$, *i.e.,* the profile intersects the cut-off surface $r = r_c$ at $x = (\ell - \epsilon)/2$. Another useful scale in the bulk surface is the minimal radius r_m which it reaches in the bulk, which appears as $r_m = r(x = 0, w = \ell)$.

Given the background metric (2.4) and our ansatz $r(x, \ell)$ for the profile of the bulk surface, we find that eq. (1.63) reduces to the following simple expression

$$S = \frac{2\pi}{\ell_{\rm P}^{d-1}} \int_m d^{d-1}x\, \frac{e^{(d-2)A}\left(e^{2A} + (1 + 2\,\lambda L^2\, A'^2)\,\dot{r}^2\right)}{\sqrt{e^{2A} + \dot{r}^2}}\,. \tag{2.26}$$

where $\dot{r} = \partial r/\partial x$ and $A' = dA/dr$. Now one may treat the above expression as an action which is varied to find a second-order differential equation to determine the profile $r(x, \ell)$. However, since the integrand above has no explicit dependence on the coordinate x, the following is a conserved quantity along the radial profile[6]

$$K_d(\ell) \;\equiv\; \frac{e^{-dA}\,(e^{2A} + \dot{r}^2)^{3/2}}{e^{2A} + (1 - 2\,\lambda L^2\, A'^2)\,\dot{r}^2}\,. \tag{2.27}$$

This leaves us with a first-order equation for the profile, which should be easier to solve. In principle then, our goal is to solve for $r(x, \ell)$ in a given holographic RG flow geometry, *i.e.,* for a specific conformal factor $A(r)$, and then substitute the solution back into eq. (2.26) to calculate the entanglement entropy.

[6] If we denote the integrand in eq. (2.26) as $\mathcal{L}$, then $K_d(\ell)^{-1} = \mathcal{L} - \frac{d\mathcal{L}}{d\dot{r}}\,\dot{r}$.

Before going on to consider the entanglement entropy and c-function for RG flow geometries, let us first examine the results when the bulk geometry is simply AdS space, *i.e.*, at a fixed point of the flow where the boundary theory is conformal. Recall that for the AdS vacuum $A(r) = r/\tilde{L}$. Let us begin by setting $\lambda = 0$ and considering the results for Einstein gravity in the bulk.[7] The case of three-dimensional AdS or a $d = 2$ boundary CFT is special since the entanglement entropy yields a logarithmic UV divergence

$$S_{\rm CFT} \;=\; \frac{4\,\pi \tilde{L}}{\ell_{\rm P}}\,\log\left(\frac{\ell}{\delta}\right)\,. \tag{2.28}$$

If we recall that the central charge of the boundary CFT is given by $c = 12\pi\,\tilde{L}/\ell_{\rm P}$, we see that this expression precisely reproduces the expected result (2.3) for the entanglement entropy of a two-dimensional CFT. Next turning to Einstein gravity with $d \geq 3$, the entanglement entropy for the interval is given by [16]

$$S_{\rm CFT} \;=\; \frac{4\pi}{d-2}\,\frac{\tilde{L}^{d-1}}{\ell_{\rm P}^{d-1}}\left(\frac{H}{\delta}\right)^{d-2} - \frac{2^d\,\pi^{(d+1)/2}}{(d-2)}\left(\frac{\Gamma(\frac{d}{2(d-1)})}{\Gamma(\frac{1}{2(d-1)})}\right)^{d-1}\frac{\tilde{L}^{d-1}}{\ell_{\rm P}^{d-1}}\left(\frac{H}{\ell}\right)^{d-2}\,. \tag{2.29}$$

Here we see the general structure given in eq. (2.23) with two terms, a power law divergence proportional to $(H/\delta)^{d-2}$ and a finite contribution proportional to $(H/\ell)^{d-2}$. Next for $\lambda = 0$, both of the central charges in eqs. (2.14) and (2.15) are identical and we use this fact to define $\mathcal{C}_d$ in eq. (2.23) for Einstein gravity: $\mathcal{C}_d(\lambda = 0) \equiv \pi^{d/2}/\Gamma(d/2)\,(\tilde{L}/\ell_{\rm P})^{d-1} = C_{\rm T} = a^*_d$. As described previously then, we can extract this central charge from the above entanglement entropy using eq. (2.24), which yields

$$\mathcal{C}_d = \beta_d\,\frac{\ell^{d-1}}{H^{d-2}}\,\frac{\partial S_{\rm CFT}}{\partial \ell} \quad \text{with} \quad \beta_d = \frac{1}{\sqrt{\pi}\,2^d\,\Gamma(d/2)}\left(\frac{\Gamma(\frac{1}{2(d-1)})}{\Gamma(\frac{d}{2(d-1)})}\right)^{d-1}\,. \tag{2.30}$$

Hence we have identified the precise value of β_d (for $d \geq 3$) which appears as the coefficient in eq. (2.25) of the c-function.

Finally let us apply the above formulae to calculate holographic entanglement entropy with the strip geometry for the boundary CFT dual to the AdS vacuum in GB gravity (2.10). To simplify the final results, it is convenient to first treat r as the independent variable, in which case to fix the profile of the bulk surface, we must determine $x(r)$. Next we choose a new radial coordinate $\tau = K^{-1/(d-1)}\,e^{-r/\tilde{L}}$ and define $h \equiv e^{2r/\tilde{L}}\,(\partial_r x)^2$. Note

[7] Note that in this case, the AdS curvature is given by simply $\tilde{L} = L$.

that as $r \to \infty$, $\tau \to 0$ and further one can show at $r = r_m$, $\tau = 1$. Now with these choices, eq. (2.27) becomes

$$\frac{\tau^{d-1}\,(1+h)^{3/2}}{\sqrt{h}\,(1-2\lambda f_\infty + h)} = 1\,. \tag{2.31}$$

In general, this equation yields three roots for $h(\tau)$ and the relevant solution is the real root which can be continuously connected to the $\lambda = 0$ solution: $h = \tau^{2(d-2)}/(1-\tau^{2(d-2)})$. Now it is straightforward to see that the entanglement entropy (2.26) can be written as

$$\begin{aligned} S_{\rm CFT} \;=\; & \frac{4\pi}{d-2}\,(1+2\lambda f_\infty)\,\frac{\tilde{L}^{d-1}}{\ell_{\rm P}^{d-1}}\left(\frac{H}{\delta}\right)^{d-2} - \frac{4\pi}{d-2}\,(1+2\lambda f_\infty)\,\frac{\tilde{L}^{d-1}}{\ell_{\rm P}^{d-1}}\left(\frac{H}{\ell}\right)^{d-2} \\ & \times\, I^{d-2}\left[1+(d-2)\int_0^1 \frac{d\tau}{\tau^{d-1}}\left(1-\frac{1+2\lambda f_\infty + h}{(1+2\lambda f_\infty)\,\sqrt{1+h}}\right)\right], \end{aligned} \tag{2.32}$$

where $I \equiv \int_0^1 d\tau\sqrt{h}$. Then applying eq. (2.30), we can express the central charge in the finite contribution as[8]

$$\begin{aligned} \mathcal{C}_d(\lambda) \;=\; & 4\pi\beta_d\,(1+2\lambda f_\infty)\,\frac{\tilde{L}^{d-1}}{\ell_{\rm P}^{d-1}}\,I^{d-2} \\ & \times\left[1+(d-2)\int_0^1 \frac{d\tau}{\tau^{d-1}}\left(1-\frac{1+2\lambda f_\infty + h}{(1+2\lambda f_\infty)\,\sqrt{1+h}}\right)\right]. \end{aligned} \tag{2.33}$$

Regrettably, we do not have a closed analytic expression for $\mathcal{C}_d(\lambda)$ in terms of the two central charges $C_{\rm T}$ and a_d^*. Hence we have numerically evaluated the above expression and plotted $\mathcal{C}_d(\lambda)/a_d^*$ as a function of $C_{\rm T}/a_d^*$ in figure 2.2a for several values of d. Note that in this figure, $\mathcal{C}_d(\lambda)/a_d^* = 1$ at $C_{\rm T}/a_d^* = 1$ for all of the values of d since this corresponds to $\lambda = 0$ or Einstein gravity in the bulk. From these curves, we can infer that $\mathcal{C}_d(\lambda)$ is a complicated nonlinear function of both $C_{\rm T}$ and a_d^*. We can also illustrate this fact as follows: In the vicinity of $\lambda \simeq 0$ or $C_{\rm T} \simeq a_d^*$, we can make a linearized analysis of eq. (2.33) to find

$$\mathcal{C}_d(\lambda) = \mathcal{C}_d(0)\left(1+\frac{3(d-1)}{2}\lambda + O(\lambda^2)\right) = \mathcal{C}_L(\lambda) + O(\lambda^2) \tag{2.34}$$

[8]Note that analogous results were given for the case $d = 4$ in [62]. However, we note that the calculations presented there did not include the 'Gibbons-Hawking' surface term in eq. (1.63) and hence their expressions do not match those presented here. However, we have verified numerically that the effective central charge in [62] agrees with eq. (2.33) when $d = 4$. We also observe that the leading divergent term in eq. (2.32) is proportional to $C_{\rm T}$ while without the 'Gibbons-Hawking' term, this term is proportional to a_d^*.

where

$$\mathcal{C}_L(\lambda) \equiv \frac{(d-1)(d-2)}{2}\, C_{\rm T} + \frac{d(d-3)}{2}\, a^*_d\,. \tag{2.35}$$

Here, we have defined $\mathcal{C}_L(\lambda)$ as the linear combination of the two central charges in eqs. (2.14) and (2.15) which yields an $O(\lambda)$ expansion which precisely matches that for $\mathcal{C}_d(\lambda)$. Next, we consider the ratio of $\mathcal{C}_d(\lambda)$ and $\mathcal{C}_L(\lambda)$ over the full (physical) range of λ. Since $\mathcal{C}_L(\lambda)$ can vanish in this range, it is convenient plot the ratio $\mathcal{C}_L(\lambda)/\mathcal{C}_d(\lambda)$ as a function of $C_{\rm T}/a^*_d$, as shown in figure 2.2b. This figure illustrates even more dramatically our previous observation that $\mathcal{C}_d(\lambda)$ is a complicated nonlinear function of both $C_{\rm T}$ and a^*_d. At this point, let us add that since $\mathcal{C}_d(\lambda) \neq a^*_d$, the central charge identified in [87, 88] as satisfying a c-theorem, we might not expect that our new effective central charge $\mathcal{C}_d(\lambda)$ will always flow monotonically in holographic RG flows for general λ.

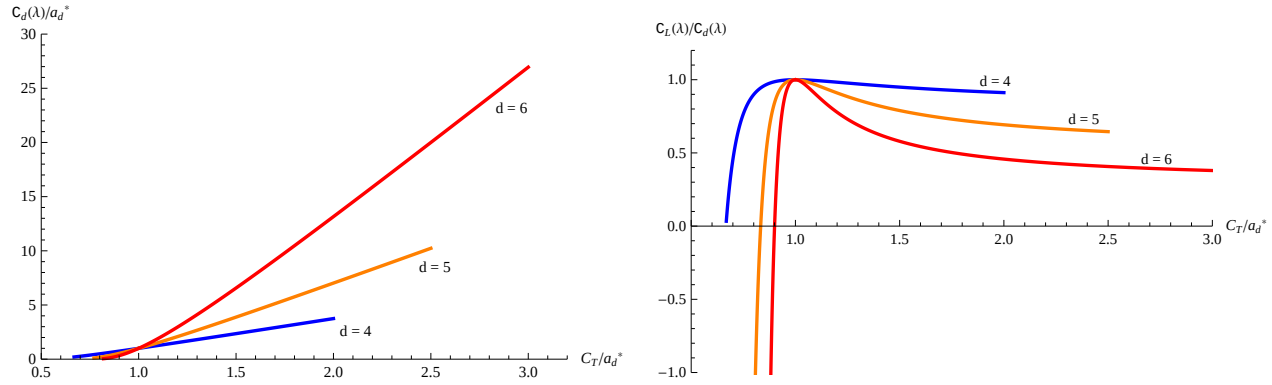

Figure 2.2: (Colour Online) Panel (a) plots $\mathcal{C}_d(\lambda)/a^*_d$ as a function of $C_{\rm T}/a^*_d$ for GB gravity, while panel (b) is a plot of $\mathcal{C}_L(\lambda)/\mathcal{C}_d(\lambda)$ as a function of $C_{\rm T}/a^*_d$. Note that both $\mathcal{C}_d(\lambda)/a^*_d = 1 = \mathcal{C}_L(\lambda)/\mathcal{C}_d(\lambda)$ at $C_{\rm T}/a^*_d = 1$ which corresponds to Einstein gravity in the bulk (*i.e.*, $\lambda = 0$). Each curve runs over the physically allowed range of $C_{\rm T}/a^*_d$ for the given value of d — see eq. (2.16) for more details.

2.3 Holographic flow of c-function with Einstein gravity

In this section, we examine the behavior of the c-function (2.25) in a general holographic RG flow dual to Einstein gravity. We will first discuss the flow of the c-function in $d = 2$

and then generalize it to arbitrary dimensions.

For $d = 2$, the bulk theory is three-dimensional Einstein gravity coupled to, *e.g.,* a scalar field with a nontrivial potential, as described in section 2.1. Our holographic expression (2.26) for the entanglement entropy of a strip can be written as

$$S \;=\; \frac{4\pi}{\ell_{\rm P}} \int_0^{\frac{\ell-\epsilon}{2}} dx\, \sqrt{\dot{r}^2 + e^{2A}}\,. \tag{2.36}$$

Note that the integration above runs over half of the range, *i.e.,* $x \in [\,0, (\ell-\epsilon)/2\,]$. Further the conserved charge (2.27) simplifies to

$$K_2(\ell) \;=\; e^{-2A(r)}\, \sqrt{\dot{r}^2 + e^{2A}}\,. \tag{2.37}$$

To calculate $dS/d\ell$, we note that $\dot{r} = \dot{r}(x,\ell)$ and $A = A(r(x,\ell))$, *i.e.,* the profile of the extremal surface implicitly depends on the strip width ℓ. If we vary S with respect to ℓ, keeping the UV cut-off $r = r_c$ fixed, we will get two contributions: one coming from change in the limits of the integration and second from change in the solution $r(x,\ell)$. We write them as

$$\frac{dS}{d\ell} \;=\; \frac{4\,\pi}{\ell_{\rm P}} \frac{1}{\sqrt{\dot{r}^2 + e^{2A(r)}}} \left[\frac{1}{2}\left(1 - \frac{d\epsilon}{d\ell}\right)(\dot{r}^2 + e^{2A(r)}) + \dot{r}\,\frac{\partial r}{\partial \ell}\right]\Bigg|_{x=\frac{\ell-\epsilon}{2}}, \tag{2.38}$$

where we have used the equation of motion for $r(x,\ell)$

$$\ddot{r} - A'\,\left(2\dot{r}^2 + e^{2A}\right) \;=\; 0\,, \tag{2.39}$$

to cancel the bulk contribution. Since the UV cut-off r_c is fixed while performing the variation, we get some extra constraints between $\dot{r} = \partial_x r$ and $r' = \partial_\ell r$ at the asymptotic boundary. Taking variation of relation $r(\frac{\ell-\epsilon}{2}, \ell) = r_c$ with respect to ℓ, we get

$$\left[\frac{\dot{r}(x,\ell)}{2}\left(1 - \frac{d\epsilon}{d\ell}\right) + \frac{\partial r(x,\ell)}{\partial \ell}\right]_{x=\frac{\ell-\epsilon}{2}} \;=\; 0\,. \tag{2.40}$$

Substituting this relation, as well as eq. (2.37), into eq. (2.38) gives us following expression for $dS/d\ell$:

$$\frac{dS}{d\ell} \;=\; -\frac{4\pi}{\ell_{\rm P}\, K_2(\ell)}\, \frac{1}{\dot{r}}\, \frac{\partial r}{\partial \ell}\bigg|_{x=\frac{\ell-\epsilon}{2}}. \tag{2.41}$$

In the above relation, the partial derivatives of $r(x,\ell)$ are evaluated near the asymptotic boundary. To further simplify this expression, we use the Fefferman-Graham expansion

near the boundary [95, 96]. In terms of the radial coordinate r, this expansion takes the form [47]

$$ds^2 \;=\; dr^2 + e^{2r/\tilde{L}}\, f(r)\, \eta_{ij}\, dx^i\, dx^j\,, \tag{2.42}$$

where

$$f(r) \;=\; 1 + a_1\phi_0^2\, e^{-2\alpha r/\tilde{L}} + a_3\phi_0^3\, e^{-3\alpha r/\tilde{L}} + \cdots\,. \tag{2.43}$$

In this expansion, $\tilde{L}$ is the AdS radius in the UV region (*i.e.,* as $r \to \infty$) and $\alpha = d - \Delta$ where Δ is the conformal weight of the operator dual to the bulk scalar field. Near the boundary, the coordinate r is very large and hence it is sufficient to work with only the leading order term in the expansion (2.43). Although $A(r)$ has a complicated profile deep inside the bulk, near the boundary it will have the simple form

$$A(r) \;=\; r/\tilde{L}\,. \tag{2.44}$$

For this $A(r)$, eq. (2.37) can be re-expressed as the following equation of motion: $dx/dr = e^{-2r/\tilde{L}}/\sqrt{K_2^2 - e^{-2r/\tilde{L}}}$. The latter is easily integrated to yield the following solution

$$x - \frac{\ell}{2} \;=\; \tilde{L}\sqrt{K_2^2 - e^{-2r/\tilde{L}}} - \tilde{L}K_2\,. \tag{2.45}$$

where the integration constant was chosen so that $x \to \ell/2$ as $r \to \infty$. Next we differentiate the above solution with respect to x and ℓ to find $\dot{r}$ and $\partial r/\partial\ell$, treating that $K_2(\ell)$ as a function of ℓ – see section 2.7.1 for further details. Taking the limit $r \to \infty$ in ratio of $\partial r/\partial\ell$ and $\dot{r}$ appearing in eq. (2.41), we find that

$$\frac{1}{\dot{r}}\frac{\partial r}{\partial \ell}\bigg|_{x=\ell/2} \;=\; -\frac{1}{2}\,. \tag{2.46}$$

This relation not only simplifies eq. (2.41) but also ensures that the first derivative of S is indeed finite for all RG flow solutions. Using this relation in eq. (2.41), we arrive at following elegant form of the c-function (2.22) for arbitrary RG flow backgrounds:

$$c_2 \;=\; 3\,\ell\,\frac{dS}{d\ell} \;=\; \frac{6\pi}{\ell_{\rm P}}\frac{\ell}{K_2(\ell)}\,. \tag{2.47}$$

The next step is to show that this c-function increases monotonically along holographic RG flows. Implicitly, the extremal bulk surfaces v on which we are evaluating the Ryu-Takayanagi formula (1.56) extend to infinite r at $x = \pm\ell/2$ and pass through a minimum $r = r_m$ at $x = 0$. The latter radius gives us an indication of which degrees of freedom the

entanglement entropy is probing, *i.e.,* for smaller values of r_m, we expect the entropy and c_2 responds more to the IR structure of the RG flow. Hence in the following, we will study behavior of c_2 as a function of the turning point radius r_m and we wish to establish the 'c-theorem' as $dc_2/dr_m \geq 0$ – at least for background geometries that satisfy appropriate constraints.

Comparing to the field theory construction of [80, 81], we note that there the c-theorem was formulated as $dc_2/d\ell \leq 0$. Naively, this result matches with the holographic inequality which we wish to establish since we expect that as the width of the strip increases, the minimal area surface will explore deeper regions in the bulk geometry. The two inequalities would be rigorously connected if we could prove a second inequality $d\ell/dr_m \leq 0$ for consistent holographic models. However, as we will see in the next section, in fact this inequality does not hold for all extremal surfaces. However, we will still find $dc_2/d\ell \leq 0$ in all cases of interest. The violations of the previous inequality are associated with unstable saddle-points which do not contribute to the physical entanglement entropy. Hence, in section 2.4, we will find that the behaviour of the entanglement entropy in general holographic RG flows provides a richer story than might have been naively anticipated.

Returning to the flow of the c-function, we note that at the minimum of the bulk surface, we will have $r(0,\ell) = r_m$ and $\dot{r}(0,\ell) = 0$. Hence considering eq. (2.37) at this turning point, we find

$$K_2(r_m) \,=\, e^{-A(r_m)}\,. \tag{2.48}$$

Here it is natural to treat this constant of the motion as a function of r_m, rather than ℓ. We will also work with width of the strip ℓ as function of r_m. Then combining eqs. (2.47) and (2.48) yields

$$\frac{dc_2}{dr_m} \,=\, \frac{6\pi}{\ell_{\rm P} K_2(r_m)}\left(\frac{d\ell}{dr_m} + A'(r_m)\,\ell\right)\,. \tag{2.49}$$

Now to express ℓ in terms of r_m, we begin with the relation

$$\frac{\ell}{2} \,=\, \int_0^{\ell/2} dx \,=\, \int_{r_m}^{\infty}\frac{dr}{\dot{r}} \,=\, \int_{r_m}^{\infty} dr \frac{e^{-2A}\,A'}{\sqrt{K_2^2 - e^{-2A}}}\frac{1}{A'}\,. \tag{2.50}$$

Here in the final expression we have used eq. (2.37). Now above, we will apply integration by parts using

$$\int dr\,\frac{e^{-2A}A'}{\sqrt{K_2^2 - e^{-2A}}} = \sqrt{K_2^2 - e^{-2A}}\,. \tag{2.51}$$

to find that

$$\ell \,=\, 2\tilde{L}K_2 + 2\int_{r_m}^{\infty} dr \frac{A''}{A'^2}\sqrt{K_2^2 - e^{-2A}}\,, \tag{2.52}$$

where we have used eq. (2.44) to evaluate $A'(r)$ at $r = \infty$. Further we can differentiate this expression with respect to r_m to get

$$\frac{d\ell}{dr_m} \;=\; -2\tilde{L}A'(r_m)\,K_2 - 2A'(r_m)\int_{r_m}^{\infty} dr\frac{A''}{A'^2}\frac{K_2^2}{\sqrt{K_2^2 - e^{-2A}}}\,. \tag{2.53}$$

Now substituting eqs. (2.52) and (2.53) into eq. (2.49), we find

$$\begin{aligned}\frac{dc_2}{dr_m} &= -\frac{12\,\pi A'(r_m)}{\ell_{\rm P}\,K_2(r_m)}\int_{r_m}^{\infty} dr\frac{A''}{A'^2}\frac{e^{-2A}}{\sqrt{K_2^2 - e^{-2A}}} \\ &= -\frac{12\,\pi A'(r_m)}{\ell_{\rm P}\,K_2(r_m)}\int_0^{\ell} dx\,\frac{A''}{A'^2}\,, \\ &= -\frac{12\,\pi A'(r_m)}{\ell_{\rm P}\,K_2(r_m)}\int_0^{\ell} dx\,\frac{1}{A'^2}\,\left(T^t{}_t - T^r{}_r\right) \geq 0\,.\end{aligned} \tag{2.54}$$

In the second line, we have used eq. (2.37) to convert the integration over r to one over x. In the last line, we have used Einstein's equations to replace A'' by the components of the stress tensor. As for the discussion of holographic c-theorems in section 2.1, the final inequality assumes that the bulk matter fields driving the holographic RG flow satisfy the null energy condition. The latter ensures that the integrand is negative. The overall inequality also requires $K_2(r_m) > 0$ and $A'(r_m) > 0$. The first condition is obvious from eq. (2.48) while the second can be established as follows: Given the null energy condition, it follows that $A'' \leq 0$ which means that A' is everywhere a decreasing function of radial coordinate r. Implicitly, we are assuming the bulk geometry approaches AdS space asymptotically, *i.e.,* the dual field theory approaches a conformal fixed point in the UV. Hence with $r \to \infty$, we see the minimal value of A' is $A' = 1/\tilde{L}$, where $\tilde{L}$ is the asymptotic AdS scale. Since this minimal value is positive, it must be that A' is positive everywhere along the holographic RG flow. Hence dc_2/dr_m is positive and our two-dimensional c-function increases monotonically along the RG flow if the bulk matter satisfies the null energy condition.

We now turn to proving the monotonic flow of the c-function (2.25) for higher dimensions. The required analysis is a straightforward extension of the above calculations with $d = 2$. In particular, one finds that eq. (2.47) generalizes to

$$c_d \;=\; \frac{2\,\pi\,\beta_d}{\ell_{\rm P}^{d-1}}\frac{\ell^{d-1}}{K_d(\ell)}\,, \tag{2.55}$$

with d boundary dimensions. The conserved quantity (2.27) is now given by

$$K_d \;=\; e^{-dA(r)}\sqrt{\dot{r}^2 + e^{2A(r)}}\,. \tag{2.56}$$

We have relegated the detailed derivation of eq. (2.55) to section 2.7.1. However, we can see from this result that all the complexities of determining the c-function boil down to evaluating the conserved charge (2.56) for the minimal area surface. We might note that we can evaluate this expression at the minimal radius (where $\dot{r} = 0$) to find

$$K_d(r_m) = e^{-(d-1)A(r_m)}\,, \tag{2.57}$$

which generalizes eq. (2.48) to general d.

Combining eqs. (2.55) and (2.57), we further find

$$\frac{dc_d}{dr_m} = \frac{2\,(d-1)\pi\,\beta_d\,\ell^{d-2}}{K_d}\left(\frac{d\ell}{dr_m} + A'(r_m)\,\ell\right)\,. \tag{2.58}$$

To express ℓ in terms of r_m, eq. (2.50) now becomes

$$\frac{\ell}{2} = \int_0^{\ell/2} dx = \int_{r_m}^{\infty}\frac{dr}{\dot{r}} = \int_{r_m}^{\infty} dr\,\frac{A'\,e^{-dA(r)}}{\sqrt{K_d^2 - e^{-2(d-1)A}}}\,\frac{1}{A'}\,, \tag{2.59}$$

where the last expression follows by using eq. (2.56). To make further progress, we observe that

$$\begin{aligned}\int dr\,\frac{A'\,e^{-dA(r)}}{\sqrt{K_d^2 - e^{-2(d-1)A}}} &= -\frac{e^{-dA}}{d\,K_d}\;{}_2F_1\left[\frac{1}{2}, \frac{d}{2(d-1)}; \frac{3d-2}{2(d-1)}; \frac{e^{-2(d-1)A(r)}}{K_d^2}\right] \\ &= e^{-(d-2)A}\sqrt{K_d^2 - e^{-2(d-1)A}} - \frac{e^{-(d-3)A}\,K_d^2}{\sqrt{K_d^2 - e^{-2(d-1)A}}}\;{}_2F_1\left[\frac{1}{2}, -\frac{d-2}{2(d-1)}; \frac{d}{2(d-1)}; \frac{e^{-2(d-1)A(r)}}{K_d^2}\right]\,.\end{aligned} \tag{2.60}$$

We have presented the second expression above to illustrate that this result is simply an extension of eq. (2.51) for general d but in the following, we will use the more compact expression given in the first line. With eq. (2.60), we can integrate by parts in eq. (2.59) to find

$$\begin{aligned}\ell &= \frac{2\sqrt{\pi}\,K_d^{1/(d-1)}}{dA'(r_m)}\,\frac{\Gamma\left(\frac{3d-2}{2(d-1)}\right)}{\Gamma\left(\frac{2d-1}{2(d-1)}\right)} \\ &\qquad -2\int_{r_m}^{\infty} dr\,\frac{A''}{A'^2}\,\frac{e^{-dA}}{d\,K_d}\;{}_2F_1\left[\frac{1}{2}, \frac{d}{2(d-1)}; \frac{3d-2}{2(d-1)}; \frac{e^{-2(d-1)A(r)}}{K_d^2}\right]\,.\end{aligned} \tag{2.61}$$

Differentiating this result with respect to r_m and making various simplifications yields

$$\begin{aligned}\frac{d\ell}{dr_m} &= -\frac{2\sqrt{\pi}\,K_d^{1/(d-1)}}{d}\,\frac{\Gamma\left(\frac{3d-2}{2(d-1)}\right)}{\Gamma\left(\frac{2d-1}{2(d-1)}\right)} - 2A'(r_m)\int_{r_m}^{\infty} dr\,\frac{A''}{A'^2}\frac{e^{-dA}}{\sqrt{K_d^2 - e^{-2(d-1)A}}} \\ &\quad +2A'(r_m)\int_{r_m}^{\infty} dr\,\frac{A''}{A'^2}\,\frac{e^{-dA}}{d\,K_d}\;{}_2F_1\left[\frac{1}{2},\frac{d}{2(d-1)};\frac{3d-2}{2(d-1)};\frac{e^{-2(d-1)A(r)}}{K_d^2}\right].\end{aligned} \tag{2.62}$$

Now substituting eqs. (2.61) and (2.62) into eq. (2.58), we find

$$\begin{aligned}\frac{dc_d}{dr_m} &= -\frac{4\,\pi(d-1)\beta_d\,\ell^{d-2}\,A'(r_m)}{\ell_{\rm P}^{d-1}\,K_d(r_m)}\int_{r_m}^{\infty} dr\,\frac{A''}{A'^2}\frac{e^{dA}}{\sqrt{K_d^2 - e^{-2(d-1)A}}} \\ &= -\frac{4\,\pi(d-1)\beta_d\,\ell^{d-2}\,A'(r_m)}{\ell_{\rm P}^{d-1}\,K_d(r_m)}\int_0^{\ell} dx\,\frac{A''}{A'^2} \\ &= -\frac{4\,\pi\beta_d\,\ell^{d-2}\,A'(r_m)}{\ell_{\rm P}^{d-1}\,K_d(r_m)}\int_0^{\ell} dx\,\frac{1}{A'^2}\,\left(T^t{}_t - T^r{}_r\right) \geq 0\,.\end{aligned} \tag{2.63}$$

The steps here are essentially the same as in our analysis of eq. (2.54) with $d = 2$. The key requirement for the final inequality to hold is that the bulk matter fields driving the holographic RG flow must satisfy the null energy condition. With this assumption then, dc_d/dr_m is positive and our d-dimensional c-function increases monotonically along the RG flow for holographic boundary theories dual to Einstein gravity in the bulk.

2.4 Explicit geometries and Phase transitions

In this section, we consider some simple bulk geometries describing holographic RG flows. This allows us to explicitly demonstrate that the c-function (2.25) indeed flows monotonically for boundary field theories dual to Einstein gravity. However, we will also find that for some RG flows, there is a 'first order phase transition' in the entanglement entropy as the width of the strip ℓ passes through a critical value. Technically, denoting the behaviour in the entanglement entropy as a phase transition is inappropriate – after all, the system itself, *i.e.,* the state of the boundary field theory, does not change at all. However, as we will see below, in our holographic calculation of the entanglement entropy, there are competing saddle points and the dominant saddle point shifts at a critical value of the width. Of course, this behaviour is reminiscent of that seen in holographic calculations describing thermodynamic phase transitions [123, 124, 125] and so we adopt the nomenclature 'phase transition' to convey this picture. The phase transition is first order and

so the entanglement entropy is continuous at the critical width ℓ_t, however, the derivative $dS/d\ell$ is discontinuous at this point. As a result, the c-function drops discontinuously at the phase transition.

Implicitly, we are assuming that the holographic RG flows studied below are solutions of Einstein gravity and hence the entanglement entropy is determined by eq. (1.56). Explicitly, our RG flow geometries take the form given in eq. (2.4) and so are defined by giving the conformal factor $A(r)$. Here we note that in all of the examples we consider, $A''(r) \leq 0$ and so the geometry could solve Einstein's equations with matter fields satisfying the null energy condition. In section 2.7.3, we consider one approach to constructing an appropriate scalar field theory that could realize the latter. In any event with $A''(r) \leq 0$, the holographic c-theorem of section 2.3 will be satisfied. That is, $dc_d/dr_m \geq 0$ or alternatively, the c-function decreases monotonically as the corresponding extremal surface extends deeper into the bulk geometry, as will be shown below.

In general, we will consider arbitrary values of the boundary dimension in the following. However, to begin, we consider a very simple example of a step flow and the discussion will be limited to the case $d = 2$, *i.e.,* a three-dimensional bulk. The step profile consists of two AdS geometries with different curvature scales are patched together at some finite radius. With such a simple profile, the behaviour of the entanglement entropy and the c-function can be determined analytically. Our analysis with $d = 2$ is easily extended to higher d but we do not present the results here. In the subsequent subsection, we also examine smooth profiles describing an holographic RG flow and allow for arbitrary d. However, numerical analysis is required to understand the behaviour of the entanglement entropy for these smooth profiles.

2.4.1 Step profile

We limit the discussion here to three-dimensional gravity and consider a bulk geometry[9] which patches together two AdS regions with different curvatures at some finite radius $r = r_0$. Using the metric ansatz in eq. (2.4), the conformal factor $A(r)$ is given by

$$A(r) = \begin{cases} A_{IR}(r) = \frac{r - r_0}{L_{IR}} + \frac{r_0}{L_{UV}} & \text{for } r \leq r_0 \\ A_{UV}(r) = \frac{r}{L_{UV}} & \text{for } r \geq r_0 \end{cases} , \tag{2.64}$$

where L_{UV} and L_{IR} correspond to the AdS radius in the UV and IR regions, which we denote as AdS_{UV} and AdS_{IR} in the following. The constant term added to $A(r)$ in the

[9]Various aspects of the flow of entanglement entropy in this example was also studied in [93] for $d = 2$, 3 and 4.

IR region ensures that the conformal factor is continuous at $r = r_0$. Of course, it is not differentiable there and some stress energy with δ-function support would be required to make this geometry a solution of Einstein's equations. As discussed in previous sections, there is a conserved quantity (2.37) which plays an important role in determining to the entanglement entropy and the c-function. Clearly, there are two classes of minimal area surfaces in this geometry, namely those that stay only in AdS_{UV} and those that penetrate deep enough into the bulk so that the minimal radius r_m is in AdS_{IR}. In either case, the conserved quantity K_2 is given by eq. (2.48) and hence we have $K_{UV} = e^{-A_{UV}(r_m)}$ for $r_m \geq r_0$ and $K_{IR} = e^{-A_{IR}(r_m)}$ for $r_m \leq r_0$. To regulate the entanglement entropy, all of these surfaces are terminated at a large cut-off radius $r = r_c$ in the UV region.

To find the minimal area surface, we will solve eq. (2.37) for $x = x(r)$. First, we can invert the latter equation to find

$$\frac{dx}{dr} = \frac{e^{-2A(r)}}{\sqrt{K_2^2 - e^{-2A(r)}}}\,. \tag{2.65}$$

Above we have discarded the root with an overall minus sign because we will only consider the branch of solutions covering the interval $x \in [0, \ell/2]$ in the following, for which $dx/dr \geq 0$. For the minimal surfaces that stay entirely in AdS_{UV}, we can easily integrate (2.65) to find

$$x = L_{UV}\sqrt{K_{UV}^2 - e^{-2r/L_{UV}}}\,, \tag{2.66}$$

using A_{UV} as given in eq. (2.64). The integration constant is chosen here so that $x = 0$ at $r = r_m$, which also implies that

$$\ell = 2L_{UV}K_{UV} = 2L_{UV}e^{-r_m/L_{UV}}\,. \tag{2.67}$$

As noted above, this solution is valid for $r_m \geq r_0$, which implies $\ell \leq \ell_2$ where

$$\ell_2 \equiv 2L_{UV}e^{-r_0/L_{UV}}\,. \tag{2.68}$$

Next we turn to the second class of minimal area surfaces, which penetrate into AdS_{IR}. In this case, we have $K_2 = K_{IR} = e^{-A_{IR}(r_m)}$ with the turning point r_m in AdS_{IR}. We divide the relevant solutions of eq. (2.65) in two parts: $x_{IR}(r) \in [0, x_t]$ describes the portion of the extremal surface in AdS_{IR} and $x_{UV}(r) \in [x_t, \ell/2]$ represents the part in AdS_{UV}. Here we have defined the transition point x_t such that $x_t = x_{IR}(r_0) = x_{UV}(r_0)$. Now integrating eq. (2.65) with the appropriate conformal factor (2.64) for each segment, we find

$$\begin{aligned} x_{IR} &= L_{IR}\sqrt{K_{IR}^2 - e^{-2A_{IR}(r)}} \\ x_{UV} &= L_{UV}\sqrt{K_{IR}^2 - e^{-2A_{UV}(r)}} + \frac{\ell}{2} - L_{UV}K_{IR}\,. \end{aligned} \tag{2.69}$$

Above, the integration constants were chosen so that $x_{IR} = 0$ at $r = r_m$ and $x_{UV} = \ell/2$ as $r \to \infty$. Combining these solutions at $x_{IR}(r_0) = x_{UV}(r_0) = x_t$, we find

$$x_t = \frac{L_{IR}}{L_{UV} - L_{IR}} \left(L_{UV} K_{IR} - \frac{\ell}{2} \right) , \tag{2.70}$$

$$\ell = 2L_{UV} K_{IR} - 2(L_{UV} - L_{IR}) \sqrt{K_{IR}^2 - e^{-2r_0/L_{UV}}} \, . \tag{2.71}$$

Here we have ensured that the solution (2.69) is continuous at $r = r_0$ but the first derivative is also continuous at this transition point because of the form of eq. (2.65) and the continuity of the conformal factor. Implicitly, eq. (2.71) gives the relation between ℓ and r_m since $K_{IR} = e^{-A_{IR}(r_m)}$. As the physically relevant quantity in the boundary theory is ℓ, we invert this relation to find the following two solutions for K_{IR}:

$$K_{IR\pm} = \frac{L_{UV}\ell \pm (L_{UV} - L_{IR}) \sqrt{\ell^2 - 4L_{IR}(2L_{UV} - L_{IR}) e^{-2r_0/L_{UV}}}}{2L_{IR}(2L_{UV} - L_{IR})} \, . \tag{2.72}$$

Above, both of these roots provide real solutions for $\ell \geq \ell_1$ with

$$\ell_1 \equiv 2\sqrt{L_{IR}(2L_{UV} - L_{IR})} \, e^{-r_0/L_{UV}} \, . \tag{2.73}$$

It is also useful to define r_1, the value of the minimum radius at $\ell = \ell_1$, for which we find

$$e^{-r_1/L_{IR}} \equiv \frac{L_{UV}}{\sqrt{L_{IR}(2L_{UV} - L_{IR})}} \, e^{-r_0/L_{IR}} \, . \tag{2.74}$$

Now the root K_{IR+} is a monotonically increasing function of ℓ over the range $\ell_1 \leq \ell \leq \infty$ and for any ℓ in this range, there is a consistent solution for the extremal surface. The corresponding values of the minimal radius are $r_1 \geq r_m \geq -\infty$. Now the second root K_{IR-} decreases for $\ell \sim \ell_1$, however, it is an increasing function for large values of ℓ. K_{IR-} has a single minimum at $\ell = \ell_2$, *i.e.,* precisely the width defined in eq. (2.68) for the discussion of solutions remaining entirely in AdS_{UV}. At this minimum, K_{IR-} takes the value $e^{-A_{IR}(r_0)} = e^{-r_0/L_{UV}}$. We find that K_{IR-} yields a consistent solution for the extremal surface as long as $\ell_1 \leq \ell \leq \ell_2$. However, for $\ell > \ell_2$, the solutions corresponding to K_{IR-} are inconsistent, *e.g.,* dx/dr is not positive throughout the range $x \in [0, \ell/2]$. We note that for the consistent solutions, while ℓ runs from ℓ_1 to ℓ_2, the minimum radius of these surfaces r_m increases from r_1 to r_0. That is, in contrast to the previous two families of solutions, here we have $d\ell/dr_m > 0$!

Hence the following picture has emerged for the extremal surfaces: Beginning with the minimal radius in the range $\infty > r_m \geq r_0$, there is a family of extremal solutions

which remain entirely in AdS_{UV}. As can be seen from eq. (2.67), the width ℓ increases monotonically as r_m decreases, reaching the maximum $\ell = \ell_2$ when $r_m = r_0$. Below this point, we make a transition to a new family of solutions which begin to penetrate into AdS_{IR}. For $r_0 \geq r_m \geq r_1$, the relevant family of extremal surfaces corresponds to the branch with K_{IR-}. In this regime, ℓ actually decreases as r_m continues to decrease, *i.e.,* $d\ell/dr_m > 0$. When r_m reaches r_1, as given in eq. (2.74), $\ell = \ell_1$ and we make another transition to the third family of extremal surfaces. These solutions correspond to the branch with K_{IR+}. In this regime $r_1 > r_m > -\infty$, ℓ again increases monotonically as r_m decreases. Figure 2.3 illustrates this behaviour for all three families of extremal surfaces. Now for any particular value of the turning point radius r_m, we see there is unique extremal surface. However, if we consider the solutions as a function of the strip width ℓ, there is a unique solution for $\ell < \ell_1$ and $\ell > \ell_2$. In the intermediate range $\ell_1 \leq \ell \leq \ell_2$, there are in fact three possible extremal surfaces for any given width. Given three possible saddle points, we are instructed in eq. (1.56) to find the extremal surface with the minimum area in order to evaluate the entanglement entropy. This situation with multiple saddle points is also the typical scenario that one encounters in the holographic description of a thermodynamic phase transition [123, 124, 125] and in fact, we will find the latter extends to the present situation. That is, we see below that the entanglement entropy undergoes a 'first order phase transition'.

Hence having found the solutions for the extremal surfaces, we will present an entropy, *i.e.,* $S = 2\pi A(v)/\ell_{\text{P}}$, for each of these surfaces. But, of course, in the intermediate regime described above, the true entanglement entropy is given by the solution which minimizes this quantity. Let us begin with the solutions (2.66) which remain entirely in AdS_{UV}. For this case, the entropy turns out to be

$$S_{UV} = \frac{4\pi L_{UV}}{\ell_{\text{P}}} \log\left(\frac{\ell}{\delta}\right) + \mathcal{O}(\delta)\,. \tag{2.75}$$

Here the result is expressed in terms of a short-distance cut-off in the boundary theory δ, which is related to the radial cut-off by[10]

$$r_c = L_{UV} \log\left(L_{UV}/\delta\right)\,. \tag{2.76}$$

Now let us consider the extremal surfaces given by eqs. (2.69) to (2.72), which penetrate

[10]This matches the standard cut-off $z_{min} = \delta$ in Poincaré coordinates where the AdS metric takes the form $ds^2 = (L_{UV}^2/z^2)\left(\eta_{ij}dx^i dx^j + dz^2\right)$ – *e.g.,* see [59].

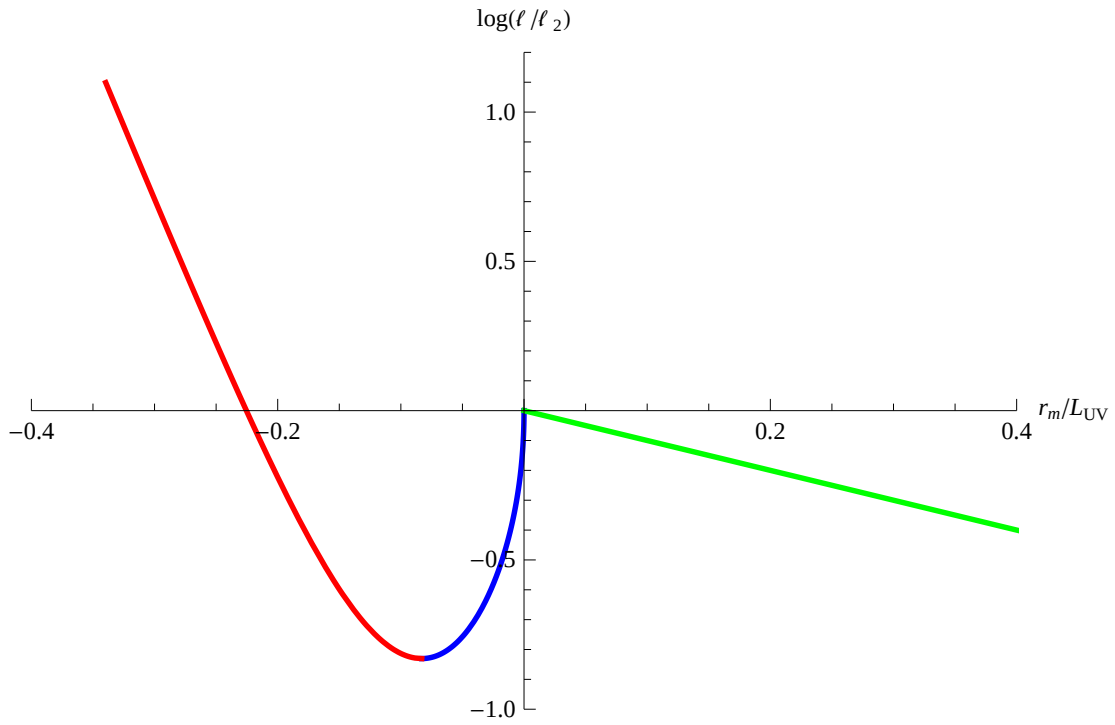

Figure 2.3: (Colour Online) This plot illustrates the behaviour of ℓ as a function of r_m for all three families of extremal surfaces. The red, blue and green portions of the curve correspond to the contributions coming from $S_{IR}(K_{IR+})$, $S_{IR}(K_{IR-})$ and S_{UV}, respectively. In particular, we see that $d\ell/dr_m \leq 0$ for $S_{IR}(K_{IR+})$ and S_{UV}, while $d\ell/dr_m \geq 0$ for $S_{IR}(K_{IR-})$. For this plot, we chose $L_{UV} = 1$, $L_{IR} = 0.1$ and $r_0 = 0$.

into AdS$_{IR}$. For this case, the calculation of entanglement entropy results

$$\begin{aligned} S_{IR} &= \frac{4\pi}{\ell_{\rm P}} \int_0^{x_t} dx \, \sqrt{e^{2A_{IR}(r)} + \dot{r}^2} + \frac{4\pi}{\ell_{\rm P}} \int_{x_t}^{(\ell-\epsilon)/2} dx \, \sqrt{e^{2A_{UV}(r)} + \dot{r}^2} \\ &= \frac{2\pi L_{IR}}{\ell_{\rm P}} \log\left[\frac{L_{IR}K_{IR} + x_t}{L_{IR}K_{IR} - x_t}\right] + \frac{2\pi L_{UV}}{\ell_{\rm P}} \log\left[\frac{4L_{UV}K_{IR} - \epsilon}{4L_{UV}K_{IR} - \ell + 2x_t} \frac{\ell - 2x_t}{\epsilon}\right] . \end{aligned} \tag{2.77}$$

We convert the cut-off ϵ above to δ using $r(x = (\ell - \epsilon)/2, \ell) = r_c$, which yields

$$\epsilon \simeq \frac{\delta^2}{L_{UV}K_{IR}} . \tag{2.78}$$

Using this relation, we can write

$$S_{IR} = \frac{4\pi L_{UV}}{\ell_{\rm P}} \log\left[\frac{2L_{UV}K_{IR}}{\delta}\right] + \frac{2\pi L_{IR}}{\ell_{\rm P}} \log\left[\frac{L_{IR}K_{IR}+x_t}{L_{IR}K_{IR}-x_t}\right] - \frac{2\pi L_{UV}}{\ell_{\rm P}} \log\left[\frac{4L_{UV}K_{IR}-\ell+2x_t}{\ell-2x_t}\right] . \tag{2.79}$$

This result is valid for both of the roots $K_{IR\pm}$ given in eq. (2.72).

Now as described above, the UV family of solutions (2.66) provide the unique extremal surface for any $\ell < \ell_1$ and hence the entanglement entropy is given by $S = S_{UV}$ in this regime. Similarly, for $\ell > \ell_2$, the extremal surface is again unique and hence the entanglement entropy is given by $S = S_{IR}(K_{IR+})$. In the intermediate regime $\ell_1 \le \ell \le \ell_2$, we have three extremal surfaces and we must identify which of these yields the minimal entropy. In particular, we always find $S_{IR}(K_{IR+}) \le S_{IR}(K_{IR-})$ and hence the branch with K_{IR-} never plays a role in determining the physical entanglement entropy. Therefore the latter is found by comparing S_{UV} and $S_{IR}(K_{IR+})$. It turns out that these two entropies are equal for some critical width ℓ_t with $\ell_1 \le \ell_t \le \ell_2$. Further $S_{UV} > S_{IR}(K_{IR+})$ for $\ell > \ell_t$ and $S_{UV} < S_{IR}(K_{IR+})$ for $\ell < \ell_t$. Hence we find that, the entanglement entropy for the step profile (2.64) is given by

$$S = \begin{cases} S_{UV}(\ell) & \text{for } \ell \le \ell_t \\ S_{IR}(K_{IR+}(\ell)) & \text{for } \ell \ge \ell_t \,, \end{cases} \tag{2.80}$$

with ℓ_t defined by $S_{UV}(\ell_t) = S_{IR}(K_{IR+}(\ell_t))$. In particular, we observe that the entanglement entropy exhibits a first order phase transition at the critical width $\ell = \ell_t$. Further, we note that at transition, $S(\ell)$ is continuous but not differentiable. We have illustrated all of this behaviour in figure 2.4, which plots $S(\ell) - S(\ell_2)$ versus $\log(\ell/\ell_2)$ for specific values of the parameters, L_{UV}, L_{IR} and r_0, defining the profile.[11]

Given the entanglement entropy (2.80), we turn to the calculation of the c-function defined in eq. (2.22). We could proceed here by explicitly differentiating the various expressions above, *e.g.,* eq. (2.79), with respect to ℓ to determine c_2. However, this calculation only verifies the final result which was already determined in our general analysis in section 2.3, namely eq. (2.47). In fact, this result applies for all three families of extremal surfaces and so we have

$$c_2 = \begin{cases} \frac{6\pi}{\ell_{\rm P}} \frac{\ell}{K_{UV}} & \text{from } S_{UV} \\ \frac{6\pi}{\ell_{\rm P}} \frac{\ell}{K_{IR-}} & \text{from } S_{IR}(K_{IR-}) \\ \frac{6\pi}{\ell_{\rm P}} \frac{\ell}{K_{IR+}} & \text{from } S_{IR}(K_{IR+}) \,, \end{cases} \tag{2.81}$$

[11] Since $S(\ell)$ diverges as $\delta \to 0$, we plot the difference $S(\ell) - S(\ell_2)$ which is independent of δ.

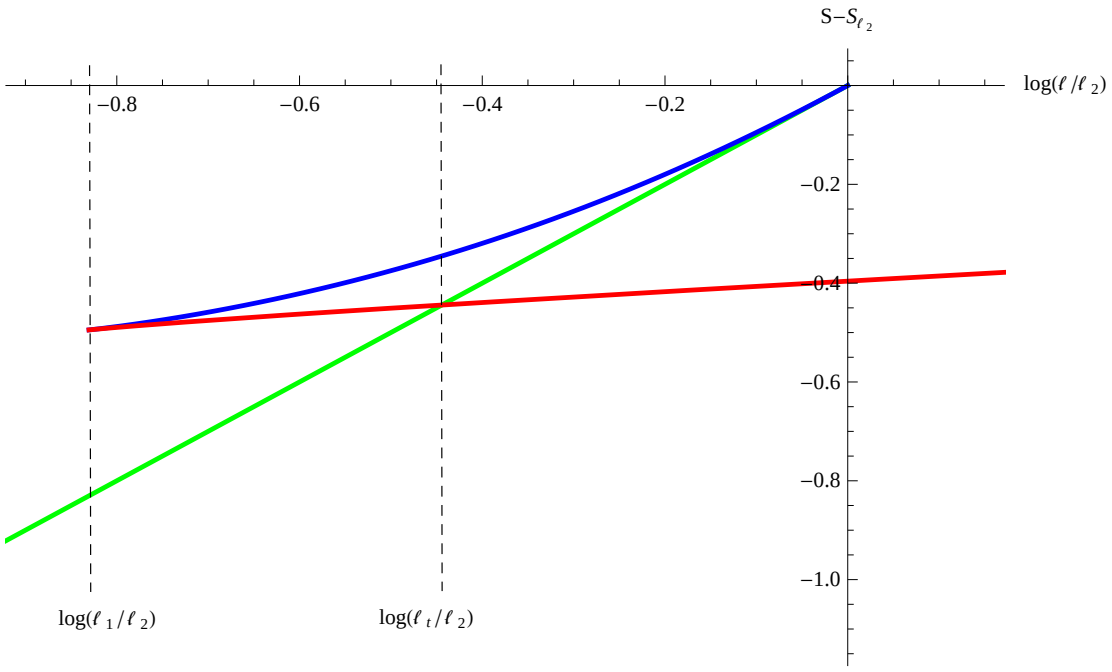

Figure 2.4: (Colour Online) This plot illustrates the entropy for all three families of extremal surfaces as a function of the width of the strip ℓ. The green curve corresponds to S_{UV}; the red, to $S_{IR}(K_{IR-+})$; and the blue, to $S_{IR}(K_{IR-})$. The phase transition occurs at $\ell = \ell_t$ where the red and green curves cross. For this plot, we have chosen $L_{UV} = 1$, $L_{IR} = 0.5$ and $r_0 = 0$.

where $K_{UV} = \ell/(2L_{UV})$ and $K_{IR\pm}$ are given in eq. (2.72). Figure 2.5a plots c_2 as a function of the turning point radius – or rather $e^{r_m/L_{UV}}$. We see that $dc_2/dr_m \geq 0$ everywhere in the figure, which is again in keeping with the expectations of our general analysis in section 2.3. However, because of the phase transition, not all values of r_m are relevant for the c-function (2.22) evaluated on the physical entanglement entropy (2.80). In figure 2.5a, the region between the vertical dashed lines is excluded and the physical c-function jumps discontinuously between the values at the points labeled A and B. This behaviour is also illustrated in figure 2.5b where the c-function in eq. (2.81) is plotted as a function of the ratio ℓ/ℓ_t. The phase transition at $\ell = \ell_t$ again takes c_2 between the points labeled A and B, which now lie on the same vertical dashed line in this figure. That is, at this critical value of the strip width, the c-function drops from the value given by S_{UV} (on the green curve) to that given by $S_{IR}(K_{IR+})$ (on the red curve). Again this discontinuity arises because of the first order nature of the phase transition, *i.e.,* the entanglement entropy is

continuous but not differentiable at this point. If we consider only the physical values of c_2, then we also find $dc_2/d\ell \leq 0$ in keeping with the general expectations of field theory analysis of [80, 81]. Of course, figure 2.5b also illustrates that $dc_2/d\ell > 0$ on the branch associated with K_{IR-}. However, as emphasized above, this family of saddle points is not relevant of the physical entanglement entropy (2.80). The 'unusual' behaviour of the c-function on this branch arises because $d\ell/dr_m \geq 0$ for this family of solutions. Given the behaviour illustrated by this simple example, it seems likely that in general any branch of extremal surfaces with the latter property will correspond to unstable saddle points which are not physically relevant.

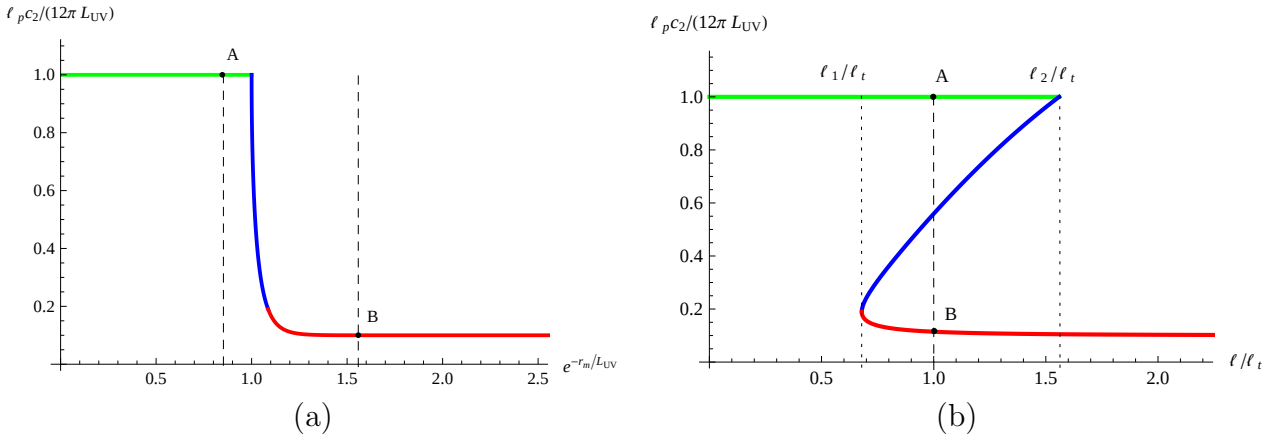

Figure 2.5: (Colour Online) Panel (a) plots the c-function (2.81) as a function of $e^{-r_m/L_{UV}}$. This plot clearly illustrates that c_2 decreases monotonically as r_m decreases, in accord with the analysis of section 2.3. However, the region between the vertical dashed lines is excluded by the phase transition in the entanglement entropy. Rather the physical c-function jumps from the point labeled A to that labeled B. Panel (b) plots the c-function with respect to ℓ/ℓ_t. One can see that c_2 is multi-valued in the region $\ell_1 \leq \ell \leq \ell_2$, as noted in eq. (2.81). Again at $\ell = \ell_t$, the c-function drops discontinuously between the points labeled A and B. The red, blue and green portions of both curves correspond to the contributions coming from $S_{IR}(K_{IR+})$, $S_{IR}(K_{IR-})$ and S_{UV}, respectively. For this plot, we chose $L_{UV} = 1$, $L_{IR} = 0.1$ and $r_0 = 0$.

2.4.2 Smooth profiles

The simple example in the previous section has alerted us to the possibility that the entanglement entropy $S(\ell)$ may experience a phase transition with respect to changing the

strip width ℓ. However, one should worry that this result is an artifact of the artificial shape of the step profile in eq. (2.64). Hence we consider some smooth profiles in this section and examine to what extent this phase transition survives for these more realistic holographic RG flows. Again our definition of the holographic entanglement entropy is given in eq. (1.56) and so implicitly we are assuming that the bulk geometry is a solution of Einstein's equations. In section 2.7.3, we consider the scalar field theory that would be necessary to realize the latter. In this section, we will consider arbitrary values of the boundary dimension d.

Let us first consider a smooth flow between the UV and IR fixed points with the following conformal factor

$$e^{A(r)} \;=\; e^{r/L}\left(2\cosh(r/R)\right)^{-\gamma}, \tag{2.82}$$

Notice that $A(r) \simeq r/L - \gamma r/R$ in the limit $r \to +\infty$ and $A(r) \simeq r/L + \gamma r/R$ for $r \to -\infty$. Hence the geometry approaches AdS space in both of these limits with

$$\frac{1}{L_{UV}} \;\equiv\; \frac{1}{L} - \frac{\gamma}{R} \quad \text{and} \quad \frac{1}{L_{IR}} \;\equiv\; \frac{1}{L} + \frac{\gamma}{R}\,. \tag{2.83}$$

The parameter R controls the sharpness of the transition in the holographic flow between the UV and IR fixed points while the change in the AdS scale is controlled by the combination γ/R. In the limit $R \to 0$ with γ/R fixed, we would recover a step profile of the form given in eq. (2.64).

To proceed further in examining the possibility of a phase transition, we used the analysis presented in previous sections and examined the extremal surfaces numerically for the above holographic flow profile. First, using eq. (2.56), the equation determining the shape of the extremal surfaces is reduced to a first order equation,

$$\frac{dx}{dr} \;=\; \frac{e^{-dA(r)}}{\sqrt{K_d^2 - e^{-2(d-1)A(r)}}}\,. \tag{2.84}$$

as appears in eq. (2.65) for $d = 2$. Then families of surfaces are easily constructed as a function of the turning point radius r_m using eq. (2.57). Numerically integrating from the turning point out to the asymptotic region, we can then determine $\ell(r_m)$.

Let us add a few more details about the numerical analysis: Near $r = r_m$, one finds that $x \sim \sqrt{r - r_m}$ and hence eq. (2.84) is singular precisely at $r = r_m$, the putative starting point of our numerical integration. So to simplify the numerical analysis, we define

$$y(r) = \sqrt{r - r_m}\, x(r)\,, \tag{2.85}$$

for which the equation of motion (2.84) becomes

$$\frac{dy}{dr} = \frac{y}{2(r-r_m)} + \frac{\sqrt{r-r_m}\, e^{-dA(r)}}{\sqrt{K_d^2 - e^{-2(d-1)A(r)}}}\,. \tag{2.86}$$

With this new coordinate, $y \sim (r-r_m)$ near $r = r_m$ and the right hand side of the equation of motion (2.86) is finite. To set the initial conditions, we use eq. (2.86) to find the leading terms in a series expansion of $y(r)$ in $r - r_m$. Now we can numerically integrate eq. (2.86) out from the turning point $r = r_m$ to large asymptotic values of r and find the strip width ℓ using the relation

$$\ell = \lim_{r\to\infty} \frac{2\, y(r)}{\sqrt{r-r_m}}\,. \tag{2.87}$$

Now as discussed previously, the appearance of a phase transition is directly related to the appearance of a regime where $d\ell/dr_m > 0$. Figure 2.6 illustrates that such behaviour still arises for a range of parameters in the smooth profile (2.82). However, as shown in the figure when R grows (holding γ/R fixed), this region decreases and eventually $d\ell/dr_m < 0$ for all values of r_m. That is, there exists a critical value R_c such that, for $R < R_c$ there is a first order phase transition while for $R > R_c$, we observe a smooth cross-over. At precisely $R = R_c$, there is a single point where $d\ell/dr_m = 0$ and the slope is otherwise negative. In this case, the phase transition would be second order.

Of course, one can go beyond the above analysis to identify the precise point where the phase transition occurs given specific values of the parameters in eq. (2.82) which produce a regime where $d\ell/dr_m > 0$. Hence for some range of the width ℓ, there will be multiple surfaces which locally extremize the entropy functional (2.120). Determining which surface provides the dominant saddle point requires carefully regulating the entanglement entropy and comparing the values of finite parts of entropy for the competing saddle points. This analysis is essentially the same as in section 2.4.1, however, in the present case with a smooth conformal factor, the profile $x(r)$ and the entropy integral are evaluated numerically. We will not present any of these results here.

Let us now turn to the asymptotic expansion of the profile (2.82) and compare it to the Fefferman-Graham (FG) expansion given in eqs. (2.42) and (2.43). We find that

$$f(r) = \left(1 + e^{-2r/R}\right)^{-\gamma} \simeq 1 - \gamma e^{-2r/R} + \dots\,. \tag{2.88}$$

which yields $\alpha = L_{UV}/R$ in eq. (2.43). Now as described in section 2.1, the natural holographic interpretation of this flow would be that the UV fixed point is perturbed by a relevant operator, which would be dual to by a scalar field in the bulk theory. However, as

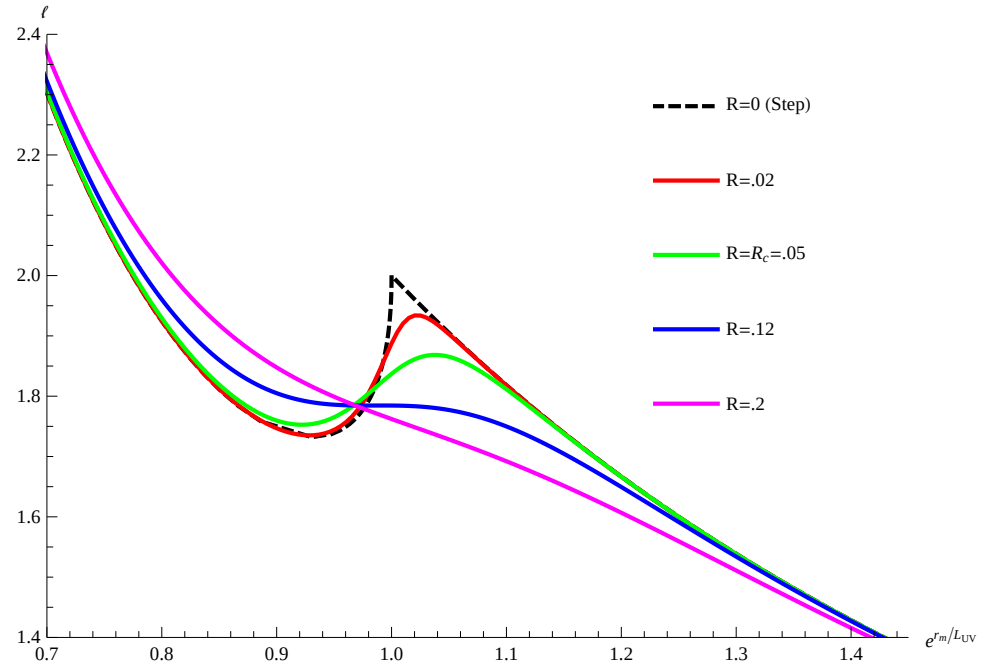

Figure 2.6: (Colour Online) Plot of strip width ℓ as a function of $e^{r_m/L_{UV}}$ for various values of the profile width R. With small R, there is a regime where $d\ell/dr_m > 0$. However, for large R, $d\ell/dr_m < 0$ everywhere. There is a critical value R_c for which $d\ell/dr_m$ reaches zero at a single point and is otherwise negative. The plot was prepared using the smooth profile (2.82) with $L = 0.66$ and $\gamma = 0.5R$, as well as $d = 2$. These parameter values yield $L_{IR} = 0.5$ and $L_{UV} = 1$.

discussed in section 2.7.3, applying this interpretation to the bulk solution yields an upper bound on the parameter α appearing in the FG expansion (2.43), *i.e.*, $\alpha \leq \frac{d}{2} + 1$. This bound then becomes a constraint on R, the width of the holographic profile (2.82). That is,

$$R \geq \frac{2L_{UV}}{d+2}\,. \tag{2.89}$$

Previously we found that the smooth holographic RG flows described by eq. (2.82) will still yield a first order phase transition in the entanglement entropy provided the width is sufficiently small, *i.e.*, $R \leq R_c$. Hence the lower bound given in eq. (2.89) creates a certain tension. Namely, if R_c does not satisfy this lower bound, it seems likely that the phase transition is still an artifact of the artificial shape of the profile in eq. (2.82). We examine

this question in figure 2.7a, where we have plotted $(d+2)R_c/2L_{UV}$ for different values of L_{UV}/L_{IR}. The bound (2.89) implies that $(d+2)R/2L_{UV} > 1$ and as the figure illustrates, the latter can only be satisfied for sufficiently large d, *i.e.*, $d \geq 6$. Hence the possibility of a phase transition is called into question for the physical dimensions $d = 2, 3, 4$.

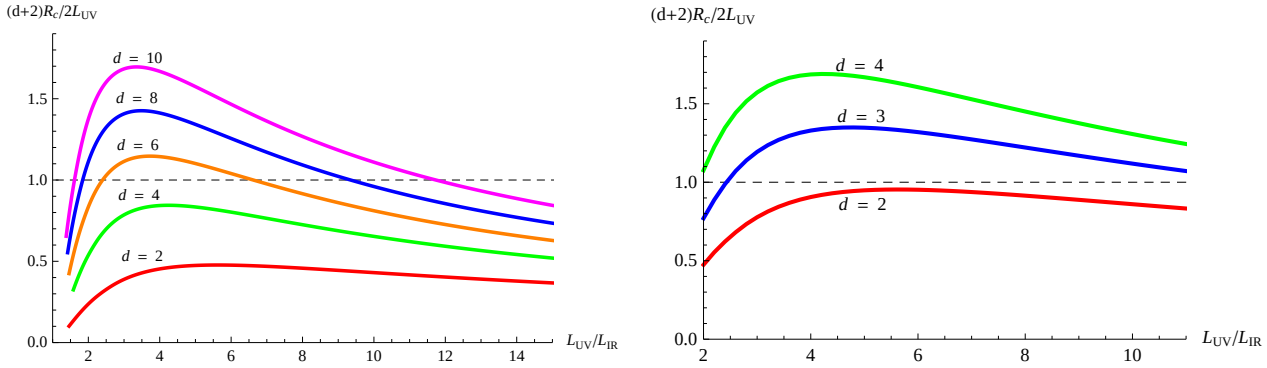

Figure 2.7: (Colour Online) Panel (a) plots $\frac{(d+2)R_c}{2L_{UV}}$ as a function of $\frac{L_{UV}}{L_{IR}}$ for various dimensions with the two-parameter conformal factor (2.82). Eq. (2.89) implies $\frac{(d+2)R_c}{2L_{UV}} > 1$ for a consistent interpretation of the holographic RG flow. Panel (b) plots $\frac{(d+2)R_c}{2L_{UV}}$ as a function of $\frac{L_{UV}}{L_{IR}}$ for the three-parameter conformal factor (2.90) with $\sigma = 5 \times 10^{-4}$.

Now the profile (2.82) was constructed to give a simple example which would smooth out the step potential studied in the previous subsection. One can easily generalize this profile to include more independent parameters and study the effect on the phase transition. Hence as another simple example, we consider the following conformal factor

$$e^{A(r)} \;=\; e^{r/L}\left(e^{2r/R} + 2\sigma + e^{-2r/R}\right)^{-\gamma/2} \,. \tag{2.90}$$

Of course, if one chooses $\sigma = 1$, this profile reduces to the previous one in eq. (2.82).[12] Hence the AdS scales in the UV and IR limits are again given by eq. (2.83) with the new expression. However, in this case, the sharpness of the transition between the asymptotic UV and IR geometries is effectively controlled by both R and σ. Given this new profile, we can readily extend the previous analysis to find in which parameter regime (R, σ) the entanglement entropy undergoes a phase transition. We do not present any details but a

[12] With the choice $\sigma = 0$, eq. (2.90) also reduces to eq. (2.82) upon substituting $R \to 2R$ and $\gamma \to 2\gamma$.

qualitative observation is that R_c becomes larger with smaller values of σ. Now considering the FG expansion in this case, the metric function in eq. (2.43) becomes

$$f(r) \;=\; \left(1 + 2\sigma e^{-2r/R} + e^{-4r/R}\right)^{-\gamma/2} = 1 - \gamma\,\sigma\, e^{-2r/R} + \dots \,. \tag{2.91}$$

Hence we still have $\alpha = L_{UV}/R$ and the lower bound in eq. (2.89) remains unchanged. Hence, as shown in figure 2.7b, we find that R_c can now satisfy this bound for $d \geq 3$. Our expectation is that by further embellishing the form of the holographic RG flow profile, we can also find realistic geometries, *i.e.,* geometries satisfying eq. (2.89), which produce a phase transition in the entanglement entropy for $d = 2$ as well.

2.5 Holographic flow of c-function with GB gravity

In this section, we return to examining the general behaviour of the c-function (2.25) in holographic RG flows but now where the bulk geometries are solutions of GB gravity (2.10).[13] As noted in section 2.2.1, the calculation of holographic entanglement entropy in GB gravity requires that we extremize the entropy functional given in eq. (1.63) [48, 62]. Evaluating this functional for the strip geometry yields the expression in eq. (2.26). The extremal surfaces are again characterized by a conserved quantity which now takes the form given in eq. (2.27). The latter is most simply evaluated by considering the turning point of the extremal surface where $r = r_m$ and $\dot{r} = 0$ so that eq. (2.27) yields

$$K_d(r_m) \;=\; e^{-(d-1)A(r_m)}\,, \tag{2.92}$$

precisely as was found before for Einstein gravity.

Recall that with Einstein gravity, we found a simple relation between K_d and $dS/d\ell$ – see eq. (2.131). In the following, we will show that this same relation extends to GB gravity. To simplify the discussion, we denote the integrand in eq. (2.26) as $\mathcal{L}$ and then K_d can be expressed as

$$\frac{1}{K_d(\ell)} \;=\; \mathcal{L} - \frac{d\mathcal{L}}{d\dot{r}}\dot{r}\,. \tag{2.93}$$

Now we vary the entanglement entropy functional (2.26) with respect to the width of the strip ℓ to find

$$\frac{dS_{GB}}{d\ell} \;=\; \frac{4\pi H^{d-2}}{\ell_{\rm P}^{d-1}}\left[\frac{1}{2}\left(1 - \frac{d\epsilon}{d\ell}\right)\mathcal{L}\Big|_{x=\frac{\ell-\epsilon}{2}} + \int_0^{\frac{\ell-\epsilon}{2}} dx\left(\frac{\delta\mathcal{L}}{\delta r}\frac{\partial r}{\partial \ell} + \frac{\delta\mathcal{L}}{\delta \dot{r}}\frac{\partial \dot{r}}{\partial \ell}\right)\right]\,. \tag{2.94}$$

[13] We refer the interested reader to section 2.7.2 for a brief discussion describing the explicit construction of such solutions.

Note that there is an extra overall factor of 2 above to since we are only integrating over half of the bulk surface, *i.e.,* from the turning point $(x, r) = (0, r_m)$ to the boundary $(x, r) = ((\ell - \epsilon)/2, r_c)$. Now surfaces extremizing eq. (2.26) will satisfy

$$\frac{\delta \mathcal{L}}{\delta r} = \frac{\partial}{\partial x}\left(\frac{\delta \mathcal{L}}{\delta \dot{r}}\right) . \tag{2.95}$$

Further eq. (2.40) still applies in the present analysis and so allows us to express $(1 - d\epsilon/d\ell)$ in terms of derivatives of the profile $r(x, \ell)$. With both of these expressions, we are able to simplify eq. (2.94) to take the form

$$\begin{aligned} \frac{dS_{GB}}{d\ell} &= \frac{4\pi H^{d-2}}{\ell_{\rm P}^{d-1}}\left[-\frac{\mathcal{L}}{\dot{r}}\frac{\partial r}{\partial \ell}\Big|_{x=\frac{\ell-\epsilon}{2}} + \left[\frac{d\mathcal{L}}{d\dot{r}}\frac{\partial r}{\partial \ell}\right]_{x=0}^{\frac{\ell-\epsilon}{2}}\right] \\ &= -\frac{4\pi H^{d-2}}{\ell_{\rm P}^{d-1} K_d(\ell)}\frac{1}{\dot{r}}\frac{\partial r}{\partial \ell}\Big|_{x=\frac{\ell-\epsilon}{2}} . \end{aligned} \tag{2.96}$$

Here the boundary term at $x = 0$ vanishes because $\dot{r} = 0$ there. Eq. (2.93) was then used to simplify the remaining terms with $K_d(\ell)$. We note that precisely the same expression as above appeared in the analysis of $dS/d\ell$ with Einstein gravity – see eq. (2.125).

The next step is to show that the ratio $\frac{1}{\dot{r}}\frac{\partial r}{\partial \ell}$ has the same simple boundary limit as found previously in eq. (2.130) with Einstein gravity. The analogous procedure would call for solving eq. (2.27) to find $\dot{r}$. However, in the present case, we would find a cubic equation in $\dot{r}^2$ and which would in general have six distinct roots. The relevant root would be that which in the limit $\lambda \to 0$ is continuously connected to the solution (2.129) found with Einstein gravity. While it is possible to carry out this procedure analytically, it is not very illuminating. Rather we note that we are interested in the behaviour near the asymptotic boundary where the geometry approaches AdS space and the conformal factor takes the form $A(r) = r/\tilde{L}$. Now it is sufficient to expand near the boundary where e^A is very large and the leading contribution to $\dot{r}$ becomes

$$\dot{r} \simeq e^{dr/\tilde{L}} K_d \left(1 - 2\lambda f_\infty\right) . \tag{2.97}$$

This equation is easily solved to yield $x(r)$ near the boundary. Of course, the integration constant is chosen to satisfy the boundary condition $x(r \to \infty) \to \ell/2$. Using this asymptotic solution for the profile of the extremal surface, it is easy to confirm that

$$\frac{1}{\dot{r}}\frac{\partial r}{\partial \ell}\Big|_{x=\ell/2} = -\frac{1}{2} , \tag{2.98}$$

as desired. Note that this relation is independent of the GB coupling λ.

Substituting eq. (2.98) into eq. (2.96), we arrive at

$$\frac{dS_{GB}}{d\ell} = \frac{2\pi H^{d-2}}{\ell_{\rm P}^{d-1}} \frac{1}{K_d(\ell)}\,, \tag{2.99}$$

which precisely matches the expression (2.131) found with Einstein gravity. It seems that this result is quite general. The first key ingredient is, of course, the conserved quantity (2.93). The other necessary ingredient is that the asymptotic geometry approaches AdS space, which seems sufficient to produce the simple expression in eq. (2.98). Hence we expect that the expression (2.99) should be general to all cases with these two basic features.

Next, we turn to the flow of c-function (2.25) as we change the minimum radius r_m of the extremal surfaces, as considered for Einstein gravity in section 2.3. Given eq. (2.99), our starting point for the c-function (2.25) is precisely the same as in eq. (2.55), *i.e.,*

$$c_d = \frac{2\,\pi\,\beta_d}{\ell_{\rm P}^{d-1}} \frac{\ell^{d-1}}{K_d(\ell)}\,, \tag{2.100}$$

Hence using eq. (2.92), we find

$$\frac{dc_d}{dr_m} = \frac{2\,\pi(d-1)\beta_d \ell^{d-2}}{\ell_{\rm P}^{d-1} K_d} \left(\frac{d\ell}{dr_m} + A'(r_m)\,\ell\right)\,. \tag{2.101}$$

Following our previous analysis, we express ℓ in terms of r_m with

$$\frac{\ell}{2} = \int_{r_m}^{\infty} \frac{dr}{\dot{r}} = \int_{r_m}^{\infty} dr \frac{1}{A'}\frac{A'}{\dot{r}}\,. \tag{2.102}$$

However, in the present case, it is not possible to use the explicit root from eq. (2.27) for $\dot{r}$ and perform the integral. Hence we define

$$F(r, r_m) = -\int_{r}^{\infty} dr \frac{A'}{\dot{r}}\,, \tag{2.103}$$

and use integration by parts in eq. (2.102) to write

$$\begin{aligned}\frac{\ell}{2} &= \left[\frac{1}{A'}F(r,r_m)\right]_{r_m}^{\infty} + \int_{r_m}^{\infty} dr \frac{A''}{A'^2} F(r,r_m) \\ &= -\frac{F(r_m,r_m)}{A'(r_m)} + \int_{r_m}^{\infty} dr \frac{A''}{A'^2} F(r,r_m)\,.\end{aligned} \tag{2.104}$$

In eq. (2.103), we have chosen the above limits on integration because the integrand vanishes at the asymptotic boundary $r = \infty$. Further, the dependence on r_m in eq. (2.103) comes from $\dot{r}(x, r_m)$. We should remind the reader that in the following discussion, our independent parameters are the profile $r(x, \ell)$ and r_m. Now differentiating eq. (2.104), we find

$$\frac{1}{2}\frac{d\ell}{dr_m} = -\frac{1}{\dot{r}}\bigg|_{r_m} - \frac{1}{A'(r_m)}\frac{\partial}{\partial r_m}F(r, r_m)\bigg|_{r_m} + \int_{r_m}^{\infty} dr \frac{A''}{A'^2}\frac{\partial}{\partial r_m}F(r, r_m)\,. \quad (2.105)$$

The first term above arises since $\partial F(r, r_m)/\partial r = A'(r)/\dot{r}$ but note that this term should be evaluated slightly away from $r = r_m$ since $\dot{r} = 0$ there. This potential divergence will be canceled below by a contribution which is revealed in the second term below. Now substituting eqs. (2.104) and (2.105) into eq. (2.101), we find

$$\frac{dc_d}{dr_m} = \frac{4\,\pi(d-1)\beta_d\,\ell^{d-2}}{\ell_{\rm P}^{d-1}K_d}\,(I_1 - I_2)\ , \quad (2.106)$$

where

$$\begin{aligned} I_1 &= \int_{r_m}^{\infty} dr \frac{A''}{A'^2}\frac{\partial}{\partial r_m}F(r, r_m) + A'(r_m)\int_{r_m}^{\infty} dr \frac{A''}{A'^2}F(r, r_m) \\ &= -A'(r_m)\int_{r_m}^{\infty} dr \frac{A''}{A'^2}\left[\int_r^{\infty} d\tilde{r}\,\frac{A'(\tilde{r})}{\dot{\tilde{r}}^2}\left(\dot{\tilde{r}} + (d-1)K_d\frac{\partial\dot{\tilde{r}}}{\partial K_d}\right)\right] \end{aligned} \quad (2.107)$$

and

$$\begin{aligned} I_2 &= \frac{1}{\dot{r}}\bigg|_{r_m} + \frac{1}{A'(r_m)}\frac{\partial}{\partial r_m}F(r, r_m)\bigg|_{r_m} + F(r_m, r_m) \\ &= \frac{1}{\dot{r}}\bigg|_{r_m} - \int_{r_m}^{\infty} dr\,\frac{A'}{\dot{r}^2}\left(\dot{r} + (d-1)K_d\frac{\partial\dot{r}}{\partial K_d}\right)\,. \end{aligned} \quad (2.108)$$

In writing these expressions, we have used $\partial\dot{r}/\partial r_m = (\partial\dot{r}/\partial K_d)(dK_d/dr_m)$, as well as eq. (2.92). Now considering the local expression for K_d in eq. (2.27), we calculate $\partial\dot{r}/\partial K_d$ keeping r fixed. Similarly, we can differentiate eq. (2.27) with respect to x, which yields an expression involving $\ddot{r}$. We find that these two quantities are related by the following:

$$\dot{r}\,A'\left(\dot{r} + (d-1)K_d\,\frac{\partial\dot{r}}{\partial K_d}\right) = \ddot{r} + 4\lambda L^2\,A'\,A''\,\dot{r}^2\,Q \quad (2.109)$$

where

$$Q \equiv \frac{\dot{r}^2 + e^{2A}}{\dot{r}^2\,(1 - 2\,\lambda L^2 A'^2) + e^{2A}(1 + 4\,\lambda L^2\,A'^2)}\,. \quad (2.110)$$

We now use eq. (2.109) to express eqs. (2.107) and (2.108) as

$$\begin{aligned} I_1 &= -A'(r_m)\int_{r_m}^{\infty}\frac{dr}{\dot r}\frac{A''}{A'^2} - 4\lambda L^2\,A'(r_m)\int_{r_m}^{\infty}dr\,\frac{A''}{A'^2}\left[\int_r^{\infty}d\tilde r\,\frac{A'(\tilde r)\,A''(\tilde r)}{\dot{\tilde r}}\,Q(\tilde r)\right], \\ I_2 &= 4\lambda L^2\int_{\infty}^{r_m}dr\,\frac{A'\,A''}{\dot r}\,Q\,, \end{aligned} \tag{2.111}$$

where we have used $\int dr\,\ddot r/\dot r^3 = -\int dx\,\partial/\partial x(1/\dot r) = -1/\dot r$. Now inserting these expression (2.111) into eq. (2.106) and then integrating by parts, we arrive to following result

$$\begin{aligned} \frac{dc_d}{dr_m} &= -\frac{4\,\pi(d-1)\beta_d\,\ell^{d-2}\,A'(r_m)}{\ell_{\rm P}^{d-1}\,K_d(r_m)}\int_{r_m}^{\infty}dr\,\frac{A''}{\dot r A'^2}\left(1-4\lambda L^2\,A'^2Q\right) \\ &= -\frac{4\,\pi\beta_d\,\ell^{d-2}\,A'(r_m)}{\ell_{\rm P}^{d-1}\,K_d(r_m)}\int_0^{\ell}dx\,\frac{1}{A'^2}\left(T^t{}_t - T^r{}_r\right)\frac{1-4\lambda L^2\,A'^2Q}{1-2\lambda L^2\,A'^2} \end{aligned} \tag{2.112}$$

Here we used the GB equations of motion, *i.e.,* eq. (2.143), to replace A'' by various components of the matter stress tensor. Note that the final result matches that in eq. (2.63) when $\lambda = 0$. However, with $\lambda \neq 0$, it is clear that the null energy condition alone (which ensures $T^t{}_t - T^r{}_r \leq 0$) is insufficient to enforce a definite sign for dc_d/dr_m. Rather we must also be able to make a clear statement about the positivity of the last factor in the integral, *i.e.,*

$$\frac{1-4\lambda L^2\,A'^2Q}{1-2\lambda L^2\,A'^2} = \frac{\dot r^2\,(1-6\,\lambda L^2A'^2)+e^{2A}}{(1-2\lambda L^2\,A'^2)(\dot r^2\,(1-2\,\lambda L^2A'^2)+e^{2A}(1+4\,\lambda L^2\,A'^2))}\,. \tag{2.113}$$

As described above, one could use eq. (2.27) to express $\dot r^2$ in terms of the conserved charge K_d and the conformal factor A, however, the resulting expression for eq. (2.113) is lengthy and unilluminating. In the limit of small λ we observe that eq. (2.113) becomes

$$\frac{1-4\lambda L^2\,A'^2Q}{1-2\lambda L^2\,A'^2} \simeq 1-2\,\lambda L^2A'^2+\cdots\,. \tag{2.114}$$

Hence it is not clear what simplification one might expect in eq. (2.112). However, this result is still suggestive in that it is easy to see that the right hand side is positive as long as $\lambda < 0$. Unfortunately, examining the full expression in eq. (2.113), we see that this simple condition does not quite guarantee that this factor is positive. Thus while we have an expression for dc_d/dr_m in GB gravity, we are not able to make a simple statement of the conditions that are necessary to ensure that the c-function flows monotonically along holographic RG flows.

2.6 Discussion

With eq. (2.25), we constructed a simple extension to higher dimensions of the c-function (2.22) considered in ref. [80, 81] for two-dimensional quantum field theories. As described in section 2.2, while the entanglement entropy itself contains a UV divergence, this expression (2.25) is finite and, at conformal fixed points, yields a central charge that characterizes the underlying conformal field theory, as had been noted previously in [62, 52]. In section 2.3, we examined the behaviour of this c-function in holographic RG flows in which the bulk theory was described by Einstein gravity. In particular, we were able to show that the flow of the c-function was monotonic as long as the matter fields driving the holographic RG flow satisfied the null energy condition. As reviewed in section 2.1, the latter condition was precisely the constraint that appears in the standard derivation of the holographic c-theorem [84, 85, 86, 87, 88].

We observe that if the bulk geometry is such that it 'slightly' violates the null energy condition over a 'small' radial regime, the integral in eqs. (2.54) or (2.63) would remain positive and hence the flow of our c-function would still be monotonic. That is, we only need the null energy condition to be satisfied in some averaged sense. Hence the null energy condition is a sufficient but not a necessary condition for the monotonic flow of the c-function (2.25). Thus there is less sensitivity to the bulk geometry is the present construction of a holographic c-theorem using the entanglement entropy than in the original discussions [84, 85, 86]. It is intriguing that when expressed as an integral over the boundary direction x, eq. (2.63) weights the contributions of the bulk stress tensor more or less equally for each interval δx in the strip. However, when the integral is expressed as an integral over the radial direction, the integrand includes an extra factor or $1/\dot{r}$, which diverges at the minimum radius r_m of the holographic surface (but the integral remains finite). Hence in the holographic flows, the c-function responds sensitively to changes in the geometry near this radius in the bulk – a result that can be seen in the explicit flows discussed in section 2.4. Hence given the holographic connection between radius in the bulk and energy scales in the boundary theory, it seems clear that the flow of this c-function is most sensitive to the lowest energy modes probed by the entanglement entropy.

Our result for the monotonic flow of c-function in section 2.3 refers to the derivative dc_d/dr_m, *i.e.,* changes in c_d as we change the minimum energy scale probed by the entanglement entropy. To describe the flow of c_d completely in terms of the boundary theory, we would actually like to establish $dc_d/d\ell \leq 0$, *i.e.,* the c-function decreases monotonically as we increase the width of the strip for which the entanglement entropy is evaluated. In this case, we would be using the width ℓ as a proxy for the relevant energy scale along the RG flow. The desired result can be established in the present holographic framework, however,

as discussed in section 2.4, one must be careful to restrict attention to the physical saddle points in evaluating the entanglement entropy. We showed there that extremal surfaces can arise for which $d\ell/dr_m > 0$ and hence $dc_d/d\ell > 0$. However, these saddle points do not contribute when one evaluates the holographic entanglement entropy with eq. (1.56) since they are never the minimum area surface. Rather the appearance of these 'unstable' saddle points signals a first order 'phase transition' in the entanglement entropy. As a result, c_d drops discontinuously at some critical value ℓ_t of the width of the strip and the monotonic 'flow' of the c-function is preserved.

While we have only illustrated this behaviour with specific examples in section 2.3, it seems clear that the physical entanglement entropy will never be determined by such saddle points. In particular, if we are studying a holographic RG flow between two AdS geometries, we will always find $d\ell/dr_m < 0$ when r_m is well into either of these two asymptotic regions. Hence as argued in section 2.4.2, if extremal surfaces arise for which $d\ell/dr_m > 0$, it indicates that there are a number of competing saddle points in the corresponding regime. First $\ell(r_m)$ is a single-valued function since the conserved charge (2.27) dictates that there is a unique surface for each value of r_m. Hence if we assume this is a smooth function, there will always be (at least) three competing saddle points when $d\ell/dr_m > 0$. It then becomes inevitable that there will be a phase transition in the corresponding regime of ℓ. Further we note that

$$\frac{dS}{dr_m} = \frac{H^{d-2}}{\ell^{d-1}} \frac{c_d}{\beta_d} \frac{d\ell}{dr_m} \,. \tag{2.115}$$

The first two factors above are positive definite and hence the sign of dS/dr_m is controlled entirely by $d\ell/dr_m$. Given this result, it is straightforward to argue that the behaviour illustrated in figure 2.4 is in fact generic. That is, the phase transition goes between the two branches for which $d\ell/dr_m < 0$. Hence we have argued that given $dc_d/dr_m \geq 0$, it also follows that $dc_d/d\ell \leq 0$ for RG flows dual to Einstein gravity.

One may be concerned that the phase transitions noted above are an artifact of choosing a background geometry in the bulk which is unphysical in some way. However, with our analysis in section 2.4 and section 2.7.3, we argued that the phase transitions can arise for holographic backgrounds that have a natural interpretation as an RG flow in the boundary theory, but also for backgrounds where the interpretation seems to be more exotic. While this interpretation was explicitly shown to apply in examples of phase transitions with the boundary dimension $d \geq 3$, constructing further examples to extend this result to $d = 2$ does not seem difficult. However, we note that these phase transitions are undoubtedly effect of the large N limit which is implicit in our constructions. However, it may still be that similar behaviour, *i.e.,* rapid transitions in the entanglement entropy, persists in the RG flows of more conventional physical systems. In any event, it would be interesting

to better understand these phase transitions in the holographic systems. Such a transition seems to indicate that quantum correlations in underlying degrees of freedom change dramatically at some particular energy scale in the RG flow.

It is worthwhile noting that phase transitions in the holographic entanglement entropy of the kind found here and in [46] for RG flows also arise in a variety of other holographic constructions. The simplest example is to consider the case where the entangling surface contains two disjoint regions. When the two regions are relatively close together, saddle point determining the holographic entanglement entropy will be a single connected bulk surface. However, as the two regions are moved apart, there is a phase transition to a second saddle point consisting of two separate bulk surfaces [58]. A similar phase transition was also found in considering the holographic entanglement entropy of the strip geometry for a bulk background corresponding to a confining phase of the boundary theory [54, 70]. There is a strong similarity between the results for these confining theories and the present RG flows since the phase transition again arises as the width to the strip passes through some critical value and results in a discontinuous drop in the central charge c_d. Further, in both cases, the phase transition can be interpreted as being produced by a rapid and drastic restructuring in the correlations of the low energy degrees of freedom (in comparison to high energy correlations). Similar results were also found for other entangling geometries, *i.e.,* a circular surface in three-dimensional confining boundary theory [126]. Finally similar phase transitions in the entanglement entropy have also been found in holographic superconductors as the temperature is varied [127] and in the time evolution of holographic quantum quenches [128].

In section 2.5, we considered extending our results to holographic models where the gravitational theory in the bulk is Gauss-Bonnet gravity (2.10). While it is straightforward to construct an expression (2.112) for dc_d/dr_m in GB gravity, it is evident that the null energy condition is not sufficient to guarantee a monotonic flow of the c-function. Unfortunately, eq. (2.112) does not lend itself to a simple statement of the conditions that would necessary to ensure that the c-function flows monotonically along holographic RG flows in these models. Further insight into this question may be provided by examining explicit holographic RG flows. In section 2.4, we assumed that the holographic backgrounds were solutions of Einstein gravity and hence the entanglement entropy is determined by eq. (1.56). We could just as easily assume that the same backgrounds are solutions of GB gravity and examine the behaviour of the c-function defined by eq. (1.63). In particular, it would be interesting to see if there are violations of the monotonic flow of the c-function in certain parameter regimes.

Of course, it may not be a surprise that the monotonic flow of the c-function (2.25) is not directly connected to the null energy condition in GB gravity. As described in

section 2.1, an important feature of this theory is that at conformal fixed points, the dual boundary theory has two distinct central charges, given in eqs. (2.14) and (2.15). Using the null energy condition, ref. [87, 88] established that the charge denoted a^*_d would satisfy a c-theorem in these holographic models. However, in section 2.2, we found that the c-function (2.25) actually corresponds to a nonlinear combination of both central charges. Hence as we noted at the outset, it was improbable that a simple holographic c-theorem could be established for GB gravity with the present construction. Setting holography aside, it is known that for four-dimensional quantum field theories, there is no possible (linear) combination of the two central charges, $c = C_{\rm T}$ and $a = a^*_d$, that can satisfy a c-theorem other than a alone [39].

Of course, GB gravity only provides an interesting extension of the usual holographic framework for $d \geq 4$. For smaller values of d, the curvature-squared interaction (2.11) does not contribute to the gravitational equations of motion because of the topological origin of this term. It may be of interest to study the behaviour of our c-function for other gravity theories with higher curvature interactions for $d = 2$ and 3. Interesting families of holographic models were considered with higher curvature theories of the three-dimensional gravity in [129, 130, 131]. A defining feature of these theories was that the dual $d = 2$ boundary theory should exhibit a c-theorem. Hence these models may provide an interesting holographic framework to examine the RG flow of c_2. However, the work of [80, 81] indicates that this flow must be monotonic for any unitary and Lorentz invariant quantum field theory and so confirming this result here would really be a test that these holographic models define reasonable boundary theories.

Our construction of the c-function (2.25) can be applied quite generally, *i.e.,* outside of the context of holography. While the RG flow of c_d is not expected to be monotonic in a generic setting, we observe that the flow can be constrained somewhat following the analysis of [80, 81]. In particular, let us define a new (dimensionful) function of the following form in arbitrary d:

$$\hat{c}_d \equiv \frac{c_d}{\ell^{d-2}} = \frac{\beta_d}{H^{d-2}} \ell \frac{dS}{d\ell} \,. \tag{2.116}$$

Of course, for $d = 2$, we have $\hat{c}_2 = c_2$. In any event, we can apply directly the analysis of [80, 81] to show that $d\hat{c}_d/d\ell \leq 0$ for any d. There, the authors considered unitary and Lorentz invariant field theories and used sub-additivity of the entanglement entropy to show that $\hat{c}_2$ is a monotonically decreasing function as ℓ increases. In particular, they considered two specific surfaces b and c with a relative boost, as shown in figure 2.8. Further a and d chosen as constant time surfaces in some frame so that they are Cauchy surfaces whose causal development corresponds to the intersection and union of the causal development of the original two boosted surfaces. By construction the surfaces a, b and

c just touch the boundary of the causal development of d on either end. Two important observations are: First, if we are evaluating the entanglement entropy for these segments in the Lorentz invariant vacuum state, then it should only depend on the proper length of the corresponding interval. Second, the entanglement entropy of any of these surfaces will be the same as for any other Cauchy surface of the corresponding domains since the time evolution is assumed to be unitary. Now the authors of [80, 81] show that sub-additivity of the entanglement entropy of these regions imposes the following relation

$$S(b) - S(a) \geq S(\alpha b) - S(\alpha a)\,, \tag{2.117}$$

where they introduce the ratio of the proper lengths $\alpha = c/a = d/b \geq 1$. Now if the relative boost is taken to be small, this relation implies that $\ell\, dS/d\ell = c_2/3 = \hat{c}_2/3$ must decrease with increasing ℓ. Now these elegant arguments can also be applied without change in considering the entanglement entropy for the strip geometry in arbitrary dimensions, as long as the boundaries of the strip are orthogonal to the boost direction. That is, the segments a, b, c and d in figure 2.8 now represent the orthogonal cross-section of four specific strips. Hence with the previous arguments, we will recover the relation (2.117) for arbitrary dimensions. This implies that with the strip geometry in arbitrary dimensions, we have $d\hat{c}_d/d\ell \leq 0$ — the same observation was made in [54]. While we cannot conclude that the original c-function (2.25) must decrease with increasing ℓ, using eq. (2.116), we find an upper bound on the rate at which c_d could increase:

$$\ell\, \frac{dc_d}{d\ell} \;\leq\; (d-2)\, c_d\,. \tag{2.118}$$

This bound applies to any d-dimensional quantum field theory, subject to the provisos of Lorentz invariance, unitarity and sub-additivity of entanglement entropy.

An important feature of the entanglement entropy (2.23) for the strip geometry is that it contains a single divergent term which is independent of the width ℓ. As a result of this simple structure, the single derivative in eq. (2.25) produces a UV finite or regulator independent c-function. Now for a general smooth entangling surface, the structure of the divergent contributions to the entanglement entropy at a conformal fixed point is more complicated, as given by (1.53),

$$S \;=\; \frac{p_{d-2}}{\delta^{d-2}} + \frac{p_{d-4}}{\delta^{d-4}} + \ldots + \begin{cases} \frac{p_1}{\delta} + p_0 + \mathcal{O}(\delta) & \text{for odd } d\,, \\ \frac{p_2}{\delta^2} + p_0 \log\left(\frac{\ell}{\delta}\right) + \mathcal{O}(1) & \text{for even } d\,, \end{cases} \tag{2.119}$$

where δ is the short distance cut-off (and ℓ is some IR scale). Of course, to produce a dimensionless entanglement entropy, the coefficients p_n must have dimension length^n. At

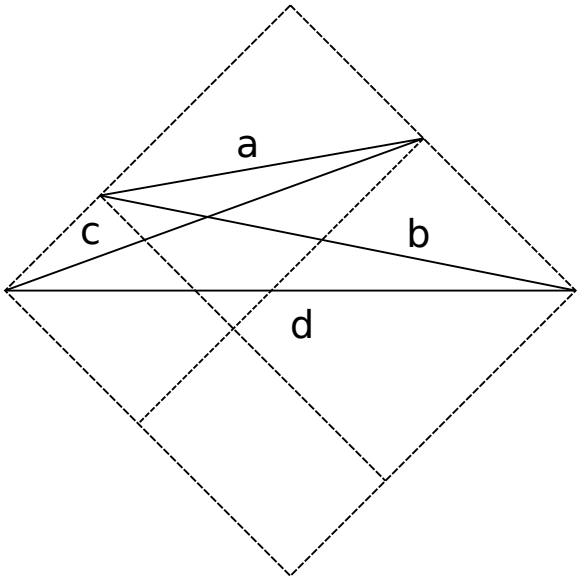

Figure 2.8: Here the boosted surfaces b and c are drawn with time and space on the vertical and horizontal axes, respectively. The casual development of the strips d and a contain the union and intersection of the causal development of b and c. The causal development for each of these surfaces is outlined with dashed lines.

a conformal fixed point, this dimensionful character is provided by scales arising from the geometry of the entangling surface and the background spacetime. For example, the first term yields the celebrated area law with $p_{d-2} \propto \mathcal{A}$, where $\mathcal{A}$ is the area of the entangling surface. If we move away from a conformal fixed point, there will be additional dimensionful couplings in underlying theory and the divergence structure of the entanglement entropy can become substantially more complicated. For example, in a holographic setting, the additional complications of relevant operators were illustrated in [47].

Of course, the conjecture by [87, 88] proposes that a central charge, which is identified using the entanglement entropy, should satisfy a c-theorem (2.1) in higher dimensions . In particular, the prescription there specifies that the entangling surface should be a (d–2)-sphere of radius R in flat space.[14] However the universal central charge was identified with the dimensionless coefficient p_0 which only appears at subleading order in eq. (2.119) for $d \geq 3$. Further since R is the only scale in the problem, one expects all of the preceding coefficients are nonvanishing with $p_n = \tilde{p}_n R^n$ for some dimensionless coefficients $\tilde{p}_n$. Hence

[14]The applicability of this geometry to the c-theorem conjectured in [87, 88] follows from the results of [59].

a single derivative with respect to the radius of the sphere will not isolate the desired coefficient in the entanglement entropy. Certainly a more sophisticated construction would be needed to remove all of the potentially divergent terms along a general RG flow. In fact, precisely such a construction was recently proposed in [46]. It would be interesting to investigate this new proposal along the lines of the analysis in sections 2.3 and 2.5. In particular, it would encouraging if the monotonic flow of the c-function identified with this construction or a similar variant could be directly related to null energy condition in holographic RG flows.

2.7 Supplementry material for Chapter 2

2.7.1 The c-function with Einstein gravity for $d \geq 3$

In this section, we describe the details of the derivation of eq. (2.55), which is our starting point for the discussion in section 2.3 of the holographic flow of the c-function in higher dimensions. The analysis here is largely an extension of that given there for $d = 2$ to an arbitrary d. For a d-dimensional boundary field theory, the holographic entanglement entropy of the strip is given by

$$S = \frac{4\pi H^{d-2}}{\ell_{\rm P}^{d-1}} \int_0^{(\ell-\epsilon)/2} dx\; e^{(d-2)A(r)}\, \sqrt{\dot{r}^2 + e^{2A(r)}} \tag{2.120}$$

and the conserved charge (2.27) reduces to

$$K_d = e^{-dA(r)} \sqrt{\dot{r}^2 + e^{2A(r)}}\,. \tag{2.121}$$

Further, for a particular extremal surface, $K_d = e^{-(d-1)A(r_m)}$ since at the turning point we have $r(0,\ell) = r_m$ and $\dot{r}(0,\ell) = 0$.

Now we differentiate the entropy (2.120) with respect to the width ℓ while holding the radial cut-off r_c fixed. In doing so, we keep in mind that both the radial profile for the surface and the cut-off in x are implicitly functions of the width ℓ, *i.e.*, $r = r(x,\ell)$ and $\epsilon = \epsilon(\ell)$. Hence we find

$$\frac{dS}{d\ell} = \frac{4\,\pi H^{d-2}\, e^{(d-2)A(r)}}{\ell_{\rm P}^{d-1}\, \sqrt{\dot{r}^2 + e^{2A(r)}}} \left[\frac{1}{2}\left(1 - \frac{d\epsilon}{d\ell}\right)(\dot{r}^2 + e^{2A(r)}) + \dot{r}\,\frac{\partial r}{\partial \ell}\right]\Bigg|_{x=(\ell-\epsilon)/2}, \tag{2.122}$$

where $\dot{r} = \partial r(x,\ell)/\partial x$. In simplifying $dS/d\ell$ to produce the expression above, we have used $\dot{r}(0,\ell) = 0$ to eliminate the boundary terms at $x = 0$, as well as removing the bulk variation using the equation of motion which follows from eq. (2.120),

$$\ddot{r} - A' \left(d\,\dot{r}^2 + (d-1)\, e^{2A} \right) \;=\; 0\,. \tag{2.123}$$

The cut-off ϵ is defined by the relation: $r(x = (\ell-\epsilon)/2, \ell) = r_c$. We can vary ℓ in the latter expression while holding r_c fixed, as in the variation in eq. (2.122), to find

$$\left[\frac{\dot{r}(x,\ell)}{2} \left(1 - \frac{d\epsilon}{d\ell} \right) + \frac{\partial r(x,\ell)}{\partial \ell} \right] \Bigg|_{x=(\ell-\epsilon)/2} \;=\; 0\,. \tag{2.124}$$

This result was already presented in eq. (2.40). Using this expression and also eq. (2.121), we can now simplify eq. (2.122) to take the form

$$\frac{dS}{d\ell} \;=\; -\frac{4\,\pi H^{d-2}}{\ell_{\rm P}^{d-1} K_d(\ell)}\, \frac{1}{\dot{r}}\, \frac{\partial r}{\partial \ell} \Bigg|_{x=(\ell-\epsilon)/2}\,. \tag{2.125}$$

Further progress requires that we consider the bulk geometry in the far UV region, which we assume approaches AdS space asymptotically with

$$A(r) \;=\; r/\tilde{L}\,. \tag{2.126}$$

Now recall that eq. (2.121) yields a simple expression for dx/dr, as presented in eq. (2.65). With the simple conformal factor (2.126), this equation is easily integrated to yield

$$x - \frac{\ell}{2} \;=\; -\frac{\tilde{L}\, e^{-dr/\tilde{L}}}{d\, K_d(\ell)}\; {}_2F_1\left[\frac{1}{2}, \frac{d}{2(d-1)}; \frac{3d-2}{2(d-1)}; \frac{e^{-2(d-1)r/\tilde{L}}}{K_d(\ell)^2} \right]\,, \tag{2.127}$$

where we are imposing the boundary condition that $x \to \ell/2$ as $r \to \infty$. We note that the same hypergeometric function appears in eq. (2.60). This is not a coincidence because in the present case A' is simply a constant and so we are essentially performing the same integration here as in eq. (2.60). Further note that this complicated expression reduces to eq. (2.66) for $d = 2$. Taking the partial derivative of eq. (2.127) with respect to ℓ, we find

$$\begin{aligned} \frac{\partial r(x,\ell)}{\partial \ell} \;=\; & -\frac{1}{2}\, e^{dr/\tilde{L}} \sqrt{K_d^2 - e^{-2(d-1)r/\tilde{L}}} \\ & + \frac{\tilde{L}}{(d-1)K_d}\, \frac{dK_d}{d\ell} \left(\frac{\sqrt{K_d^2 - e^{-2(d-1)r/\tilde{L}}}}{d\, K_d}\; {}_2F_1\left[\frac{1}{2}, \frac{d}{2(d-1)}; \frac{3d-2}{2(d-1)}; \frac{e^{-2(d-1)r/\tilde{L}}}{K_d(\ell)^2} \right] - 1 \right) \end{aligned} \tag{2.128}$$

Now using eq. (2.121) with the conformal factor (2.126), we find

$$\dot{r} \;=\; e^{dr/\tilde{L}}\,\sqrt{K_d^2 - e^{-2(d-1)r/\tilde{L}}}\,. \tag{2.129}$$

Then we consider the ratio of these two expressions and take the limit $x \to \ell/2$ and $r \to \infty$ to find

$$\frac{1}{\dot{r}}\frac{\partial r}{\partial \ell}\bigg|_{x=\ell} \;=\; -\frac{1}{2}\,. \tag{2.130}$$

Essentially this result indicates that with the limit $r_c \to \infty$, $d\epsilon/d\ell$ vanishes in eq. (2.124). Now substituting eq. (2.130) into eq. (2.125) yields

$$\frac{dS}{d\ell} \;=\; \frac{2\,\pi H^{d-2}}{\ell_{\rm P}^{d-1}}\,\frac{1}{K_d(\ell)}\,. \tag{2.131}$$

We use this simple form of derivative of entanglement entropy to produce the expression for the c-function in eq. (2.55).

2.7.2 RG flow solutions for GB gravity

In section 1.3.1 of previous chapter, we discussed the RG flow in the AdS/CFT correspondence, where dual gravity is Einstein gravity. Now, we are interested in holographic RG flow solutions for the action (2.10) in which GB gravity is coupled to a scalar field, *i.e.,*

$$I = \frac{1}{2\ell_{\rm P}^{d-1}}\int d^{d+1}x\sqrt{-g}\left[R + \frac{\lambda L^2}{(d-2)(d-3)}\mathcal{X}_4 - \frac{1}{2}\left(\partial\phi\right)^2 - V(\phi)\right]\,, \tag{2.132}$$

where $\mathcal{X}_4$ is given by eq. (2.11). First, we will examine the equations of motion for holographic RG flows in some detail. This will allow us to explicitly verify the result used in eq. (2.19) to prove the holographic c-theorem for GB gravity [87, 88]. Then we discuss a simple approach to explicitly construct analytic solutions for GB gravity describing holographic RG flows. This construction is a simple extension of the 'superpotential' approach developed for Einstein gravity in [28, 29]. This approach was already extended to GB gravity with four boundary dimensions in [132] and here we provide the generalization to arbitrary $d \geq 4$.

In the action (2.132) above, the cosmological constant term has been absorbed into the scalar potential and we assume that $V(\phi)$ has various critical points where the potential energy is negative as in eq. (1.28). As described in section 2.1, for each of these critical

points, there is an AdS vacuum solution where the curvature scale is given by $\tilde{L}^2 = L^2/f_\infty$ where L is some canonical scale appearing in the potential and the curvature squared interaction while the (dimensionless) constant f_∞ is given by eq. (2.13). To consider solutions describing holographic RG flows, we begin by writing the scalar and gravitational equations of motion as

$$\nabla^2\phi - \frac{\delta V}{\delta\phi} = 0\,, \tag{2.133}$$

$$R_{ab} - \frac{1}{2}R g_{ab} + \frac{\lambda L^2}{(d-2)(d-3)} H_{ab} = T_{ab}\,, \tag{2.134}$$

where

$$H_{ab} = R_{acde}R_b{}^{cde} - 2R_{ac}R_b{}^c - 2R_{acbd}R^{cd} + RR_{ab} - \frac{1}{4}\mathcal{X}_4 g_{ab}\,. \tag{2.135}$$

Further the stress tensor for the scalar field is given by

$$T_{ab} = \frac{1}{2}\partial_a\phi\,\partial_b\phi - \frac{1}{2}\,g_{ab}\left(\frac{1}{2}\,(\partial\phi)^2 + V(\phi)\right)\,. \tag{2.136}$$

As in the main text, we consider the following ansatz for the metric:

$$ds^2 = e^{2A(r)}\,\eta_{ij}\,dx^i dx^j + dr^2\,, \tag{2.137}$$

For nontrivial RG flows, we also include a simple ansatz for the scalar: $\phi = \phi(r)$. In particular then, this ansatz maintains Lorentz invariance in the boundary directions. Now with these metric and scalar ansatz, there are two nontrivial components of the gravitational equations (2.134):

$$d(d-1)(A'^2 - \lambda L^2\,A'^4) = 2\,T_r{}^r\,, \tag{2.138}$$

$$2\,(d-1)(1-2\,\lambda L^2\,A'^2)A'' + d(d-1)(A'^2 - \lambda L^2\,A'^4) = 2\,T_t{}^t\,. \tag{2.139}$$

Again 'prime' denotes a derivative with respect to r. Using eq. (2.136), we find the following components of stress tensor

$$T_r{}^r = \frac{1}{4}(\phi')^2 - \frac{1}{2}V(\phi)\,, \tag{2.140}$$

$$T_i{}^j = -\,\delta_i{}^j\left(\frac{1}{4}(\phi')^2 + \frac{1}{2}V(\phi)\right)\,. \tag{2.141}$$

With the present ansatz, the equation of motion for the bulk scalar (2.133) becomes

$$\phi'' + d\,A'\,\phi' - \frac{\delta V}{\delta\phi} = 0\,. \tag{2.142}$$

Of course, the three equations of motion above are not all independent. For example, one can derive eq. (2.139) by differentiating eq. (2.138) and then substituting in eqs. (2.138) and (2.142).

Taking the difference of eqs. (2.138) and (2.139), we find

$$T_t^{\,t} - T_r^{\,r} \;=\; (d-1)(1-2\,\lambda L^2\,A'^2)A''\,, \tag{2.143}$$

which is the result used to establish the holographic c-theorem for GB gravity in eq. (2.19). Eqs. (2.138), (2.139) and (2.143) are written for GB gravity coupled to a general matter field Lagrangian and as long as the matter sector satisfies the null energy condition, the combination of components of T_{ab} in eq. (2.143) are negative (or zero). In the particular case considered here, *i.e.,* the action (2.132) with a scalar field, we find $T^t{}_t - T^r{}_r = -(\phi')^2/2$ and so the sign of eq. (2.143) is obvious.

Given eqs. (2.138–2.142), a simple set of explicit solutions can be constructed by extending an approach developed for Einstein gravity in [28, 29]. The key idea is to consider a special class of scalar potentials that can be defined in terms of a 'superpotential' and then express the solution in terms of this superpotential. This construction was extended from Einstein gravity to GB gravity in five dimensions (*i.e.,* $d = 4$) in [132] and here we provide the generalization to arbitrary $d \geq 4$. First, we write the scalar potential in terms of a superpotential $W(\phi)$ as follows:

$$V(\phi) = 2\,(d-1)^2\,\left(\frac{\delta W}{\delta\phi}\right)^2\,\left(1-2\,\lambda L^2 W^2\right)^2 - d(d-1)W^2\,(1-\lambda L^2\,W^2)\,. \tag{2.144}$$

With a potential of this form, the equations of motion above can be re-expressed as first order equations:

$$\begin{aligned} \phi' &= -2\,(d-1)\,\left(1-2\,\lambda L^2\,W^2\right)\,\frac{\delta W}{\delta\phi}\,, \\ A' &= W\,. \end{aligned} \tag{2.145}$$

Given these first order equations, we may now solve for the metric (2.137) and the scalar profile in quadratures. We note that the same equations appear in the construction of domain wall solutions for 'new massive gravity' in higher dimensions [133]. The action studied there differs from the GB action (2.132) by the addition of an action proportional to the square of the Weyl tensor, *i.e.,* $-\frac{\lambda\,L^2}{(d-2)(d-3)}C_{abcd}C^{abcd}$. This additional interaction does not influence the equations of motion in the present setting because the metric ansatz (2.137) for the holographic RG flows is conformally flat.

2.7.3 Scalar potentials for section 2.4.2

In section 2.4.2, we analyzed the flow of the entanglement entropy in various bulk geometries which were defined by specifying an explicit conformal factor, *e.g.,* as in eq. (2.82). Here we would like to show that these profiles can arise as solutions of Einstein gravity coupled to a scalar field with an appropriate potential. In particular, we use the 'superpotential' approach described in section 1.3.1 and at the end of the last section.

With $\lambda = 0$, the expression of scalar potential and equations of motion in terms of the superpotential are give by (1.39) and (1.40). Now using these equations, we would like to construct $V(\phi)$ given $A(r)$. First from eq. (1.40), we find

$$A'' = \frac{\delta W}{\delta \phi}\,\phi' = -2(d-1)\,\left(\frac{\delta W}{\delta \phi}\right)^2 = -\frac{1}{2(d-1)}\,(\phi')^2\,. \tag{2.146}$$

Hence if we let $\phi = \phi_{\rm UV}$ at the critical point in the UV, *i.e.,* $\phi(r \to \infty) \to \phi_{\rm UV}$, then we can write

$$\phi(r) \;=\; \phi_{\rm UV} - \int_r^\infty d\tilde{r}\,\phi'(\tilde{r}) \;=\; \phi_{\rm UV} - \int_r^\infty d\tilde{r}\,\Big[-2(d-1)\,A''(\tilde{r})\Big]^{1/2}\,. \tag{2.147}$$

Similarly combining eq. (1.39) with eqs. (1.40) and (2.146), we may write the value of potential along the flow as

$$V(r) = -(d-1)\,A'' - d(d-1)\,(A')^2\,. \tag{2.148}$$

Given these two expressions, one can easily make a parametric plot of the potential V as a function of ϕ, at least over the range of the scalar covered in the holographic flow. Alternatively, if eq. (2.147) can be integrated analytically and inverted, *i.e.,* one can write $r = r(\phi)$, then eq. (2.148) will yield an analytic expression for $V(\phi)$. We use both of these approaches to describe the potential corresponding to the conformal factors presented in section 2.4.2.

Let us begin with the conformal factor given in eq. (2.82). In this case, it is straightforward to integrate eq. (2.147) with the result being

$$\tan\left(\frac{\pi}{2}\,\frac{\phi}{\phi_{\rm UV}}\right) \;=\; e^{r/R} \qquad \text{with} \quad \phi_{\rm UV} = \pi\,\sqrt{2\gamma(d-1)}\,. \tag{2.149}$$

We also note that at the far IR of the holographic flow, $\phi \to 0$ as $r \to -\infty$. Given this expression (2.149) and the conformal factor (2.82), it is straightforward to calculate the

superpotential $W(\phi)$ using eq. (1.40),

$$W(\phi) = \frac{1}{L} + \frac{\gamma}{R}\cos\left(\pi\frac{\phi}{\phi_{\rm UV}}\right) , \tag{2.150}$$

and the potential $V(\phi)$ using eq. (2.148),

$$V(\phi) = \frac{(d-1)\gamma}{R^2}\sin^2\left(\pi\frac{\phi}{\phi_{\rm UV}}\right) - d(d-1)\left[\frac{1}{L} + \frac{\gamma}{R}\cos\left(\pi\frac{\phi}{\phi_{\rm UV}}\right)\right]^2 . \tag{2.151}$$

Hence we have produced a analytic result for the scalar potential necessary to produce the bulk geometry with $A(r)$ as in eq. (2.82) as a solution of Einstein gravity. In figure 2.9, the curve with $\sigma = 1$ illustrates the behaviour of the potential (2.151). Figure 2.10 also shows the potential for various values of the parameters.

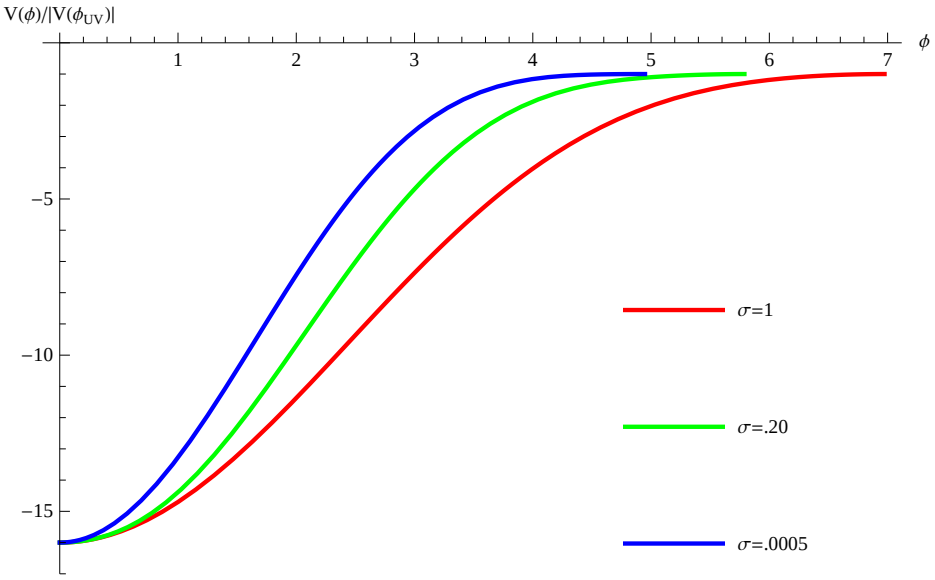

Figure 2.9: A parametric plot of $V(\phi)/|V_{\rm UV}|$ versus ϕ for eq. (2.152) with various values of parameter σ. The other parameters in the potential are set to $L = .40$, $R = .55$ and $\gamma = .825$, as well as setting $d = 4$.

Now let us consider the conformal factor given in eq. (2.90). Using the same equations

as before, we now find

$$\begin{aligned} \frac{d\phi}{dr} &= \frac{2\sqrt{\gamma(d-1)}}{R}\,\frac{\sqrt{1+\sigma\cosh(2r/R)}}{\sigma+\cosh(2r/R)} \\ V(r) &= \frac{2\gamma(d-1)}{R^2}\,\frac{1+\sigma\cosh(2r/R)}{(\sigma+\cosh(2r/R))^2} - d(d-1)\left(\frac{1}{L}-\frac{\gamma}{R}\,\frac{\sinh(2r/R)}{\sigma+\cosh(2r/R)}\right)^2 . \end{aligned} \tag{2.152}$$

In this case, we were not able to analytically integrate ϕ'. However, it is straightforward to perform a numerical integration and produce a parametric plot of the potential V as a function of ϕ, as shown in figure 2.9. In this figure, the boundary dimension was chosen to be $d = 4$ and the potential parameters are fixed as $L = .40$, $R = .55$ and $\gamma = .825$, while σ is varied as indicated on the plot. The plot shows that qualitatively this potential has the same shape as the analytic potential found for the previous conformal factor in eq. (2.151) – recall that in fact, this new potential will agree with eq. (2.151) when $\sigma = 1$. However, the new potential is becoming steeper as the parameter σ becomes smaller. The plots only show the potential over the range relevant for the holographic RG flow, *i.e.,* from $\phi = \phi_{\rm IR} = 0$ to $\phi_{\rm UV}$. However, the full potential would be symmetric about both $\phi_{\rm IR}$ and $\phi_{\rm UV}$ and so it would be periodic with a period $\Delta\phi = 2(\phi_{\rm UV} - \phi_{\rm IR})$. Further we note that for the parameters chosen in figure 2.9, the entanglement entropy undergoes a phase transition for $\sigma = .0005$ but there is no phase transition for either $\sigma = .2$ or 1.

While we were not able to produce an analytic expression for the full potential from eq. (2.152), it is still possible to consider a perturbative expansion around the UV critical point, *i.e.,*

$$V(\delta\phi) = V_{\rm UV} + \frac{1}{2}\,m^2_{\rm UV}\,\delta\phi^2 + \frac{1}{24}\,\lambda_{\rm UV}\,\delta\phi^4 + \cdots , \tag{2.153}$$

where $\delta\phi = \phi - \phi_{\rm UV}$. One can easily verify that there are no odd powers of $\delta\phi$ appearing in this expansion. As an example, we note that the mass parameter above would be calculated as

$$m^2_{\rm UV} = \left.\frac{\delta^2 V}{\delta\phi^2}\right|_{\phi=\phi_{\rm UV}} = \left.\frac{1}{\phi'}\,\frac{d}{dr}\left(\frac{1}{\phi'}\,\frac{dV}{dr}\right)\right|_{r\to\infty} . \tag{2.154}$$

The results for the first few parameter is the expansion (2.153) are:

$$\begin{aligned} V_{\rm UV} &= -\frac{d(d-1)}{L^2_{UV}}\,, \qquad\qquad m^2_{\rm UV} = \frac{1}{R^2} - \frac{d}{L_{UV}R} \\ \lambda_{\rm UV} &= -\frac{3d\,\sigma^2\,L_{UV}R + d(2-7\sigma^2)\,L_{IR}R - 8(1-2\sigma^2)\,L_{IR}L_{UV}}{2(d-1)\sigma^2\,(L_{UV}-L_{IR})R^3}\,, \end{aligned} \tag{2.155}$$

where we are using the expressions in eq. (2.83) for L_{UV} and L_{IR}. Of course, the value of $V_{\rm UV}$ above corresponds to the expected value of the cosmological constant in the asymptotic AdS geometry. We note that the mass parameter $m^2_{\rm UV}$ is independent of the extra parameter σ appearing in the conformal factor (2.90). Hence these first two parameters precisely match those in the analogous expansion of the analytic potential in eq. (2.151), as is readily verified. As shown in eq. (2.155), the additional parameter σ first makes its appearance the quartic coupling $\lambda_{\rm UV}$. In this case, one can still verify that $\lambda_{\rm UV}(\sigma = 1)$ matches the analogous quartic coupling found in expanding the analytic potential (2.151) about $\phi = \phi_{\rm UV}$. To provide some qualitative insight for this quartic coupling, we add that typically (*e.g.,* for the parameters chosen in figure 2.9), $\lambda_{\rm UV}$ is negative for $\sigma \sim 1$ but it becomes positive for small values of σ (and diverges as $\sigma \to 0$).

At this point, we would like to consider the holographic interpretation of these geometries in more detail. Recall that the standard description begins with a discussion in the boundary theory where a UV critical point is perturbed by some relevant operator $\mathcal{O}$ and the latter triggers an RG flow to a new critical point in the IR. A natural assumption in this discussion is that $\mathcal{O}$ is relevant, *i.e.,* that it has a conformal dimension $\Delta < d$. Now in the gravity description, as discussed in section 1.3.1, this operator is dual to the bulk scalar ϕ and the conformal dimension is related to the scalar mass by the standard formula $m^2_{\rm UV} L^2_{UV} = \Delta(\Delta - d)$ [26]. Inverting the latter relation yields two roots for Δ, *i.e.,*

$$\Delta_\pm = \frac{d}{2} \pm \sqrt{\frac{d^2}{4} + m^2_{\rm UV} L^2_{UV}}\,, \tag{2.156}$$

where the standard choice corresponds to $\Delta = \Delta_+$. The scalar will have two independent solutions asymptotically [26],

$$\phi \simeq e^{\Delta_- r/L_{UV}}\, \phi^{(-)} + e^{\Delta_+ r/L_{UV}}\, \phi^{(+)}\,, \tag{2.157}$$

where the coefficient of the more slowly decaying solution $\phi^{(-)}$ corresponds to the coupling for the dual operator while $\phi^{(+)}$ is proportional to the expectation value $\langle \mathcal{O} \rangle$.

Now turning to the scalar mass in eq. (2.155), we observe that the result can be written as $m^2_{\rm UV} L^2_{UV} = \alpha(\alpha - d)$ where $\alpha = L_{UV}/R$. Further by combining eq. (2.91) and $\phi' \propto \sqrt{-A''}$ from eq. (2.146), we see that α is precisely the exponent controlling the asymptotic decay of $\delta\phi$. Now there are four regimes of α which we consider separately: (a) $0 < \alpha \leq d/2$, (b) $d/2 < \alpha < (d+2)/2$, (c) $(d+2)/2 < \alpha < d$ and (d) $d \leq \alpha$. In the interval (a), the holographic interpretation of the flow geometry precisely matches that described above. That is, $\alpha = \Delta_-$ with $\Delta_+ = d - \Delta_- < d$. Hence the dual operator is relevant and leading contribution in the asymptotic decay of $\delta\phi$ reflects the fact that corresponding coupling

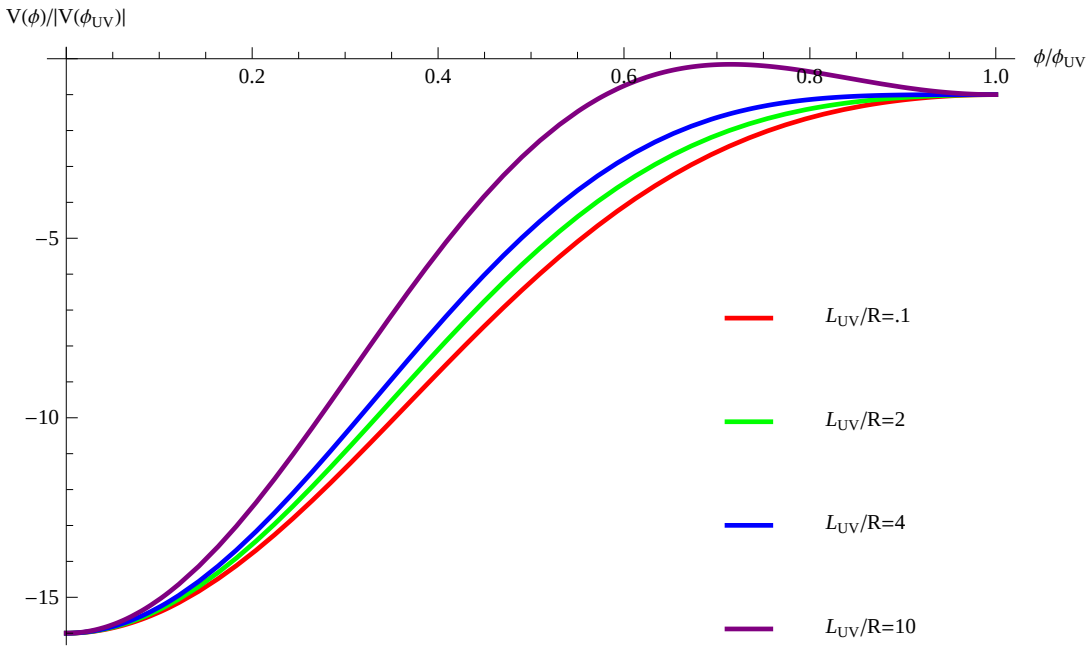

Figure 2.10: Plot of $V(\phi)/|V_{\rm UV}|$ versus $\phi/\phi_{\rm UV}$ for eq. (2.151) with various values of parameter L_{UV}/R. The parameters in the potential are chosen to fix $L_{UV} = 1$ and $L_{IR} = .25$ and we set $d = 4$.

is nonvanishing in the boundary theory. In the intervals (b) and (c), we have instead $\alpha = \Delta_+ < d$ and hence the interpretation is that $\mathcal{O}$ is relevant but the boundary coupling for this operator vanishes. Rather holographic interpretation of the bulk solution is that $\mathcal{O}$ has a nonvanishing expectation value in the UV, which then triggers the RG flow to a new IR fixed point. Of course, this appears to be a somewhat unconventional description of RG flows.[15] We have distinguished the interval (b) with $\frac{d}{2} < \alpha < \frac{d}{2} + 1$ because in the regime, one can imagine the standard interpretation of the bulk solution still holds for the 'alternate quantization' of the holographic theory [31]. In the latter approach, the roles of $\phi^{(-)}$ and $\phi^{(+)}$ are reversed and the dimension of the boundary operator is given by $\Delta = \Delta_-$. Note that in these first three intervals (a), (b) and (c), we have $m^2_{\rm UV} \leq 0$ and $m^2_{\rm UV}$ reaches its minimum value at $\alpha = d/2$, where it coincides precisely

[15] Similar flows arising in a supergravity construction were studied in [134]. However, the flows described there would all fall into the interval (b).

with the Breitenlohner-Freedman bound [23, 24, 25], *i.e.*, $m^2_{\rm UV}L^2_{UV} = -d^2/4$. Finally in the interval (d), we have $\alpha = \Delta_+ \geq d$ and hence in this regime, $\mathcal{O}$ is no longer a relevant operator. Rather we have an irrelevant (or marginal) operator again with a nonvanishing expectation value which triggers the flow to a new fixed point in the IR. Note that with $\alpha > d$, $m^2_{\rm UV} > 0$ and the scalar potential must have a third extremum ϕ_3 between the UV and IR critical points where $V(\phi_3) > V_{\rm UV}$.[16] This extra extremum is distinguished from the UV and IR critical points since by construction, the latter are critical points of the superpotential, whereas the new critical point satisfies $\delta V/\delta\phi|_{\phi=\phi_3} = 0$ but $\delta W/\delta\phi|_{\phi=\phi_3} \neq 0$. The changing structure of the potential as L_{UV}/R varies through these different regimes is illustrated in figure 2.10. As already noted, the interpretation of the RG flows in cases (c) and (d) in the boundary theory seems somewhat exotic. Hence one must worry that the underlying holographic model for these constructions is unphysical in some way. For example, it could be that for a consistent boundary CFT, once the dimension Δ of the operator is fixed, the quartic coupling in eq. (2.155) must be constrained in some way, along the lines of various bounds found in [101, 102, 103, 104, 105, 106, 107, 108, 109] or [135, 136, 137, 138, 139]. Alternatively, it could be that these background solutions are simply unstable in the corresponding parameter regime. In any event, in the main text, we focus our attention on the models in the intervals (a) and (b) for which the holographic RG flows have a conventional interpretation – see the discussion around eq. (2.89).

To close this section, we note that one can also consider a perturbative expansion of the scalar potential as in eq. (2.153) but about the IR critical point, *i.e.*,

$$V(\widetilde{\delta\phi}) = V_{\rm IR} + \frac{1}{2}\, m^2_{\rm IR}\, \widetilde{\delta\phi}^{\,2} + \frac{1}{24}\, \lambda_{\rm IR}\, \widetilde{\delta\phi}^{\,4} + \cdots\,, \tag{2.158}$$

where $\widetilde{\delta\phi} = \phi - \phi_{\rm IR}$ with $\phi_{\rm IR} \equiv \phi(r \to -\infty)$. As before, there are no odd powers of $\widetilde{\delta\phi}$ appearing in eq. (2.158). The first few parameters in this IR expansion are:

$$\begin{aligned} V_{\rm IR} &= -\frac{d(d-1)}{L^2_{IR}}\,, \qquad\qquad m^2_{\rm IR} = \frac{1}{R^2} + \frac{d}{L_{IR}R} \\ \lambda_{\rm IR} &= -\frac{-d\,(2-7\sigma^2)\,L_{UV}R - 3d\,\sigma^2\,L_{IR}R - 8(1-2\sigma^2)\,L_{IR}L_{UV}}{2(d-1)\sigma^2\,(L_{UV}-L_{IR})R^3}\,. \end{aligned} \tag{2.159}$$

As in the UV expansion, we see that the parameter σ first appears here in the quartic coupling $\lambda_{\rm IR}$. Hence one can easily verify that $V_{\rm IR}$ and $m^2_{\rm IR}$ precisely match the corresponding couplings in the IR expansion of the analytic potential in eq. (2.151), while $\lambda_{\rm IR}$ matches the quartic coupling in this expansion when $\sigma = 1$. Note that $m^2_{\rm IR} > 0$ and so the dual

[16] In fact, for L_{UV}/R sufficiently large, one finds $V(\phi_3) > 0$.

operator is always irrelevant at the IR critical point. The behaviour of the quartic coupling is qualitatively the same as described above for $\lambda_{\rm IR}$, *i.e.,* it is typically negative for $\sigma \sim 1$ and positive for $\sigma \sim 0$.

Chapter 3

Entanglement entropy for singular surfaces

As discussed in section 1.3.3, the typical calculation of entanglement entropy in quantum field theory begins by choosing a particular spatial region V and integrating out the degrees of freedom in the complement $\bar{V}$. Then with the resulting density matrix $\rho_{\rm V}$, one calculates: $S_{\rm EE} = -{\rm Tr}\,(\rho_{\rm V}\,\log\rho_{\rm V})$. Unfortunately, this calculation generically yields a UV divergent answer because the result is dominated by short distance correlations in the vicinity of the boundary ∂V. However, if we regulate the calculation by introducing a short distance cut-off δ, the entanglement entropy exhibits an interesting geometric structure [140, 46]. For example, with a QFT in d spacetime dimensions, this allows us to organize the results as in (1.53):

$$S_{\rm EE} = \frac{p_{d-2}}{\delta^{d-2}} + \frac{p_{d-4}}{\delta^{d-4}} + \cdots\,, \tag{3.1}$$

where each of the coefficients p_i involves an integration over the boundary ∂V. In particular, the first two coefficients may be written as

$$p_{d-2} = \int_{\partial V} d^{d-2}y\,\sqrt{h}\,h_2 = h_2\,\mathcal{A}_{\partial V}\,, \tag{3.2}$$

$$p_{d-4} = \int_{\partial V} d^{d-2}y\,\sqrt{h}\,\left[h_{4,1}\,\mathcal{R} + h_{4,2}\,K^{\hat{\imath}\,a}_{a}K^{\hat{\imath}\,b}_{b}\right]\,. \tag{3.3}$$

Of course, the leading term then yields the famous 'area law' result [8, 9]. The geometry of the boundary becomes even more evident in the second coefficient p_{d-4} with the appear-

ance of $\mathcal{R}$ and $K^{\hat{\imath}}_{ab}$, the intrinsic Ricci scalar and the extrinsic curvature of this surface.[1] The coefficients $h_{i,a}$ above will depend on the detailed structure of the underlying QFT. In particular, we note that they may become functions of the cut-off through their dependence on mass scales μ_i in the QFT since the latter will only appear in the dimensionless combination $\mu_i\delta$, *i.e.*, $h_{i,a} = h_{i,a}(\mu_i\delta)$ [46]. The geometric character of the entanglement entropy illustrated here naturally follows from the implicit choice of a covariant regulator in the QFT and the fact that the UV divergences are local.

Unfortunately, the coefficients appearing in the expansion above are scheme dependent. Clearly, if we shift $\delta \to \alpha\delta$, we find $h_{i,a} \to \hat{h}_{i,a} = \alpha^{i-d} h_{i,a}(\alpha\mu_i\delta)$. Hence the regulator dependence here comes both from the implicit dependence on mass scales in the QFT and the 'classical' engineering dimension of the individual coefficients. Of course, the latter can be avoided by carrying the expansion in eq. (3.1) to sufficiently high orders. In particular, one may find a logarithmic contribution to the entanglement entropy

$$S_{\text{univ}} = c_d \, \log(\delta/\ell) \tag{3.4}$$

where ℓ is some (macroscopic) scale in the geometry of ∂V. At this order in the expansion, the coefficient c_d is dimensionless. Further it may be natural to eliminate any intrinsic scales in the QFT by focussing on fixed point theories of the RG flow.[2] In this case, shifting δ as above makes a finite shift in the entanglement entropy but c_d is left unchanged. Hence one expects that this coefficient contains universal information that characterizes the underlying CFT. For example, from (1.55) in four dimensions, this universal coefficient is simply given by [51][3]

$$c_4 = \frac{1}{2\pi}\int_{\partial V} d^2y\sqrt{h}\,\left[\, c\,\left(K^{\hat{\imath}\,b}_a K^{\hat{\imath}\,a}_b - \frac{1}{2}K^{\hat{\imath}\,a}_a K^{\hat{\imath}\,b}_b\right) + \, a\,\mathcal{R}\,\right] , \tag{3.5}$$

where a and c are the two central charges of the CFT. In principle then, this provides an approach to determine these central charges. For example, calculating the entanglement entropy for a sphere yields $c_d \propto a$, while only c appears for a cylinder [51].

The preceding discussion implicitly assumes that the boundary of the region in question is smooth. The purpose of this chapter is to explore the effects of geometric singularities in this 'entangling surface' ∂V. In part, our motivation comes from the observation that

[1] We are assuming here that the background geometry is simply d-dimensional flat space. Otherwise additional contributions could appear in p_4 involving the background curvature.

[2] Universal terms may also appear in other circumstances, either as a finite contribution, *e.g.,* [67, 68, 69] or when explicit mass scales are present [141, 47].

[3] Again, we are assuming that the background geometry is flat.

in three dimensions, if the boundary contains corners or kinks, the corresponding entanglement entropy will contain additional logarithmic contributions [78, 79]

$$S_{\text{kink}} = k_3(\Delta\theta)\, \log(\delta/L)\,, \tag{3.6}$$

where $\Delta\theta$ is the opening angle of the kink – see figure 3.1. As a function of $\Delta\theta$, coefficient $k(\Delta\theta)$ satisfies certain simple properties [78, 54]. In particular, $k_3(\Delta\theta = \pi) = 0$ since the ∂V becomes a smooth surface when the angle is set to π. If the QFT is in a pure state, we have $S_{\text{EE}}(V) = S_{\text{EE}}(\bar{V})$ and so $k_3(\Delta\theta) = k_3(2\pi - \Delta\theta)$ in this case. Further in examples [78, 79, 54], one finds for a small opening angle: $k_3(\Delta\theta \to 0) \propto 1/\Delta\theta$. However, we must add that the precise universal information contained in $k_3(\Delta\theta)$ remains to be understood.

A natural question is to ask whether similar contributions arise for singular entangling surfaces in higher dimensions. If yes, we can ask what the geometric dependence of these new terms is. Further, if we focus on CFT's, we might ask if the coefficients in these contributions have a simple dependence on the central charges, analogous to that in eq. (3.5). Now using the AdS/CFT framework for entanglement entropy in section 1.3.4, we may begin to address these questions. In fact, using the standard calculation of holographic entanglement entropy, the logarithmic contribution (3.6) associated with a kink in three dimensions has already been identified in [54]. More generally, this approach allows us to easily study boundary CFT's in a variety of dimensions and further the geometric structure of the entanglement entropy becomes readily evident in holographic calculations [47, 48]. In the following then, we use holography to study some simple singular entangling surfaces in higher dimensions and we find a variety of new universal contributions. While these are just first steps towards a full understanding of these universal terms, our results indicate a rich geometric structure for the entanglement entropy of singular surfaces.

The remainder of this chapter is organized as follows: In the next section, we give a brief overview of our calculations and summarize our main results. In section 3.2, we consider entangling surfaces with a conical singularity for boundary CFT's with $d = 4$, 5 and 6. In these cases, the singularity in the geometry of the entangling surface is confined to a single point and so we broaden our calculations to consider extended singularities in section 3.3. There we find that the appearance of universal terms in the entanglement entropy depends on the dimension and the curvature of the singular locus. Section 3.4 presents calculations of holographic entanglement entropy for singular surfaces in boundary CFT's which are dual to the Gauss-Bonnet gravity. These calculations allow us to examine the dependence of the universal terms on the central charges of the underlying CFT. In section 3.5, we briefly discuss our results and consider future directions. Section 3.6 contains supplementary material for this chapter. Section 3.6.1 describes an alternate calculation of the entanglement entropy associated with a conical singularity. In particular, we make

a conformal transformation from R^d to $R \times S^{d-1}$ and so the conical entangling surface becomes a cylinder in the latter background. In section 3.6.2, we give certain details for lengthy calculations presented in sections 3.2, 3.3 and 3.4.

3.1 Singular entangling surfaces and summary of results

In the sections 3.2, 3.3 and 3.4, we will describe in detail various holographic calculations of the entanglement entropy for certain singular surfaces. Each of these calculations is quite lengthy and individually they are not very enlightening. Hence in this section, we provide an overview of these calculations and a summary of our results. We begin by describing the kinds of singular entangling surfaces which we will consider.

Let us go back to eq. (3.6) for three dimensions. In this case, the entangling surface is a one-dimensional curve and the 'singular surface' would be one containing a kink or a corner where the direction of the tangent vector changes discontinuously at a point. We can characterize this behaviour by saying that the geodesic curvature of the curve contains a δ-function singularity. In higher dimensions, the entangling surface is a $(d-2)$-dimensional submanifold which divides into two a time slice of the d-dimensional background spacetime. In this case, the natural extension of geodesic curvature is the extrinsic curvature of these surfaces. However, a distinct feature characterizing the geometry of these higher dimensional surfaces is now their intrinsic curvature. Of course, for a fixed background, these two curvatures will be related to each other (and the background curvature) through the Gauss-Codazzi equations. However, it is worth noting that in discussing singular surfaces, we might consider singularities in either the extrinsic curvature or the intrinsic curvature. In particular, as we show with simple examples below, it is possible to construct surfaces where the intrinsic curvature is everywhere smooth while the extrinsic curvature is singular. The other possibility which we consider is when both the extrinsic and intrinsic curvatures have singularities.[4] In either case, the examples which we consider below contain δ-function singularities. That is, in all of our examples, the curvatures characterizing the entangling surface are finite and smooth everywhere, except for a particular locus or subset of points.

In considering such singular entangling surfaces, we introduce an intuitive nomenclature to simplify the discussion: *kink*, *cone* and *crease*. Examples of each are illustrated in figure

[4]We will assume the geometry of the background is everywhere smooth in the following. Combined with the Gauss-Codazzi equations, this assumption rules out the possibility that the extrinsic curvature may be smooth while the intrinsic curvature is singular.

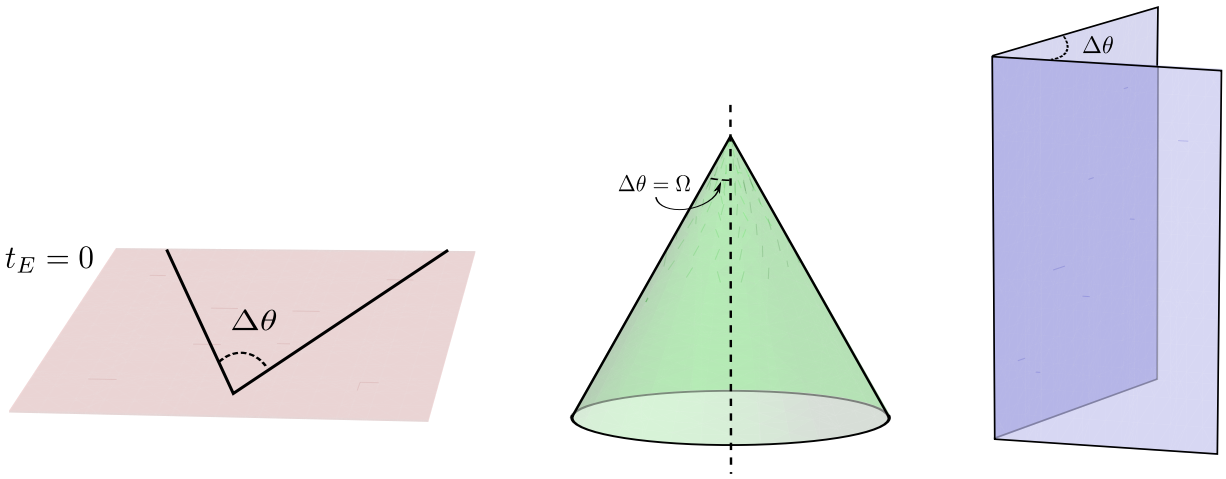

(a) (b) (c)

Figure 3.1: (Colour Online) Panel (a) shows a kink in constant Euclidean time t_E slice in $d = 3$. Panel (b) shows the cone c_1. Panel (c) shows the crease $k \times R^1$.

3.1. To explain these terms, it suffices to consider evaluating the entanglement entropy in flat d-dimensional background R^d. With Euclidean signature, the metric can then be written in 'cylindrical' coordinates as

$$ds^2 = dt_{\rm E}^2 + d\rho^2 + \rho^2 \left(d\theta^2 + \sin^2\theta\, d\Omega_n^2\right) + \sum_{i=1}^{m} \left(dx^i\right)^2 \tag{3.7}$$

where $d\Omega_n^2$ denotes the round metric on a unit n-sphere. Hence we have $d = 3+n+m$. The entangling surface will be a $(d-2)$-dimensional geometry embedded in this background (on a surface of constant $t_{\rm E}$).

The natural model of a *kink* is then given in $d = 3$ ($n = 0 = m$) as the union of two rays: $k = \{t_{\rm E} = 0, \rho = [0, \infty), \theta = \pm\Omega\}$. With this choice of angles, the opening angle between the two rays is $\Delta\theta = 2\Omega$. Similarly, our prototype for a *cone* is given in $d = 3 + n$ as the surface: $c_n = \{t_{\rm E} = 0, \rho = [0, \infty), \theta = \Omega\}$. Hence with this construction, we are only considering cones with a spherical cross-section S^n. We define a *crease* to be the higher dimensional extension of either of these singular surfaces where we take the direct product of a kink k or a cone c_n with some other manifold. With the flat background (3.7) above, the natural extension of the previous constructions gives the crease $k \times R^m$ in $d = 3 + m$ or a conical crease $c_n \times R^m$ in $d = 3 + n + m$.

In a certain sense the kink is simply a lower dimensional version of a cone, *i.e.,* $k = c_0$. However, we prefer to distinguish these two classes to highlight the difference in the singularities noted above. If we consider the crease $k \times R^m$, the intrinsic geometry of this submanifold is smooth everywhere including $\rho = 0$ and in fact for the construction above, the intrinsic curvature vanishes everywhere. On the other hand, the extrinsic curvature contains a δ-function singularity at the tip of the kink, *i.e.,* $\rho = 0$. Again for the above construction, the extrinsic curvature vanishes everywhere away from this singularity. Now considering the conical crease $c_n \times R^m$, one finds that both the intrinsic and extrinsic curvatures have δ-function singularities at the tip of the cone, *i.e.,* $\rho = 0$. For the prototype constructed above, the intrinsic curvature vanishes away from this singular point but the extrinsic curvature is nonvanishing.

In our calculations of the entanglement entropy, it will also be useful to consider the CFT in a background of the form $R^{3+n} \times S^m$, for which we write the metric as

$$ds^2 \;=\; dt_{\rm E}^2 + d\rho^2 + \rho^2 \left(d\theta^2 + \sin^2\theta d\Omega_n^2\right) + R^2\, d\Omega_m^2\,. \tag{3.8}$$

This allows us to consider creases of the form $k \times S^m$ or $c_n \times S^m$. With these geometries, the intrinsic curvature of the entangling surface is nonvanishing everywhere but in particular, the geometry of the singular locus is now S^m.

Now after this description of our singular surfaces, we briefly explain our holographic calculations and the results. We use the AdS/CFT correspondence to calculate the holographic entanglement entropy for a boundary CFT with the above singular entangling surfaces. In different calculations, we use the following bulk geometries:

$$ds^2 \;=\; \frac{L^2}{z^2}\left(dz^2 + dt_{\rm E}^2 + d\rho^2 + \rho^2 \left(d\theta^2 + \sin^2\theta d\Omega_n^2\right) + \sum_{i=1}^{m} \left(dx^i\right)^2\right)\,, \tag{3.9}$$

$$ds^2 \;=\; \frac{L^2}{z^2}\Big(dz^2 + f_1(z)\left[dt_{\rm E}^2 + d\rho^2 + \rho^2 \left(d\theta^2 + \sin^2\theta d\Omega_n^2\right)\right] + f_2(z)\, R^2\, d\Omega_m^2\Big)\,. \tag{3.10}$$

Here L is the AdS curvature scale and z is the radial coordinate with the asymptotic boundary at $z = 0$. Of course, eq. (3.9) is just AdS_{d+1} where $d = 3 + n + m$ as above and with a flat boundary metric written in the coordinates given in eq. (3.7). The geometry in eq. (3.10) approaches AdS_{d+1} asymptotically with the curved boundary metric given in eq. (3.8). However, because this boundary geometry is not conformally flat, the bulk geometry is not purely AdS_{d+1} and the functions, f_1 and f_2, must be determined by evaluating the gravitational equations of motion. With these bulk metrics, (3.9) and (3.10), we can readily calculate the holographic entanglement entropy for the kink, cone or crease geometries described above.

To calculate the holographic entanglement entropy, we use the prescription by Ryu and Takayanagi [16, 52], discussed in section 1.3.4. The details of our holographic calculations of the entanglement entropy for kinks, cones and creases are given in the following sections. As expected, these calculations contain a variety of divergences that must be regulated. However, we pay particular attention to the question of whether there are new singular contributions associated with geometric singularity in the entangling surface. Further, in certain cases, we find that the singularity produces new universal contributions. Table 3.1 summarizes our results.

d	Background spacetime	Geometry of entangling surface	Crease dimension	Crease curvature	Expected Divergences	New Divergences
3	R^3	k	0	–	$1/\delta$	$\log(\delta)^*$
4	R^4	c_1	0	–	$1/\delta^2\,,\ \log(\delta)$	$\log^2(\delta)^*$
5	R^5	c_2	0	–	$1/\delta^3\,,\ 1/\delta$	$\log(\delta)^*$
6	R^6	c_3	0	–	$1/\delta^4\,,\ 1/\delta^2\,,\ \log(\delta)$	$\log^2(\delta)^*$
>3	R^d	$k \times R^{d-3}$	$d-3$	flat	$1/\delta^{d-2}$	$1/\delta^{d-3}$
4	$R^3 \times S^1$	$k \times S^1$	1	flat	$1/\delta^2$	$1/\delta$
5	$R^3 \times S^2$	$k \times S^2$	2	curved	$1/\delta^3\,,\ 1/\delta$	$1/\delta^2\,,\ \log(\delta)^*$
6	$R^3 \times S^3$	$k \times S^3$	3	curved	$1/\delta^4\,,\ 1/\delta^2$	$1/\delta^3\,,\ 1/\delta$
6	$R^4 \times S^2$	$k \times (R^1 \times S^2)$	3	curved	$1/\delta^4\,,\ 1/\delta^2$	$1/\delta^3\,,\ 1/\delta$
5	R^5	$c_1 \times R^1$	1	flat	$1/\delta^3\,,\ 1/\delta$	$\log(\delta)/\delta$
6	R^6	$c_1 \times R^2$	2	flat	$1/\delta^4\,,\ 1/\delta^2\,,\ \log(\delta)^*$	$\log(\delta)/\delta$
7	R^7	$c_1 \times R^3$	3	flat	$1/\delta^5\,,\ 1/\delta^3\,,\ 1/\delta$	$\log(\delta)/\delta^3$
5	$R^4 \times S^1$	$c_1 \times S^1$	1	flat	$1/\delta^3\,,\ 1/\delta$	$\log(\delta)/\delta$
6	$R^4 \times S^2$	$c_1 \times S^2$	2	curved	$1/\delta^4\,,\ 1/\delta^2\,,\ \log\delta$	$\log^2(\delta)^*$
7	$R^4 \times S^3$	$c_1 \times S^3$	3	curved	$1/\delta^5\,,\ 1/\delta^3\,,\ 1/\delta$	$\log(\delta)/\delta^3$
6	R^6	$c_2 \times R^1$	1	flat	$1/\delta^4\,,\ 1/\delta^2\,,\ \log(\delta)^*$	$1/\delta$
7	R^7	$c_2 \times R^2$	2	flat	$1/\delta^5\,,\ 1/\delta^3\,,\ 1/\delta$	$1/\delta^2$
6	$R^5 \times S^1$	$c_2 \times S^1$	1	flat	$1/\delta^4\,,\ 1/\delta^2\,,\ \log(\delta)^*$	$1/\delta$
7	$R^5 \times S^2$	$c_2 \times S^2$	2	curved	$1/\delta^5\,,\ 1/\delta^3\,,\ 1/\delta$	$1/\delta^2\,,\ \log(\delta)^*$

Table 3.1: Summary of the divergent terms for various singular surfaces from our holographic calculations. Here d is the spacetime dimension of the CFT background, which can be both flat or curved. The 'expected' divergences are those which can arise with a smooth entangling surface – see discussion in the introduction. The 'new' divergences are produced by the singularity in the surface and vanish when the surface is smooth, *i.e.*, $\Omega = \pi/2$. Any universal terms are marked with a '$*$' – see the discussion in the main text.

As described above, if the entangling surface has a kink in $d = 3$, there is a new universal contribution (3.6) to the entanglement entropy. We review the holographic calculation of [54] which reveals this result in section 3.2. These calculations are extended to creases of the form $k \times R^m$ in section 3.3 and there we find no universal contribution, *i.e.,* no $\log \delta$ term, for these cases. However, we note that in this case the locus of the singularity, *i.e.,* the tip of the crease, is flat. The results become more interesting if this locus is curved. If the singular locus is curved but odd-dimensional, we again find no logarithmic contribution. However, if the singular locus is both curved and even-dimensional, we find that the entanglement entropy of the crease contains a $\log \delta$ contribution. While we have a limited number of explicit examples of this behaviour, *i.e.,* the case of $k \times S^2$, it suggests to us that generally for creases of the form $k \times \Sigma_{2m}$, there are new universal terms of the form

$$S_{\text{univ}} \sim \int_\Sigma d^{2m}y \, \sqrt{h} \, [\mathcal{R}^m] \log \delta \tag{3.11}$$

where Σ is the singular locus on the entangling surface and $[\mathcal{R}^m]$ represents some curvature invariant containing m powers of the curvature on this submanifold.

We also consider entangling surfaces with conical singularities in section 3.2. In this case, if the boundary CFT lives in an odd-dimensional spacetime, *i.e.,* c_n with n even, we find that the singularity contributes a $\log \delta$ term to the entanglement entropy. However, for an even-dimensional boundary theory, *i.e.,* c_n with n odd, we find that the new universal contribution actually diverges as $\log^2 \delta$. However, we note, and explain in detail in section 3.5, that part of this $\log^2 \delta$ contribution can be identified with the 'smooth' contribution given in eq. (3.5). That is, part of this divergence should be associated with correlations away from the singularity and so depends on details of the smooth part of the geometry away from the tip of the cone. However, we also argue part of the contribution is associated with the singularity itself and so should still be expected to arise for more general situations, independent of this smooth geometry. Given that our boundary field theory is a CFT, we might ask if the coefficients of these new universal contributions are simple functions of the central charges. As a step in this direction, we work with Gauss-Bonnet gravity in the bulk in section 3.4, as this allows us to begin to distinguish the boundary central charges, *e.g.,* see [114]. In the case of even dimensions, we see that the coefficient of the $\log^2 \delta$ contribution is proportional to a particular central charge, *i.e.,* for $d = 4$, it is c. However, for odd dimensions, the $\log \delta$ term does not yield any such simple result.

The holographic calculations are also extended to consider conical creases of the form $c_n \times R^m$ or $c_n \times S^m$ in section 3.3. For these cases, we find that the nature of universal contributions again depends on the dimension of both the full spacetime and the singular locus, as well as the curvature of the latter. In particular, if both of these dimensions

is even and the locus is curved, *e.g.,* $c_1 \times S^2$, then a $\log^2\delta$ term arises. Alternatively, if the background is odd-dimensional but the locus is even-dimensional and curved, *e.g.,* $c_2 \times S^2$, then a $\log\delta$ contribution appears. In any other cases, the singularity does not contribute any universal terms of this form to the entanglement entropy. Our results again suggest the appearance of universal contributions of the form given in eq. (3.11) for odd-dimensional theories, while similar terms with a $\log^2\delta$ divergence seem to be present for even-dimensional CFT's.

In discussing these results, we need to be careful about an important point. As we have illustrated with eq. (3.5), in even dimensional CFT's, the smooth part of the entangling surface will already produce a universal term proportional to $\log\delta$. Hence, as noted in our description of the results for cones, we must distinguish this term from universal contributions associated with the singularity. Other cases where this issue arises include: $c_1 \times R^2$, $c_2 \times R^1$ and $c_2 \times S^1$. All of these examples are in six dimensions where we do not have the analog of the $d = 4$ expression in eq. (3.5). So while a detailed comparison is not possible, in considering the corresponding holographic calculations in detail, we see that the coefficient of the $\log\delta$ receives contributions at all values of the radius ρ and that there is no singularity at $\rho = 0$. Hence we can clearly infer that this contribution is coming from the smooth part of the geometry and the singularity is not making a universal contribution to the entanglement entropy.

To close this section, let us note that for many of the examples in table 3.1, there were no logarithmic terms in the entanglement entropy. In some of those cases, it may still be that the finite contribution exhibits some universal behaviour but we did not investigate this possibility here.

3.2 EE for singular embeddings

In this section, we will study entanglement entropy (EE) with singular entangling surfaces in a flat background for holographic CFT's which are dual to Einstein gravity. The simplest case in this category is the kink in $d = 3$ dimensional CFT. It is already known that EE for a kink has a logarithmic divergence [78, 79]. This calculation for holographic EE was first done by Hirata and Takayanagi in [54]. So before calculating EE for cones in higher dimensions, we briefly review this case.

We begin with $\{d, n, m\} = \{3, 0, 0\}$ in metric (3.9). Then the kink in the boundary is defined by $\rho \in [0, H]$ and $\theta \in [-\Omega, \Omega]$, where H is the IR cut-off. The holographic entanglement entropy for this geometry is given by (1.56), that is the area of the minimal

area surface which hangs in the bulk and is homologous to the kink on the boundary. We assume that the induced coordinate for the minimal area surface are (ρ, θ) and the radial coordinate $z = z(\rho, \theta)$. Now we can find the induced metric $h_{\mu\nu}$ over the surface and the entanglement entropy is given by

$$S_3\big|_k \;=\; \frac{2\pi}{\ell_{\rm P}^2}\int d\rho\, d\theta\, \sqrt{h} \;=\; \frac{2\pi}{\ell_{\rm P}^2}\int d\rho\, d\theta\, \frac{L^2}{z^2}\sqrt{\rho^2+\rho^2 z'^2+\dot{z}^2}\,, \tag{3.12}$$

where $z' = \partial_\rho z$ and $\dot{z} = \partial_\theta z$. Here we point out that the EE for entangling surface ∂V in d-dimensional field theory will be represented by $S_d\big|_{\partial V}$. Now we can easily find the equation of motion for $z(\rho, \theta)$. From scaling symmetry of the AdS space and the fact that there is no other scale in the problem, we can say that

$$z \;=\; \rho\, h(\theta)\,, \tag{3.13}$$

where $h(\theta)$ is such that $h \to 0$ as $\theta \to \pm\Omega$. After using this ansatz, the entropy functional reduces to

$$S_3\big|_k \;=\; \frac{4\pi L^2}{\ell_{\rm P}^2}\int_{\delta/h_0}^{H}\frac{d\rho}{\rho}\int_0^{\Omega-\epsilon} d\theta\frac{\sqrt{1+h^2+\dot{h}^2}}{h^2}\,, \tag{3.14}$$

where we have introduced the UV cut-off at $z = \delta$, $\dot{h} = dh/d\theta$ and defined h_0 such that at $\theta = 0$, $h(0) = h_0$. Note that $\dot{h}(0) = 0$ and h_0 is the maximum value of $h(\theta)$. Also, ϵ is a function of ρ defined using (3.13), such that at $z = \delta$, $h(\Omega - \epsilon) = \delta/\rho$. Further, the substitution of ansatz (3.13) in equation of motion for $z(\rho, \theta)$ gives

$$h(1+h^2)\ddot{h} + 2\dot{h}^2 + (h^2+1)(h^2+2) \;=\; 0\,. \tag{3.15}$$

For this equation of motion, we can easily see that there exists a quantity K which is conserved along θ translation and is given by

$$K \;=\; \frac{1+h^2}{h^2\sqrt{1+h^2+\dot{h}^2}} \;=\; \frac{\sqrt{1+h_0^2}}{h_0^2}\,, \tag{3.16}$$

where we have used $\dot{h}(0) = 0$ and $h(0) = h_0$ to get the expression on the right hand side. Now plan is to convert θ integral in (3.14) to integral over h and then separate the divergent part in the integral. We also make the coordinate transformation to $y = \sqrt{1/h^2 - 1/h_0^2}$, where $y \to \infty$ as we approach the boundary. After this coordinate transformation, the integrand has following divergence in the limit $y \to \infty$:

$$\sqrt{\frac{1+h_0^2(1+y^2)}{2+h_0^2(1+y^2)}} \sim 1 + \mathcal{O}\left(\frac{1}{y^3}\right)\,. \tag{3.17}$$

So now we can write EE as

$$S_3\big|_k = \frac{4\pi L^2}{\ell_{\rm P}^2}\int_{\delta/h_0}^{H}\frac{d\rho}{\rho}\int_0^{\sqrt{(\rho/\delta)^2-1/h_{01}^2}}dy\left(\sqrt{\frac{1+h_0^2(1+y^2)}{2+h_0^2(1+y^2)}}-1\right) + \frac{4\pi L^2}{\ell_{\rm P}^2}\int_{\delta/h_0}^{H}\frac{d\rho}{\rho}\sqrt{\frac{\rho^2}{\delta^2}-\frac{1}{h_{01}^2}}\,, \tag{3.18}$$

which can be simplified to give

$$S_3\big|_k = \frac{4\pi L^2}{\ell_{\rm P}^2}\left(\frac{H}{\delta}-q_3(\Omega)\log\left(\frac{H}{\delta}\right)+\mathcal{O}(\delta)\right)\,, \tag{3.19}$$

where $q_3(\Omega)$ is

$$q_3(\Omega) = \int_0^\infty dy\left[1-\sqrt{\frac{1+h_0^2(1+y^2)}{2+h_0^2(1+y^2)}}\right]\,. \tag{3.20}$$

Note that $q_3(\Omega)$ is the cut-off independent term in the EE for the kink. After this quick review of the calculations by Hirata and Takaynagi, we turn towards the cone in higher dimensions where we will see $\log^2\delta$ divergence for even d.

3.2.1 Cone in $d = 4, 5$ and 6 CFT

In this section, we will calculate EE for cone c_n in some even and odd dimensional space-time. We will give detailed calculations for c_1 in $d = 4$ and discuss the final results for c_2 and c_3 in $d = 5, 6$ dimensional CFT's[5]. However, in the beginning of the calculations, we will keep the discussion general for arbitrary d.

With $m = 0$ in the bulk metric (3.9), we can define the cone geometry by $\theta \in [0, \Omega]$ and $\rho \in [0, H]$, where H is the IR cut-off for the geometry. Now, we define the minimal area surface, that gives the entanglement entropy, by coordinates (ρ, θ, Ω_n) where Ω_n are coordinates on sphere S^n in (3.9). As for the cone c_n, we have a rotational symmetry $SO(n+1)$ along the sphere S^n, the radial coordinate z will depend only on θ, *i.e.*, $z = z(\rho, \theta)$. Then, the induced metric is given by

$$h = \begin{bmatrix} \frac{L^2}{z^2}(1+z'^2) & \frac{L^2}{z^2}z'\dot{z} & \\ \frac{L^2}{z^2}z'\dot{z} & \frac{L^2}{z^2}(\rho^2+\dot{z}^2) & \\ & & \frac{L^2\rho^2}{z^2}\sin^2\theta\, g_{ab}(S^n) \end{bmatrix}\,, \tag{3.21}$$

[5]The cone in $d = 4$ CFT is also discussed in [142].

where $\dot{z} = \partial_\theta z$, $z' = \partial_\rho z$ and $g_{ab}(S^n)$ represents the metric over unit S^n. We also regulate the minimal area surface by stopping it at the UV cut-off $z = \delta$. Now the entropy functional becomes

$$S_d\big|_{c_{d-3}} = \frac{2\pi\, L^{d-1}\Omega_{d-3}}{\ell_{\rm P}^{d-1}} \int d\rho\, d\theta\, \frac{\rho^{d-3}\sin^{d-3}(\theta)}{z^{d-1}} \sqrt{(\rho^2 + (\partial_\theta z)^2 + \rho^2(\partial_\rho z)^2)}\,, \quad (3.22)$$

where Ω_{d-3} is the surface area of the unit $(d-3)$-sphere. Note that here we have used $n = d-3$. From this entropy functional, we can find the equation of motion for $z(\rho, \theta)$.

$$\begin{aligned} 0 \;=\; & \rho^2 \sin(\theta) z \left(\rho^2 + \dot{z}^2\right) z'' + \rho^2 \sin(\theta) z \left(1 + z'^2\right) \ddot{z} - 2\rho^2 \sin(\theta) z \dot{z} z' \dot{z}' \\ & + (d-1)\rho^2 \sin(\theta) \left(\dot{z}^2 + \rho^2 \left(1 + z'^2\right)\right) + z(d-3)\cos(\theta)\dot{z} \left(\dot{z}^2 + \rho^2 \left(1 + z'^2\right)\right) \\ & + \rho z \sin(\theta) z' \left((d-1)\dot{z}^2 + (d-2)\rho^2 \left(1 + z'^2\right)\right) \end{aligned} \quad (3.23)$$

To proceed further, we use the scaling symmetry of the AdS background. As the background geometry is scale invariant and the only scale in our discussion is ρ, solution of $z(\rho, \theta)$ should be of the following form

$$z(\rho, \theta) \;=\; \rho\, h(\theta)\,, \quad (3.24)$$

where $h(\theta)$ is a function of θ such that as $\theta \to \Omega$, $h \to 0$. Also at $\theta = 0$, z achieves its maximum value and we have $\dot{h}(0) = dh/d\theta|_{\theta=0} = 0$. We also define h_0 such that $h_0 = h(\theta = 0)$. Now to extract the cut-off independent term, first we change the integration over θ to integration over h:

$$S_d\big|_{c_{d-3}} = \frac{2\pi\, L^{d-1}\Omega_{d-3}}{\ell_{\rm P}^{d-1}} \int_{\delta/h_0}^{H} \frac{d\rho}{\rho} \int_{h_0}^{\delta/\rho} dh\, \frac{\sin^{d-3}(\theta)}{\dot{h} h^{d-1}} \sqrt{1 + h^2 + \dot{h}^2}\,. \quad (3.25)$$

Now the plan is to make the integral over h finite. To do so, we find the solution of $\sin(\theta)$ and $\dot{h}$ near the boundary and then see how the integrand diverges in the limit $h \to 0$. Then, we subtract the terms up to order $1/h$ in the integrand of (3.25) to make it finite. At this step, we will find that it is convenient to write the asymptotic solution for $\sin(\theta)$ for each $d \geq 4$ separately. Hence, now we work case by case.

First, we consider $d = 4$ and find $\dot{h}$ and $\sin(\theta)$ in terms of h in the asymptotic limit, where $h \to 0$. To do so, we make a change of variable $y = \sin\theta$ and invert (3.23) into equation of motion for $y = y(h)$. Using $\dot{h} = \sqrt{1-y^2}/y'(h)$ and $\ddot{h} = -(yy'^2 + (1-y^2)y'')/y'^3$, we find that

$$\begin{aligned} 0 \;=\; & h\left(1 + h^2\right) y \left(1 - y^2\right) y'' - y y' \left(3 + h^2 + \left(3 + 5h^2 + 2h^4\right) y'^2\right) + 2h y^2 \left(1 + \left(1 + h^2\right) y'^2\right) \\ & - h \left(1 + \left(1 + h^2\right) y'^2\right) + \left(3 + h^2\right) y^3 y' - h y^4\,, \end{aligned} \quad (3.26)$$

where $y' = dy/dh$ and $y'' = d^2y/dh^2$. We can solve this equation of motion perturbatively near the boundary and find that

$$y = \sin(\Omega) - \frac{1}{4}\cos(\Omega)\cot(\Omega)h^2 + \left(\frac{1}{64}(3-\cos(2\Omega))\cot^2(\Omega)\csc(\Omega)\log(h) + y_0\right)h^4 + \mathcal{O}(h^6)\,, \tag{3.27}$$

where we have used $y(\theta = \Omega) = y(h = 0) = \sin(\Omega)$. In the above expression, y_0 is a constant and its value is fixed by using the fact that $y(h)$ has an extrema at $h = h_0$. Further, this solution also contains $\log(h)$, which will appear in solutions for even d. As a next step, we find $\dot{h}(\theta)$ near the boundary in terms of h. For that, we define $f(h) = \dot{h}(\theta)$ and write (3.26) as

$$\begin{aligned} 0 \;=\; & h\left(1+h^2\right) yff' + h\sqrt{1-y^2}f^3 + \left(3+h^2\right)yf^2 \\ & + h\left(1+h^2\right)\sqrt{1-y^2}f + \left(3+5h^2+2h^4\right)y\,. \end{aligned} \tag{3.28}$$

Now using (3.27) we can solve this equation near the boundary and find

$$f(h) \;=\; -\frac{2\tan(\Omega)}{h} - \frac{1}{2}h(3-\cos(2\Omega))\csc(2\Omega)\log(h) + f_0 h + \dots\,, \tag{3.29}$$

where f_0 is a constant. Now using (3.27), (3.29) and $d = 4$ in integrand of (3.25), we find that for small h

$$\frac{\sin\theta}{\dot{h}h^3}\sqrt{1+h^2+\dot{h}^2} \sim -\frac{\sin(\Omega)}{h^3} + \frac{\cos(\Omega)\cot(\Omega)}{8h} + \mathcal{O}(h)\,. \tag{3.30}$$

This implies that the h integral in the entropy functional has only divergences coming from first two terms in the limit $h \to \delta/\rho$. We can separate these divergent terms and for $d = 4$, write the entropy functional (3.25) in the following form

$$S_4\big|_{c_1} \;=\; \frac{4\,\pi^2\,L^3}{\ell_{\rm P}^3}\,(I_1 + I_2)\,. \tag{3.31}$$

where

$$\begin{aligned} I_1 \;&=\; \int_{\delta/h_0}^{H}\frac{d\rho}{\rho}\int_{h_0}^{\delta/\rho} dh\,\left[\frac{\sin\theta}{\dot{h}h^3}\sqrt{1+h^2+\dot{h}^2} + \frac{\sin(\Omega)}{h^3} - \frac{\cos(\Omega)\cot(\Omega)}{8h}\right]\,, \\ I_2 \;&=\; -\int_{\delta/h_0}^{H}\frac{d\rho}{\rho}\int_{h_0}^{\delta/\rho} dh\left(\frac{\sin(\Omega)}{h^3} - \frac{\cos(\Omega)\cot(\Omega)}{8h}\right)\,. \end{aligned}$$

If we series expand I_1 in terms of UV cut-off δ, we find that leading term is of order $\log(\delta)$. To see that, we use (3.30) and find that in I_1, integration over h is actually finite if we set

the upper limit $h = 0$. As all the subleading terms will be of higher order in powers of δ, we find that

$$I_1 \;=\; -\log(\delta)\int_{h_0}^{0} dh\,\left[\frac{\sin\theta}{\dot{h}h^3}\sqrt{1+h^2+\dot{h}^2}+\frac{\sin(\Omega)}{h^3}-\frac{\cos(\Omega)\cot(\Omega)}{8h}\right]+\mathcal{O}(\delta^0)\,. \quad (3.32)$$

Simultaneously, we can evaluate I_2 and find that

$$\begin{aligned} I_2 \;=\;& \frac{H^2\sin(\Omega)}{4\delta^2}-\frac{1}{16}\cos(\Omega)\cot(\Omega)\log(\delta/H)^2 \\ &+\left(\frac{1}{8}\cos(\Omega)\cot(\Omega)\log(h_0)+\frac{\sin(\Omega)}{2h_0^2}\right)\log(\delta/H)+\mathcal{O}(\delta^0)\,. \end{aligned} \quad (3.33)$$

Now using (3.32) and (3.33) in (3.31), we find the complete structure of divergences in the entanglement entropy for cone:

$$S_4\big|_{c_1} \;=\; \frac{4\,\pi^2\,L^3}{\ell_{\rm P}^3}\left[\frac{H^2\sin(\Omega)}{4\delta^2}-\frac{1}{16}\cos(\Omega)\cot(\Omega)\log(\delta/H)^2+q_4\log(\delta/H)+\mathcal{O}(\delta^0)\right], \quad (3.34)$$

where

$$\begin{aligned} q_4 \;=\;& \frac{1}{8}\cos(\Omega)\cot(\Omega)\log(h_0)+\frac{\sin(\Omega)}{2h_0^2} \\ &+\int_0^{h_0} dh\,\left[\frac{\sin\theta}{\dot{h}h^3}\sqrt{1+h^2+\dot{h}^2}+\frac{\sin(\Omega)}{h^3}-\frac{\cos(\Omega)\cot(\Omega)}{8h}\right] \end{aligned} \quad (3.35)$$

So we find that EE for a cone in $d = 4$ CFT has a double logarithmic term. We can notice from expression of I_2 that one of the log terms comes from integration over h and then second from integration over ρ. Here, first integration over h or θ actually brings us close to the cut-off at the smooth part of the entangling surface. Further, when second integration over ρ is performed, we approach to the singularity. This idea is consistent with the fact that in EE for even dimensions, we get a logarithmically divergent term according to [51].

Now, as a next step, we generalize our discussion to cones in higher dimensions. First, we calculate EE for cone in $d = 5$ CFT. In this case the calculations proceeds similar to the $d = 4$ and the complete expression for the EE is given in the section 3.6.2. However, we find that that cut-off independent term is the coefficient of $\log\delta$ divergence and it is given by

$$S_5^{\log}\big|_{c_2} \;=\; \frac{8\,\pi^2\,L^4}{\ell_{\rm P}^4}q_5\log(\delta/H)\,, \quad (3.36)$$

where

$$q_5 = -\frac{4\cos^2(\Omega)}{9\,h_0} + \frac{\sin^2(\Omega)}{3\,h_0^3} + \int_0^{h_0} dh\,\left[\frac{\sin^2(\theta)}{\dot{h}\,h^4}\sqrt{1+h^2+\dot{h}^2} + \frac{\sin^2(\Omega)}{h^4} - \frac{4\cos^2(\Omega)}{9\,h^2}\right]. \tag{3.37}$$

We further draw this universal term in figure 3.2. There, $\log|q_d|$ is plotted as a function of $\log(\sin\Omega)$ for $d=3$ and 5. In the limit $\Omega\to 0$, we see that $\log|q_5|$ asymptotes to a straight line with slop -1. This implies that for small Ω,

$$q_5 \propto \frac{1}{\Omega}\,. \tag{3.38}$$

Finally for $d=6$, we find that the cut-off independent term is

$$S_6^{\log^2}\big|_{c_3} = \frac{4\,\pi^3\,L^5}{\ell_{\rm P}^5}\frac{9\cos(\Omega)\cot(\Omega)(31-\cos(2\Omega))}{8192}\log\left(\delta/H\right)^2\,. \tag{3.39}$$

It is straight forward to see from (3.25) that all the even dimensions will produce a $\log^2\delta$ divergence. For even dimensions, the number of powers of h in the denominator is odd. When separating the divergences, similar to (3.30), it will produce a $1/h$ factor. This term integrated over h and then over ρ, similar to I_2, will produce a $\log^2\delta$ divergence. Of course these results will persist in field theories in curved backgrounds and for dual gravities with higher derivative curvatures. We will discuss these examples in sections 3.3 and 3.4.

3.3 EE for extended singularities

In this section, we will calculate the entanglement entropy for various creases. Obviously the crease can have two types of locus of singularities: flat or curved. By studying these examples, we will argue that the contribution from the singularity will be non-zero only if the locus is even dimensional and curved.

In the first subsection, we will study creases with a flat locus of singularity. We will see that in this case, we don't find any new logarithmic divergence coming from the singularity. The geometries we will be considering are kinks $k\times R^1$, $k\times R^2$ and cone $c_1\times R^2$.

In second subsection, we will mainly consider the singular geometries of the form $k\times S^m$ and $c_n\times S^m$. In these cases, a generic calculation for arbitrary curvature is tedious. So

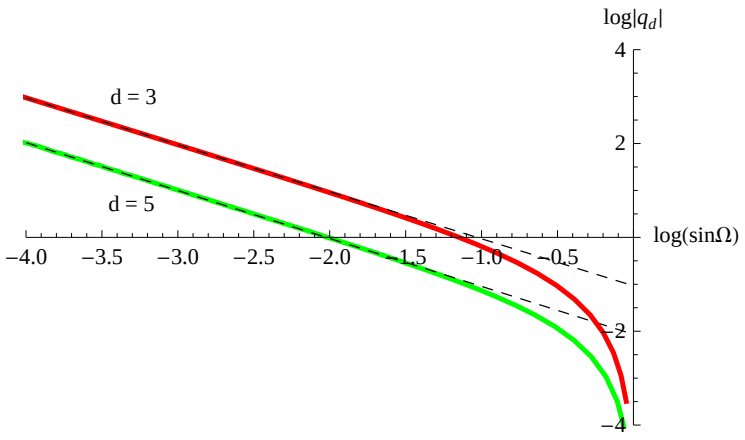

Figure 3.2: (Color online) We have drawn $\log|q_d|$ as a function of $\log(\sin\Omega)$ for $d = 3$ and 5. In the limit $\Omega \to 0$, it is known that $\log|q_3| = -\log(\sin\Omega) + \ldots$ [54]. For $d = 5$, we observe similar behavior and find that for small Ω, the linear fit is $\log|q_5| = -\log(\sin\Omega) - 2.1$.

we will work in certain limits where curvature of the locus of singularity is very small and show how the leading order terms behave in these cases. In the calculations, we will use following approach: If the curvature of the locus is related to $1/R_1$, then in the limit $R_1 \to \infty$, the boundary geometry will become flat. Now we make R_1 finite but keep it very large and, calculate the leading order corrections to EE in this limit. In this process, we will find that leading correction to EE, in a proper normalization, will be of order $\mathcal{O}(1/R_1^2)$ but not $\mathcal{O}(1/R_1)$. Now, this approach has one more advantage. As we are going to argue now, for some simple background geometries like $R^3 \times S^2$, the coefficient of the logarithmic term at order $1/R_1^2$ will be the complete contribution from the kink. We will note in our calculations that the only dimensionful quantities in the problem will be R_1, the UV cut-off δ and the IR cut-off H. As the coefficient of the logarithmic divergence should be dimensionless and if we series expand it in terms of $1/R_1$, the numerator can either be δ or H. So the new logarithmic contribution will be of the form

$$S_{new} = R_1^2 \left(\frac{C_0}{R_1^2} + \mathcal{O}\left(\frac{\delta^2}{R_1^4}\right) + \mathcal{O}\left(\frac{H^2}{R_1^4}\right) + \ldots \right) \log(\delta)\,. \tag{3.40}$$

In this case, the terms with δ in the numerator are not UV cut-off invariant and terms with H in the numerator are not really the contribution from the kink. That is because H is the scale of the bulk part of the entangling surface and a term arising from the singularity should be independent of it. So we only need to focus on the leading order correction which is precisely the contribution from the singularity. This issue will again be discussed when

we rigorously calculate EE in section 3.3.2.

Let us summarize our strategy for the calculations here: for cases where boundary theory is on curved background, we use the Fefferman-Graham expansion to find the dual gravity near the boundary. For flat boundary, we don't need to go through this step. Then, we calculate the entanglement entropy for the kinks and use the Fefferman-Graham expansion to separate the logarithmic divergence from the singularities. We will see that first few terms of the Fefferman-Graham expansion will be sufficient to find the leading order corrections to the logarithmic divergences in the limit $R_1 \to \infty$. To begin with, we will calculate EE for some singular geometries with flat locus in the next subsection.

3.3.1 EE for singularity with a flat locus

In this section, we will calculate entanglement entropy for following two types of geometries[6]: $k \times R^m$ and $c_n \times R^m$. We will particularly see EE for cases where $n = 1, 2$ and $m = 1, 2, 3$.

3.3.1.1 Crease $k \times R^m$

In this section, we will work in the dual Einstein's gravity with bulk metric (3.9) and $n = 0$. The crease $k \times R^m$ geometry is given by $\theta \in [-\Omega, \Omega]$, $\rho \in [0, \infty]$ and $x_i \in [-\infty, \infty]$. We pick (ρ, θ, x_i) as the induced coordinates over the minimal area surface and the radial coordinate is $z = z(\rho, \theta)$. Now the induced metric becomes

$$h = \begin{bmatrix} \frac{L^2}{z^2}(1+z'^2) & \frac{L^2}{z^2}z'\dot{z} & & & \\ \frac{L^2}{z^2}z'\dot{z} & \frac{L^2}{z^2}(\rho^2+\dot{z}^2) & & & \\ & & \frac{L^2}{z^2} & & \\ & & & \ddots & \\ & & & & \frac{L^2}{z^2} \end{bmatrix}, \tag{3.41}$$

and the EE is given by

$$S_d\big|_{k\times R^{d-3}} = \frac{2\pi\, L^{d-1}\tilde{H}^{d-3}}{\ell_{\rm P}^{d-1}} \int d\rho\, d\theta\, \frac{1}{z^{d-1}} \sqrt{(\dot{z}^2 + \rho^2(1+z'^2))}\,, \tag{3.42}$$

[6]The EE for wedge $k \times R^1$ is also calculated in [142].

where $\dot{z} = \partial_\theta z$, $z' = \partial_\rho z$ and we have substituted $m = d-3$. We have also imposed an IR cut-off such that $x_i \in [-\tilde{H}/2, \tilde{H}/2]$. From this functional, we can find the equation of motion for $z(\rho,\theta)$ and it turns out to be

$$\begin{aligned} 0 \;=\; & \rho z\left(\rho^2+\dot{z}^2\right) z'' + \rho z\left(1+z'^2\right)\ddot{z} - 2\rho z\dot{z}z'\dot{z}' \\ & + \dot{z}^2((d-1)\rho + 2zz') + \rho^2((d-1)\rho + zz')\left(1+z'^2\right) \end{aligned} \tag{3.43}$$

Now, in the limit $h \to \infty$, ρ is the only scale in the problem. Hence, using scaling symmetry of AdS, we can argue that

$$z \;=\; \rho\, h(\theta)\,. \tag{3.44}$$

Using this in (3.42), we find that

$$S_d\big|_{k\times R^{d-3}} \;=\; \frac{4\pi\, L^{d-1}\tilde{H}^{d-3}}{\ell_{\rm P}^{d-1}} \int_{\delta/h_0}^{H} \frac{d\rho}{\rho^{d-2}} \int_{h_0}^{\delta/\rho} dh \frac{1}{\dot{h}h^{d-1}} \sqrt{\dot{h}^2+h^2+1}\,, \tag{3.45}$$

where we have put the UV cut-off at $z=\delta$ and defined $h_0 = h(0)$. Further, we have used (3.44) to find the limits of the integrations and the extra factor of two comes from changing the range of the integration from $\theta \in [-\Omega,\Omega]$ to $\theta \in [0,\Omega]$. Using (3.44) in (3.43), we find the equation of motion for h

$$h(1+h^2)\ddot{h} + (d-1)\dot{h}^2 + h^4 + dh^2 + (d-1) \;=\; 0\,. \tag{3.46}$$

In this case, although it is not explicit, we can find a constant along the θ translation from (3.46). It is straight forward to see that

$$K_d \;=\; \frac{(1+h^2)^{(d-1)/2}}{h^{(d-1)}\sqrt{\dot{h}^2+h^2+1}} \;=\; \frac{(1+h_0^2)^{(d-2)/2}}{h_0^{(d-1)}} \tag{3.47}$$

is a conserved quantity and it satisfies the equation of motion. Now we can use (3.47) to separate the divergences in the EE (3.45). Using the fact that h decreases near the boundary and hence $\dot{h}$ should be negative, we find

$$\dot{h} \;=\; -\frac{\sqrt{1+h^2}\sqrt{(1+h^2)^{d-2} - K_d^2\, h^{2(d-1)}}}{K_d\, h^{d-1}}\,. \tag{3.48}$$

Using this in integrand of (3.45), in the limit $h \to 0$, we find that

$$\frac{\sqrt{\dot{h}^2+h^2+1}}{\dot{h}h^{d-1}} \sim -\frac{1}{h^{d-1}} - \frac{1}{2}K_d^2\, h^{d-1} + \mathcal{O}(h^{d+1})\,. \tag{3.49}$$

Now in (3.45), we can add and subtract $1/h^{d-1}$ in the integrand and write

$$S_d\big|_{k\times R^{d-3}} = \frac{4\pi\, L^{d-1}\tilde{H}^{d-3}}{\ell_{\rm P}^{d-1}}\left[\frac{H}{(d-2)\delta^{d-2}} - \frac{1}{(d-3)h_0\delta^{d-3}} + \mathcal{O}(\delta^0) + I_1\right], \quad (3.50)$$

where

$$I_1 = \int_{\delta/h_0}^{H}\frac{d\rho}{\rho^{d-2}}\int_{h_0}^{\delta/\rho} dh\left(\frac{\sqrt{\dot{h}^2+h^2+1}}{\dot{h}h^{d-1}} + \frac{1}{h^{d-1}}\right).$$

In (3.50), first few term are coming from h and ρ integration of $1/h^{d-1}$. To find the divergences in I_1, first we represent the integrand by $J(h)$ and from (3.49), $J(h)\sim h^{d-1}$ as $h\to 0$. We perform the integration by parts and write I_1 as

$$\begin{aligned} I_1 &= -\frac{1}{(d-3)H^{d-3}}\int_{h_0}^{\delta/H} dh\, J(h) - \frac{\delta}{(d-3)}\int_{\delta/h_0}^{H}\frac{d\rho}{\rho^{d-1}}J(h)\big|_{h=\delta/\rho} \\ &= -\frac{1}{(d-3)H^{d-3}}\int_{h_0}^{\delta/H} dh\, J(h) - \frac{\delta}{(d-3)}\, I_2\,. \end{aligned} \quad (3.51)$$

Now to separate the divergences in I_2, we make a change of variable from ρ to $q=\delta/\rho$ and then Taylor expand the terms around $\delta=0$:

$$\begin{aligned} I_2 &= -\frac{1}{\delta^{d-2}}\int_{h_0}^{\delta/H} dq\, q^{d-3}J(q) \\ &= -\frac{1}{\delta^{d-2}}\left[\int_{h_0}^{0} dq\, q^{d-3}J(q) + \frac{\delta}{H}\left(q^{d-3}J(q)\right)_{q=\delta/H} + \dots\right] \\ &= -\frac{1}{\delta^{d-2}}\int_{h_0}^{0} dq\, q^{d-3}J(q) + (O)(\delta^3)\,. \end{aligned} \quad (3.52)$$

In the above expression, the integral over q is finite because from (3.49), $q^{d-3}J(q)\sim q^{2d-4}$ for small q. Combining (3.50)-(3.52), we can write

$$\begin{aligned} S_d\big|_{k\times R^{d-3}} = \frac{4\pi\, L^{d-1}\tilde{H}^{d-3}}{\ell_{\rm P}^{d-1}}\Bigg[&\frac{H}{(d-2)\delta^{d-2}} \\ &+ \left(\int_{h_0}^{0} dq\, q^{d-3}J(q) - \frac{1}{h_0}\right)\frac{1}{(d-3)\delta^{d-3}} + \mathcal{O}(\delta^0)\Bigg]. \end{aligned} \quad (3.53)$$

Remarkably, we find that as soon as we add a flat locus to the kink, the log divergence disappears. However, there is a new divergent term of order $1/\delta^{d-3}$ which does not arise

in smooth entangling surfaces. This clearly shows that logarithmic contribution from the crease depends on the curvature of the locus of the singularity. Further, there can be a logarithmic term from the smooth part of the entangling surface in even d. However, the entangling surface in $k \times R^m$ is flat apart from the singularity and such contributions vanish. This example clearly shows that when the locus is flat, there is no contribution from the singularity. However, we will see ahead that as soon as we turn on the curvature of the locus, the logarithmic divergence will appear only for the cases where locus is even dimensional.

3.3.1.2 Crease $c_n \times R^m$

In this section, we will calculate EE for the geometries $c_n \times R^m$. Although such a calculation can be extended for general n and m, we will particularly focus on $n = 1, 2$ and $m = 1, 2$. To begin with, we consider the metric (3.9) for the dual gravity with arbitrary m. The conically singular geometry $c_n \times R^m$ is given by $\rho \in [0, \infty]$ and $\theta \in [0, \Omega]$ in gravitational dual (3.9). We assume that the induced coordinates over the minimal area surface are (ρ, θ, Ω_n), where Ω_n are coordinates over unit sphere S^n. As we have rotational symmetry over the sphere S^n, the radial coordinate for the minimal area surface will be given by $z = z(\rho, \theta)$. Now, the induced metric over the surface is

$$h = \begin{bmatrix} \frac{L^2}{z^2}\left(1+z'^2\right) & \frac{L^2}{z^2}z'\dot{z} & & & & \\ \frac{L^2}{z^2}z'\dot{z} & \frac{L^2}{z^2}\left(\rho^2+\dot{z}^2\right) & & & & \\ & & \frac{L^2\rho^2\sin^2(\theta)}{z^2}g_{ab}(S^n) & & & \\ & & & \frac{L^2}{z^2} & & \\ & & & & \ddots & \\ & & & & & \frac{L^2}{z^2} \end{bmatrix}, \tag{3.54}$$

where $g_{ab}(S^n)$ represents the metric over the unit sphere S^n and the EE is given by

$$S_d\big|_{c_n\times R^m} = \frac{2\pi\, L^{d-1}\tilde{H}^m\Omega_n}{\ell_{\rm P}^{d-1}}\int d\rho\, d\theta\, \frac{\rho^n\sin^n(\theta)}{z^{d-1}}\sqrt{\left(\dot{z}^2+\rho^2(1+z'^2)\right)}\,, \tag{3.55}$$

where Ω_n is the area of the unit n-sphere, $\dot{z} = \partial_\theta z$ and $z' = \partial_\rho z$. Note that we have integrated over the x^i's and used the IR cut-off $x^i \in [-\tilde{H}/2, \tilde{H}/2]$. Now for this case, the equation of motion becomes

$$\begin{aligned} 0 \;=\; & \rho^2 z\left(\rho^2+\dot{z}^2\right)z'' + \rho^2 z\left(1+z'^2\right)\ddot{z} - 2\rho^2 z\dot{z}z'\dot{z}' + (d-1)\rho^2\left(\dot{z}^2+\rho^2\left(1+z'^2\right)\right) \\ & + z\left(d'\cot(\theta)\dot{z}^3 + (d'+2)\rho\dot{z}^2z' + d'\rho^2\cot(\theta)\dot{z}\left(1+z'^2\right) + (d'+1)\rho^3z'\left(1+z'^2\right)\right). \end{aligned} \tag{3.56}$$

Once again, here we can use the scaling arguments and say that

$$z(\rho,\theta) \;=\; \rho\, h(\theta)\,. \tag{3.57}$$

Then, EE reduces to

$$S_d\big|_{c_n\times R^m} \;=\; \frac{2\pi\, L^{d-1}\tilde{H}^m\Omega_n}{\ell_{\rm P}^{d-1}}\int_{\delta/h_0}^{H}\frac{d\rho}{\rho^{d-n-2}}\int_{h_0}^{\delta/\rho}dh\,\frac{\sin^n(\theta)\sqrt{\dot{h}^2+h^2+1}}{\dot{h}\,h^{d-1}}\,, \tag{3.58}$$

and equation of motion for h becomes

$$\begin{aligned} 0 \;=\;& h(1+h^2)\ddot{h}+n\cot(\theta)h\dot{h}^3+(d+nh^2-1)\dot{h}^2+n\cot(\theta)h(1+h^2)\dot{h}\\ &+(n+1)h^4+(d+n)h^2+d-1\,. \end{aligned} \tag{3.59}$$

In (3.58), we have changed the integration from θ to over h. We have also introduced the UV cut-off $z=\delta$ and defined $h_0=h(0)$.

Now we set $n=1$ and $d=5$ (that also mean that $m=1$), and calculate EE for the singular surface $c_1\times R^1$. First, we need to find $y=\sin(\theta)$ near the boundary in terms of h. For that, we invert the equation of motion (3.56) and get

$$\begin{aligned} 0 \;=\;& h\left(1+h^2\right)y\left(1-y^2\right)y''-2\left(2+3h^2+h^4\right)yy'^3\\ &-h\left(1+h^2\right)\left(1-2y^2\right)y'^2-\left(4+h^2\right)y\left(1-y^2\right)y'-h\left(-1+y^2\right)^2\,. \end{aligned} \tag{3.60}$$

Now solving this equation perturbatively near the boundary, we get the solution

$$y \;=\; \sin(\Omega)-\frac{1}{6}h^2\cos(\Omega)\cot(\Omega)-\frac{1}{432}h^4(19-5\cos(2\Omega))\cot^2(\Omega)\csc(\Omega)+\mathcal{O}(h^5)\,, \tag{3.61}$$

where we have used that at $h=0$, $y(0)=\sin(\Omega)$. Further, we can define $\dot{h}(\theta)=f(h)$ and write the equation (3.59) in the form

$$\begin{aligned} 0 \;=\;& h\left(1+h^2\right)yff'+h\sqrt{1-y^2}f^3+\left(4+h^2\right)yf^2\\ &+h\left(1+h^2\right)\sqrt{1-y^2}f+2\left(2+3h^2+h^4\right)y\,, \end{aligned} \tag{3.62}$$

where $y'=dy/dh$. Using y from (3.61) and solving this equation near the asymptotic boundary, we find

$$\begin{aligned} f \;=\;& -\frac{3\tan(\Omega)}{h}+\frac{1}{3}h(8-\cos(2\Omega))\csc(2\Omega)+f_0h^2\\ &-\frac{1}{216}h^3(435-404\cos(2\Omega)+52\cos(4\Omega))\csc^3(\Omega)\sec(\Omega)+\mathcal{O}(h^4)\,, \end{aligned} \tag{3.63}$$

where f_0 is a constant which is fixed by the condition $f(h_0) = 0$. Now it is straight forward to see that near the boundary

$$\frac{\sin(\theta)\sqrt{1+h^2+\dot{h}^2}}{\dot{h}h^4} \sim -\frac{\sin(\Omega)}{h^4} + \frac{\cos(\Omega)\cot(\Omega)}{9h^2} - \frac{1}{18}\cos(\Omega)\cot(\Omega) + \dots , \tag{3.64}$$

and we can use it to make h integral in entropy functional finite. So we write EE as

$$\begin{aligned} S_5\big|_{c_1\times R^1} &= \frac{4\,\pi^2\,L^4\tilde{H}}{\ell_{\rm P}^4}\Bigg[\frac{H^2\sin(\Omega)}{6\delta^3} + \frac{\cos(\Omega)\cot(\Omega)}{9\delta}\log(\delta/H) \\ &+ \frac{2h_0^2\cos(\Omega)\cot(\Omega)\,(1-\log(h_0)) - 9\sin(\Omega)}{18h_0^2\delta} \\ &+ \int_{\delta/h_0}^{H}\frac{d\rho}{\rho^2}\int_{h_0}^{\delta/\rho} dh\left(\frac{\sin^{d'}(\theta)\sqrt{\dot{h}^2+h^2+1}}{\dot{h}h^{d-1}} + \frac{\sin(\Omega)}{h^4} - \frac{\cos(\Omega)\cot(\Omega)}{9h^2}\right) + \mathcal{O}(h^0)\Bigg], \end{aligned} \tag{3.65}$$

where we have already performed the integrations over some terms. Now let us call the term with integration I_1 and the integrand $J_5(h)$. Then, near the boundary $J_5(h) \sim \mathcal{O}(h^0)$. Now using integration by parts, we can write

$$\begin{aligned} I_1 &= \int_{\delta/h_0}^{H}\frac{d\rho}{\rho^2}\int_{h_0}^{\delta/\rho} dh J_5(h) \\ &= -\frac{1}{H}\int_{h_0}^{\delta/H} dh J_5(h) - \delta\int_{\delta/h_0}^{H}\frac{d\rho}{\rho^3}J_5(h)|_{h=\delta/\rho} \end{aligned}$$

We further make the coordinate transformation $\rho = \delta/q$ and Taylor expand the second term in δ:

$$\begin{aligned} I_1 &= -\frac{1}{H}\int_{h_0}^{\delta/H} dh J_5(h) + \frac{1}{\delta}\int_{h_0}^{\delta/H} dq\, q J_5(q) \\ &= -\frac{1}{H}\int_{h_0}^{0} dh J_5(h) + \frac{1}{\delta}\int_{h_0}^{0} dq\, q^2 J_5(q) - \frac{\delta}{18H^3}\cos(\Omega)\cot(\Omega) + \mathcal{O}(\delta)\,, \end{aligned} \tag{3.66}$$

where we have used (3.64) to get the final expression. Combining (3.65) and (3.66), we can write

$$\begin{aligned} S_5\big|_{c_1\times R^1} &= \frac{4\,\pi^2\,L^4\tilde{H}}{\ell_{\rm P}^4}\Bigg[\frac{H^2\sin(\Omega)}{6\delta^3} + \frac{1}{\delta}\int_{h_0}^{0} dq\, q J_5(q) + \frac{\cos(\Omega)\cot(\Omega)}{9}\frac{\log(\delta/H)}{\delta} \\ &+ \frac{2h_0^2\cos(\Omega)\cot(\Omega)\,(1-\log(h_0)) - 9\sin(\Omega)}{18h_0^2\delta} + \mathcal{O}(\delta^0)\Bigg], \end{aligned} \tag{3.67}$$

Note that in the above expression, we have a new divergence of the form $\log(\delta/H)/\delta$ which does not arise in EE for smooth entangling surfaces. This term should be a contribution from the singularity. Further, we note that as soon as we add a one-dimensional locus to the conical singularity, both double log and logarithmic divergences disappear. Recall that in the previous case for cone c_1 in $d = 4$, *i.e.,* eqn. (3.34), we got a double log and log terms.

We can easily generalize the above calculations to the crease $c_1 \times R^2$. For this case, the integrand near the boundary and complete expression for EE are given by (3.254) and (3.255). Once again we find a divergent term of the order $\log(\delta/H)/\delta$ in EE. Also, now the cut-off independent term is

$$S_6^{\log}\big|_{c_1\times R^2} = \frac{4\,\pi^2\,L^5\tilde{H}^2}{\ell_{\rm P}^5}\frac{3(13-19\cos(2\Omega))\cot^2(\Omega)\csc(\Omega)}{8192H^2}\log(\delta/H)\,. \tag{3.68}$$

Note that for singular geometry $c_1 \times R^2$ in $d = 6$, we only have log divergence instead of $\log^2\delta$ as compared to the cone c_1 in equations (3.34). Also, recall that in (3.39), we saw that a cone without a locus, c_3 in $d = 6$ gives a $\log^2\delta$ divergence. In (3.68), this $\log^2\delta$ term disappears because of flat locus we have added. We will see in section 3.3.2.2 that as soon as the curvature of the locus turned on, the $\log^2\delta$ divergence will reappear in (3.186) in $d = 6$. In (3.68), the logarithmic contribution can be attributed to the fact that in even dimensions, the entangling surface has a logarithmic divergence. We can explicitly verify that logarithmic term in (3.68) comes from integration over $1/h$ in expansion (3.254). As ρ need not to be near the singularity, this contribution is from smooth part of the entangling surface. Further, it is straight forward to find that for cone $c_1 \times R^3$ in $d = 7$ dimensional CFT, the EE has no double log or log divergence. Which is expected because for entangling surface in odd d, there is no logarithmic divergence and as the locus is odd dimensional and flat, there should not be any logarithmic contribution from the singularity either.

We can further extend these calculations for the case $n = 2$ and $m = 1, 2$. For crease $c_2 \times R^1$, we find that the universal term in EE is a logartihmic divergence and it is given by

$$S_6^{\log}\big|_{c^2\times R^1} = \frac{8\,\pi^2\,L^5\tilde{H}}{\ell_{\rm P}^5}\frac{(7-9\cos(2\Omega))\cot^2(\Omega)}{256\,H}\log(\delta/H)\,. \tag{3.69}$$

We also find a new contribution from the singularity at the order $1/\delta$. In $c^2 \times R^1$, the locus of the singularity is odd dimensional and hence singularity doesn't contribute in the universal term. However, smooth part of the entangling surface contributes through a log in $d = 6$ and this is the contribution (3.69). It can be verified that this log term arise from integration over h away from the singularity. Further, we can also calculate EE for crease

$c_2 \times R^2$ and find that there is a new divergence from singularity of order $1/\delta^2$. However, there is neither a log nor a $\log^2$ term in EE. Note that for crease $c_2 \times R^2$, the locus of the singularity is even dimensional but flat. So singularity does not contribute through a log term. However, as we will see in (3.191) that for a curved locus, we get a log contribution.

3.3.2 EE for singularity with curved locus

In this subsection, we will consider several singular embeddings which have a curved locus. As soon as the curvature of the locus is turned on, the double log and log terms from singularity will make appearance. In this section, we will consider the creases $k \times \Sigma$ and $c_n \times \Sigma$, where locus Σ will take the form S^m or $S^{m-p} \times R^p$. These cases will be slightly more involved and hence we will do two things: first, we will always work in the limit where curvature of the locus is very small and we will do the calculations perturbatively. In certain cases, we will see that these perturbative calculations are sufficient to pick out the complete contributions from the singularity. Second, for calculations in this section, we will foliate our minimal area surface in different way. In all the previous cases, the induced coordinates on the minimal area surface were $(\rho, \theta, \dots)$ and we assumed that the radial coordinate $z = z(\rho, \theta)$. However, we will find that it is more convenient to do the calculations in a coordinate system where bulk radial coordinate z is one of the induced coordinates on the minimal area surface and we have $\rho = \rho(z, \theta)$. We have shown in figure 3.3, how these different induced coordinates foliate the minimal area surface in the bulk. Note that the new set of induced coordinate $(z, \theta, \dots)$ are not the well-defined coordinates on the boundary as $\rho = \rho(z, \theta)$ will be multivalued for $z = 0$ and $\theta = \pm\Omega$. However, until unless we put the UV cut-off, we find that $\rho = \rho(z, \theta)$ is a well-behaved function and we can work with it. Now, in the next subsection we will begin with the geometries $k \times \Sigma$ and then we will move on to conical singularities $c_n \times \Sigma$.

3.3.2.1 Crease $k \times \Sigma$

In this section, we will mainly consider the geometries $k \times S^2$, $k \times R \times S^2$ and $k \times S^3$. We will see that singularities with even dimensional locus will contribute through a logarithmic term.

To begin with, let us consider $d = 5$ CFT on background $R^3 \times S^2$. Before we construct the singular entangling surface in this geometry and calculate holographic EE, we need to

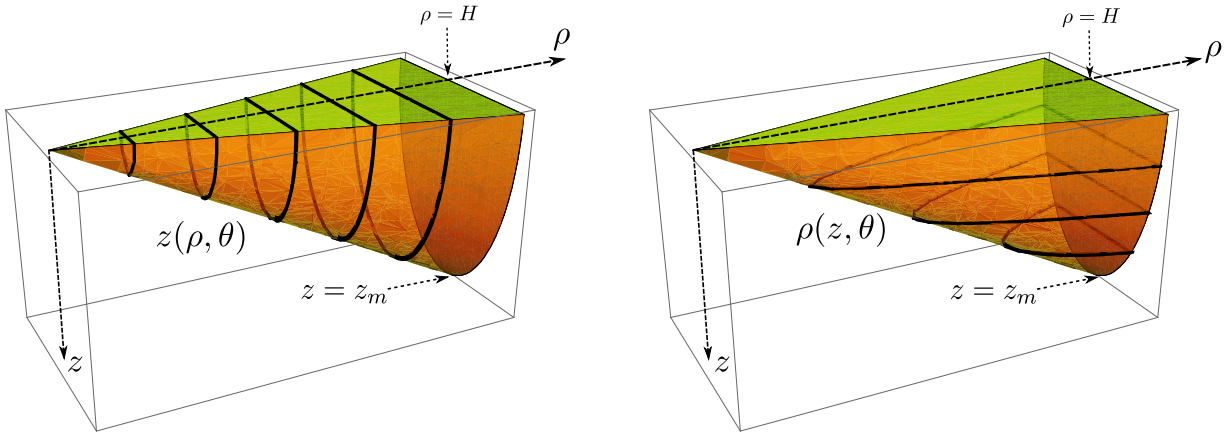

(a) (b)

Figure 3.3: Panel (a) shows how minimal area surface is foliated when we have the induced coordinates $(\rho, \theta, \dots)$ and minimal area surface is given by $z = z(\rho, \theta)$. Panel (b) shows the foliation of the minimal area surface when induced coordinates are $(z, \theta, \dots)$ and we have $\rho = \rho(z, \theta)$. Note that $z = z_m$ is the maximum value of z on the surface such that $\rho(0, z_m) = H$.

find the dual gravity. So we begin with the action for six-dimensional dual Einstein gravity

$$I_6 \,=\, \frac{1}{\ell_{\rm P}^4}\int d^6x\sqrt{-g}\left[\frac{20}{L^2}+R\right]\,, \tag{3.70}$$

for which, the equation of motion is given by

$$R_{\mu\nu}-\frac{10}{L^2}g_{\mu\nu}\,=\,0\,. \tag{3.71}$$

Now we ansatz that the bulk metric, which has the boundary $R^3 \times S^2$, is of the form

$$ds^2 \,=\, \frac{L^2}{z^2}\left(dz^2+f_1(z)\left(dt^2+d\rho^2+\rho^2 d\theta^2\right)+f_2(z)R_1^2\,d\Omega_2^2\right)\,, \tag{3.72}$$

where $d\Omega_2^2 = d\xi_0^2 + \sin^2(\xi_0)d\xi_1^2$ represents the metric over two-sphere and, f_1 and f_2 are functions of the radial coordinate. Here R_1 is the radius of the sphere on the boundary and in the limit $R_1 \to \infty$, we recover the flat boundary. To find f_1 and f_2, we use the Fefferman-Graham expansion near the boundary $z = 0$. The idea is to insert the ansatz

(3.72) in the equation of motion (3.71) and then solve it near $z = 0$ to find

$$\begin{aligned} f_1 &= 1 + \frac{z^2}{12R_1^2} + \frac{17z^4}{576R_1^4} + \dots \quad \text{and} \\ f_2 &= 1 - \frac{z^2}{4R_1^2} - \frac{5z^4}{192R_1^4} + \dots . \end{aligned} \tag{3.73}$$

Knowing the dual geometry near the boundary, we can calculate EE for the geometry $k \times S^2$. On the boundary, this geometry is defined by $\rho \in [0, H]$ and $\theta \in [-\Omega, \Omega]$, where H is the IR cut-off. Now to define the minimal area surface, we use slightly different coordinates compared to the previous sections. We choose the induced coordinates to be $(z, \theta, \xi_0, \xi_1)$ and because of the rotational symmetry on the sphere, $\rho = \rho(z, \theta)$. Although, $\rho(z, \theta)$ is not a well defined function at the boundary $z = 0$ but we can definitely work with it until we impose the UV cut-off and assume that the boundary is at some finite $z = \delta$. With this coordinate choice, the induced metric becomes

$$h = \begin{bmatrix} \frac{L^2}{z^2}\left(f_1\rho'^2 + 1\right) & \frac{L^2 f_1}{z^2}\dot{\rho}\rho' & & \\ \frac{L^2 f_1}{z^2}\dot{\rho}\rho' & \frac{L^2 f_1}{z^2}\left(\dot{\rho}^2 + \rho^2\right) & & \\ & & \frac{L^2 f_2\, R_1^2}{z^2} & \\ & & & \frac{L^2 f_2\, R_1^2}{z^2}\sin^2(\xi_0) \end{bmatrix}, \tag{3.74}$$

where $\dot{\rho} = \partial_\theta \rho$, $\rho' = \partial_z \rho$ and hence, the entanglement entropy is given by

$$S_5\big|_{k\times S^2} = \frac{8\,\pi^2 L^4 R_1^2}{\ell_{\rm P}^4} \int dz\, d\theta\, \frac{\sqrt{f_1 f_2}}{z^4} \sqrt{\dot{\rho}^2 + \rho^2(1 + f_1\rho'^2)}\,. \tag{3.75}$$

We can easily find the equation of motion of $\rho(z, \theta)$ to be

$$\begin{aligned} 0 = \;& 2z f_1 f_2 \rho \left(\rho^2 + \dot{\rho}^2\right)\rho'' + 2z f_2 \rho \left(1 + f_1\rho'^2\right)\ddot{\rho} - 4z f_1 f_2 \rho\dot{\rho}\rho'\dot{\rho}' \\ & + 2z f_1 f_2' \rho\rho' \left(\dot{\rho}^2 + \rho^2\left(1 + f_1\rho'^2\right)\right) - f_2\Big(4z\dot{\rho}^2 + \rho\left(8f_1 - 3z f_1'\right)\dot{\rho}^2\rho' \\ & + 2z\rho^2\left(1 + f_1\rho'^2\right) - \rho^3\rho'\left(3z f_1' - 8f_1^2\rho'^2 - 2f_1\left(4 - z f_1'\rho'^2\right)\right)\Big), \end{aligned} \tag{3.76}$$

where $\ddot{\rho} = \partial_\theta^2 \rho$, $\rho'' = \partial_z^2 \rho$ and $\dot{\rho}' = \partial_z \partial_\theta \rho$.

As discussed earlier, we will be working in the approximation $R_1 \to \infty$. In this approximation, we will find that leading order correction to the EE will be of the order $\mathcal{O}(1/R_1^2)$. To show this, first we need to find the form of the solution $\rho(z, \theta)$ in this approximation. For that, we make following ansatz:

$$\rho(z, \theta) = \frac{z}{h(\theta)} + \frac{z^2}{R_1} g_2(\theta) + \frac{z^3}{R_1^2} g_3(\theta) + \dots . \tag{3.77}$$

This ansatz is made on the basis of the available dimensionful quantities in the problem. Now we are going to argue that in the following expansion, the θ dependent functions g_{2n} are zero. To see that, we insert the ansatz (3.77) in the equation of motion for $\rho(z,\theta)$ and find following equations of motion for h, g_2 and g_3:

$$h\left(1+h^2\right)\ddot{h}+4\dot{h}^2+\left(1+h^2\right)\left(4+h^2\right) = 0\,, \tag{3.78}$$

$$\begin{aligned} h^2\left(1+h^2\right)^2 g_2''+2h\left(7+2h^2\right)\left(1+h^2\right)\dot{h}g_2' \\ +g_2\left(14\dot{h}^2-2h^4(8-\dot{h}^2)-h^6-31h^2-16\right) &= 0\,, \end{aligned} \tag{3.79}$$

$$\begin{aligned} h^2\left(1+h^2\right)^2\ddot{g}_3+4h\left(4+h^2\right)\left(1+h^2\right)\dot{h}\dot{g}_3 \\ -g_3\left(h^6+h^2\left(35-2\dot{h}^2\right)+4\left(5-6\dot{h}^2\right)+2h^4\left(8-\dot{h}^2\right)\right) &= \mathcal{S}_1\,, \end{aligned} \tag{3.80}$$

where $\mathcal{S}_1$ is given by

$$\begin{aligned} \mathcal{S}_1 &= \frac{1}{12h}\left(8+7h^4+3\dot{h}^2+h^2\left(15+7\dot{h}^2\right)\right) \\ &+\frac{2h}{\left(1+h^2\right)}\Bigg(h^2\left(1+h^2\right)^2\left(4+h^2\right)g_2'^2+2h\left(8+7h^2+h^6\right)\dot{h}g_2g_2' \\ &+\left(h^2\left(32-15\dot{h}^2\right)+h^6\left(8+\dot{h}^2\right)+2h^4\left(15+\dot{h}^2\right)+2\left(5+8\dot{h}^2\right)\right)g_2^2\Bigg)\,. \end{aligned} \tag{3.81}$$

Note that here we have arranged the equations of motion such that on the left hand side, we have the homogeneous part of the equation and on the right hand side, we have the source terms. So $\mathcal{S}_1$ is source for g_3 and in (3.81), terms in first line come from the corrections to f_1 and f_2, and terms in last two lines are second order in g_2. We also note that in (3.79) and (3.80), we have used equations of motion to eliminate the second derivatives of h and g_2. Now we notice following points: first, the corrections to f_1 and f_2 are of even powers of $1/R_1$ and hence they only source g_{2n+1}'s. Second, g_{2n} are sourced only by g_{2i}'s, where $i<n$. Third, in flat boundary, precisely in the limit $R_1\to\infty$, we have $h\neq 0$ and $g_2=0$. So above arguments conclude that as we make R_1 finite, only $g_{2n+1}(\theta)$'s will be turned on and all the $g_{2n}=0$, which clearly are solution of these equations of motion.

Now to separate the logarithmic divergence in entanglement entropy, first let us write $\rho=\rho_0(z,\theta)+\rho_1(z,\theta)/R_1^2$, where $\rho_0=z/h(\theta)$ and ρ_1 is higher order corrections for large R_1. Using this and (3.73) in (3.75), and keeping only the leading order terms in R_1, we

find that

$$S_5\big|_{k\times S^2} = \frac{8\,\pi^2 L^4 R_1^2}{\ell_{\rm P}^4}\int_{z_m}^{\delta} dz \int_{-\Omega+\epsilon}^{\Omega-\epsilon} d\theta \Bigg[\frac{\sqrt{\dot\rho_0^2+\rho_0^2\,(1+\rho_0'^{\,2})}}{z^4} - \frac{(\dot\rho_0\,(5z^2\dot\rho_0-24\dot\rho_1)-24\rho_0\rho_1\,(1+\rho_0'^{\,2})+\rho_0^2\,(5z^2+4z^2\rho_0'^{\,2}-24\rho_0'\rho_1'))}{24z^4R_1^2\sqrt{\dot\rho_0^2+\rho_0^2\,(1+(\rho_0')^{\,2})}}\Bigg], \tag{3.82}$$

where δ is the UV cut-off and $\epsilon=\epsilon(z)$ is defined such that $\rho(z,\Omega-\epsilon)=H$ and further, z_m is defined such that $\rho(z_m,0)=H$ or $\epsilon(z_m)=\Omega$. We can also insert this ansatz in (3.76) and find the equation of motion for ρ_0 and ρ_1 by series expanding it in terms of R_1. In the second term of (3.82), we can convert ρ_1' and $\dot\rho_1$ into ρ_1 using the integration by parts and then use equation of motion for ρ_0 to simplify the coefficient of ρ_1 to zero. This process will leave us with some boundary terms and we find that

$$\begin{aligned} S_5\big|_{k\times S^2} = \frac{4\,\pi^2 L^4 R_1^2}{\ell_{\rm P}^4}\int_{z_m}^{\delta} dz \int_{-\Omega+\epsilon}^{\Omega-\epsilon} d\theta \Bigg[&\frac{\sqrt{\dot\rho_0^2+\rho_0^2\,(1+(\rho_0')^{\,2})}}{z^4} - \frac{(5\dot\rho_0^2+\rho_0^2\,(5+4\rho_0'^{\,2}))}{24\,R_1^2z^2\sqrt{\dot\rho_0^2+\rho_0^2\,(1+(\rho_0')^{\,2})}} + \frac{\partial}{\partial\theta}\left(\frac{\dot\rho_0\rho_1}{R_1^2z^4\sqrt{\dot\rho_0^2+\rho_0^2\,(1+(\rho_0')^{\,2})}}\right) \\ &+\frac{\partial}{\partial z}\left(\frac{\rho_0^2\rho_0'\rho_1}{R_1^2z^4\sqrt{\dot\rho_0^2+\rho_0^2\,(1+\rho_0'^{\,2})}}\right)\Bigg]. \end{aligned} \tag{3.83}$$

Now we can insert the ansatz $\rho_0=z/h(\theta)$ and $\rho_1=z^3g_3(\theta)$ and simplify the functional to

$$\begin{aligned} S_5\big|_{k\times S^2} = \frac{16\,\pi^2 L^4 R_1^2}{\ell_{\rm P}^4}\int_{z_m}^{\delta} dz \int_{h_0}^{h_{1c}} \frac{dh}{\dot h}\Bigg[&\frac{\sqrt{1+h^2+\dot h^2}}{z^3h^2} - \frac{4+5h^2+5\dot h^2}{24\,R_1^2zh^2\sqrt{1+h^2+\dot h^2}}\Bigg] \\ &-\frac{14\,\pi^2L^4}{\ell_{\rm P}^4}\int_{z_m}^{\delta}\frac{dz}{z}\frac{g_3\dot h}{\sqrt{1+h^2+\dot h^2}}\Big|_{\theta=\Omega-\epsilon}, \end{aligned} \tag{3.84}$$

where we have changed the integration limits from $(-\Omega,\Omega)$ to $(0,\Omega)$ and also changed the integration variable to $h(\theta)$. Note that the boundary term with derivative with respect to z turns out to zero up to leading order. We have also defined $h_0=h(0)$ and $h_{1c}(\rho)=h(\Omega-\epsilon)$ and used $h_1'(0)=0$ in getting the boundary terms.

Now to separate the logarithmic divergences, we consider all the contributing factors one by one. We will see that the first term in the first line of (3.84) will not contain any logarithmic divergence. The second term and the boundary terms will contain logarithmic divergence. Note that we also need to be careful and consider the divergences coming from

the limits of the integrals. To begin with, we first study the behavior of h and g_3 near the asymptotic boundary. The equations of motion for h and g_3 are given by (3.78) and (3.80) with $g_2 = 0$. Now similar to (3.47), we find that equation of motion for h can be integrated once to get

$$K_5 \;=\; \frac{(1+h^2)^2}{h^4\sqrt{1+h^2+\dot{h}^2}}\,, \tag{3.85}$$

where K_5 is a constant and it can be further related to $h(0)$ using $\dot{h}(0) = 0$.

To extract the logarithmic divergence, we will only need the asymptotic behavior of h and g_3. Hence we solve g_3 in terms of h in asymptotic limit, where h is small. To do so, we use (3.80) and change the variable from θ to h by expressing $\ddot{g}_3(\theta) = d^2g_3/d\theta^2$ and $\dot{g}_3(\theta) = dg_3/d\theta$ in terms of $\ddot{g}_3(h) = d^2g_3/dh^2$ and $\dot{g}_3(h1) = dg_3/dh$. We further use (3.85) to express $h1'(\theta)$ in terms of K_5 and h. Finally, the equation of motion for $g_3(h)$ becomes

$$\begin{aligned} 0 \;=\;& 12h^3\left(1+h^2\right)^2\left(h^8K_5^2-\left(1+h^2\right)^3\right)\ddot{g}_3+12\,h^2\Big(h^8\left(1+h^2\right)\left(16+5h^2\right)K_5^2 \\ & -4\left(1+h^2\right)^4\left(3+h^2\right)\Big)\dot{g}_3-12h\Big(2\left(1+h^2\right)^3\left(12+h^2+h^4\right) \\ & -h^8\left(44+17h^2+3h^4\right)K_5^2\Big)g_3+\left(1+h^2\right)^3\left(3+7h^2\right)+5h^8K_5^2\,. \end{aligned} \tag{3.86}$$

Now this equation has two solutions when we solve it perturbatively in the limit $h \to 0$. The leading terms of these solutions go like $1/h^3$ and $1/h^8$. However, g_3 must be such that ρ is finite in the limit $h \to 0$ and $\delta \to 0$. As g_3 appears at order δ^3 in (3.73), it can only go like $1/h^3$. Hence, one of the constants, which is the coefficient of $1/h^8$, is fixed to zero. As a result, the asymptotic solution turns out to be

$$g_3 \;=\; \frac{b_3}{h^3}+\frac{1+88b_3}{56h}+\frac{4+72b_3}{189}h-\frac{4+72b_3}{693}h^3+\dots\,, \tag{3.87}$$

where b_3 is a constant such that $g_3(\theta)$ has an extrema at $\theta = 0$.

Before we begin discussing divergences of various terms, we find the series expansion of h_{1c} in terms of the UV cut-off δ. As $h_{1c} = h(\Omega-\epsilon)$ and $z = \delta$ at the cut-off, we can use (3.77) and perturbative solution (3.87) to find following series expansion for h_{1c}

$$h_{1c}(\delta) \;=\; \left(\frac{1}{H}+\frac{b_3H}{R_1^2}\right)\delta+\frac{(1+88b_3)\,\delta^3}{56HR_1^2}+\frac{(4+72b_3)\,\delta^5}{189H^3R_1^2}+\mathcal{O}(\delta^6)\,. \tag{3.88}$$

Note that we have kept only leading corrections in R_1 at any order in δ.

Now we return to (3.84) and analyze the divergences for each term. First, we use (3.85) in the integrand of first two terms of (3.84) and find that in the asymptotic limit

$$\frac{\sqrt{1+h^2+\dot{h}^2}}{\dot{h}h^2} \sim -\frac{1}{h^2}-\frac{1}{2}K_5^2h^6+\mathcal{O}(h^8) \tag{3.89}$$

$$\frac{5\dot{h}^2+5h^2+4}{24\dot{h}\,h^2\sqrt{1+h^2+\dot{h}^2}} \sim -\frac{5}{24h^2}-\frac{K_5^2h^6}{16}+\mathcal{O}(h^8)\,. \tag{3.90}$$

So we can make the integrands finite by organizing the terms in following form

$$\begin{aligned} I_1 &= \int_{z_m}^{\delta}\frac{dz}{z^3}\int_{h_0}^{h_{1c}}dh\frac{\sqrt{1+h^2+\dot{h}^2}}{\dot{h}h^2} \\ &= \int_{z_m}^{\delta}\frac{dz}{z^3}\int_{h_0}^{h_{1c}}dh\left[\frac{\sqrt{1+h^2+\dot{h}^2}}{\dot{h}h^2}+\frac{1}{h^2}\right]+\int_{z_m}^{\delta}\frac{dz}{z^3}\left(\frac{1}{h_{1c}}-\frac{1}{h_0}\right) \qquad (3.91)\\ &= I_1'+I_2'\,, \qquad (3.92)\end{aligned}$$

and

$$\begin{aligned} I_2 &= \int_{z_m}^{\delta}\frac{dz}{z}\int_{h_0}^{h_{1c}}dh\frac{5\dot{h}^2+5h^2+4}{24\dot{h}h^2\sqrt{1+h^2+\dot{h}^2}} \\ &= \int_{z_m}^{\delta}\frac{dz}{z}\int_{h_0}^{h_{1c}}dh\left[\frac{5\dot{h}^2+5h^2+4}{24\dot{h}h^2\sqrt{1+h^2+\dot{h}^2}}+\frac{5}{24h^2}\right]+\int_{z_m}^{\delta}dz\frac{5}{24z}\left(\frac{1}{h_{1c}}-\frac{1}{h_0}\right) \qquad (3.93)\\ &= I_3'+I_4'\,. \qquad (3.94)\end{aligned}$$

In (3.92), I_1' and I_2' represent the first and second integrals in (3.91). Similarly in (3.94), I_3' and I_4' are the first and second integrals in (3.93). Now first we consider I_1'. We differentiate it with respect to the UV cut-off δ and look for $1/\delta$ divergent terms. After taking the derivative, we find

$$\begin{aligned} \frac{dI_1'}{d\delta} &= \frac{1}{\delta^3}\int_{h_0}^{h_{1c}(\delta)}dh\left[\frac{\sqrt{1+h^2+\dot{h}^2}}{\dot{h}h^2}+\frac{1}{h^2}\right] \\ &= \frac{1}{\delta^3}\int_{h_0}^{0}dh\left[\frac{\sqrt{1+h^2+\dot{h}^2}}{\dot{h}h^2}+\frac{1}{h^2}\right]+\frac{1}{\delta^2}\frac{dh_{1c}(\delta)}{d\delta}\left[\frac{\sqrt{1+h^2+\dot{h}^2}}{\dot{h}h^2}+\frac{1}{h^2}\right]_{h=h_{1c}(\delta)}+\ldots \\ &= \frac{1}{\delta^3}\int_{h_0}^{0}dh\left[\frac{\sqrt{1+h^2+\dot{h}^2}}{\dot{h}h^2}+\frac{1}{h^2}\right]-\frac{K_5^2}{2H^5}\left(\frac{1}{H^2}+\frac{7b_3}{R_1^2}\right)\delta^4+\mathcal{O}(\delta^6)\,, \qquad (3.95)\end{aligned}$$

where we have Taylor expanded the integrand in the second line and in the third line, we have used (3.85) and (3.88) to find the leading order divergence. Here we don't have any term of order $1/\delta$ and of $\log(\delta)/\delta$, which come consecutively from divergences of order $\log(\delta)$ and $\log(\delta)^2$ in I_1'.

Similar to I_1', we can take a derivative of I_2' with respect to δ and use (3.88) to find

$$\frac{dI_2'}{d\delta} = \left(1-\frac{b_3H^2}{R_1^2}\right)\frac{H}{\delta^4} - \frac{1}{h_0\delta^3} - \frac{1+88b_3}{56R_1^2}\frac{H}{\delta^2} - \frac{4+72b_3}{189\,R_1^2H} + \mathcal{O}(\delta)\,. \tag{3.96}$$

So we find that I_1 doesn't have any logarithmic divergence. We can use similar steps to find

$$\begin{aligned}\frac{dI_3'}{d\delta} &= \frac{1}{\delta}\int_{h_0}^{0} dh\left[\frac{5\dot{h}^2+5h^2+4}{24\dot{h}h^2\sqrt{1+h^2+\dot{h}^2}}+\frac{5}{24h^2}\right] \\ &\qquad -\frac{K_5^2}{H^5}\left(\frac{1}{16H^2}+\frac{7b_3}{16R_1^2}\right)\delta^5+\mathcal{O}(\delta^6) \qquad (3.97)\\ \frac{dI_4'}{d\delta} &= \frac{5H}{24\delta^2}\left(1-\frac{b_3H^2}{R_1^2}\right)-\frac{5}{24h_0}\frac{1}{\delta}+\mathcal{O}(\delta^0) \qquad (3.98)\end{aligned}$$

We can also use the same procedure on the boundary term and find that

$$\begin{aligned}\frac{d}{d\delta}\int_{z_m}^{\delta}\frac{dz}{z}\frac{g_3\dot{h}}{\sqrt{1+h^2+\dot{h}^2}}\Big|_{\theta=\Omega-\epsilon} &= \frac{b_3H^3}{\delta^4}\left(1-\frac{3b_3H^2}{R_1^2}\right) \qquad (3.99)\\ &\quad +\frac{(1+88b_3)\,H\,(-4b_3H^2+R_1^2)}{56R_1^2\delta^2} \\ &\quad +\left(\frac{4+72b_3}{189H}-\frac{(27+16b_3\,(521+17100b_3))\,H}{84672R_1^2}\right) \\ &\quad +\mathcal{O}(\delta)\,.\end{aligned}$$

So from (3.95) - (3.99), we can find the logarithmic divergence in the EE for $k\times S^2$ geometry:

$$S_5^{log}\big|_{k\times S^2} = \frac{16\,\pi^2L^4}{\ell_{\rm P}^4}\left(-\int_{h_0}^{0}dh\left[\frac{5\dot{h}^2+5h^2+4}{24\dot{h}h^2\sqrt{1+h^2+\dot{h}^2}}+\frac{5}{24h^2}\right]+\frac{5}{24h_0}\right)\log(\delta)\,. \tag{3.100}$$

From (3.95) - (3.99), we also notice a divergence of order $1/\delta^2$ in EE which does not appear in EE for smooth entangling surfaces. Note that such a term also appeared in EE

for $k \times R^m$ in (3.53). We further notice that logarithmic contribution in (3.100) is of next to the leading order for large R_1. As we are working in odd dimensional space-time, there is no logarithmic contribution from the surface itself.

Now we turn to our next example. Having seen the logarithmic contribution from a even dimensional curved locus, now we consider odd dimensional locus. We will calculate the entanglement entropy for $k \times S^3$ geometry in CFT on $R^3 \times S^3$. For this case, the locus is S^3 and we will see that there will be no log contribution from the singularity. However, as the CFT is in even dimensional space-time, we should be getting a logarithmic contribution coming from the entangling surface. In this case, the metric for the dual geometry is given by

$$ds^2 = \frac{L^2}{z^2}\left(dz^2 + f_1(z)\left(dt^2 + d\rho^2 + \rho^2 d\theta^2\right) + f_2(z) R_1^2\, d\Omega_3^2\right), \tag{3.101}$$

where $d\Omega_3^2 = d\xi_0^2 + \sin^2(\xi_0) d\xi_1^2 + \sin^2(\xi_0)\sin^2(\xi_1) d\xi_2^2$ is the unit three-sphere and f_1 and f_2 are following

$$\begin{aligned} f_1 &= 1 + \frac{3z^2}{20R_1^2} + \frac{69z^4}{1600R_1^4} + \dots, \\ f_2 &= 1 - \frac{7z^2}{20R_1^2} - \frac{11z^4}{1600R_1^4} + \dots. \end{aligned} \tag{3.102}$$

Once again we choose the induced coordinates on the minimal area surface to be $(z, \theta, \xi_0, \xi_1, \xi_2)$ and assume $\rho = \rho(z, \theta)$. Then the induced metric over the minimal area surface will be given by

$$h = \begin{bmatrix} \frac{L^2}{z^2}\left(f_1 \rho'^2 + 1\right) & \frac{L^2 f_1}{z^2}\dot\rho\rho' & & & & \\ \frac{L^2 f_1}{z^2}\dot\rho\rho' & \frac{L^2 f_1}{z^2}\left(\dot\rho^2 + \rho^2\right) & & & & \\ & & \frac{L^2 f_2\, R_1^2}{z^2} & & & \\ & & & \frac{L^2 f_2\, R_1^2}{z^2}\sin^2(\xi_0) & & \\ & & & & \frac{L^2 f_2\, R_1^2}{z^2}\sin^2(\xi_0)\sin^2(\xi_1) & \end{bmatrix}, \tag{3.103}$$

where $\dot\rho = \partial_\theta \rho$, $\rho' = \partial_z \rho$ and now the entanglement entropy is given by

$$S_6\big|_{k\times S^3} = \frac{4\,\pi^3 L^5 R_1^3}{\ell_{\rm P}^5} \int dz\, d\theta\, \frac{\sqrt{f_1 f_2^3}}{z^5} \sqrt{\dot\rho^2 + \rho^2(1 + f_1 \rho'^2)}\,. \tag{3.104}$$

We can easily find the equation of motion for $\rho(z,\theta)$ to be

$$\begin{aligned} 0 \;=\;& 2zf_1f_2\rho\left(\rho^2+\dot\rho^2\right)\rho'' + 2f_2\rho\left(z+zf_1\rho'^2\right)\ddot\rho - 4zf_1f_2\rho\dot\rho\rho'\dot\rho' \\ & +3zf_1\rho f_2'\rho'\left(\dot\rho^2+\rho^2\left(1+f_1\rho'^2\right)\right) - f_2\Big(4z\dot\rho^2+\rho\left(10f_1-3zf_1'\right)\dot\rho^2\rho' + 2\rho^2\left(z+zf_1\rho'^2\right) \\ & -\rho^3\rho'\left(3zf_1'-10f_1^2\rho'^2+2f_1\left(-5+zf_1'\rho'^2\right)\right)\Big)\,, \end{aligned} \tag{3.105}$$

where $\ddot\rho=\partial_\theta^2\rho$, $\rho''=\partial_z^2\rho$ and $\dot\rho'=\partial_z\partial_\theta\rho$. Once again, we can write $\rho=\rho_0+\rho_1/R_1^2$ and keep only the leading order correction to the entanglement entropy. We can further series expand the equation of motion (3.105) to get equation of motion for ρ_0 and ρ_1. We find that, using these equations of motion and integration by parts, the entropy functional can be simplified to

$$\begin{aligned} S_6\big|_{k\times S^3} \;=\;& \frac{4\,\pi^3L^5R_1^3}{\ell_{\rm P}^5}\int_{z_m}^{\delta}dz\int_{-\Omega+\epsilon}^{\Omega-\epsilon}d\theta\Bigg[\frac{\sqrt{\dot\rho_0^2+\rho_0^2\left(1+\rho_0'^2\right)}}{z^5} \\ & -\frac{3\left(6\dot\rho_0^2+\rho_0^2\left(6+5\rho_0'^2\right)\right)}{40R_1^2z^3\sqrt{\dot\rho_0^2+\rho_0^2\left(1+\rho_0'^2\right)}} + \frac{\partial}{\partial\theta}\left(\frac{\dot\rho_0\rho_1}{R_1^2z^5\sqrt{\dot\rho_0^2+\rho_0^2\left(1+\rho_0'^2\right)}}\right) \\ & +\frac{\partial}{\partial z}\left(\frac{\rho_0^2\rho_0'\rho_1}{R_1^2z^5\sqrt{\dot\rho_0^2+\rho_0^2\left(1+\rho_0'^2\right)}}\right)\Bigg]\,. \end{aligned} \tag{3.106}$$

Further, we can substitute $\rho_0=z/h(\theta)$ and $\rho_1=z^3g_3(\theta)$. The equations of motion for h and g_3 from (3.105) becomes

$$h\left(1+h^2\right)\ddot h+5\dot h^2+\left(1+h^2\right)\left(5+h^2\right) \;=\; 0\,, \tag{3.107}$$

$$\begin{aligned} & h^2\left(1+h^2\right)^2\ddot g_3+2h\left(9+11h^2+2h^4\right)\dot h\dot g_3 \\ & -g_3\left(25+45h^2+21h^4+h^6-\left(27-h^2+2h^4\right)\dot h^2\right) \;=\; \mathcal{S}_1\,, \end{aligned} \tag{3.108}$$

where source terms for g_3 are

$$\mathcal{S}_1 \;=\; \frac{3\left(10+19h^2+9h^4+\left(4+9h^2\right)\dot h^2\right)}{20h}\,. \tag{3.109}$$

Here, as in (3.47), we can integrate the equation of motion for h once and write it as

$$K_6 \;=\; \frac{\left(1+h^2\right)^{5/2}}{h^5\sqrt{1+h^2+\dot h^2}}\,, \tag{3.110}$$

where K_6 is a constant and we can relate it to h_0 by using $\dot{h}(0) = 0$. We can further simplify (3.106) to

$$S_6\big|_{k\times S^3} = \frac{8\,\pi^3 L^5 R_1^3}{\ell_{\rm P}^5}\left(I_1 + \frac{I_2}{R_1^2} + \frac{I_3}{R_1^2} + \frac{I_4}{R_1^2}\right), \tag{3.111}$$

where

$$I_1 = \int_{z_m}^{\delta} dz \int_{h_0}^{h_{1c}} \frac{dh}{\dot{h}} \frac{\sqrt{1+h^2+\dot{h}^2}}{z^4 h^2}, \tag{3.112}$$

$$I_2 = -\int_{z_m}^{\delta} dz \int_{h_0}^{h_{1c}} \frac{dh}{\dot{h}} \frac{3\left(5+6h^2+6\dot{h}^2\right)}{40R_1^2 z^2 h^2\sqrt{1+h^2+\dot{h}^2}}, \tag{3.113}$$

$$I_3 = -\int_{z_m}^{\delta} \frac{dz}{z^2} \frac{g_3\dot{h}}{\sqrt{1+h^2+\dot{h}^2}}\bigg|_{\Omega-\epsilon}, \tag{3.114}$$

$$I_4 = -\int_{z_m}^{\delta} \frac{dz}{z^2} \int_{h_0}^{h_{1c}} \frac{dh}{\dot{h}} \frac{g_3}{h\sqrt{1+h^2+\dot{h}^2}}. \tag{3.115}$$

Note that the last term I_4 is not being integrated over z. That's because $h_{1c}(z)$ appears in the limit of θ integral. Now, we can use (3.110) in (3.108) to find following equation of motion for g_3 in terms of h:

$$\begin{aligned} 0 = {} & 20h^3\left(1+h^2\right)^2\left(h^{10}K_6^2 - \left(1+h^2\right)^4\right)\ddot{g}_3 + 20h^2(1+h^2)\Big(h^{10}\left(18+5h^2\right)K_6^2 \\ & - \left(1+h^2\right)^5\left(13+4h^2\right)\Big)\dot{g}_3 + 20h\Big(h^{10}\left(52+19h^2+3h^4\right)K_6^2 \\ & - \left(1+h^2\right)^4\left(27-h^2+2h^4\right)\Big)g_3 + 3\left(1+h^2\right)^4\left(4+9h^2\right) + 18h^{10}K_6^2\,. \end{aligned} \tag{3.116}$$

This equation can be solved perturbatively for small h near the asymptotic boundary. We find that this second order equation of motion has two different solutions which go like $1/h^3$ and $1/h^9$. As ρ is finite at the boundary, the solution can go only with power $1/h^3$. So the solution near the boundary becomes

$$g_3(h) = \frac{b_3}{h^3} + \frac{3+140b_3}{80h} + \frac{3+36b_3}{64}h - \frac{1+12b_3}{96}h^3 + \frac{5+60b_3}{1536}h^5 + \dots, \tag{3.117}$$

where constant b_3 is fixed by the condition that $\dot{g}_3(h_0) = 0$. We use this in $\rho = z/h + z^3 g_3/R_1^2$ and evaluate it at $z = \delta$, $\rho = H$ and $h = h_{1c}(\delta)$. By inverting the relation and keeping only leading order terms in R_1, we find

$$h_{1c}(\delta) = \left(\frac{1}{H} + \frac{b_3 H}{R_1^2}\right)\delta + \frac{(3+140b_3)\,\delta^3}{80HR_1^2} + \frac{(3+36b_3)\,\delta^5}{64H^3R_1^2} + \mathcal{O}(\delta^6). \tag{3.118}$$

Now we use this to separate logarithmic divergence. Using (3.110), we find that the integrands in I_1, I_2, I_3 and I_4 are of following form for small h:

$$\begin{aligned}
\frac{\sqrt{1+h^2+\dot{h}^2}}{\dot{h}h^2} &\sim -\frac{1}{h^2}-\frac{1}{2}K_6^2h^8+\mathcal{O}(h^9)\,,\\
-\frac{3\left(5+6h^2+6\dot{h}^2\right)}{40\dot{h}h^2\sqrt{1+h^2+\dot{h}^2}} &\sim \frac{9}{20h^2}+\frac{3}{20}K_6^2h^8+\mathcal{O}(h^9)\\
-\frac{g_3\dot{h}}{\sqrt{1+h^2+\left(\dot{h}\right)^2}} &\sim \frac{b_3}{h^3}+\frac{3+140b_3}{80h}+\frac{3}{64}\left(1+12b_3\right)h-\frac{1}{96}\left(1+12b_3\right)h^3+\mathcal{O}(h^5)\\
\frac{g_3}{\dot{h}h\sqrt{1+h^2+\dot{h}^2}} &\sim b_3K_6^2h^6+\mathcal{O}(h^7)\,.
\end{aligned}\tag{3.119}$$

Using these relations, now we can make the integral over h finite and organize the terms in following form

$$\begin{aligned}
I_1 &= \int_{z_m}^{\delta}\frac{dz}{z^4}\int_{h_0}^{h_{1c}}dh\left(\frac{\sqrt{1+h^2+\dot{h}^2}}{\dot{h}h^2}+\frac{1}{h^2}\right)+\int_{z_m}^{\delta}\frac{dz}{z^4}\left(\frac{1}{h_{1c}(z)}-\frac{1}{h_0}\right)\\
&= I_1'+I_2'\,,
\end{aligned}\tag{3.120}$$

$$\begin{aligned}
I_2 &= -\int_{z_m}^{\delta}\frac{dz}{z^2}\int_{h_0}^{h_{1c}}dh\left(\frac{3\left(5+6h^2+6\dot{h}^2\right)}{40h^2\sqrt{1+h^2+\dot{h}^2}}+\frac{9}{20h^2}\right)-\frac{9}{20}\int_{z_m}^{\delta}\frac{dz}{z^2}\left(\frac{1}{h_{1c}(z)}-\frac{1}{h_0}\right)\\
&= I_3'+I_4'\,.
\end{aligned}\tag{3.121}$$

In (3.120), I_1' and I_2' represent the first and second integral in the expression of I_1. Similarly in (3.121), I_3' and I_4' are the first and second integral in expression for I_2. We can further take derivative of I''s with respect to δ and then Taylor expand the integrals to get

$$\frac{dI_1'}{d\delta} = \frac{1}{\delta^4}\int_{h_0}^{0}dh\frac{\sqrt{1+h^2+\dot{h}^2}}{\dot{h}h^2}-\frac{K_6^2\left(9\,b_3H^2+R_1^2\right)}{2\,H^9R_1^2}\delta^5+\mathcal{O}(\delta^6)\,,\tag{3.122}$$

$$\frac{dI_2'}{d\delta} = \frac{H}{\delta^5}\left(1-\frac{b_3\,H^2}{R_1^2}\right)-\frac{1}{h_0\delta^4}-\frac{\left(3+140\,b_3\right)H}{80\,R_1^2\delta^3}-\frac{3+36\,b_3}{64\,H\,R_1^2\delta}+\mathcal{O}(\delta^0)\,,\tag{3.123}$$

$$\frac{dI_3'}{d\delta} = -\frac{1}{\delta^2}\int_{h_0}^{0}dh\left(\frac{3\left(5+6\,h^2+6\,\dot{h}^2\right)}{40\,h^2\sqrt{1+h^2+\dot{h}^2}}\right)+\frac{3\,K_6^2\left(9\,b_3H^2+R_1^2\right)\delta^7}{20\,H^9R_1^2}+\mathcal{O}(\delta^{10})\,,\tag{3.124}$$

$$\frac{dI_4'}{d\delta} = -\frac{9\,H}{20\,\delta^3}\left(1-\frac{b_3H^2}{R_1^2}\right)+\frac{9}{20\,h_0\delta^2}+\frac{9\left(3+140\,b_3\right)H}{1600\,R_1^2\delta}+\mathcal{O}(\delta)\,.\tag{3.125}$$

Also, we can simplify the boundary terms in a similar fashion and find that

$$\frac{dI_3}{d\delta} = \left(1-\frac{3\,b_3H^2}{R_1^2}\right)\frac{b_3H^3}{\delta^5}+\left(7\,b_3+\frac{3}{20}-\frac{b_3\,(3+140\,b_3)\,H^2}{5\,R_1^2}\right)\frac{H}{4\,\delta^3} + \left(\frac{3+36\,b_3}{64\,H}-\frac{(9+1440\,b_3+26800\,b_3^2)\,H}{6400\,R_1^2}\right)\frac{1}{\delta}+\mathcal{O}(\delta^0)\,, \quad (3.126)$$

$$\frac{dI_4}{d\delta} = -\frac{1}{\delta^2}\int_{h_0}^{0} dh\frac{g_3}{h\,\dot{h}\sqrt{1+h^2+\dot{h}^2}}+\mathcal{O}(\delta^5)\,. \quad (3.127)$$

Now using (3.111) and (3.120)-(3.127), first we notice that there are new divergent terms of order $1/\delta^3$ and $1/\delta$ which does not arise in EE for smooth entangling surfaces in $d=6$. We also find that the logarithmic divergence of the entanglement entropy are

$$S_6^{log}\big|_{k\times S^3} = \frac{8\,\pi^3L^5R_1}{\ell_{\rm P}^5}\left(0+\mathcal{O}\left(\frac{1}{R_1^4}\right)\right)\log(\delta)\,. \quad (3.128)$$

Remarkably, the contribution to the logarithmic divergence at the leading order is zero. At higher order, *i.e.,* at order $\mathcal{O}\,(1/R_1^4)$, there should be logarithmic contribution coming from the bulk part of the entangling surface. According to [48], the logarithmic contribution from four-dimensional entangling surface will have the coefficient of the form $\int dx^4C$, where C is a combination of various curvature squared terms. These terms will contribute with $1/R_1^4$ and so does the smooth part of the entangling surface. So up to leading order, there is no logarithmic contribution from the singularity because the locus is odd dimensional. We might ask if there can be any contribution from the singularity alone at higher order in $1/R_1$. However, we discard such a possibility. It is easy to see that all the higher order terms will be of even powers of $1/R_1$ and to make the coefficient dimensionless, the only other available scale will be H. As H is related to the size of the surface, all such contributions actually result from the contribution from the bulk surface and not the singularity alone. Hence, we expect that there is no contribution from the singularity in this case.

Next, we see one more example where odd dimensional locus doesn't contribute to logarithmic dimensions, in spite of non-zero curvature. We are going to consider $k\times R^1\times S^2$ geometry. We consider the background geometry for CFT to be $R^4\times S^2$. Then the bulk metric for boundary $R^4\times S^2$ is given by

$$ds^2 = \frac{L^2}{z^2}\left(dz^2+f_1(z)\left(dt^2+d\rho^2+\rho^2d\theta^2+dx^2\right)+f_2(z)R_1^2\,d\Omega_2^2\right)\,, \quad (3.129)$$

and f_1 and f_2 become

$$\begin{aligned} f_1 &= 1+\frac{z^2}{20R_1^2}+\frac{z^4}{100R_1^4}+\dots\,, \\ f_2 &= 1-\frac{z^2}{5R_1^2}-\frac{7z^4}{800R_1^4}+\dots\,. \end{aligned} \tag{3.130}$$

The $k\times R^1\times S^2$ geometry is given by $\theta\in[-\Omega,\Omega]$, $x\in[-\infty,\infty]$ and $\rho\in[0,\infty]$. We put IR cut-offs on x and ρ directions such that $x\in[-\tilde{H}/2,\tilde{H}/2]$ and $\rho\in[\rho_m,H]$, where ρ_m is related to the UV cut-off δ. We choose (z,θ,x,ξ_0,ξ_1) as induced coordinates on the minimal area surface with $\rho=\rho(z,\theta)$. Then, the induced metric over the minimal area surface will become

$$h = \begin{bmatrix} \frac{L^2}{z^2}\left(f_1\rho'^2+1\right) & \frac{L^2 f_1}{z^2}\dot{\rho}\rho' & & & \\ \frac{L^2 f_1}{z^2}\dot{\rho}\rho' & \frac{L^2 f_1}{z^2}\left(\dot{\rho}^2+\rho^2\right) & & & \\ & & \frac{L^2 f_1}{z^2} & & \\ & & & \frac{L^2 f_2\, R_1^2}{z^2} & \\ & & & & \frac{L^2 f_2\, R_1^2}{z^2}\sin^2(\xi_0) \end{bmatrix}, \tag{3.131}$$

where $\dot{\rho}=\partial_\theta\rho$, $\rho'=\partial_z\rho$ and now the entanglement entropy is given by

$$S_6\big|_{k\times R^1\times S^2} = \frac{8\,\pi^2 L^5 R_1^2\tilde{H}}{\ell_{\rm P}^5}\int dz\,d\theta\,\frac{f_1 f_2}{z^5}\sqrt{\dot{\rho}^2+\rho^2(1+f_1\rho'^2)}\,. \tag{3.132}$$

Note that here we have already performed integration over x. In this case, the equation of motion for $\rho(z,\theta)$ becomes

$$\begin{aligned} 0 = \;& 2z f_1 f_2\rho\left(\rho^2+\dot{\rho}^2\right)\rho''+2z f_2\rho\left(1+f_1\rho'^2\right)\ddot{\rho}-2z f_2\left(\rho^2+2\dot{\rho}^2\right)\dot{\rho}' \\ & +2\rho\left(2z f_2 f_1'+f_1\left(-5f_2+z f_2'\right)\right)\left(\rho^2+\dot{\rho}^2\right)\rho'-2z f_1 f_2\rho^2\rho'^2 \\ & +f_1\rho^3\left(3z f_2 f_1'+2f_1\left(-5f_2+z f_2'\right)\right)\rho'^3\,. \end{aligned} \tag{3.133}$$

where $\ddot{\rho}=\partial_\theta^2\rho$, $\rho''=\partial_z^2\rho$ and $\dot{\rho}'=\partial_z\partial_\theta\rho$. Once again, we can write $\rho=\rho_0+\rho_1/R_1^2$ and keep only the leading order correction to the entanglement entropy. We can further series expand the equation of motion (3.133) to get equation of motion for ρ_0 and ρ_1. We find that, using these equations of motion and integration by parts, the entropy functional can

be simplified to

$$S_6\big|_{k\times R^1\times S^2} = \frac{8\,\pi^2 L^5 R_1^2 \tilde{H}}{\ell_{\rm P}^5}\int_{z_m}^{\delta} dz \int_{-\Omega+\epsilon}^{\Omega-\epsilon} d\theta \Bigg[\frac{\sqrt{\dot{\rho}_0^2+\rho_0^2\,(1+\rho_0'^{\,2})}}{z^5} - \frac{3\,(6\dot{\rho}_0^2+\rho_0^2\,(6+5\rho_0'^{\,2}))}{40R_1^2 z^3\sqrt{\dot{\rho}_0^2+\rho_0^2\,(1+\rho_0'^{\,2})}} + \frac{\partial}{\partial\theta}\left(\frac{\dot{\rho}_0\rho_1}{R_1^2 z^5\sqrt{\dot{\rho}_0^2+\rho_0^2\,(1+\rho_0'^{\,2})}}\right) + \frac{\partial}{\partial z}\left(\frac{\rho_0^2\rho_0'\rho_1}{R_1^2 z^5\sqrt{\dot{\rho}_0^2+\rho_0^2\,(1+\rho_0'^{\,2})}}\right)\Bigg]. \tag{3.134}$$

Further, we can substitute $\rho_0 = z/h(\theta)$ and $\rho_1 = z^3 g_3(\theta)$. The equations of motion for h and g_3 from (3.133) becomes

$$h\left(1+h^2\right)\ddot{h} + 5\dot{h}^2 + \left(1+h^2\right)\left(5+h^2\right) = 0\,, \tag{3.135}$$

$$h^2\left(1+h^2\right)^2\ddot{g}_3 + 2h\left(9+11h^2+2h^4\right)\dot{h}\dot{g}_3 - g_3\left(25+45h^2+21h^4+h^6-\left(27-h^2+2h^4\right)\dot{h}^2\right) = \mathcal{S}_1\,, \tag{3.136}$$

where source terms for g_3 are

$$\mathcal{S}_1 = \frac{\left(10+19h^2+9h^4+(4+9h^2)\left(\dot{h}\right)^2\right)}{20h}\,. \tag{3.137}$$

Note that homogeneous part of the equations of motion for h and g_3 are same as the case of kink in $R^3\times S^3$. Similar to (3.47), we can further integrate the equation of motion for h to get a conserved quantity

$$K_6 = \frac{(1+h^2)^{5/2}}{h^5\sqrt{1+h^2+\dot{h}^2}}\,. \tag{3.138}$$

The simplified expression for the entanglement entropy then becomes

$$S_6\big|_{k\times R^1\times S^2} = \frac{16\,\pi^2 L^5 \tilde{H} R_1^2}{\ell_{\rm P}^5}\left(I_1+\frac{I_2}{R_1^2}+\frac{I_3}{R_1^2}+\frac{I_4}{R_1^2}\right), \tag{3.139}$$

where

$$I_1 = \int_{z_m}^{\delta} dz \int_{h_0}^{h_{1c}} \frac{dh}{\dot{h}} \frac{\sqrt{1+h^2+\dot{h}^2}}{z^4 h^2}\,, \tag{3.140}$$

$$I_2 = -\int_{z_m}^{\delta} dz \int_{h_0}^{h_{1c}} \frac{dh}{\dot{h}} \frac{\left(5+6h^2+6\dot{h}^2\right)}{40R_1^2 z^2 h^2 \sqrt{1+h^2+\dot{h}^2}}\,, \tag{3.141}$$

$$I_3 = -\int_{z_m}^{\delta} \frac{dz}{z^2} \frac{g_3 \dot{h}}{\sqrt{1+h^2+\dot{h}^2}}\bigg|_{\Omega-\epsilon}\,, \tag{3.142}$$

$$I_4 = -\int_{z_m}^{\delta} \frac{dz}{z^2} \int_{h_0}^{h_{1c}} \frac{dh}{\dot{h}} \frac{g_3}{h\sqrt{1+h^2+\dot{h}^2}}\,. \tag{3.143}$$

Now we can convert the equation of motion for $g_3(\theta)$ into equation of motion for $g_3(h)$ and solve it perturbatively near the boundary in the limit $h \to 0$. We find that

$$g_3 = \frac{b_3}{h^3} + \frac{1+140b_3}{80h} + \frac{1}{64}(1+36b_3)\,h - \frac{1}{288}(1+36b_3)\,h^3 + \frac{(5+180b_3)\,h^5}{4608} + \mathcal{O}(h^5)\,, \tag{3.144}$$

where constant b_3 is fixed by the condition $\dot{g}_3(h_0) = 0$. Using this in $\rho = z/h + z^3 g_3/R_1^2$ and evaluating at $z = \delta$, $\rho = H$ and $h = h_{1c}(\delta)$, we find

$$h_{1c}(\delta) = \left(\frac{1}{H} + \frac{b_3 H}{R_1^2}\right)\delta + \frac{(1+140b_3)\,\delta^3}{80HR_1^2} + \frac{(1+36b_3)\,\delta^5}{64H^3R_1^2} + \mathcal{O}(\delta^6)\,. \tag{3.145}$$

Note that we have only kept the terms of order $1/R_1^2$ in the above expansion. Now for small h, the integrands in I_i's behave as

$$\begin{aligned}
\frac{\sqrt{1+h^2+\dot{h}^2}}{\dot{h}h^2} &\sim -\frac{1}{h^2} - \frac{1}{2}K_6^2 h^8 + \mathcal{O}(h^9)\,,\\
-\frac{\left(5+6h^2+6\dot{h}^2\right)}{40\dot{h}h^2\sqrt{1+h^2+\dot{h}^2}} &\sim \frac{3}{20h^2} + \frac{1}{20}K_6^2 h^8 + \mathcal{O}(h^9)\,,\\
-\frac{g_3\dot{h}}{\sqrt{1+h^2+\left(\dot{h}\right)^2}} &\sim \frac{b_3}{h^3} + \frac{1+140b_3}{80h} + \frac{(1+36b_3)}{64}h - \frac{(1+36b_3)}{288}h^3 + \mathcal{O}(h^5)\,,\\
\frac{g_3}{\dot{h}h\sqrt{1+h^2+\dot{h}^2}} &\sim b_3 K_6^2 h^6 + \mathcal{O}(h^7)\,.
\end{aligned} \tag{3.146}$$

Using these, we can make θ integrals in I_1 and I_2 finite by separating the divergences:

$$\begin{aligned} I_1 &= \int_{z_m}^{\delta}\frac{dz}{z^4}\int_{h_0}^{h_{1c}}dh\left(\frac{\sqrt{1+h^2+\dot{h}^2}}{\dot{h}h^2}+\frac{1}{h^2}\right)+\int_{z_m}^{\delta}\frac{dz}{z^4}\left(\frac{1}{h_{1c}(z)}-\frac{1}{h_0}\right) \\ &= I_1'+I_2'\,, \end{aligned} \tag{3.147}$$

$$\begin{aligned} I_2 &= -\int_{z_m}^{\delta}\frac{dz}{z^2}\int_{h_0}^{h_{1c}}dh\left(\frac{\left(5+6h^2+6\dot{h}^2\right)}{40h^2\sqrt{1+h^2+\dot{h}^2}}+\frac{3}{20h^2}\right)-\frac{3}{20}\int_{z_m}^{\delta}\frac{dz}{z^2}\left(\frac{1}{h_{1c}(z)}-\frac{1}{h_0}\right) \\ &= I_3'+I_4'\,. \end{aligned} \tag{3.148}$$

In (3.147), I_1' and I_2' are first and second integrals in I_1 and similarly in (3.148), I_3' and I_4' represent first and second integrals in I_2. Now we can further differentiate I_i's with respect to δ and Taylor expand the expressions to separate the divergences

$$\frac{dI_1'}{d\delta} = \frac{1}{\delta^4}\int_{h_0}^{0}dh\frac{\sqrt{1+h^2+\dot{h}^2}}{\dot{h}h^2}-\frac{K_6^2\left(9b_3H^2+R_1^2\right)}{2H^9R_1^2}\delta^5+\mathcal{O}(\delta^6)\,, \tag{3.149}$$

$$\frac{dI_2'}{d\delta} = \frac{H}{\delta^5}\left(1-\frac{b_3H^2}{R_1^2}\right)-\frac{1}{h_0\delta^4}-\frac{\left(1+140b_3\right)H}{80R_1^2\delta^3}-\frac{1+36b_3}{64HR_1^2\delta}+\mathcal{O}(\delta^0)\,, \tag{3.150}$$

$$\frac{dI_3'}{d\delta} = -\frac{1}{\delta^2}\int_{h_0}^{0}dh\left(\frac{\left(5+6h^2+6\dot{h}^2\right)}{40h^2\sqrt{1+h^2+\dot{h}^2}}\right)+\frac{K_6^2\left(9b_3H^2+R_1^2\right)\delta^7}{20H^9R_1^2}+\mathcal{O}(\delta^{10})\,, \tag{3.151}$$

$$\frac{dI_4'}{d\delta} = -\frac{3H}{20\delta^3}\left(1-\frac{b_3H^2}{R_1^2}\right)+\frac{3}{20h_0\delta^2}+\frac{3\left(3+140b_3\right)H}{1600R_1^2\delta}+\mathcal{O}(\delta)\,. \tag{3.152}$$

Also, we can simplify the boundary terms in a similar fashion and find that

$$\begin{aligned} \frac{dI_3}{d\delta} &= \left(1-\frac{3b_3H^2}{R_1^2}\right)\frac{b_3H^3}{\delta^5}+\left(1-\frac{4b_3H^2}{R_1^2}\right)\frac{H(1+140b_3)}{80\delta^3} \\ &\quad+\left(\frac{1+36b_3}{64H}-\frac{\left(1+480b_3+26800b_3^2\right)H}{6400R_1^2}\right)\frac{1}{\delta}+\mathcal{O}(\delta^0)\,, \end{aligned} \tag{3.153}$$

$$\frac{dI_4}{d\delta} = -\frac{1}{\delta^2}\int_{h_0}^{0}dh\frac{g_3}{h\dot{h}\sqrt{1+h^2+\dot{h}^2}}+\mathcal{O}(\delta^5)\,. \tag{3.154}$$

Using (3.139) and (3.147)-(3.154), we find new divergence of order $1/\delta^3$ and $1/\delta$, and the universal term in the entanglement entropy

$$S_6{}^{log}\big|_{k\times R^1\times S^2} = \frac{16\,\pi^2L^5\tilde{H}}{\ell_{\rm P}^5}\left(0+\mathcal{O}\left(\frac{1}{R_1^2}\right)\right)\log(\delta)\,. \tag{3.155}$$

Once again, we find that leading contribution in logarithmic divergence disappears, which is consistent with the fact that there is no contribution from the singularity with odd dimensional locus. In the next subsection, we will consider some more geometries with conical singularities to push our hypothesis.

3.3.2.2 Crease $c_n \times \Sigma$

In this section, we will calculate EE for conical singularities of the form $c_n \times S^m$. We will mainly consider following singular geometries: $c_1 \times S^1$, $c_1 \times S^2$, $c_1 \times S^3$, $c_2 \times S^1$ and $c_2 \times S^2$. The case with $\{n, m\} = \{1, 1\}$ will turn out to be trivial and it will be straightforward to see that there is no new contribution to the $\log^2\delta$ or log divergence. For $\{n, m\} = \{1, 2\}$, we will find that there is a $\log^2\delta$ contribution in EE which had disappeared when the locus was taken to be flat in (3.68). For $\{n, m\} = \{1, 3\}$, we will see that there is no $\log^2\delta$ contribution from the singularity as the locus is odd dimensional. Finally for $\{n, m\} = \{2, 1\}$ and $\{2, 2\}$, we will find that entanglement entropy contains a logarithmic divergence. In $\{n, m\} = \{2, 1\}$, this contribution is actually coming from the smooth part of the surface as $d = 6$ and logarithmic contribution from the trace anomaly is non-zero. In $\{n, m\} = \{2, 2\}$, the logarithmic contribution comes from the singularity and this is consistent with the idea that for even dimensional curved locus, the singularity in odd d will contribute through a logarithmic divergence.

To begin with, we consider the simplest case with $m = 1$. In this case, the background geometry for the CFT is $R^4 \times S^1$. Then, the dual bulk geometry is given by

$$ds^2 = \frac{L^2}{z^2}\left(dz^2 + f_1(z)\left(dt^2 + d\rho^2 + \rho^2 d\theta^2 + \rho^2 \sin^2(\theta) d\phi^2\right) + f_2(z) R_1^2\, d\xi_0^2\right), \tag{3.156}$$

where $f_1 = 1 + \mathcal{O}(1/R_1^6)$ and $f_2 = 1 + \mathcal{O}(1/R_1^6)$. For this bulk, we consider the singular surface given by $\theta \in [0, \Omega]$, $\phi \in [0, 2\pi]$ and $\rho \in [0, H]$. For the minimal area surface which gives us the entanglement entropy, we assume that $\rho = \rho(z, \theta)$. Then, EE is given by

$$S_5\big|_{c_1 \times S^1} = \frac{4\,\pi^2 L^4 R_1}{\ell_{\rm P}^4} \int dz\, d\theta\, \frac{\sin(\theta)\rho f_1 \sqrt{f_2}}{z^4} \sqrt{\dot\rho^2 + \rho^2(1 + f_1 \rho'^2)}\,, \tag{3.157}$$

where $\dot\rho = \partial_\theta \rho$ and $\rho' = \partial_z \rho$. Using this, we can find the equation of motion for $\rho(z, \theta)$ to

be

$$\begin{aligned} 0 = \; & 2zf_1f_2\sin(\theta)\rho^2\left(\rho^2+\dot\rho^2\right)\rho'' + 2zf_2\sin(\theta)\rho^2\left(1+f_1\rho'^2\right)\ddot\rho \\ & -4zf_1f_2\sin(\theta)\rho^2\dot\rho\rho'\dot\rho' + 2zf_1f_2\rho^2\left(-2\sin(\theta)\rho+\cos(\theta)\dot\rho\right)\rho'^2 \\ & +f_1\sin(\theta)\rho^4\left(3zf_2f_1' + f_1\left(-8f_2+zf_2'\right)\right)\rho'^3 + 2zf_2\Big(\cos(\theta)\dot\rho\left(\rho^2+\dot\rho^2\right) \\ & -\sin(\theta)\rho\left(2\rho^2+3\dot\rho^2\right)\Big) + \sin(\theta)\rho^2\left(4zf_2f_1' + f_1\left(-8f_2+zf_2'\right)\right)\left(\rho^2+\dot\rho^2\right)\rho' \,. \end{aligned} \tag{3.158}$$

As the conical singularity has a one dimensional locus, we expect that there will be no logarithmic contribution from the singularity. Now we substitute $\rho = \rho_0 + \rho_1/R_1^2$ in (3.157) and find the leading order correction to the entanglement entropy. However, when we use the equation of motion for ρ_0 and simplify the entropy functional, the contribution depending on the coefficients of leading order terms of f_1 and f_2 will vanish because $f_1 = 1+\mathcal{O}(1/R_1^6)$ and $f_2 = 1+\mathcal{O}(1/R_1^6)$. So we find that simplified expression has following form

$$\begin{aligned} S_5\big|_{c_1\times S^1} = \; & \frac{4\,\pi^2 L^4 R_1}{\ell_{\rm P}^4}\int dz\,d\theta\Bigg[\frac{\sin(\theta)\rho_0}{z^4}\sqrt{\dot\rho_0^2+\rho_0^2(1+\rho_0'^2)} \\ & +\frac{1}{R_1^2}\frac{\partial}{\partial\theta}\left(\frac{\rho_0\dot\rho_0\rho_1}{z^4\sqrt{\dot\rho_0^2+\rho_0^2\left(1+\rho_0'^2\right)}}\right)+\frac{1}{R_1^2}\frac{\partial}{\partial z}\left(\frac{\rho_0^3\rho_0'\rho_1}{z^4\sqrt{\dot\rho_0^2+\rho_0^2\left(1+\rho_0'^2\right)}}\right)\Bigg]\,. \end{aligned} \tag{3.159}$$

Now we can insert the ansatz $\rho_0 = z/h(\theta)$ and $\rho_1 = z^3 g_3(\theta)$ in the functional and find that

$$\begin{aligned} S_5\big|_{c_1\times S^1} = \; & \frac{4\,\pi^2 L^4 R_1}{\ell_{\rm P}^4}\Bigg[\int_{z_m}^{\delta}\frac{dz}{z^2}\int_{h_0}^{h_{1c}(z)}\frac{dh}{\dot h}\frac{\sin(\theta)\sqrt{1+h^2+\dot h^2}}{h^3} \\ & -\frac{1}{R_1^2}\int_{z_m}^{\delta}dz\frac{g_3\sin(\theta)\dot h}{h\sqrt{1+h^2+\dot h^2}}\Big|_{h_{1c}(z)} + \frac{1}{R_1^2}\int_{z_m}^{\delta}dz\int_{h_0}^{h_{1c}(z)}\frac{dh}{\dot h}\frac{g_3\sin(\theta)}{h^2\sqrt{1+h^2+\dot h^2}}\Bigg]\,. \end{aligned} \tag{3.160}$$

Also from (3.158), the equations of motion for h and g_3 reduces to

$$\begin{aligned} 0 = \; & \ddot h h\left(1+h^2\right)\sin(\theta)+\cos(\theta)h\dot h^3+\left(4+h^2\right)\sin(\theta)\dot h^2 \\ & +\cos(\theta)\left(1+h^2\right)h\dot h+2\left(2+3h^2+h^4\right)\sin(\theta) \end{aligned} \tag{3.161}$$

$$\begin{aligned} 0 = \; & h^2\left(1+h^2\right)^2\sin(\theta)\ddot g_3 + h\left(1+h^2\right)\Big(2\left(8+3h^2\right)\sin(\theta)\dot h \\ & +\cos(\theta)h\left(1+h^2+3\dot h^2\right)\Big)\dot g_3 - \Big(2\left(1+h^2\right)\left(10+8h^2+h^4\right)\sin(\theta) \\ & +3\left(8+3h^2+h^4\right)\sin(\theta)\dot h^2+2\cos(\theta)h\left(4+h^2\right)\dot h^3\Big)g_3\,. \end{aligned} \tag{3.162}$$

Now, we find that g_3 is not sourced by h and hence, a homogeneous solution $g_3 = 0$ will be the exact solution for this case. This implies that excluding the first term in the above expression, all the other terms will vanish. As g_3 is zero, there will not be any new contribution to the limits of the integrations either. This result is consistent with the idea that singularity will contribute in EE only if the locus is curved and even dimensional.

As a next example, we consider the singular geometry $c_1 \times S^2$ in CFT background $R^4 \times S^2$. For this case, the bulk metric is given by

$$ds^2 = \frac{L^2}{z^2}\left(dz^2 + f_1(z)\left(dt^2 + d\rho^2 + \rho^2 d\theta^2 + \rho^2 \sin^2(\theta) d\phi^2\right) + f_2(z) R_1^2\, d\Omega_2^2\right), \qquad (3.163)$$

where $d\Omega_2^2 = d\xi_0^2 + \sin^2(\xi_0) d\xi_0^2$ is metric over unit two-sphere and

$$\begin{aligned} f_1 &= 1 + \frac{z^2}{20R_1^2} + \frac{z^4}{100R_1^4} + \dots, \\ f_2 &= 1 - \frac{z^2}{5R_1^2} - \frac{7z^4}{800R_1^4} + \dots. \end{aligned} \qquad (3.164)$$

Now the entanglement entropy is given by

$$S_6\big|_{c_1\times S^2} = \frac{16\,\pi^3 L^5 R_1^2}{\ell_{\rm P}^5}\int dz d\theta \frac{f_1 f_2 \sin(\theta)\rho\sqrt{\dot\rho^2 + \rho^2\left(1 + f_1 \rho'^2\right)}}{z^5}, \qquad (3.165)$$

and equation of motion for $\rho(z,\theta)$ becomes

$$\begin{aligned} 0 &= 2z f_1 f_2 \sin(\theta)\rho^2\left(\rho^2 + \dot\rho^2\right)\rho'' + 2z f_2 \sin(\theta)\rho^2\left(1 + f_1\rho'^2\right)\ddot\rho - 4\,z\,f_1 f_2 \sin(\theta)\rho^2\dot\rho\,\rho'\,\dot\rho' \\ &\quad + 2z\cos(\theta) f_2 \dot\rho\left(\dot\rho^2 + \rho^2\left(1 + f_1\rho'^2\right)\right) + \sin(\theta)\rho\Big(-2\,z f_2(2\,\rho^2 + 3\dot\rho^2) \\ &\quad + 2\,\rho\left(2\,z\,f_2 f_1' + f_1(-5\,f_2 + z\,f_2')\right)(\rho^2 + \dot\rho^2)\rho' - 4\,z\,f_1 f_2 \rho^2 \rho'^2 \\ &\quad + f_1\rho^3\left(3\,z\,f_2 f_1' + 2\,f_1\left(-5\,f_2 + z\,f_2'\right)\right)\rho'^3\Big). \end{aligned} \qquad (3.166)$$

Now we can plug in the ansatz $\rho = \rho_0 + \rho_1/R_1^2$ in the entropy functional and equation of motion. We can Taylor expand the entropy functional in R_1 and keep the leading correction. In this leading correction, we can use the integration by parts and the equation

of motion for ρ_0 to simplify the entropy functional to

$$\begin{aligned} S_6\big|_{c_1\times S^2} &= \frac{16\,\pi^3 L^5 R_1^2}{\ell_{\rm P}^5}\int_{z_m}^{\delta} dz \int_0^{\Omega-\epsilon} d\theta \Bigg[\frac{\sin(\theta)\rho_0}{z^5}\sqrt{\dot\rho_0^2+\rho_0^2\,(1+\rho_0'^{\,2})} \\ &\quad -\frac{\sin(\theta)\rho_0\,(6\dot\rho_0^2+\rho_0^2\,(6+5\rho_0'^{\,2}))}{40R_1^2 z^3\sqrt{\dot\rho_0^2+\rho_0^2\,(1+\rho_0'^{\,2})}} - \frac{\partial}{\partial z}\left(\frac{\sin(\theta)\rho_0^3\rho_0'\rho_1}{z^5 R_1^2\sqrt{\dot\rho_0^2+\rho_0^2\,(1+\rho_0'^{\,2})}}\right)\Bigg] \\ &\quad +\frac{16\,\pi^3 L^5}{\ell_{\rm P}^5}\int_{z_m}^{\delta} dz \frac{\sin(\theta)\rho_0\dot\rho_0\rho_1}{z^5\sqrt{\dot\rho_0^2+\rho_0^2\,(1+\rho_0'^{\,2})}}\Bigg|_{\theta=\Omega-\epsilon}. \end{aligned} \tag{3.167}$$

We can further use $\rho_0 = z/h(\theta)$ and $\rho_1 = z^3 g_3(\theta)$ and find that

$$S_6\big|_{c_1\times S^2} = \frac{16\,\pi^3 L^5 R_1^2}{\ell_{\rm P}^5}\left[I_1+\frac{I_2}{R_1^2}+\frac{I_3}{R_1^2}\right], \tag{3.168}$$

where

$$I_1 = \int_{z_m}^{\delta}\frac{dz}{z^3}\int_{h_0}^{h_{1c}(z)} dh\frac{\sin(\theta)\sqrt{1+h^2+\dot h^2}}{\dot h\, h^3}, \tag{3.169}$$

$$I_2 = -\int_{z_m}^{\delta}\frac{dz}{z}\int_{h_0}^{h_{1c}(z)} dh\frac{\sin(\theta)\left(5+6h^2+6\dot h^2\right)}{40\,\dot h\, h^3\sqrt{1+h^2+\dot h^2}}, \tag{3.170}$$

$$I_3 = -\int_{z_m}^{\delta}\frac{dz}{z}\frac{g_3\sin(\theta)\dot h}{h\sqrt{1+h^2+\dot h^2}}\Bigg|_{h=h_{1c}(z)}. \tag{3.171}$$

Note that term with derivative with respect to z in (3.167) vanishes. Now using the above ansatz in (3.166), we can also find the equations of motion for h and g_3. For these equations, we can make a change of variable from θ to $y=\sin(\theta)$ and find

$$\begin{aligned} 0 &= y(1-y^2)h(1+h^2)\ddot h + (1-y^2)^2 h\dot h^3 + y(1-y^2)(5+h^2)\dot h^2 \\ &\quad +(1-2y^2)h(1+h^2)\dot h + y(1+h^2)(5+2h^2) \end{aligned} \tag{3.172}$$

$$\begin{aligned} \mathcal{S}_1 &= y(1-y^2)h^2(1+h^2)^2\ddot g_3 + h\Big(\left(1-2y^2\right)h\left(1+h^2\right)^2 \\ &\quad +6y\left(1-y^2\right)\left(3+4h^2+h^4\right)\dot h + 3\left(1-y^2\right)^2 h\left(1+h^2\right)\dot h^2\Big)\dot g_3 \\ &\quad -\Big(y\left(1+h^2\right)\left(25+21h^2+2h^4\right) - 3y\left(1-y^2\right)\left(9+2h^2+h^4\right)\dot h^2 \\ &\quad -2\left(1-y^2\right)^2 h\left(4+h^2\right)\dot h^3\Big)\dot g_3\,, \end{aligned} \tag{3.173}$$

where $\mathcal{S}_1$ is the source terms and it is given by

$$\mathcal{S}_1 = \frac{y\left(1+h^2\right)\left(10+9h^2\right)+4y\left(1-y^2\right)\left(1+2h^2\right)\dot{h}^2+\left(1-y^2\right)^2 h\dot{h}^3}{20h}\,. \tag{3.174}$$

Now to separate the logarithmic divergence, we want to find the asymptotic behavior of integrand in terms of h, where $h \to 0$. So we invert equation (3.172) using $\ddot{h}(y) = -((1-y^2)\,y'' + yy'^2)/y'^3$ and $\dot{h}(y) = \sqrt{1-y^2}/y'$, where on the right hand side we have $y = y(h)$ and $y' = dy/dh$. We can also change the independent variable in (3.109) from y to h. Apart from previous two relations, we also use

$$\begin{aligned} \dot{g}_3(\theta) &= \dot{g}_3(h)\frac{\sqrt{1-y^2}}{y'} \\ \ddot{g}_3(\theta) &= \frac{\sqrt{1-y^2}}{y'}\frac{d}{dh}\left(\frac{\dot{g}_3(h)\sqrt{1-y^2}}{y'}\right)\,. \end{aligned} \tag{3.175}$$

Finally, we can rewrite (3.172) and (3.173) as

$$\begin{aligned} 0 &= h\left(1+h^2\right)y\left(1-y^2\right)y'' - \left(5+7h^2+2h^4\right)yy'^3 \\ &\quad -h\left(1+h^2\right)\left(1-2y^2\right)y'^2 - \left(5+h^2\right)y\left(1-y^2\right)y' - h\left(1-y^2\right)^2 \end{aligned} \tag{3.176}$$

$$\begin{aligned} \mathcal{S}_2 &= h^2\left(1+h^2\right)^2 y\left(1-y^2\right)y'\ddot{g}_3 + h\left(1+h^2\right)\Big(2h\left(1-y^2\right)^2 \\ &\quad +\left(13+5h^2\right)y\left(1-y^2\right)y' - \left(1+h^2\right)\left(5+2h^2\right)yy'^3\Big)\dot{g}_3 + \Big(2h\left(4+h^2\right)\left(1-y^2\right)^2 \\ &\quad +3\left(9+2h^2+h^4\right)y\left(1-y^2\right)y' - \left(1+h^2\right)\left(25+21h^2+2h^4\right)yy'^3\Big)g_3\,, \end{aligned} \tag{3.177}$$

where now $\dot{g}_3 = dg_3/dh$ and

$$\mathcal{S}_2 = \frac{h\left(1-y^2\right)^2 - 4\left(1+2h^2\right)y\left(1-y^2\right)y' - \left(1+h^2\right)\left(10+9h^2\right)yy'^3}{20h}\,. \tag{3.178}$$

Now we can try to solve these equations perturbatively in terms of h near the boundary, where h is small. As $y = \sin(\Omega)$ at $h = 0$, we find the solution

$$y = \sin(\Omega) - \frac{\cos(\Omega)\cot(\Omega)}{8}h^2 + \frac{1}{512}\left(2\csc(\Omega) - 7\csc^3(\Omega) + 5\sin(\Omega)\right)h^4 + \dots\,. \tag{3.179}$$

Using this in (3.177) and solving it perturbatively, we find that

$$g_3 = -\frac{1}{20h} + \frac{1+\csc^2(\Omega)}{96}h\,\log(h) + b_3 h + \dots\,, \tag{3.180}$$

where b_3 is a constant and it is fixed by the condition $\dot{g}_3(0) = 0$. Now, we evaluate the expression $\rho = z/h + z^3 g_3/R_1^2$ at $z = \delta$, $\rho = H$ and $h(z) = h_{1c}$. In this relation, we use (3.180) and invert it to find

$$h_{1c} = \frac{\delta}{H} - \frac{\delta^3}{20HR_1^2} + \frac{(96b_3 + (1+\csc^2(\Omega))\log(\delta/H))\,\delta^5}{96H^3R_1^2} + \mathcal{O}(\delta^6)\,. \tag{3.181}$$

Now, we can use (3.179) and (3.180) in integrands of I_1 and I_2 to find their behavior near the boundary:

$$\begin{aligned}
\frac{\sin(\theta)\sqrt{1+h^2+\dot{h}^2}}{\dot{h}h^3} &\sim -\frac{\sin(\Omega)}{h^3} + \frac{3\cos(\Omega)\cot(\Omega)}{32h} \\
&\quad - \frac{3h(13-19\cos(2\Omega))\cot^2(\Omega)\csc(\Omega)}{4096} + \mathcal{O}(h^3) \\
\frac{\sin(\theta)\left(5+6h^2+6\dot{h}^2\right)}{40\dot{h}h^3\sqrt{1+h^2+\dot{h}^2}} &\sim -\frac{3\sin(\Omega)}{20h^3} + \frac{\cos(\Omega)\cot(\Omega)}{64h} \\
&\quad - \frac{h(67-157\cos(2\Omega))\cot^2(\Omega)\csc(\Omega)}{81920} + \mathcal{O}(h^3)\,.
\end{aligned} \tag{3.182}$$

Using these, we can make the integrations in I_1 and I_2 finite and write in the form

$$\begin{aligned}
I_1 &= \int_{z_m}^{\delta}\frac{dz}{z^3}\int_{h_0}^{h_{1c}(z)} dh\left[\frac{\sin(\theta)\sqrt{1+h^2+\dot{h}^2}}{\dot{h}h^3} + \frac{\sin(\Omega)}{h^3} - \frac{3\cos(\Omega)\cot(\Omega)}{32h}\right. \\
&\qquad \left. + \frac{3h(13-19\cos(2\Omega))\cot^2(\Omega)\csc(\Omega)}{4096}\right] \\
&\quad + \int_{z_m}^{\delta}\frac{dz}{z^3}\left(\frac{\sin(\Omega)}{2}\left(-\frac{1}{h_{1c}^2}+\frac{1}{h_0^2}\right) + \frac{3}{32}\cos(\Omega)\cot(\Omega)\log(h_{1c}/h_0)\right. \\
&\qquad \left. + \frac{3\,(h_0^2-h_{1c}^2)\,(13-19\cos(2\Omega))\cot^2(\Omega)\csc(\Omega)}{8192}\right) \\
&= I_1' + I_2'\,,
\end{aligned} \tag{3.183}$$

and

$$\begin{aligned} I_2 &= -\int_{z_m}^{\delta}\frac{dz}{z}\int_{h_0}^{h_{1c}(z)}dh\left[\frac{\sin(\theta)\left(5+6h^2+6\dot{h}^2\right)}{40R_1^2\dot{h}h^3\sqrt{1+h^2+\dot{h}^2}}+\frac{3\sin(\Omega)}{20h^3}-\frac{\cos(\Omega)\cot(\Omega)}{64h}\right.\\ &\qquad\left.+\frac{(67-157\cos(2\Omega))\cot^2(\Omega)\csc(\Omega)h}{81920}\right]\\ &\quad+\int_{z_m}^{\delta}\frac{dz}{z}\left(\frac{3\sin(\Omega)}{40}\left(\frac{1}{h_0^2}-\frac{1}{h_{1c}^2}\right)+\frac{\cos(\Omega)\cot(\Omega)}{64}\log(h_0/h_{1c})\right.\\ &\qquad\left.-\frac{(h_0^2+h_{1c}^2)\,(67-157\cos(2\Omega))\cot^2(\Omega)\csc(\Omega)}{163840}\right)\\ &= I_3'+I_4'\,. \end{aligned} \tag{3.184}$$

In (3.183) and (3.184), I_1' and I_2' are first and second integrals in I_1 and I_3' and I_4' are first and second integrals in I_2. Now we can take derivatives of I_i''s with respect to δ, and then Taylor expand the terms to find:

$$\begin{aligned} \frac{dI_1'}{d\delta} &= \frac{1}{\delta^3}\int_{h_0}^{0}dh\left[\frac{\sin(\theta)\sqrt{1+h^2+\dot{h}^2}}{\dot{h}h^3}+\frac{\sin(\Omega)}{h^3}-\frac{3\cos(\Omega)\cot(\Omega)}{32h}\right.\\ &\qquad\left.+\frac{3h(13-19\cos(2\Omega))\cot^2(\Omega)\csc(\Omega)}{4096}\right]\\ &\qquad+\frac{3\left(\csc(\Omega)+11\csc^3(\Omega)+3\csc^5(\Omega)-15\sin(\Omega)\right)}{8192H^4}\delta\log(\delta/H)+\dots\,,\\ \frac{dI_2'}{d\delta} &= \frac{H^2\sin(\Omega)}{2\delta^5}+\cdots-\frac{\csc(\Omega)+\sin(\Omega)}{96R_1^2}\frac{\log(\delta/H)}{\delta}+\mathcal{O}(1/\delta)\,,\\ \frac{dI_3'}{d\delta} &= -\frac{1}{\delta}\int_{h_0}^{0}dh\left[\frac{\sin(\theta)\left(5+6h^2+6\dot{h}^2\right)}{40R_1^2\dot{h}h^3\sqrt{1+h^2+\dot{h}^2}}+\frac{3\sin(\Omega)}{20h^3}-\frac{\cos(\Omega)\cot(\Omega)}{64h}\right.\\ &\qquad\left.+\frac{(67-157\cos(2\Omega))\cot^2(\Omega)\csc(\Omega)h}{81920}\right]+\mathcal{O}(\delta^3)\,,\\ \frac{dI_4'}{d\delta} &= -\frac{3H^2\sin(\Omega)}{40\delta^3}-\frac{\cos(\Omega)\cot(\Omega)}{64}\frac{\log(\delta)}{\delta}+\mathcal{O}(1/\delta)\,,\\ \frac{dI_3}{d\delta} &= -\frac{H^2\sin(\Omega)}{20\delta^3}+\frac{(3-\cos(2\Omega))\csc(\Omega)}{192}\frac{\log(\delta)}{\delta}+\mathcal{O}(1/\delta)\,. \end{aligned} \tag{3.185}$$

Now using (3.183)-(3.185) in (3.168), we find that the double log contribution in the EE

becomes

$$S_6^{\log^2}\big|_{c_1\times S^2} = -\frac{\pi^3 L^5 \cos(\Omega)\cot(\Omega)}{8\,\ell_{\rm P}^5}\log(\delta)^2\,. \tag{3.186}$$

Note that there are other contribution to the double log term but they are of higher order in R_1. As the only other dimensionful quantity in the problem is the IR cut-off H, these terms will be of the form $\mathcal{O}(H^2/R_1^2)$. Interestingly, all such terms, which scale with H are contributions from the smooth part of the entangling surface. Hence (3.186) is the complete contribution from the singularity alone. In section 3.3.1.2, we saw that there was no such double logarithmic term when the locus of the singularity was either flat or it is odd dimensional. Hence, (3.186) is also consistent with the idea that similar to (3.11), generically the contribution from the singularity should be of the following form

$$S_{univ} \sim \int_\Sigma d^{2m}y\,\sqrt{h}\,[\mathcal{R}^m]\,\log(\delta)^2\,. \tag{3.187}$$

Here Σ is the $2m$-dimensional locus of the singularity and $[\mathcal{R}^m]$ is the curvature invariants with m powers of the curvatures.

Having seen the appearance of the $\log^2\delta$ divergence for even dimensional curved locus, now we turn towards odd dimensional locus. So we consider EE for geometry $c_1\times S^3$. For this case, the calculations proceed in a similar fashion and we find that, near the boundary $y=\sin(\theta)$ and g_3 in terms of h are given by

$$\begin{aligned} y(h) &= \sin(\Omega) - \frac{1}{10}\cos(\Omega)\cot(\Omega)h^2 - \frac{(63-17\cos(2\Omega))\cot^2(\Omega)\csc(\Omega)h^4}{6000} \\ &\quad + \frac{(373\csc(\Omega) - 1853\csc^3(\Omega) - 889\csc^5(\Omega) + 2369\sin(\Omega))\,h^6}{450000} + \mathcal{O}(h^7)\,, \\ g_3(h) &= -\frac{1}{12h} - \frac{h(39-11\cos(2\Omega))\csc^2(\Omega)}{2250} + b_3\,h^2 + \mathcal{O}(h^3)\,, \end{aligned} \tag{3.188}$$

where b_3 is a constant and it is fixed by the condition that g_3 has a minimum at $\theta=0$. However, we will see that this constant is zero. If we calculate EE, we find that there is no $\log^2\delta$ term but there is a log term in EE at the order next to the leading order in R_1:

$$S_7^{\log}\big|_{c_1\times S^3} = -\frac{8\,\pi^4 L^6 R_1}{H\ell_{\rm P}^6} b_3\,\sin(\Omega)\log(\delta)\,. \tag{3.189}$$

Now, we are going to argue that this logarithmic term is not coming from the singularity. We can see that, if we set $\Omega=\pi/2$, the conical singularity in the entangling surface disappears. However, the logarithmic term in (3.189) is still non-zero. Hence, this contribution

is actually coming from the non-singular part of the entangling surface. Further, as we are considering the EE in odd dimensional CFT's, there should not be any log term from the smooth part of the entangling surface. Hence, the contribution (3.189) should be zero and this is only if $b_3 = 0$. This result further assures that a singularity with odd dimensional locus does not contribute through a log or $\log^2\delta$ term.

We can further calculate EE for singularity $c_2 \times S^1$ in $d = 6$. In this case, the singularity has an odd dimensional, curved locus which does not contribute in the universal term. However, as d is even, we find that the smooth part of the surface contribute through a log term and it is given by

$$S_6^{\log}\big|_{c_2\times S^1} = \frac{\pi^3 L^5 R_1}{\ell_{\rm P}^5}\frac{(7-9\cos(2\Omega))\cot^2(\Omega)}{16\,H}\log(\delta/H)\,. \tag{3.190}$$

Further, there is a new divergent term of the order $1/\delta$ in this case. Note that this term matches with the logarithmic term in EE for $c_2\times R^1$ in (3.69). Finally, we give results for the case where a conical singularity in odd dimensions have a curved, even-dimensional locus. In background $R^5\times S^2$, we can consider the singular geometry $c_2\times S^2$ which contains a new divergence of order $1/\delta^2$. Further, in odd d the smooth part of the entangling geometry does not contribute through a logarithmic term. However, a singularity will contribute through a $\log(\delta)$ term if the locus of the singularity is even dimensional and curved. Precisely this is what we see in EE for $c_2\times S^2$ and find following universal term in EE

$$\begin{aligned} S_7^{\log}\big|_{c_2\times S^2} &= \frac{32\,\pi^3 L^6}{\ell_{\rm P}^6}\log(\delta)\bigg[-\int_0^{h_0} dh\left(\frac{\mathcal{L}_0}{\dot h}-\frac{7\sin^2\Omega}{60\,h^4}+\frac{\cos^2\Omega}{25\,h^2}\right)\\ &\qquad +\frac{7\sin^2\Omega}{180\,h_0^3}-\frac{\cos^2\Omega}{25\,h_0}\bigg]\,, \end{aligned} \tag{3.191}$$

where $\dot h = dh/d\theta$ and

$$\mathcal{L}_0 = -\frac{\sin^2(\theta)\left(7\,\dot h^2+7\,h^2+6\right)}{60\,h^4\sqrt{\dot h^2+h^2+1}}\,. \tag{3.192}$$

Note that similar to previous cases, h is defined such that $\rho = z/h(\theta)+z^3\,g_3(\theta)/R_1^2$ and it is the solution of following equation of motion

$$\begin{aligned} 0 &= h(1+h^2)\ddot h+2\cot^2(\theta)\,h\,\dot h^3+2\left(h^2+3\right)\dot h^2\\ &\qquad +2\cot(\theta)h_1\left(1+h_1^2\right)\dot h+3\left(2+3h^2+h^4\right)\,, \end{aligned} \tag{3.193}$$

with $h_0 = h(0)$. The log divergence (3.191) is a contribution from the singularity and it is non-zero because the locus of the singularity is even dimensional and curved. So the

examples in this section reaffirm that an extended singularity contributes in the cut-off independent terms through log or $\log^2\delta$ terms only if its locus is even dimensional and curved.

3.4 Universal terms and the central charges

In previous sections, we calculated the EE for various surfaces and found that singularity produces new log and $\log^2\delta$ terms in the EE. As it has been seen that cut-off independent coefficients contain central charges, it is natural to ponder what function of central charges appear in these new cut-off independent contributions from the singularities. In the cases being discussed, we have been working with CFT's which are dual to the Einstein gravity. For these CFT's, all the central charges are equal and there is no way to distinct these in the universal term of EE. To explore this question, we need to consider the dual geometries which contain extra parameters and for which the central charges differentiate from each other. Hence, in this case, we will calculate EE for some singular geometries in Gauss-Bonnet gravities and take first step towards guessing the functional form of the log terms in terms of central charges.

3.4.1 Singular embedding

In this section, we will discuss EE for cone geometry in $d = 4, 5, 6$ dimensional CFT's. We will first calculate the EE for $d = 4$ systematically and discuss the results for other cases.

For the Gauss-Bonnet gravity in $(d+1)$-dimensional space-time, the action is given by

$$I_d = \frac{1}{2\ell_{\rm P}^{d-2}} \int d^{d+1}x\sqrt{-g}\left[R + \frac{d(d-1)}{L^2} + \frac{\lambda L^2}{(d-2)(d-3)}\mathcal{X}_2\right], \tag{3.194}$$

where

$$\mathcal{X}_2 = R_{abcd}R^{abcd} - 4R_{ab}R^{ab} + R^2 \tag{3.195}$$

is Euler density on two-dimensional submanifold. We have introduced L as a canonical scale in the curvature-squared interaction so that strength of this term is controlled by λ, a dimensionless coupling constant. Now in arbitrary d, we would like to use following two

central charges of the CFT

$$C_{\rm T} = \frac{\pi^{d/2}}{\Gamma(d/2)}\left(\frac{\tilde{L}}{\ell_{\rm P}}\right)^{d-1}[1-2\lambda f_\infty]\,, \tag{3.196}$$

$$a^*_d = \frac{\pi^{d/2}}{\Gamma(d/2)}\left(\frac{\tilde{L}}{\ell_{\rm P}}\right)^{d-1}\left[1-2\frac{d-1}{d-3}\lambda f_\infty\right]\,, \tag{3.197}$$

where $\tilde{L}$ is the AdS radius of solutions of (3.194) in the asymptotic limit and it is given by (3.200). These central charges were defined in [114] and has special significance in arbitrary dimensions. The central charge $C_{\rm T}$ controls the leading singularity of the two-point function of the stress tensor and a^*_d is shown to satisfy a holographic c-theorem in arbitrary dimensions [87, 88]. Soon we will calculate the EE for various singular surfaces and would like to see if the universal terms can be identified in terms of these central charge.

Now in Gauss-Bonnet gravity, the holographic EE is given by [48, 62]

$$S_d = \frac{2\pi}{\ell_{\rm P}^{d-1}}\int d^{d-1}x\sqrt{h}\left[1+\frac{2\lambda L^2}{(d-2)(d-3)}\mathcal{R}\right]\,, \tag{3.198}$$

where $\mathcal{R}$ is the Ricci scalar for the induced metric h. In five-dimensional space-time, the AdS solution of action (3.194) is given by

$$ds^2 = \frac{\tilde{L}^2}{z^2}\left(dz^2+dt^2+d\rho^2+\rho^2 d\theta^2+\rho^2\sin^2(\theta)\,d\phi^2\right)\,, \tag{3.199}$$

where $\tilde{L}$ is the AdS radius and it is related to canonical scale L by the following relation

$$\tilde{L}^2 = L^2/f_\infty \quad \text{where} \quad f_\infty = \frac{1-\sqrt{1-4\lambda}}{2\lambda}\,. \tag{3.200}$$

Further, the central charges of the dual CFT defined by the gravitational trace anomalies are given by

$$c = \pi^2\frac{\tilde{L}^3}{\ell_{\rm P}^3}(1-2\lambda f_\infty) \quad \text{and} \quad a = \pi^2\frac{\tilde{L}^3}{\ell_{\rm P}^3}(1-6\lambda f_\infty)\,. \tag{3.201}$$

Note that in $d=4$, these central charges precisely coincide with the central charges $C_{\rm T}$ and a^*_4 defined in (3.196) and (3.197).

Now the cone geometry is defined by $\rho \in [0, H]$, $\theta \in [0, \Omega]$ and $\phi \in [0, 2\pi]$. We consider the induced coordinates to be (ρ, θ, ϕ) and radial coordinate $z = z(\rho, \theta)$. For this case, the induced metric becomes

$$h = \begin{bmatrix} \frac{\tilde{L}^2}{z^2}\left(1 + (\partial_\rho z)^2\right) & \frac{\tilde{L}^2}{z^2}\partial_\rho z \partial_\theta z & 0 \\ \frac{\tilde{L}^2}{z^2}\partial_\rho z \partial_\theta z & \frac{\tilde{L}^2}{z^2}\left(\rho^2 + (\partial_\theta z)^2\right) & 0 \\ 0 & 0 & \frac{\tilde{L}^2}{z^2}\rho^2 \sin^2(\theta) \end{bmatrix} . \tag{3.202}$$

For this metric, the expression for Ricci scalar $\mathcal{R}$ in (3.198) contains the terms like $\partial_\rho^2 z$ and $\partial_\theta^2 z$. However, it is straightforward to see that the equation of motion is still second order. This is because Gauss-Bonnet term is topological in nature. Further, We impose the UV cutoff at $z = \delta$ and define $\epsilon(\rho)$ such that at $\theta = \Omega - \epsilon$, $z(\rho, \Omega - \epsilon) = \delta$. As the background geometry has scaling symmetry and apart from ρ, there are no dimensionful quantities in the problem, the solution for z should be of the following form

$$z = \rho\, h(\theta) . \tag{3.203}$$

Here $h(\theta)$ is a function such that $h(\Omega) = 0$ and $\dot{h}(0) = 0$. Also, the maximum value of $h(\theta)$ is $h(0) = h_0$. By plugging this ansatz in equation of motion for $z(\rho, \theta)$, which we get by applying the variational principle on entropy functional (3.198) with $d = 4$, the equation of motion for $h(\theta)$ turns out to be

$$\begin{aligned} 0 \;=\; & h\left(1+h^2\right)\left(\left(1+h^2\right)\sin(\theta)\left(1+4\lambda f_\infty\right) + 6\lambda\cos(\theta) h f_\infty \dot{h} + \sin(\theta)\left(1-2\lambda f_\infty\right)\dot{h}^2\right)\ddot{h} \\ & + \cos(\theta) h\left(1-2\lambda f_\infty\right)\dot{h}^5 - \left(3+h^2\right)\sin(\theta)\left(-1+2\lambda f_\infty\right)\dot{h}^4 \\ & + 2\cos(\theta) h\left(1+h^2+\lambda\left(1-2h^2\right) f_\infty\right)\dot{h}^3 \\ & + 3\left(1+h^2\right)\sin(\theta)\left(2+h^2-2\lambda\left(1+h^2\right) f_\infty\right)\dot{h}^2 \\ & + \cos(\theta) h\left(1+h^2\right)^2\left(1+4\lambda f_\infty\right)\dot{h} + \left(1+h^2\right)^2\sin(\theta)\left(3+2h^2\left(1+\lambda f_\infty\right)\right) . \end{aligned} \tag{3.204}$$

Further, we can simplify the entropy functional using this equation of motion and find that

$$S_4\big|_{c_1} = \frac{4\,\pi^2 \tilde{L}^3}{\ell_{\rm P}^3} \int_{\delta/h_0}^{H} \frac{d\rho}{\rho} \int_{h_0}^{\delta/\rho} dh \frac{\sin(\theta)\mathcal{L}_1}{\mathcal{L}_2} , \tag{3.205}$$

where we have changed the integration from θ to h and

$$\begin{aligned}\mathcal{L}_1 &= \left(1+h^2+\dot{h}^2\right)\Big(\sin(\theta)\left(1+h^2+\dot{h}^2\right)-2\lambda f_\infty\Big(\left(h^2\cos(\theta)\cot(\theta)+4\sin(\theta)\right)\dot{h}^2 \\ &\quad +2h^3\cos(\theta)\dot{h}+\left(2+h^2\right)^2\sin(\theta)\Big)\Big)+4\lambda^2 f_\infty^2\Big(\left(h^2\cos(\theta)\cot(\theta)+3\sin(\theta)\right)\dot{h}^4 \\ &\quad -2h\left(3-h^2\right)\cos(\theta)\dot{h}^3+h^2\left(2+h^2+2\cos(2\theta)\right)\csc(\theta)\dot{h}^2+2h^3\left(1+h^2\right)\cos(\theta)\dot{h} \\ &\quad +h^4\left(1+h^2\right)\sin(\theta)\Big), \qquad (3.206) \\ \mathcal{L}_2 &= h^3\dot{h}\sqrt{1+h^2+\dot{h}^2}\Big(\sin(\theta)\left(1+h^2+\dot{h}^2\right)+2\lambda f_\infty\Big(3h\cos(\theta)\dot{h} \\ &\quad +\sin(\theta)\left(2+2h^2-\dot{h}^2\right)\Big)\Big).\end{aligned}$$

Now we want to make h integrand in (3.205) finite. For that, we define $y=\sin(\theta)$ and find y and $\dot{h}$ in terms of h near the asymptotic boundary. For that, we convert (3.204) into the equation of motion for y with independent variable h. Solving this equation of motion perturbatively, we find that near the boundary

$$\begin{aligned}y(h) &= \sin(\Omega)-\frac{1}{4}h^2\cos(\Omega)\cot(\Omega) \\ &\quad +\frac{1}{64}h^4\log(h)(3-\cos(2\Omega))\cot^2(\Omega)\csc(\Omega)+c_0h^4+\dots, \qquad (3.207)\end{aligned}$$

where we have used the condition $y(0)=\sin(\Omega)$ and c_0 is a constant which is fixed by the condition that $y'(h_0)=0$. We can now assume $y=y(\theta)$ and $h=h(\theta)$ in (3.207) and then invert it to find

$$\begin{aligned}\dot{h}(\theta) &= -\frac{2\tan(\theta)}{h}-\frac{(3-\cos(2\Omega))\csc(2\Omega)}{2}h\log(h) \\ &\quad -\frac{\sec(\Omega)\left(256c_0\tan^2(\theta)-5\cos(2\Omega)\csc(\Omega)+7\right)}{16}h\dots. \qquad (3.208)\end{aligned}$$

Now using (3.207) and (3.208), we can find that near the boundary

$$\frac{\sin(\theta)\mathcal{L}_1}{\mathcal{L}_2} \sim -\frac{\sin(\Omega)\left(1-6\lambda f_\infty\right)}{h^3}+\frac{\cos(\Omega)\cot(\Omega)\left(1-2\lambda f_\infty\right)}{8h}+\mathcal{O}(h), \qquad (3.209)$$

which can be used to write the EE as

$$\begin{aligned} S_4\big|_{c_1} &= \frac{4\,\pi^2\tilde{L}^3}{\ell_{\rm P}^3}\Bigg[\frac{H^2\sin(\Omega)\,(1-6\lambda f_\infty)}{4\delta^2}-\frac{1}{16}\cos(\Omega)\cot(\Omega)\,(1-2\lambda f_\infty)\log^2(\delta/H) \\ &\quad+\left(\frac{\sin(\Omega)\,(1-6\lambda f_\infty)}{2h_0^2}+\frac{1}{8}\log(h_0)\cos(\Omega)\cot(\Omega)\,(1-2\lambda f_\infty)\right)\log(\delta/H) \\ &\quad+\int_{\delta/h_0}^{H}\frac{d\rho}{\rho}\int_{h_0}^{\delta/\rho}dh\left(\frac{\sin(\theta)\mathcal{L}_1}{\mathcal{L}_2}+\frac{\sin(\Omega)\,(1-6\lambda f_\infty)}{h^3}-\frac{\cos(\Omega)\cot(\Omega)\,(1-2\lambda f_\infty)}{8h}\right)\Bigg]. \end{aligned} \tag{3.210}$$

In the last term, the h integration is finite in the limit $\delta\to 0$ and hence the leading order divergence is logarithmic. Hence, we write

$$\begin{aligned} S_4\big|_{c_1} &= \frac{4\,\pi^2\tilde{L}^3}{\ell_{\rm P}^3}\Bigg[\frac{H^2\sin(\Omega)\,(1-6\lambda f_\infty)}{4\delta^2}-\frac{1}{16}\cos(\Omega)\cot(\Omega)\,(1-2\lambda f_\infty)\log^2(\delta/H) \\ &\quad+\log(\delta/H)\left(\frac{\sin(\Omega)\,(1-6\lambda f_\infty)}{2h_0^2}+\frac{1}{8}\log(h_0)\cos(\Omega)\cot(\Omega)\,(1-2\lambda f_\infty)\right. \\ &\quad\left.+\int_0^{h_0}dh\left[\frac{\sin(\theta)\mathcal{L}_1}{\mathcal{L}_2}+\frac{\sin(\Omega)\,(1-6\lambda f_\infty)}{h^3}-\frac{\cos(\Omega)\cot(\Omega)\,(1-2\lambda f_\infty)}{8h}\right]\right) \\ &\quad+\mathcal{O}(\delta^0)\Bigg]. \end{aligned} \tag{3.211}$$

Now we can compare the coefficient of the $\log^2\delta$ divergence with the central charge (3.196) and find that

$$\begin{aligned} S_4^{\log^2}\big|_{c_1} &= -\frac{C_{\rm T}}{4}\cos(\Omega)\cot(\Omega)\log^2(\delta/H) \\ &= -\frac{c}{4}\cos(\Omega)\cot(\Omega)\log^2(\delta/H)\,, \end{aligned} \tag{3.212}$$

where the second equation follow from (3.201). So we find that for EE of a cone in $d=4$, the singularity contributes in the universal term through the central charge $C_{\rm T}$. Here, we should point out that only half of the above contribution is from the singularity. The other half can be calculated using the contribution of the trace anomaly in EE, *i.e.,* using eq. (3.5). We discuss this point in more detail in section 3.5.

We can also calculate the EE for five-dimensional cone in Gauss-Bonnet gravity. For this case, the action for bulk geometry is (3.194) with $d=5$ and canonical scale L is related

to $\tilde{L}$ by relation (3.200). Now the complete expression of entanglement entropy is given by (3.257) and the universal term is

$$S_5^{\log}\big|_{c_2} = -\frac{8\,\pi^2\tilde{L}^4}{\ell_{\rm P}^4}\left(\frac{\left(2\cos^2(\Omega)\,(2-7\lambda f_\infty)\,h_0^2-3\sin^2(\Omega)\,(1-4\lambda f_\infty)\right)}{9h_0^3}+\int_0^{h_0}dh\frac{\mathcal{L}_3}{\mathcal{L}_4}\right)\log(\delta/H)\,, \tag{3.213}$$

where $\mathcal{L}_3$ and $\mathcal{L}_4$ are given by (3.258). In this case, we can further compare the universal term with the central charges (3.196) and (3.197). However, we observe from expression of $\mathcal{L}_3$ and $\mathcal{L}_4$ in (3.258) that there are terms of order $\mathcal{O}(\lambda^2)$ in the universal term. This implies that the expression (3.213) is not a simple function of the central charges $C_{\rm T}$ and a_5^* and in particular, it is not a linear function.

Further, we calculate the EE for cone in $d=6$ and find that the cut-off independent terms is $\log^2\delta$ and it is given by

$$S_6^{\log^2}\big|_{c_3} = \frac{12\,\pi^3\tilde{L}^5\cos(\Omega)\cot(\Omega)}{\ell_{\rm P}^5}\left(\frac{93-190\lambda f_\infty}{8192}-\frac{3-2\lambda f_\infty}{8192}\cos(2\Omega)\right)\log^2(\delta/H)\,. \tag{3.214}$$

We have given the complete expression of EE in the section 3.6.2 in eqn. (3.259). In this expression, we would like to compare the Ω independent coefficients with the central charges of the CFT. So there are two terms, $(93-190\lambda f_\infty)$ and $(3-2\lambda f_\infty)$, which we can express in terms of $C_{\rm T}$ and a_6^*. Using equations (3.196) and (3.197), we find that the universal terms in EE for c_3 can be written as

$$S_6^{\log^2}\big|_{c_3} = \frac{3\cos(\Omega)\cot(\Omega)}{1024}\Big[(90\,C_{\rm T}+3\,a_6^*)-(6\,C_{\rm T}-3\,a_6^*)\cos(2\Omega)\Big]\log^2(\delta/H)\,. \tag{3.215}$$

Now in $d=6$, we do not know the precise expression of the contribution of the trace anomaly to EE, *i.e.*, $d=6$ generalization of (3.5). Hence, now we can not distinguish the contribution from the trace anomaly with the contribution from the singularity in (3.215). Hence, we can not say what part of the universal term comes from the singularity and particularly, we can not confirm if singularity contributes only through the central charge $C_{\rm T}$.

3.4.2 Singularity with a curved locus

In this section, we will repeat the calculation of EE for geometry $k \times S^2$ in $d = 5$ CFT, which is dual to the Gauss-Bonnet gravity. For this case, the bulk action and EE are given by (3.194) and (3.198). We further consider the metric ansatz

$$ds^2 = \frac{\tilde{L}^2}{z^2}\left(dz^2 + f_1(z)\left(dt^2 + d\rho^2 + \rho^2 \sin^2(\theta)\right) + R_1^2 f_2(z) d\Omega_2^2\right) , \tag{3.216}$$

where $d\Omega_2^2$ is metric over the two-sphere. Further, similar to (3.200), $\tilde{L}^2 = L^2/f_\infty$ where $f_\infty = (1-\sqrt{1-4\lambda})/2\lambda$. Here f_1 and f_2 are functions of z and one can use the Fefferman-Grahm expansion to find their values near the boundary.

Now, to calculate EE, we first use Fefferman-Grahm expansion and find that

$$\begin{aligned} f_1(z) &= 1 + \frac{z^2}{12R_1^2} + \frac{z^4(51-58\lambda f_\infty)}{1728R_1^4(1-2\lambda f_\infty)} + \dots , \\ f_2(z) &= 1 - \frac{z^2}{4R_1^2} - \frac{z^4(15-2\lambda f_\infty)}{576R_1^4(1-2\lambda f_\infty)} + \dots . \end{aligned} \tag{3.217}$$

Once again, we choose the parametrization $\rho = \rho(z,\theta)$ and similar to (3.74), we can find the induced metric for the entropy functional. Here, we restrain to give the complete expression for the entropy functional but the important point to note is that now there are terms with higher derivatives, like ρ'', $\ddot{\rho}$ and $\dot{\rho}'$ in the entropy functional. However, in spite of this, the equation of motion for $\rho(z,\theta)$ is still second order and that is because of the topological nature of the Gauss-Bonnet terms. Now we can simplify the entropy function by inserting the ansatz $\rho = \rho_0 + \rho_1/R_1^2$ and then series expending it for large R_1. We find that up to the leading order, the EE is given by

$$\begin{aligned} S_5\big|_{k\times S^2} = \frac{16\,\pi^2 \tilde{L}^4 R_1^2}{\ell_{\rm P}^4}\int_{z_m}^{\delta} dz \int_0^{\Omega-\epsilon} d\theta \Bigg(\mathcal{L}_0(\rho_0) + \frac{1}{R_1^2}\Big(\mathcal{L}_N(\rho_0) + \mathcal{L}_f(\rho_0, \mathbf{c}_1, \mathbf{c}_2) \\ + \rho_1' \mathcal{L}_1(\rho_0) + \dot{r}\,\dot{h}\,\mathcal{L}_2(\rho_0) + \ddot{\rho}_1 \mathcal{L}_3(\rho_0) + \rho_1 \mathcal{L}_4(\rho_0) + \dot{\rho}_1 \mathcal{L}_5(\rho_0) + \rho_1 \mathcal{L}_6(\rho_0)\Big)\Bigg) , \end{aligned} \tag{3.218}$$

where $\mathcal{L}_0(\rho_0)$ is the term which comes from the limit $R_1 \to \infty$ in the original lagrangian. The term $\mathcal{L}_N(\rho_0)$ is a new term which doesn't appear for $\lambda = 0$ case. This term comes from the contribution of sphere in the Ricci scalar in (3.198). The term $\mathcal{L}_f(\rho_0, \mathbf{c}_1, \mathbf{c}_2)$ is the term which is independent of ρ_1 and comes from the leading order corrections in $f_1 = 1 + \mathbf{c}_1 z^2/R_1^2$ and $f_2 = 1 + \mathbf{c}_2 z^2/R_1^2$, where $\mathbf{c}_1 = 1/12$ and $\mathbf{c}_2 = -1/4$. Further, terms

with $\mathcal{L}_1(\rho_0)$-$\mathcal{L}_6(\rho_0)$ are independent of $\mathbf{c}_1$ and $\mathbf{c}_2$ and are linear in ρ_1, as it is written. Now, we can write

$$\begin{aligned}
\rho_1'\mathcal{L}_1 &= \partial_z(\mathcal{L}_1\rho_1 - \mathcal{L}_1'\rho_1) + \mathcal{L}_1''\rho_1\,,\\
\dot\rho_1'\mathcal{L}_2 &= \partial_z(\mathcal{L}_2\dot\rho_1) - \partial_\theta(\mathcal{L}_2'\rho_1) + \dot{\mathcal{L}}_1{}'\rho_1\,,\\
\ddot\rho_1\mathcal{L}_3 &= \partial_\theta(\mathcal{L}_3\dot\rho_1) - \partial_\theta(\dot{\mathcal{L}}_3\rho_1) + \ddot{\mathcal{L}}_3\rho_1\,,\\
\rho_1\mathcal{L}_4 &= \partial_z(\mathcal{L}_4\rho_1) - \mathcal{L}_4'\rho_1\,,\\
\dot\rho_1\mathcal{L}_5 &= \partial_\theta(\mathcal{L}_5\rho_1) - \mathcal{L}_5'\rho_1\,,
\end{aligned} \tag{3.219}$$

where prime and upper dot denote the partial derivative with respect to z and θ. Using these in (3.218), we write

$$\begin{aligned}
S_5\big|_{k\times S^2} &= \frac{16\,\pi^2\tilde L^4 R_1^2}{\ell_{\rm P}^4}\int_{z_m}^{\delta}dz\int_0^{\Omega-\epsilon}d\theta\Big(\mathcal{L}_0(\rho_0)+\frac{1}{R_1^2}\Big(\mathcal{L}_N(\rho_0)+\mathcal{L}_f(\rho_0,\mathbf{c}_1,\mathbf{c}_2)\\
&\qquad +\rho_1(\mathcal{L}_1''+\dot{\mathcal{L}}_2{}'+\ddot{\mathcal{L}}_3-\mathcal{L}_4'-\dot{\mathcal{L}}_5)+\partial_z(\mathcal{L}_1\rho_1-\mathcal{L}_1'\rho_1+\mathcal{L}_2\dot\rho_1+\mathcal{L}_4\rho_1)\Big)\Big)\\
&\quad +\frac{16\,\pi^2\tilde L^4}{\ell_{\rm P}^4}\int_{z_m}^{\delta}dz\,\Big(-\mathcal{L}_2'\rho_1+\mathcal{L}_3\dot\rho_1-\dot{\mathcal{L}}_3\rho_1+\mathcal{L}_5\rho_1\Big)_{\theta=\Omega-\epsilon}\,,
\end{aligned} \tag{3.220}$$

where the coefficient of the ρ_1 vanishes from the equation of motion of ρ_0 and we have performed the integration over θ in terms in the last line. Note that we can not integrate over z in any term as $\epsilon=\epsilon(z)$ and both θ and z integrations don't commute. Now we further insert the ansatz $\rho_0 = z/h(\theta)$ and $\rho_1 = z^3 g_3(\theta)$ in the above entropy functional and in the equations of motion for ρ_0 and ρ_1 to find the equations of motion for h and g_3. Once again, we restrain to give the complete expression of the equations of motion as they are not very illuminating. Similar to (3.84), at this stage we find that the terms with the partial derivative with respect to z vanish. Finally, the entropy functional reduces to

$$\begin{aligned}
S_5\big|_{k\times S^2} &= \frac{16\,\pi^2\tilde L^4 R_1^2}{\ell_{\rm P}^4}\int_{z_m}^{\delta}dz\int_{h_0}^{h_{1c}(z)}\frac{dh}{\dot h}\left(\frac{\hat{\mathcal{L}}_0(h)}{z^3}+\frac{1}{R_1^2}\frac{\hat{\mathcal{L}}_N(h)+\hat{\mathcal{L}}_f(h,\mathbf{c}_1,\mathbf{c}_2)}{z}\right)\\
&\quad +\frac{16\,\pi^2\tilde L^4}{\ell_{\rm P}^4}\int_{z_m}^{\delta}dz\,\frac{\hat{\mathcal{L}}_B|_{\theta=\Omega-\epsilon}}{z}\,,
\end{aligned} \tag{3.221}$$

where we have defined $\mathcal{L}_0=\hat{\mathcal{L}}_0(h)/z^3$, $\mathcal{L}_N=\hat{\mathcal{L}}_N(h)/z$, $\mathcal{L}_f=\hat{\mathcal{L}}_f(h,\mathbf{c}_1,\mathbf{c}_2)/z$ and expressions for $\hat{\mathcal{L}}$'s are given by (3.262) in section 3.6.2. Now we can solve the equations of motion

for h and g_3 near the asymptotic boundary to find

$$\begin{aligned}\dot{h} &= -\frac{a_1}{h^4}-\frac{2a_1}{h^2}-a_1+\frac{h^4\left(1-6f_\infty\lambda\right)}{2a_1\left(1-2f_\infty\lambda\right)}-\frac{h^6\left(1-10f_\infty\lambda\right)}{2a_1\left(1-2f_\infty\lambda\right)}+\dots\,, \\ g_3 &= \frac{b_3}{h^3}+\frac{9-26f_\infty\lambda+792b_3\left(1-2f_\infty\lambda\right)}{504h\left(1-2f_\infty\lambda\right)}+\frac{4h\left(3-11f_\infty\lambda+54b_3\left(1-2f_\infty\lambda\right)\right)}{567\left(1-2f_\infty\lambda\right)}+\dots\,,\end{aligned} \tag{3.222}$$

where a_1 and b_3 are constants which are fixed by ensuring that both h and g_3 have extrema at $\theta=0$. Note that here a_1 is related to a quantity which is conserved along the θ translation similar to (3.85). Using these solutions near the boundary, we first find the value of $h_{1c}(z)$ at the UV cut-off $z=\delta$. To do that, we use the above solutions in the ansatz $\rho=z/h+z^3g_3/R_1^2$ and inverting the relations iteratively, we find

$$\begin{aligned}h_{1c}(\delta) &= \left(\frac{1}{H}+\frac{b_3H}{R_1^2}\right)\delta+\frac{\left(9-26f_\infty\lambda+792b_3\left(1-2f_\infty\lambda\right)\right)\delta^3}{504HR_1^2\left(1-2f_\infty\lambda\right)} \\ &\quad+\frac{4\left(3-11f_\infty\lambda+54b_3\left(1-2f_\infty\lambda\right)\right)\delta^5}{567H^3R_1^2\left(1-2f_\infty\lambda\right)}+\dots\,.\end{aligned} \tag{3.223}$$

Note that above relation reduces to (3.88) for $\lambda=0$. Now we use (3.222) to study the behavior of integrands in (3.221) near the asymptotic boundary, where we have $h\to 0$:

$$\begin{aligned}\frac{\hat{\mathcal{L}}_0}{\dot{h}} &\sim -\frac{1-4f_\infty\lambda}{h^2}+\mathcal{O}(h^4)\,, \\ \frac{\hat{\mathcal{L}}_N+\hat{\mathcal{L}}_f}{\dot{h}} &\sim \frac{15-68f_\infty\lambda}{72h^2}+\mathcal{O}(h^2)\,.\end{aligned} \tag{3.224}$$

Using these, similar to (3.91) and (3.93), we can make the integrands in (3.262) finite. We can break the terms in following components

$$I_1 = \int_{z_m}^{\delta}\frac{dz}{z^3}\int_{h_0}^{h_{1c}(z)}dh\left(\frac{\hat{\mathcal{L}}_0}{\dot{h}}+\frac{1-4f_\infty\lambda}{h^2}\right)\,, \tag{3.225}$$

$$I_2 = -\int_{z_m}^{\delta}\frac{dz}{z^3}\int_{h_0}^{h_{1c}(z)}dh\,\frac{1-4f_\infty\lambda}{h^2}\,, \tag{3.226}$$

$$I_3 = -\int_{z_m}^{\delta}\frac{dz}{z}\int_{h_0}^{h_{1c}(z)}dh\left(\frac{\hat{\mathcal{L}}_N+\hat{\mathcal{L}}_f}{\dot{h}}-\frac{15-68f_\infty\lambda}{72h^2}\right)\,, \tag{3.227}$$

$$I_4 = -\int_{z_m}^{\delta}\frac{dz}{z}\int_{h_0}^{h_{1c}(z)}dh\,\frac{15-68f_\infty\lambda}{72h^2}\,, \tag{3.228}$$

and then take a derivative with respect to δ and find following series expansion:

$$\begin{aligned}
\frac{dI_1}{d\delta} &= \frac{1}{\delta^3}\int_{h_0}^{0} dh\left(\frac{\hat{\mathcal{L}}_0}{\dot{h}}+\frac{1-4f_\infty\lambda}{h^2}\right)+\mathcal{O}(\delta^4)\\
\frac{dI_2}{d\delta} &= \left(1-\frac{b_3H^2}{R_1^2}\right)\frac{H\left(1-4f_\infty\lambda\right)}{\delta^4}-\frac{1-4f_\infty\lambda}{h_0\delta^3}\\
&\quad -\frac{H\left(1-4f_\infty\lambda\right)\left(9-26f_\infty\lambda+792b_3\left(1-2f_\infty\lambda\right)\right)}{504\left(1-2f_\infty\lambda\right)R_1^2\delta^2}+\mathcal{O}(\delta^0)\\
\frac{dI_3}{d\delta} &= -\frac{1}{\delta}\int_{h_0}^{0} dh\left(\frac{\hat{\mathcal{L}}_N+\hat{\mathcal{L}}_f}{\dot{h}}-\frac{15-68f_\infty\lambda}{72h^2}\right)+\mathcal{O}(\delta^5) \qquad (3.229)\\
\frac{dI_4}{d\delta} &= -\left(1-\frac{b_3H^2}{R_1^2}\right)\frac{H\left(15-68f_\infty\lambda\right)}{72\delta^2}+\frac{15-68f_\infty\lambda}{72h_0\delta}+\mathcal{O}(\delta^0)\\
\frac{d}{d\delta}\int_{z_m}^{\delta} dz\,\frac{\hat{\mathcal{L}}_B|_{\theta=\Omega-\epsilon}}{z} &= \left(1-\frac{3b_3H^2}{R_1^2}\right)\frac{b_3H^3\left(1-4f_\infty\lambda\right)}{\delta^4}\\
&\quad +\left(1-\frac{4b_3H^2}{R_1^2}\right)\frac{H\left(1-4f_\infty\lambda\right)\left(9-26f_\infty\lambda+792b_3\left(1-2f_\infty\lambda\right)\right)}{504\left(1-2f_\infty\lambda\right)\delta^2}\\
&\quad +\mathcal{O}(\delta^0)\,.
\end{aligned}$$

Note that we have done the same with the boundary term in (3.221) too. Using these relations, we can read off the logarithmic term in the EE, which is given by

$$\begin{aligned}
S_5^{\log}\big|_{k\times S^2} &= \frac{16\,\pi^2\tilde{L}^4}{\ell_{\rm P}^4}\left(\int_{h_0}^{0} dh\left(\frac{\hat{\mathcal{L}}_N+\hat{\mathcal{L}}_f}{\dot{h}}-\frac{15-68f_\infty\lambda}{72h^2}\right)\right.\\
&\qquad \left.+\frac{15-68f_\infty\lambda}{72h_0}\right)\log(\delta/H)\,, \qquad (3.230)
\end{aligned}$$

where $\hat{\mathcal{L}}_N$ and $\hat{\mathcal{L}}_f$ are given by (3.262). Now we can try to compare this cut-off independent term with the central charges (3.196) and (3.197). However, by looking at the expression of $\hat{\mathcal{L}}_N$ and $\hat{\mathcal{L}}_f$, we find that there are terms of order $\mathcal{O}(\lambda^2)$. Hence the universal term is not a simple (and particularly linear) function of the central charges.

Now, it would have been interesting to further investigate the universal term for the geometry $c_1\times S^2$. In this case, the singularity has a even dimensional, curved locus and we will get a $\log^2\delta$ divergence. So it would have been very interesting to see if this contribution from the locus is a specific central charge. However, this calculate is tedious and demands more patience and ingenuous simplifications.

3.5 Discussion

In this chapter, we have used holography to study entanglement entropy for various singular surfaces in higher dimensions. In particular, in section 3.2.1, we considered cones in various dimensions. For $c_2 = R^+ \times S^2$ in $d = 5$, we found that an additional universal contribution appears:

$$S_{\text{univ}} = k_d(\Omega)\, \log(\delta/L)\,, \tag{3.231}$$

where Ω is the opening angle of the cone, as shown in figure 3.1. While the expression for the coefficient $k(\Omega)$ is left implicit in eq. (3.36), we showed that it satisfies the required properties: (a) $k_d(\Omega = \pi/2) = 0$ since the entangling surface is actually a flat plane for this angle and (b) $k_d(\Omega) = k_d(\pi - \Omega)$ since the entanglement entropy of the CFT ground state is identical for the density matrix describing the degrees of freedom inside or outside of the cone. Further we found that $k_d(\Omega \to 0) \propto 1/\Omega$ as in (3.38). Our expectation is that this behaviour extends generally to cones for odd-dimensional theories. That is, the entanglement entropy acquires a universal contribution of the form given in eq. (3.231) for a cone $c_{d-3} = R^+ \times S^{d-3}$ in any odd d.

Further we add that in eq. (3.36), the coefficient k_5 is proportional to L^4/ℓ_{P}^4 which can be identified with a central charge in the dual boundary CFT. However, with Einstein gravity in the bulk, all of the central charges in the five-dimensional boundary theory are identical and so in section 3.4.1, we extended the calculation to Gauss-Bonnet gravity in the bulk, which allows us to distinguish at least two such central charges, as described there. However, given the result for $k_5(\Omega)$ implicit in eq. (3.213) and (3.258), it appears that this coefficient is a complicated nonlinear function of both central charges. It may in fact be that this coefficient is not determined by the central charges alone – this would then be similar to the results found for Renyi entropies in [114].

The case of even dimensions was particularly interesting. In section 3.2.1 with $d = 4$ and 6, we found that a cone yields a universal contribution of the form:

$$S_{\text{univ}} = \hat{k}_d(\Omega)\, \log^2(\delta/L)\,, \tag{3.232}$$

where Ω is again the opening angle, as shown in figure 3.1. Again we believe this is a generic result for even-dimensional theories. In our holographic examples, the coefficient functions have a relatively simple form, as shown in eqs. (3.34) and (3.39). Hence for these examples, it is straightforward to verify that $\hat{k}_d(\Omega)$ satisfies the same properties as described for $k_d(\Omega)$ in the previous paragraph. From these results, we also see that $\hat{k}_d(\Omega \to 0) \propto 1/\Omega$, which parallels the behaviour known for k_3 in eq. (3.6). Further, in section 3.4.1, using Gauss-Bonnet gravity, we were able to verify that this coefficient is proportional to the central

charge (3.196) which controls the leading singularity of the two-point function of the stress tensor. In particular, for $d = 4$, we have a simple result (3.212) which yields

$$\hat{k}_4 = -\frac{c}{4}\,\frac{\cos^2\Omega}{\sin\Omega}\,. \tag{3.233}$$

We might note that with even d, there are also contributions proportional to a single power of $\log \delta/L$, however, these terms are no longer universal. Rather the corresponding coefficient will vary if the details of the cut-off (or the macroscopic scale L) are changed because of the presence of the $\log^2 \delta/L$ term – see further discussion below.

Recall that the trace anomaly in an even-dimensional CFT gives rise a universal contribution in the entanglement entropy with a smooth entangling surface [52, 51, 143, 87]. In particular, if we consider a four-dimensional CFT in a flat background, this contribution takes the form given in eq. (3.5). Given this explicit expression, it is interesting to compare this contribution for a conical entangling surface c_1 in $d = 4$ to the universal term (3.212) found in our holographic calculation.

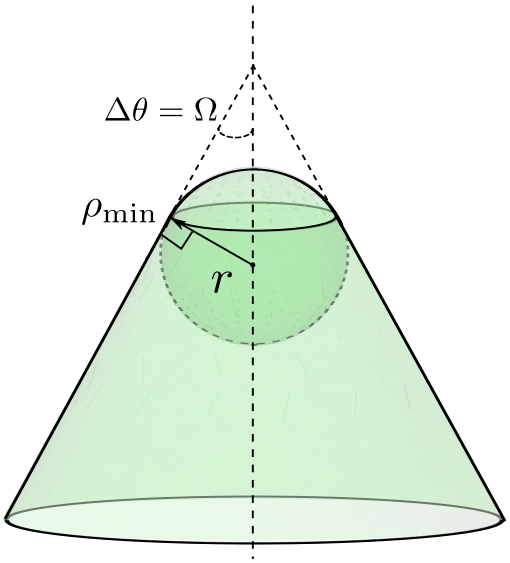

Figure 3.4: (Colour Online) The illustration shows regulated cone $\tilde{c}_1$, where the tip is replaced by a spherical cap.

Of course, eq. (3.5) is only expected to apply for a smooth entangling surface and so cannot be applied directly to the cone c_1. Hence our approach is to construct a 'regulated cone' $\tilde{c}_1$ by cutting off the cone at some $\rho_{\min}$ and replacing the tip with a spherical cap of

radius $r = \rho_{\min} \tan\Omega$, as shown in figure 3.4. Hence $\tilde{c}_1$ provides a smooth model of the desired conical entangling surface to which we can apply eq. (3.5) and we can consider the limit $\rho_{\min} \to 0$ to recover the result for the singular surface c_1. Hence working first with finite $\rho_{\min}$, it is relatively straightforward to show that eq. (3.5) yields[7]

$$S_{\text{univ}} = -\frac{c}{2}\frac{\cos^2\Omega}{\sin\Omega}\,\log(\delta/L)\log(\rho_{\min}/L) + 2\,a\,(1-\sin\Omega)\,\log(\delta/L)\,. \tag{3.234}$$

Unfortunately the first term will diverge if we take the limit $\rho_{\min} \to 0$. However, if the underlying CFT has been regulated with the cut-off δ, it should not be able to resolve any features in geometry at shorter distances. Hence it is natural to consider the limit $\rho_{\min} \to \delta$ which yields

$$S_{\text{univ}} = -\frac{c}{2}\frac{\cos^2\Omega}{\sin\Omega}\,\log^2(\delta/L) + 2\,a\,(1-\sin\Omega)\,\log(\delta/L)\,. \tag{3.235}$$

With this construction, the universal contribution (3.5) contains terms proportional to both $\log^2(\delta/L)$ and $\log(\delta/L)$. The most surprising aspect of this result is that the coefficient of the leading term is almost identical to the holographic result in eq. (3.212). However, there is a mismatch by a factor of two.[8] Our interpretation of this result is that with the conical entangling surface c_1, part of the $\log^2(\delta/L)$ divergence should be associated with correlations across the smooth part of the entangling surface away from the singularity. The above calculation then suggests a pile up of short distance correlations in the vicinity of the tip. However, the full accumulation of correlations near the tip of the cone does not have (precisely) the form expected from the 'smooth' expression (3.5). Hence a part of this universal contribution should be thought of as intrinsic to the singularity at the tip of the cone itself.

As already noted, if we examine our holographic entanglement entropy for c_1 in eq. (3.34), we also find a term proportional to $\log(\delta/L)$. The angular dependence of the corresponding coefficient is different from that for the $\log^2(\delta/L)$ term and so one might envision that certain universal aspects can still be extracted from this coefficient. For example, in eq. (3.235), the second central charge a appears in the $\log(\delta/L)$ term and so one might hope to extract this charge by studying the entanglement entropy for cones with various opening angles Ω. However, we wish to emphasize that this $\log(\delta/L)$ contribution is simply not universal in the presence of the $\log^2(\delta/L)$ term. For example, let us return to our

[7] On the conical portion of $\tilde{c}_1$, $\mathcal{R} = 0$ while the only nontrivial component of the extrinsic curvature is $K^{\hat{\theta}}_{\phi\phi} = \rho\,\sin\Omega\,\cos\Omega$. On the spherical cap, $\mathcal{R} = 2/r^2$ while the combination of extrinsic curvatures in eq. (3.5) vanishes.

[8] This observation was also made in [142]. We also note that the same result appears in an alternate calculation of the holographic entanglement entropy presented in section 3.6.1. There the mismatch can be regarded as an anomaly resulting from a singular conformal transformation.

regulated model of cone above where we argued it was natural to take the limit $\rho_{\min} \to \delta$ for the radius of the spherical cap. The latter was motivated by observing that δ is a short distance cut-off in the underlying CFT and so the latter can not resolve any geometric features involving shorter distance scales. However, let us note that the radius of the spherical cap was $r = \rho_{\min} \tan\Omega$ and so even if we set $\rho_{\min} = \delta$, for small Ω, the cap is effectively much smaller than the short distance cut-off. Hence one might instead choose

$$\rho_{\min} = \begin{cases} \delta & \text{for } \Omega > \pi/4\,, \\ \frac{\delta}{\tan\Omega} & \text{for } \Omega \leq \pi/4\,. \end{cases} \tag{3.236}$$

While such a choice leaves the $\log^2(\delta/L)$ term unchanged, the coefficient in the $\log(\delta/L)$ contribution acquires a complicated new angular dependence. We have presented this discussion simply to illustrate that all of the details (including the angular dependence) of the coefficient of the $\log(\delta/L)$ can be expected to depend on the precise choice of the regulator in the calculation of the entanglement entropy. While eq. (3.236) gives an illustrative example, we might observe that the same regulator in the holographic calculations is far more subtle. The analog of eq. (3.236) would be $\rho_{\min} = \delta/h_0$ in section 3.2.1.

We also extended our holographic analysis to consider creases or extended singularities in section 3.3. Examining the examples summarized in table 3.1, we find that the crease of the form $k \times R^m$ or $c_n \times R^m$ creates no new universal contributions.[9] However, in general, we found that creases can contribute additional universal terms, but singular locus must have an even dimension and must be curved. These results suggest that these new universal contributions to the entanglement entropy take the form given in eq. (3.11) with a $\log\delta$ divergence in odd dimensions and $\log^2\delta$ in even dimensions. These results indicate that there is a rich variety of new geometric contributions to entanglement entropy that can be associated with singular entangling surfaces. However, our analysis only considered simple families of singularities and does not suffice to reveal the full geometric structure of these universal terms. It would, of course, be interesting to consider more general singularities, *e.g.,* a crease of the form $k \times R^1$ but where the opening angle varies along R^1 or where R^1 was not entirely straight. Another step towards a clearer picture of these geometric coefficients would be to carry out the holographic calculations using the Fefferman-Grahm expansion [95, 96] to compute entanglement entropy along the lines discussed in [47].

In part, our motivation for these studies was the possibility that these new universal contributions may be used to identify the central charges of the underlying CFT. Recently

[9] Let us re-iterate that we are ignoring certain cases here, *e.g.,* $c_1 \times R^2$, where a $\log\delta$ term appears but it can be attributed to the smooth part of the entangling surface. We also do not consider the possibility that the finite contributions may exhibit some new universal behaviour.

there has been a great deal of interest in using entanglement to identify central charges that obey a c-theorem, in particular for odd spacetime dimensions, *e.g.,* see [46, 142, 87, 88, 144, 145]. In this regard, our results only point towards a clear result for even dimensions, namely that the coefficient of the $\log^2\delta$ contribution is proportional to a particular central charge. Unfortunately, this central charge $C_{\rm T}$ is not the one expected to satisfy a c-theorem.[10] However, our holographic result seems particularly simple and so it may be that there is a general derivation for any CFT, perhaps connected to the trace anomaly as for the universal terms identified for smooth surfaces [52, 51, 87, 143]. In odd dimensions, our results in section 3.4.1 indicate that the universal terms associated with singularities in the entangling surface will be complicated nonlinear functions of many parameters in the underlying CFT. Here it must be said that we refer to these contributions as universal since they will be independent of the details of the UV regulator and so should characterize properties of the underlying CFT (or QFT more generally). However, the precise nature of the information contained in these terms remains to be understood. A similar result was found for Renyi entropies of spherical entangling surfaces in [114].

It would also be interesting to study these universal contributions to entanglement entropy in non-holographic theories. In particular, one might consider heat kernel methods for free field theories for simple surfaces, *e.g.,* along the lines of [141, 146]. We have been informed [147] that similar $\log^2\delta$ terms have been found in the entanglement entropy for surfaces with a conical singularity in non-holographic calculation. It would also be interesting to further investigate the Renyi entropy for the singular entangling surfaces [114].

3.6 Supplementry material for chapter 3

3.6.1 Conformal transformations and EE for c_{d-3}

In this section, we consider an alternate approach to calculating the entanglement entropy associated with a conical singularity. In particular, we begin by performing a conformal transformation which takes R^d to $R \times S^{d-1}$. Under such a conformal transformation, the conical entangling surface c_{d-3}, considered in sections 3.1 and 3.2, becomes simply a uniform cylinder $R \times S^{d-3}$ in the latter background. The analogous mapping was applied to calculating the cusp anomaly for a Wilson loop with a sharp corner in N=4 SYM, *e.g.,*

[10] Setting holography aside, it was shown that for four-dimensional QFT's, there is no possible (linear) combination of the two central charges, $C_{\rm T}$ and $a = a_d^*$, that can satisfy a c-theorem apart from a alone [39].

see [148]. In this case, calculating the cusp anomaly becomes problem of determining the quark-antiquark potential on a three-sphere. In fact, the holographic calculation of the leading result corresponds to determining an extremal surface in the bulk with a 'kink' boundary condition and so precisely it matches the calculation of the holographic EE for a kink in $d = 3$ [149, 148].

Note that in the background geometry $R \times S^{d-1}$, the time coordinate is compactified and the length of the cylinder is along R. Then we would like to calculate EE using the simple cylindrical geometry and in particular, to see if we get the same $\log \delta$ and $\log^2 \delta$ terms that appeared in our previous calculations. The key feature in these calculations is that the entangling surface $R \times S^{d-3}$ now has an infinite length along the R direction and so this length must be regulated to properly account for the logarithmic divergences, as we will discuss bellow in section 3.6.1.1 when we calculate the holographic EE. We first discuss desired conformal transformation in the CFT and then we consider how this transformation is implemented with a coordinate transformation in the dual bulk spacetime.

In the flat background (3.8) with $\{n, m\} = \{d-3, 0\}$, we can make the coordinate transformations $t_E = r \cos \xi$ and $\rho = r \sin \xi$ and find following metric

$$ds^2 \;=\; dr^2 + r^2(d\xi^2 + \sin^2 \xi \, (d\theta^2 + \sin^2 \theta \, d\Omega_{d-3}^2)) \,. \tag{3.237}$$

In these coordinates, the cone geometry discussed in section 3.1 translates to the surface: $c_{d-3} = \{r = [0, \infty), \xi = \pi/2, \theta = \Omega\}$. We can further perform the coordinate transformation $r = L \, e^{Y/L}$, and a Weyl transformation to remove the overall factor $e^{2Y/L}$ from the resulting metric. After these transformations, we find background geometry becomes $R \times S^{d-1}$ with the metric

$$ds^2 \;=\; dY^2 + L^2(d\xi^2 + \sin^2 \xi \, (d\theta^2 + \sin^2 \theta \, d\Omega_{d-3}^2)) \,, \tag{3.238}$$

where $Y \in [-\infty, \infty]$. Further, the conical entangling surface above is now mapped to a cylinder of infinite length, *i.e.,*

$$c_{d-3} = \{Y = (-\infty, \infty), \xi = \pi/2, \theta = \Omega\} \,. \tag{3.239}$$

Next we discuss the coordinate transformation in the bulk geometry which implements the conformal transformation between the two boundary metrics in eqs. (3.237) and (3.238). We begin with the standard description of (Euclidean) AdS_{d+1} as a hyperbola embedded in the following $(d+2)$-dimensional Minkowski space

$$ds^2 \;=\; -dU^2 + dV^2 + (dX^1)^2 + \cdots + (dX^d)^2 = \; -dU^2 + dV^2 + dR^2 + R^2 d\Omega_{d-1}^2 \,, \tag{3.240}$$

where in the second expression, we introduced polar coordinates on the space spanned by the X^i. Now the AdS geometry is defined by the hyperbola

$$-U^2 + V^2 + (\vec{X})^2 \;=\; -U^2 + V^2 + R^2 \;=\; -L^2\,. \tag{3.241}$$

We can solve this constraint by writing $U \;=\; \sqrt{R^2+L^2}\,\cosh(Y/L)$ and $V \;=\; \sqrt{R^2+L^2}\,\sinh(Y/L)$, in which case the induced metric on this surface becomes

$$ds^2 \;=\; \frac{1}{\left(1+\frac{R^2}{L^2}\right)} dR^2 + \left(1+\frac{R^2}{L^2}\right) dY^2 + R^2\left[d\xi^2 + \sin^2\xi\,(d\theta^2 + \sin^2\theta\, d\Omega_{d-3}^2)\right]\,, \tag{3.242}$$

where we have written $d\Omega_{d-1}^2 = d\xi^2 + \sin^2\xi\,(d\theta^2 + \sin^2\theta\, d\Omega_{d-3}^2)$. Of course, we recognize this metric as (Euclidean) AdS_{d+1} in global coordinates and this geometry is dual to the boundary CFT with the background metric (3.238). Alternatively, to get the bulk metric dual to eq. (3.237), we write $R = rL/z$ and $U+V = L^2/z$ and eq. (3.241) yields $U - V = z + r^2/z$. With these coordinates, the induced metric on the hyperbola becomes

$$ds^2 \;=\; \frac{L^2}{z^2}(dz^2 + dr^2 + r^2 d\Omega_{d-1}^2)\,, \tag{3.243}$$

which matches the 'Poincaré patch' metric (3.9) with $r^2 = t_E^2 + \rho^2$. Clearly, the boundary metric matches the desired form given in eq. (3.237). This bulk metric (3.243) was used in our calculation of the holographic EE for the cone in section 3.2. So now we calculate the same EE using the cylindrical geometry in bulk metric (3.242).

3.6.1.1 EE for cylinders

In this section, we will calculate the holographic EE for cylindrical entangling surface $R \times S^{d-3}$ on the background $R \times S^{d-1}$ for $d = 3$, 4 and 5. As we will see, the calculations here are closely related to those already presented in section 3.2. We find that the coefficient of the universal $\log\delta$ term matches our previous results for $d = 3$ and 5. In $d = 4$, the universal term is a $\log^2\delta$ contribution but we find the coefficient in the following does not give a precise match with that in eq. (3.212) from our previous calculation. In fact, the $\log^2\delta$ term here shows the same mismatch by a factor of two that we found in eq. (3.235) from considering the contribution of the trace anomaly on a regulated conical surface. We will show that this difference in the holographic results come from choosing different UV cut-offs in the different coordinate systems. Although these cut-offs are natural in the particular coordinate system in which they are chosen, they produce different coefficients of the $\log^2\delta$ divergence.

Now we begin with a general discussion for a d-dimensional CFT background $R \times S^{d-1}$ and later focus on the specific cases with $d = 3$, 4 and 5. The cylindrical entangling surface in the boundary is given in eq. (3.239). However, to produce a finite result, the length the cylinder must be regulated which we do by restricting $Y \in [Y_-, Y_+]$, where Y_- and Y_+ are cut-offs to be fixed below. Now the holographic EE is calculated by first finding the minimal area surface hanging into the bulk geometry with metric (3.242) and if we define this surface by coordinates $(Y, \theta, \Omega_{d-3})$, we will have a radial profile $R(\theta) = L\, g(\theta)$. In particular, note that $R(\theta)$ is independent of Y because we have translational symmetry along this direction. The only scale in the geometry is L, which also coincides with the radius of the sphere S^{d-1} on the boundary. With this ansatz, the holographic EE is given by

$$S_d|_{cylinder} = \frac{2\,\pi\, L^{d-2}\,\Omega_{d-3}}{\ell_{\rm P}^{d-1}} \int_{Y_-}^{Y_+} dY \int_0^{\Omega-\epsilon} d\theta\, g^{d-3} (\sin\theta)^{d-3} \sqrt{\dot{g}^2 + g^2 + g^4}\,, \tag{3.244}$$

where $\dot{g} = dg/d\theta$ and Ω_{d-3} represents the area of the unit $(d-3)$-sphere. Further, ϵ is related to the UV cut-off in the theory. Note that a natural way to choose UV cut-off for cylinder should keep ϵ independent of Y – the coordinate along the length of the cylinder. So a natural UV cut-off for the minimal area surface can be $R = L^2/\delta$, which will fix ϵ such that $g(\Omega - \epsilon) = L/\delta$.

To compare this expression (3.244) with our previous results, we need to relate the quantities for the cylinder with the quantities for the cone discussed in section 3.2. First we note that from the coordinate transformation taking us from eq. (3.242) to eq. (3.243), we have $\rho = r$ and $R = r\,L/z = \rho\, L/z$. In previous calculation of the holographic EE in eq. (3.14) or (3.25), we used the ansatz $z = \rho\, h(\theta)$. Hence, above relation implies that $R = L/h(\theta)$. Comparing with our ansatz above, we see that $g(\theta) = 1/h(\theta)$ and $h(\Omega - \epsilon) = \delta/L$. Now we turn to consider the cut-offs in the coordinate Y. First note that these are independent of our UV cut-off on the radial coordinate, *i.e.,* $R = L^2/\delta$. As after the conformal transformation, we want cylinder to become a cone in R^d, Y_- and Y_+ should be controlled by cut-offs in ρ appearing in eq. (3.25). We use the coordinate transformation $Y = L \log(\rho/L)$, as given above eq. (3.238), and from the range $\rho \in [\delta/h_0, H]$ in eq. (3.25), we find that $Y_- = L \log(\delta/h_0 L)$ and $Y_+ = L \log(H/L)$. Using all these results, we can now rewrite eq. (3.244) as

$$S_d|_{cylinder} = \frac{2\,\pi\, L^{d-1}\Omega_{d-3}}{\ell_{\rm P}^{d-1}} \int_{\delta/h_0}^{H} \frac{d\rho}{\rho} \int_{h_0}^{\delta/L} dh \frac{\sin^{d-3}(\theta)}{\dot{h}\, h^{d-1}} \sqrt{\dot{h}^2 + h^2 + 1}\,. \tag{3.245}$$

At first sight, this expression is identical to eq. (3.25) found in the previous calculation. However, we should notice that there is a crucial difference. Namely, the upper limit of integration over h here is a fixed constant while in eq. (3.25), it is a function of ρ.

Now we consider cylinder in different dimensions one by one. In eq. (3.244), we first take $d = 3$ to consider a cylinder dual to a kink in R^3. Note that in this case $\theta \in [-\Omega, \Omega]$ and we will also have an extra factor of two coming from change of limit of integration. We can further use the variable $y = \sqrt{1/h^2 - 1/h_0^2}$ as around eq. (3.17) and follow the steps in section 3.2. Finally, we find that for $d = 3$, eq. (3.245) will produce

$$S_3|_{cylinder} = \frac{4\pi L^2}{\ell_{\rm P}^2}\left[\frac{L}{\delta}\log(H/\delta) + \frac{L}{\delta}\log(h_0) - q_3(\Omega)\log(H/\delta) + \dots\right], \tag{3.246}$$

where q_3 is given by (3.20). We note that the universal term in EE for cylinder matches with the one in the kink. However, now the leading order divergence is different and contains an extra factor of $\log(h_0 H/\delta)$. Of course, these divergent terms are not expected to be universal.

In part, the aim of the present calculations is to show that our 'universal' terms are independent of the details of the choice of regulator. Here we chose the natural cut-off adapted to the new coordinates after the conformal transformation in the boundary geometry (or a coordinate transformation in the bulk geometry). While the entire structure of the divergent contributions was not unchanged, our universal logarithmic term matched the previous calculations. Note that in eq. (3.245), if we would have used $z = \delta$ as the UV cut-off, using $R = \rho L/z$, we would have had $g(\Omega - \epsilon) = \rho/\delta = 1/h(\Omega - \epsilon)$. In this case, eq. (3.245) (with an extra factor of two) would have become

$$\tilde{S}_3|_{cylinder} = \frac{4\pi L^2}{\ell_{\rm P}^2}\int_{\delta/h_0}^{H}\frac{d\rho}{\rho}\int_{h_0}^{\delta/\rho} dh\frac{\sqrt{\dot{h}^2 + h^2 + 1}}{h^2\dot{h}}, \tag{3.247}$$

precisely matching with eq. (3.14). However, choosing the new radial coordinate R to be a function of ρ (or more clearly Y) would not have been a natural UV cut-off in this case. Although we have found that for $d = 3$, the universal term in eqs. (3.246) and (3.14) match, this will not be the case in $d = 4$ which we discuss next.

For a cylinder in a CFT on $R \times S^3$, the EE is given by eq. (3.245) with $d = 4$. Now following the calculations and steps in section 3.2.1, we find that

$$\begin{aligned} S_4|_{cylinder} = \frac{4\pi^2 L^3}{\ell_{\rm P}^3}\Bigg[&\frac{L^2\sin^2\Omega}{2\,\delta^2}\log(H/\delta) + \frac{L^2\sin^2\Omega}{2\,\delta^2}\log(h_0) \\ &- \frac{\cos\Omega\,\cot\Omega}{8}\log^2(\delta/H) + \mathcal{O}(\log(\delta))\Bigg]. \end{aligned} \tag{3.248}$$

We can compare eqs. (3.248) with (3.35) and clearly see that the universal term is off by a factor of two. However, this $\log^2\delta$ contribution precisely matches with the contribution

from the trace anomaly as given in eq. (3.235). Here we can see that the new universal contribution from the singularity discussed in eq. (3.212) is not invariant under conformal transformation of coordinates. In eq. (3.245), if we had chosen the UV cut-off on $R = \rho L/z = L\, g(\theta)$ to be $z = \delta$, the upper limit of integration would have been δ/ρ, instead of δ/L. In that case, the results for the holographic EE here would have precisely matched our previous results for the cone c_1.

Here we would note that singularities appear in two places here. Of course, there is the geometric singularity in the entangling surface c_1. However, the conformal transformation taking us from the flat metric (3.237) to the cylindrical metric (3.238) is also singular at precisely the same point, *i.e.,* this transformation maps the origin in R^d to $Y \to -\infty$ in $R \times S^{d-1}$. Hence it seems this transformation is 'anomalous' in that it does not preserve the coefficient of the universal contribution to the entanglement entropy. This effect is somewhat reminiscent of the anomaly that arises in mapping a straight Wilson line in N=4 SYM to a circular Wilson loop, both in R^4. While the former has a vanishing expectation value, the expectation of the latter yields a nontrivial result [149, 150].

As a final example, we give the EE for a cylinder in $R \times S^4$. In this case, we insert $d = 5$ into eq. (3.245) and follow the steps in section 3.2.1 to find that

$$\begin{aligned} S_5|_{cylinder} \;=\; & \frac{8\pi^2 L^4}{\ell_{\rm P}^4}\left[\frac{L^3\sin^2\Omega}{3\,\delta^3}\log(H/\delta) + \frac{L^3\sin^2\Omega}{3\,\delta^3}\log(h_0) - \frac{4\,L\,\cos^2\Omega}{9\,\delta}\log(H/\delta)\right. \\ & \left. -\frac{4\,L\,\cos^2\Omega}{9\,\delta}\log(h_0) + q_5\log(\delta/H) + \mathcal{O}(\delta^0)\right], \end{aligned} \tag{3.249}$$

where q_5 precisely the same as given in eq. (3.37). Hence in comparing eqs. (3.249) and (3.36), we clearly see that the universal logarithmic term for a cylinder in $R \times S^4$ matches with that for cone c_2. However, as compared to EE for c_2 in (3.250), there are again new non-universal divergences, which take the form $\log(\delta)/\delta^3$ and $\log(\delta)/\delta$.

We conclude this section by saying that although we have studied examples in $d = 3, 4$ and 5, we expect that the $\log^2\delta$ term for cone c_{d-3} in even d is not invariant under the conformal mapping from flat space to a cylinder. However, for odd d, the $\log\delta$ term will be invariant under the corresponding conformal transformation.

3.6.2 Intermediate quantities for calculation of EE

In this section, we mention various intermediatory steps in calculation of EE.

3.6.2.1 EE for cone c_2 in $d = 5$

$$S_5\big|_{c_2} = \frac{8\,\pi^2\,L^4}{\ell_{\rm P}^4}\left[\frac{H^3\sin^2(\Omega)}{9\delta^3} - \frac{4H\cos^2(\Omega)}{9\delta} + q_5\log(\delta/H) + \mathcal{O}(\delta^0)\right], \tag{3.250}$$

where q_5 is given by (3.37). The $h(\theta)$ in (3.37) is solution of following equation of motion

$$\begin{aligned} h(1+h^2)\sin(\theta)\ddot{h} + 2\,h\,\cos(\theta)\dot{h}^3 + 2\,(2+h^2)\sin(\theta)\dot{h}^2 \\ +2\,h\,(1+h^2)\cos(\theta)\dot{h} + (4+7h^2+3h^4)\sin(\theta) \;=\; 0\,. \end{aligned} \tag{3.251}$$

3.6.2.2 EE for cone c_3 in $d = 6$

$$\begin{aligned} S_6\big|_{c_3} \;=\; & \frac{8\,\pi^3\,L^5}{\ell_{\rm P}^5}\left[\frac{H^4\sin^3(\Omega)}{16\delta^4} - \frac{27H^2\cos^2(\Omega)\sin(\Omega)}{128\delta^2}\right. \\ & +\frac{9\cos(\Omega)\cot(\Omega)(31-\cos(2\Omega))}{8192}\log\left(\delta/H\right)^2 \\ & +\left(q_6 + \frac{\sin^3(\Omega)}{4h_0^4} - \frac{27\cos^2(\Omega)\sin(\Omega)}{64h_0^2}\right. \\ & \left.\left. -\frac{9\cos(\Omega)\cot(\Omega)(31-\cos(2\Omega))\log(h_0)}{4096}\right)\log\left(\delta/H\right) \right. \\ & \left. +\mathcal{O}(\delta^0)\right], \end{aligned} \tag{3.252}$$

where q_6 is given by

$$\begin{aligned} q_6 \;=\; & \int_0^{h_0} dh\left[\frac{\sin^3(\theta)}{\dot{h}h^5}\sqrt{1+h^2+\dot{h}^2} + \frac{\sin^2(\Omega)}{h^5} - \frac{27\cos^2(\Omega)\sin(\Omega)}{32h^3}\right. \\ & \left. +\frac{9\cos(\Omega)(31-\cos(2\Omega))\cot(\Omega)}{4096h}\right]. \end{aligned} \tag{3.253}$$

3.6.2.3 EE for conical singularity $c_1 \times R^2$ in $d = 6$

For this case, the integrand in EE behaves as

$$\frac{\sin(\theta)\sqrt{1+h^2+\dot{h}^2}}{\dot{h}h^5} \sim -\frac{\sin(\Omega)}{h^5} + \frac{3\cos(\Omega)\cot(\Omega)}{32h^3} - \frac{3(13-19\cos(2\Omega))\cot^2(\Omega)\csc(\Omega)}{4096h} + \frac{\cot^2(\Omega)\csc^3(\Omega)(-375+348\cos(2\Omega)-45\cos(4\Omega)-128b_3\sin(2\Omega)+64b_3\sin(4\Omega))}{32768}h\log(h) + \mathcal{O}(h)\,, \tag{3.254}$$

near the boundary. Using this, we find that EE is given by

$$S_6\big|_{c_1\times R^2} = \frac{4\,\pi^2\,L^5h^2}{\ell_{\rm P}^5}\Bigg[\frac{H^2\sin(\Omega)}{8\delta^4} + \frac{3\cos(\Omega)\cot(\Omega)\log(\delta)}{64\delta^2} + \frac{3h_0^4(13-19\cos(2\Omega))\cot^2(\Omega)\csc(\Omega)+384h_0^2\cos(\Omega)\cot(\Omega)\,(1-2\log(h_0))-4096\sin(\Omega)}{16384h_0^2\delta^2} - \frac{1}{2\delta^2}\int_0^{h_0} dq\,q^2J_6(q) + \frac{3(13-19\cos(2\Omega))\cot^2(\Omega)\csc(\Omega)\log(\delta)}{8192H^2} + \mathcal{O}(\delta^0)\Bigg]\,, \tag{3.255}$$

where

$$J_6(h) = \left(\frac{\sin(\theta)\sqrt{1+h^2+\dot{h}^2}}{\dot{h}h^5} + \frac{\sin(\Omega)}{h^5} - \frac{3\cos(\Omega)\cot(\Omega)}{32h^3} + \frac{3(13-19\cos(2\Omega))\cot^2(\Omega)\csc(\Omega)}{4096h}\right). \tag{3.256}$$

3.6.2.4 EE for cone c_2 in CFT dual to Gauss-Bonnet gravity

For five-dimensional cone $R^+ \times S^2$ in CFT dual to the Gauss-Bonnet gravity, the entanglement entropy turns out to be

$$S_5\big|_{c_2} = \frac{8\,\pi^2\tilde{L}^4}{\ell_{\rm P}^4}\Bigg[\frac{H^3\sin^2(\Omega)\,(1-4\lambda f_\infty)}{9\delta^3} - \frac{2H\cos^2(\Omega)\,(2-7\lambda f_\infty)}{9\delta} - \left(\frac{\left(2\cos^2(\Omega)\,(2-7\lambda f_\infty)\,h_0^2-3\sin^2(\Omega)\,(1-4\lambda f_\infty)\right)}{9h_0^3} + \int_0^{h_0} dh\frac{\mathcal{L}_3}{\mathcal{L}_4}\right)\log(\delta/H) + \mathcal{O}(\delta^0)\Bigg]\,, \tag{3.257}$$

where

$$\begin{aligned}
\mathcal{L}_3 &= 3\sin^4(\theta)\left(1+h^2+\dot{h}^2\right)^2+4\lambda^2 f_\infty^2\Big(h^4\left(2+3h^2+h^4\right)\sin^4(\theta)\\
&\quad +4h^3\left(2+3h^2+h^4\right)\cos(\theta)\sin^3(\theta)\dot{h}\\
&\quad +h^2\left(4+6h^2+3h^4+\left(8+9h^2+3h^4\right)\cos(2\theta)\right)\sin^2(\theta)\dot{h}^2\\
&\quad -h\left(4-h^4-\left(4+3h^2+h^4\right)\cos(2\theta)\right)\sin(2\theta)\dot{h}^3\\
&\quad +\left(h^4\cos^4(\theta)-3h^2\cos^2(\theta)\sin^2(\theta)+6\sin^4(\theta)\right)\dot{h}^4\Big)\\
&\quad -2\lambda\sin^3(\theta)f_\infty\left(1+h^2+\dot{h}^2\right)\left(-4h\cos(\theta)\dot{h}+\sin(\theta)\left(6+5h^2+9\dot{h}^2\right)\right)\\
\mathcal{L}_4 &= 3h^4\dot{h}\sqrt{1+h^2+\dot{h}^2}\Big(\sin^2(\theta)\left(1+h^2+\dot{h}^2\right)+2\lambda f_\infty\Big(\left(2+3h^2+h^4\right)\sin^2(\theta)\\
&\quad +h\left(2+h^2\right)\sin(2\theta)\dot{h}+\left(h^2\cos^2(\theta)-\sin^2(\theta)\right)\dot{h}^2\Big)\Big). \qquad (3.258)
\end{aligned}$$

3.6.2.5 EE for cone c_3 in CFT dual to Gauss-Bonnet gravity

For cone $R^+\times S^3$ in $d=6$ dimensional CFT, which is dual to Gauss-Bonnet gravity, the EE is given by

$$\begin{aligned}
S_6\big|_{c_3} &= \frac{4\pi^3\tilde{L}^5}{\ell_{\rm P}^5}\Bigg[\frac{H^4\sin^3(\Omega)\left(3-10\lambda f_\infty\right)}{48\delta^4}-\frac{H^2\cos^2(\Omega)\sin(\Omega)\left(27-86\lambda f_\infty\right)}{128\delta^2}\\
&\quad +\frac{3\cos(\Omega)\cot(\Omega)\left(\left(93-190\lambda f_\infty\right)-\left(3-2\lambda f_\infty\right)\cos(2\Omega)\right)}{8192}\log(\delta/H)^2\\
&\quad +\frac{1}{12288h_0^4}\Big[-27h_0^4\cos(\Omega)(31-\cos(2\Omega))\cot(\Omega)\log\left(h_0\right)-5184h_0^2\cos^2(\Omega)\sin(\Omega)\\
&\quad +3072\sin^3(\Omega)-2\lambda f_\infty\Big(9h_0^4\cos(\Omega)(-95+\cos(2\Omega))\cot(\Omega)\log\left(h_0\right) \qquad (3.259)\\
&\quad -8256h_0^2\cos^2(\Omega)\sin(\Omega)+5120\sin^3(\Omega)\Big)+\int_0^{h_0}dh\left(\mathcal{L}_5-\mathcal{L}_5'\right)\Big]\log(\delta/H)\\
&\quad +\mathcal{O}(\delta^0)\Bigg].
\end{aligned}$$

Here $\mathcal{L}_5$ and $\mathcal{L}'_5$ are terms which come from making the h integrand in original expression of EE finite and these are given by

$$\mathcal{L}_5 = \frac{\mathcal{L}_{5N}}{\mathcal{L}_{5D}} \quad \text{with} \tag{3.260}$$

$$\begin{aligned}
\mathcal{L}_{5N} &= \sin\theta \Bigg[12\,\lambda^2 f_\infty^2 h^8 \sin^4\theta + 48\,\lambda^2 f_\infty^2 \cos\theta\, h^7 \sin^3\theta\, \dot{h} \\
&\quad +24\,\lambda f_\infty \cos\theta\, \sin^3\theta\, h\, \dot{h} \Big(1 + (1 - 5\lambda f_\infty)\, \dot{h}^2\Big) \\
&\quad +6\,\lambda\, f_\infty h^5 \sin(2\theta)\, \dot{h} \Big(\sin^2\theta + 2\,\lambda\, f_\infty \Big(5\, \sin^2\theta + 2\cos^2\theta\, \dot{h}^2\Big)\Big) \\
&\quad +\lambda\, f_\infty h^3 \sin^2\theta\, \dot{h} \Big(6\sin^2\theta\,(3 + \dot{h}^2) + 2\,\lambda\, f_\infty \Big(18\, \sin^2\theta - (1 + 17\cos(2\theta))\dot{h}^2\Big)\Big) \\
&\quad +2\,\lambda\, f_\infty h^6 \Big(3\, \sin^4\theta + \lambda\, f_\infty \Big(14\, \sin^4\theta + 9\, \sin^2(2\theta)\, \dot{h}^2\Big)\Big) \\
&\quad +2\, \sin^4\theta\, \Big(20\lambda^2 f_\infty^2 \dot{h}^4 + 3\,(1 + \dot{h}^2)^2 - 8\,\lambda\, f_\infty (1 + 3\,\dot{h}^2 + 2\,\dot{h}^4)\Big) \\
&\quad +h^2 \sin^2\theta \Big(12\, \sin^2\theta\,(1 + \dot{h}^2) + 4\,\lambda^2 f_\infty^2 \dot{h}^2 \big(7 + 17\, \cos(2\theta) - 9\, \cos^2\theta\, \dot{h}^2\big) \\
&\quad -\lambda\, f_\infty \Big(24\, \sin^2\theta + (17 - 23\, \cos(2\theta))\dot{h}^2 + 6\, \cos^2\theta\, \dot{h}^4\Big)\Big) \\
&\quad +h^4 \Big(6\, \sin^4\theta + \lambda\, f_\infty \sin^2\theta\, \big(1 + \cos(2\theta) + 6\dot{h}^2\big) \\
&\quad +4\,\lambda^2 f_\infty^2 \big(4\, \sin^4\theta + 3\,(5 + 8\cos(2\theta))\sin^2\theta\, \dot{h}^2 + 3\, \cos^4\theta\, \dot{h}^4\big)\Big)\Bigg],
\end{aligned}$$

$$\begin{aligned}
\mathcal{L}_{5D} &= 6\, h^5 \dot{h} \sqrt{1 + h^2 + \dot{h}^2} \Big(3\,\lambda\, f_\infty h^4 \sin^2\theta + 9\,\lambda\, f_\infty \cos\theta\, \sin\theta\, h\, \dot{h} + 6\,\lambda\, f_\infty \cos\theta\, \sin\theta\, h^3 \dot{h} \\
&\quad + \sin^2\theta \Big(1 + \dot{h}^2 + 2\,\lambda\, f_\infty \big(2 - \dot{h}^2\big)\Big) + h^2 \Big(\sin^2\theta + \lambda f_\infty \Big(7\, \sin^2\theta + 3\, \cos^2\theta\, \dot{h}^2\Big)\Big)\Big)
\end{aligned}$$

and

$$\begin{aligned}
\mathcal{L}'_5 &= -\frac{\sin^3\Omega\, (3 - 10\lambda\, f_\infty)}{3\, h^5} + \frac{\cos^2\Omega\, \sin\Omega\, (27 - 86\lambda f_\infty)}{32 h^3} \\
&\quad -\frac{3\cos\Omega\, \cot\Omega\, (93 - 3\cos(2\Omega) + 2\,\lambda\,(-95 + \cos(2\Omega)) f_\infty)}{4096\, h}\,.
\end{aligned} \tag{3.261}$$

Note that in the asymptotic limit, $h \to 0$ and $\mathcal{L}_5 = \mathcal{L}'_5 + \mathcal{O}(h)$.

3.6.2.6 EE for $k \times S^2$ in CFT dual to Gauss-Bonnet gravity

The values of $\hat{\mathcal{L}}$'s in eqn. (3.221) are following:

$$
\begin{aligned}
\hat{\mathcal{L}}_0 &= \frac{1}{h^2\sqrt{1+h^2+\dot{h}^2}\left(\left(1-2f_\infty\lambda\right)\dot{h}^2+\left(1-2f_\infty\lambda\right)h^2+4f_\infty\lambda+1\right)} \\
&\quad\times\Big[\left(1-6f_\infty\lambda+8f_\infty^2\lambda^2\right)\dot{h}^4+2\left(1-5f_\infty\lambda+\left(1-6f_\infty\lambda+8f_\infty^2\lambda^2\right)h^2\right)\dot{h}^2 \\
&\quad+\left(1-6f_\infty\lambda+8f_\infty^2\lambda^2\right)h^4+\left(2-10f_\infty\lambda\right)h^2-4f_\infty\lambda+1\Big], \\
\hat{\mathcal{L}}_N &= \frac{2f_\infty\lambda\sqrt{1+h^2+\dot{h}^2}}{3h^2} \\
\hat{\mathcal{L}}_f &= \frac{-1}{72h^2\left(1+h^2\right)\left(1+h^2+\dot{h}^2\right)^{3/2}\left(\left(1-2f_\infty\lambda\right)\dot{h}^2+\left(1-2f_\infty\lambda\right)h^2+4f_\infty\lambda+1\right)} \\
&\quad\times\Big[5\left(3-10f_\infty\lambda+8f_\infty^2\lambda^2\right)\left(1+h^2\right)\dot{h}^6+\Big(42-26f_\infty\lambda-56f_\infty^2\lambda^2 \\
&\quad+3\left(29-80f_\infty\lambda+64f_\infty^2\lambda^2\right)h^2+15\left(3-10f_\infty\lambda+8f_\infty^2\lambda^2\right)h^4\Big)\dot{h}^4 \\
&\quad+\Big(39+8f_\infty\lambda+48f_\infty^2\lambda^2+\left(123-172f_\infty\lambda+64f_\infty^2\lambda^2\right)h^2 \\
&\quad+3\left(43-110f_\infty\lambda+88f_\infty^2\lambda^2\right)h^4+15\left(3-10f_\infty\lambda+8f_\infty^2\lambda^2\right)h^6\Big)\dot{h}^2 \\
&\quad+5\left(3-10f_\infty\lambda+8f_\infty^2\lambda^2\right)h^8+\left(57-140f_\infty\lambda+112f_\infty^2\lambda^2\right)h^6 \\
&\quad+\left(81-146f_\infty\lambda+120f_\infty^2\lambda^2\right)h^4+\left(51-72f_\infty\lambda+48f_\infty^2\lambda^2\right)h^2-16f_\infty\lambda+12\Big] \\
\hat{\mathcal{L}}_B &= z\left(-\mathcal{L}_2'\rho+\mathcal{L}_3\dot{\rho}-\dot{\mathcal{L}}_3\rho+\mathcal{L}_5\rho\right) \qquad (3.262) \\
&= -\frac{2f_\infty\lambda h\dot{g}_3+2f_\infty\lambda h^3\dot{g}_3+\left(1-2f_\infty\lambda\right)g_3h^2\dot{h}+g_3\dot{h}\left(1+6f_\infty\lambda+\left(1-4f_\infty\lambda\right)\dot{h}^2\right)}{\left(1+h^2+\dot{h}^2\right)^{3/2}}.
\end{aligned}
$$

Chapter 4

Conclusion

The AdS/CFT correspondence has provided a remarkable tool to study various properties of the strongly coupled field theories in the large N limit. Over the years, there has been efforts to make this duality more precise and find the exact gauge/gravity dictionary. In this context, the proposal by Ryu and Takayanagi [16] has provided us with an elegant tool to calculate entanglement entropy in strongly coupled field theories. As discussed in section 1.3.4, this proposal has been tested extensively on various known results and explicit proofs are also given for certain cases [57, 59]. Now using these holographic ideas, we have studied some interesting features of entanglement entropy in quantum field theory.

In chapter 2, we have constructed a UV regulator independent c-function (2.25) from the entanglement entropy for strip geometry in arbitrary dimensions. In [80, 81], the c-function (2.22) was considered for two dimensional field theories and our c-function is its simple extension to higher dimensions. As discussed in section 2.2, although the EE for a strip is UV divergent, our c-function (2.25) is finite and at the conformal fixed points, yields the central charge that characterizes the underlying CFT. In section 2.3, we have examined the behaviour of this c-function in holographic RG flows, in which the bulk theory is described by Einstein gravity. Here, we show that our c-function flows monotonically if the matter field driving the RG flow satisfies the null energy condition. Recall that this condition is precisely the constraint that appears in the standard derivation of the holographic c-theorem [84, 85, 86, 87, 88].

We also observe that if the null energy condition is violated over a 'very small' radial regime, the integral in eqs. (2.54) or (2.63) would remain positive and hence the flow of our c-function would still be monotonic. So our c-function requires the null energy condition to be satisfied only in an averaged sense. Hence the null energy condition is a sufficient

but not a necessary condition for the monotonic flow of the c-function (2.25).

To show the monotonic flow of c-function in section 2.3, we make use of the derivative dc_d/dr_m, *i.e.,* changes in c_d as we change the minimum energy scale probed by the entanglement entropy. However, to establish the monotonic flow of the c-function completely in boundary theory, one needs to prove that $dc_d/d\ell \leq 0$, *i.e.,* the c-function decreases monotonically as we increase the width of the strip for which the entanglement entropy is evaluated. This result can be established in the holographic framework. However, as discussed in section 2.4, one must be careful to restrict attention to the physical saddle points in evaluating the entanglement entropy. There we showed that in calculation of EE, extremal surfaces can arise for which $d\ell/dr_m > 0$ and hence $dc_d/d\ell > 0$. However, these saddle points should be discarded when one evaluates the holographic entanglement entropy with eq. (1.56) since they are not the minimum area surface. In fact, the appearance of these 'unstable' saddle points introduce a first order 'phase transition' in the entanglement entropy. As a result, the c-function c_d drops discontinuously at some critical value ℓ_t of the width of the strip and the monotonic behavior of the c-function is preserved along the flow.

Further, in section 2.4 and section 2.7.3, we have discussed the phase transitions in more detail to convince ourselves that these are not an artifact of choosing background geometry in the bulk which is unphysical in some way. We have argued that such phase transitions can arise in holographic backgrounds which have a natural interpretation as an RG flow in the boundary theory. Although we have shown this interpretation explicitly in examples of phase transitions with the boundary dimension $d \geq 3$, we expect the results to extend to $d = 2$.

In section 2.5, we studied the c-function (2.25) in holographic models where the gravitational theory in the bulk is Gauss-Bonnet gravity (2.10). In this case, it is straightforward to construct an expression (2.112) for dc_d/dr_m in GB gravity, where it is evident that the null energy condition is not sufficient to guarantee a monotonic flow of the c-function. Unfortunately, eq. (2.112) can not be expressed as a simple statement of the conditions that are necessary to ensure the monotonic flow of the c-function along holographic RG in these models. As discussed in section 2.6, further insight into the behavior of c-function (2.25) may be provided by examining explicit holographic RG flows in Gauss-Bonnet gravity. In particular, it would be interesting to see if there are violations of the monotonic flow of the c-function in certain RG flows.

It may not be a surprise that the monotonic flow of the c-function (2.25) is not ensured by the null energy condition in GB gravity. As reviewed in section 2.1, an important feature of this theory is that at conformal fixed points, the dual boundary theory has two

distinct central charges, given by eqs. (2.14) and (2.15). Using the null energy condition, ref. [87, 88] established that the charge denoted a_d^* would satisfy a c-theorem in these holographic models. However, in section 2.2, we found that the c-function (2.25) actually corresponds to a nonlinear combination of both central charges. Hence it will not be reasonable to expect that a simple holographic c-theorem could be established for GB gravity with the present construction.

Recently, in four dimensional field theories, it has been showed that the central charge a_d^* given by (2.15) satisfies a c-theorem [87, 88]. Through study of holographic entanglement, it is also known that this central charge appears as the universal term in EE for spherical entangling surface [52]. Hence, it will be interesting to see if one can construct a finite c-function from the EE of spheres and determine if it satisfies a consistent c-theorem. Given the generalised form of EE in (1.53), a 'refined entanglement entropy' is defined for arbitrary dimensions in [46]. Similar to our c-function (2.25), this refined EE contains derivatives with respect to macroscopic scale of the entangling surfaces and is independent of UV regulator for specific scalable entangling surfaces. Further, it was proposed [46], and later proved in [145], that in $d = 3$ dimensional field theories, this refined EE for sphere flows monotonically along the RG flows. However, in $d = 4$ dimensional field theories, a counter example is given which shows that refined EE for sphere does not behave monotonically [46]. Now, it will be interesting to study the refined EE in detail along the line of chapter 2. It still remains to be understood if the flow of refined EE for a sphere in $d = 3$ field theories is related to the null energy condition in the holographic RG flows. Further, using holography, it will be interesting to understand why in $d = 4$, the refined EE for sphere does not flow monotonically.

As we have seen in chapter 2 and in the original studies on c-theorems [84, 85, 86, 87, 88], the null energy condition in the bulk gravity is a very useful condition. In the bulk gravity, although it refers to the stability of the system, its precise interpretation on the field theory side is still unknown. Further, the Cardy's conjecture has been proved in $d = 4$ dimensional field theories [42], however the key ideas in this proof don't extend to $d = 6$ [151]. So even if Cardy's conjecture is true in all the even dimensions, a generalized proof behind these theorems, which extends in all the even dimensions, is still elusive. Given the significant progress in holography on c-theorems, now it might be very useful to find the precise gauge-gravity dictionary for the null energy condition in the bulk. If we can understand the precise interpretation in the boundary field theory of the null energy condition in the bulk, it might help to extend the proof of c-theorems in other dimensions.

In chapter 3, we have used holography to study EE for various singular entangling surfaces in higher dimensions. In particular in section 3.2, we calculated EE for cones in various dimensions. For $d = 5$, we find that a new universal contribution (3.36), which is

linear in logarithm, appears. It is further shown in (3.38) that similar to a kink in $d = 3$, the universal term goes like $1/\Omega$ for $\Omega \to 0$, where Ω is the opening angle of the cone as shown in fig. 3.1. Now it is expected that this behavior extends to higher dimensions where a cone $c_{d-3} = R^+ \times S^{d-3}$ in any odd d acquire a universal contribution of the form (3.231). In section 3.2.1, we have also studied the EE for cones in $d = 4$ and 6. Here we found that a cone yields a universal contribution of the form (3.232), which is quadratic in logarithm. Again, we believe that this is a generic result for even-dimensional field theories. For even dimensions, as shown in eqs. (3.34) and (3.39), now the coefficient has relatively simple expression. Also, similar to odd dimensions, for small opening angle Ω, the coefficient goes as $1/\Omega$.

Further, in section 3.4.1, we calculate EE for cones in Gauss-Bonnet gravity. There, we were able to verify that the universal term in EE for a cone in $d = 4$, which is given by (3.212), is proportional to the central charge (3.196) which controls the leading singularity of the two-point function of the stress tensor. For $d = 5$, we learn from (3.213) that the universal term is a non-linear function of the central charges. However, for a cone in $d = 6$, once again the universal term (3.215) is linear in central charges (3.196) and (3.197).

In section 3.5, we also discussed that for cones in even dimensional field theories, there are also contributions proportional to a single power of $\log \delta/L$. However, these terms are no longer universal. In fact, this logarithmic contribution depends on the way the singularity of the cone is regularized in calculation of holographic entanglement entropy. Now note that the trace anomaly in an even-dimensional CFT produce a universal contribution in the entanglement entropy with a smooth entangling surface [52, 51, 143, 87]. For $d = 4$, we find that the contribution of trace anomaly (3.235) in the universal term for the cone is only half of (3.212). Hence, we expect that part of the $\log^2(\delta/L)$ divergence is associated with correlations across the smooth part of the entangling surface away from the singularity. However, another part of this universal contribution should be intrinsic to the singularity at the tip of the cone itself.

Now an interesting observation here is that the universal term (3.212) for a cone in $d = 4$ and the contribution from the trace anomaly (3.235) have the same Ω dependence apart from a factor of two, where Ω is the opening angle for cone. As we yet do not know the geometric structure of contribution of a conical singularity in universal term, it will be interesting to know if the contribution of the singularity and of trace anomaly are actually the same apart from an overall constant factor. For that, it will be interesting to calculate universal term in holographic EE for a singular entangling surface of the form $R^+ \times \Sigma^{d-3}$, where Σ^{d-3} is a geometry which is topologically equivalent to a sphere S^{d-3}, and compare it with the contribution from the trace anomaly.

Further in section 3.3, we extended our holographic analysis to consider creases or extended singularities. Using our results summarized table 3.1, we find that the crease of the form $k \times R^m$ or $c_n \times R^m$ creates no new universal contributions. However, in general, we found that creases can contribute additional universal terms, but singular locus must be curved and have an even dimension. These results suggest that these new universal contributions to the entanglement entropy take the form given in eq. (3.11) with a $\log \delta$ divergence in odd dimensions and $\log^2 \delta$ in even dimensions. These results indicate that there is a rich variety of new geometric contributions to entanglement entropy that can be associated with singular entangling surfaces. However, our analysis in this thesis is not sufficient to reveal the full geometric structure of these universal terms. It would be interesting to consider more general singularities, *e.g.,* a crease of the form $k \times R^1$ but where the opening angle varies along R^1 or where R^1 was not entirely straight. Another direction to understand these geometric coefficients is to do holographic calculations using the Fefferman-Grahm expansion [95, 96] to compute entanglement entropy along the lines discussed in [47].

Finally, it will be interesting to study these new universal terms for entanglement entropy in non-holographic theories. One might also consider heat kernel methods for free field theories for simple surfaces, *e.g.,* along the lines of [141, 146]. Some results [147] that non-holographic models do produce a $\log^2 \delta$ term in EE for conical singularity have already emerged. Further, it would also be interesting to investigate the Renyi entropy for the singular entangling surfaces [114].

Permissions

Gmail by Google

Ajay Singh <sajay.1729@gmail.com>

Permission to use our papers in my thesis

Rob Myers <rmyers@perimeterinstitute.ca> Sat, Jun 9, 2012 at 6:11 AM
To: Ajay Singh <sajay.1729@gmail.com>

yes, of course. rob

On Sat, Jun 9, 2012 at 2:12 AM, Ajay Singh <sajay.1729@gmail.com> wrote:

> Hi Rob,
>
> Can I request your permission to use the following papers written with
> you in my Ph.D. thesis:
>
> 1. R. C. Myers and A. Singh, "Comments on Holographic Entanglement
> Entropy and RG Flows," JHEP 1204, 122 (2012) [arXiv:1202.2068
> [hep-th]].
> 2. R. C. Myers and A. Singh, "Entanglement Entropy for Singular Surfaces".
>
> Thanks,
>
> --
> Ajay Singh,
> Graduate Student,
> Perimeter Institute for Theoretical Physics,
> 31 Caroline St. N., Waterloo
> Ontario, Canada
> N2L 2Y5

Ajay Singh <sajay.1729@gmail.com>

Permission request to use paper in my Ph.D. thesis

JHEP Editorial Office <jhep-eo@jhep.sissa.it> Mon, Jun 11, 2012 at 5:53 AM
Reply-To: jhep-eo@jhep.sissa.it
To: Ajay Singh <sajay.1729@gmail.com>
Cc: JHEP Editorial Office <jhep-eo@jhep.sissa.it>

Dear Dr. Singh,

Thank you for your message.

According to JHEP policy authors are granted a personal license to use all or part of their work in personal compilations or other publications of the author's own works, provided that this is for non-commercial use.

In this specific case, we would like to confirm that the permission is granted.

Should you need further information please do not hesitate to contact us.

Best regards,
Cristiana Prever
JHEP Editorial Office

On 06/09/2012 08:19 AM, Ajay Singh wrote:

> Dear Publisher,
>
> I am writing you to request your permission to include following paper in my Ph.D. thesis, which I co-authored and published in JHEP:
>
> 1. R. C. Myers and A. Singh, "Comments on Holographic Entanglement Entropy and RG Flows," JHEP 1204, 122 (2012) [arXiv:1202.2068 [hep-th]].
>
> Please note that with my thesis, I will be signing a Theses Non-Exclusive License that authorizes Library and Archives Canada to reproduce, communicate to the public on the Internet, loan, distribute or sell copies of my thesis, among other things.
>
> Thanking you,

Bibliography

[1] **DELPHI** Collaboration, K. Doroba, "Precision test of electroweak interactions: What we have learned from LEP and SLC?," *Acta Phys.Polon.* **B35** (2004) 1173–1189.

[2] T. Cheng and L. Li, *Gauge Theory of Elementry Particle Physics*. Oxford University Press, USA, 1988.

[3] M. E. Peskin and D. V. Schroeder, *An Introduction to Quantum Field Theory*. Westviewer Press, 1995.

[4] I. R. J. Aitchison and A. J. G. Hey, *Gauge Theories in Particle Physics, Vol.-1,2*. IoP, Bristol, 2004.

[5] P. T. Chrusciel, "Black holes," *Lect.Notes Phys.* **604** (2002) 61–102, arXiv:gr-qc/0201053 [gr-qc].

[6] S. Hawking, "Particle Creation by Black Holes," *Commun.Math.Phys.* **43** (1975) 199–220.

[7] J. D. Bekenstein, "Black holes and entropy," *Phys.Rev.* **D7** (1973) 2333–2346.

[8] L. Bombelli, R. K. Koul, J. Lee, and R. D. Sorkin, "A Quantum Source of Entropy for Black Holes," *Phys.Rev.* **D34** (1986) 373–383.

[9] M. Srednicki, "Entropy and area," *Phys.Rev.Lett.* **71** (1993) 666–669, arXiv:hep-th/9303048 [hep-th].

[10] G. 't Hooft, "On the Quantum Structure of a Black Hole," *Nucl.Phys.* **B256** (1985) 727.

[11] J. Callan, Curtis G. and F. Wilczek, "On geometric entropy," *Phys.Lett.* **B333** (1994) 55–61, arXiv:hep-th/9401072 [hep-th].

[12] J. Polchinski, "String theory. Vol. 1: An introduction to the bosonic string,".

[13] J. Polchinski, "String theory. Vol. 2: Superstring theory and beyond,".

[14] R. J. Szabo, "BUSSTEPP lectures on string theory: An Introduction to string theory and D-brane dynamics," arXiv:hep-th/0207142 [hep-th].

[15] C. V. Johnson, "D-brane primer," arXiv:hep-th/0007170 [hep-th].

[16] S. Ryu and T. Takayanagi, "Holographic derivation of entanglement entropy from AdS/CFT," *Phys.Rev.Lett.* **96** (2006) 181602, arXiv:hep-th/0603001 [hep-th].

[17] A. M. Polyakov, "Quantum Geometry of Bosonic Strings," *Phys.Lett.* **B103** (1981) 207–210.

[18] J. Callan, Curtis G., E. Martinec, M. Perry, and D. Friedan, "Strings in Background Fields," *Nucl.Phys.* **B262** (1985) 593.

[19] J. Callan, Curtis G., I. R. Klebanov, and M. Perry, "String Theory Effective Actions," *Nucl.Phys.* **B278** (1986) 78.

[20] F. Gliozzi, J. Scherk, and D. I. Olive, "Supersymmetry, Supergravity Theories and the Dual Spinor Model," *Nucl.Phys.* **B122** (1977) 253–290.

[21] A. Strominger and C. Vafa, "Microscopic origin of the Bekenstein-Hawking entropy," *Phys.Lett.* **B379** (1996) 99–104, arXiv:hep-th/9601029 [hep-th].

[22] J. M. Maldacena, "The Large N limit of superconformal field theories and supergravity," *Adv.Theor.Math.Phys.* **2** (1998) 231–252, arXiv:hep-th/9711200 [hep-th].

[23] P. Breitenlohner and D. Z. Freedman, "Positive Energy in anti-De Sitter Backgrounds and Gauged Extended Supergravity," *Phys.Lett.* **B115** (1982) 197.

[24] P. Breitenlohner and D. Z. Freedman, "Stability in Gauged Extended Supergravity," *Annals Phys.* **144** (1982) 249.

[25] L. Mezincescu and P. Townsend, "Stability At A Local Maximum In Higher Dimensional Anti-de Sitter Space And Applications To Supergravity," *Annals Phys.* **160** (1985) 406.

[26] O. Aharony, S. S. Gubser, J. M. Maldacena, H. Ooguri, and Y. Oz, "Large N field theories, string theory and gravity," *Phys.Rept.* **323** (2000) 183–386, arXiv:hep-th/9905111 [hep-th].

[27] J. L. Petersen, "Introduction to the Maldacena conjecture on AdS/CFT," *Int.J.Mod.Phys.* **A14** (1999) 3597–3672, arXiv:hep-th/9902131 [hep-th].

[28] K. Skenderis and P. K. Townsend, "Gravitational stability and renormalization group flow," *Phys.Lett.* **B468** (1999) 46–51, arXiv:hep-th/9909070 [hep-th].

[29] O. DeWolfe, D. Freedman, S. Gubser, and A. Karch, "Modeling the fifth-dimension with scalars and gravity," *Phys.Rev.* **D62** (2000) 046008, arXiv:hep-th/9909134 [hep-th].

[30] E. Witten, "Anti-de Sitter space and holography," *Adv.Theor.Math.Phys.* **2** (1998) 253–291, arXiv:hep-th/9802150 [hep-th].

[31] I. R. Klebanov and E. Witten, "AdS/CFT correspondence and symmetry breaking," *Nucl.Phys.* **B556** (1999) 89–114, arXiv:hep-th/9905104 [hep-th].

[32] M. Duff, "Observations on Conformal Anomalies," *Nucl.Phys.* **B125** (1977) 334.

[33] M. Duff, "Twenty years of the Weyl anomaly," *Class.Quant.Grav.* **11** (1994) 1387–1404, arXiv:hep-th/9308075 [hep-th].

[34] S. Deser and A. Schwimmer, "Geometric classification of conformal anomalies in arbitrary dimensions," *Phys.Lett.* **B309** (1993) 279–284, arXiv:hep-th/9302047 [hep-th].

[35] A. Zamolodchikov, "Irreversibility of the Flux of the Renormalization Group in a 2D Field Theory," *JETP Lett.* **43** (1986) 730–732.

[36] J. L. Cardy, "Is There a c Theorem in Four-Dimensions?," *Phys.Lett.* **B215** (1988) 749–752.

[37] H. Osborn, "Derivation of a Four-Dimensional c Theorem," *Phys.Lett.* **B222** (1989) 97.

[38] D. Anselmi, D. Freedman, M. T. Grisaru, and A. Johansen, "Nonperturbative formulas for central functions of supersymmetric gauge theories," *Nucl.Phys.* **B526** (1998) 543–571, arXiv:hep-th/9708042 [hep-th].

[39] D. Anselmi, J. Erlich, D. Freedman, and A. Johansen, "Positivity constraints on anomalies in supersymmetric gauge theories," *Phys.Rev.* **D57** (1998) 7570–7588, arXiv:hep-th/9711035 [hep-th].

[40] K. A. Intriligator and B. Wecht, "The Exact superconformal R symmetry maximizes a," *Nucl.Phys.* **B667** (2003) 183–200, arXiv:hep-th/0304128 [hep-th].

[41] E. Barnes, K. A. Intriligator, B. Wecht, and J. Wright, "Evidence for the strongest version of the 4d a-theorem, via a-maximization along RG flows," *Nucl.Phys.* **B702** (2004) 131–162, arXiv:hep-th/0408156 [hep-th].

[42] Z. Komargodski and A. Schwimmer, "On Renormalization Group Flows in Four Dimensions," *JHEP* **1112** (2011) 099, arXiv:1107.3987 [hep-th].

[43] Z. Komargodski, "The Constraints of Conformal Symmetry on RG Flows," arXiv:1112.4538 [hep-th].

[44] A. Schwimmer and S. Theisen, "Spontaneous Breaking of Conformal Invariance and Trace Anomaly Matching," *Nucl.Phys.* **B847** (2011) 590–611, arXiv:1011.0696 [hep-th].

[45] A. Adams, N. Arkani-Hamed, S. Dubovsky, A. Nicolis, and R. Rattazzi, "Causality, analyticity and an IR obstruction to UV completion," *JHEP* **0610** (2006) 014, arXiv:hep-th/0602178 [hep-th].

[46] H. Liu and M. Mezei, "A Refinement of entanglement entropy and the number of degrees of freedom," arXiv:1202.2070 [hep-th].

[47] L.-Y. Hung, R. C. Myers, and M. Smolkin, "Some Calculable Contributions to Holographic Entanglement Entropy," *JHEP* **1108** (2011) 039, arXiv:1105.6055 [hep-th].

[48] L.-Y. Hung, R. C. Myers, and M. Smolkin, "On Holographic Entanglement Entropy and Higher Curvature Gravity," *JHEP* **1104** (2011) 025, arXiv:1101.5813 [hep-th].

[49] D. V. Fursaev and S. N. Solodukhin, "On one loop renormalization of black hole entropy," *Phys.Lett.* **B365** (1996) 51–55, arXiv:hep-th/9412020 [hep-th].

[50] D. V. Fursaev and S. N. Solodukhin, "On the description of the Riemannian geometry in the presence of conical defects," *Phys.Rev.* **D52** (1995) 2133–2143, arXiv:hep-th/9501127 [hep-th].

[51] S. N. Solodukhin, "Entanglement entropy, conformal invariance and extrinsic geometry," *Phys.Lett.* **B665** (2008) 305–309, arXiv:0802.3117 [hep-th].

[52] S. Ryu and T. Takayanagi, "Aspects of Holographic Entanglement Entropy," *JHEP* **0608** (2006) 045, arXiv:hep-th/0605073 [hep-th].

[53] M. Headrick and T. Takayanagi, "A Holographic proof of the strong subadditivity of entanglement entropy," *Phys.Rev.* **D76** (2007) 106013, arXiv:0704.3719 [hep-th].

[54] T. Hirata and T. Takayanagi, "AdS/CFT and strong subadditivity of entanglement entropy," *JHEP* **0702** (2007) 042, arXiv:hep-th/0608213 [hep-th].

[55] P. Calabrese and J. L. Cardy, "Entanglement entropy and quantum field theory," *J.Stat.Mech.* **0406** (2004) P06002, arXiv:hep-th/0405152 [hep-th].

[56] G. Vidal, J. Latorre, E. Rico, and A. Kitaev, "Entanglement in quantum critical phenomena," *Phys.Rev.Lett.* **90** (2003) 227902, arXiv:quant-ph/0211074 [quant-ph].

[57] D. V. Fursaev, "Proof of the holographic formula for entanglement entropy," *JHEP* **0609** (2006) 018, arXiv:hep-th/0606184 [hep-th].

[58] M. Headrick, "Entanglement Renyi entropies in holographic theories," *Phys.Rev.* **D82** (2010) 126010, arXiv:1006.0047 [hep-th].

[59] H. Casini, M. Huerta, and R. C. Myers, "Towards a derivation of holographic entanglement entropy," *JHEP* **1105** (2011) 036, arXiv:1102.0440 [hep-th].

[60] D. Lovelock, "The Einstein tensor and its generalizations," *J.Math.Phys.* **12** (1971) 498–501.

[61] D. Lovelock, "Divergence-free tensorial concomitants," *Aequationes Mathematicae* **4** (1970) 127–138.

[62] J. de Boer, M. Kulaxizi, and A. Parnachev, "Holographic Entanglement Entropy in Lovelock Gravities," *JHEP* **1107** (2011) 109, arXiv:1101.5781 [hep-th].

[63] R. M. Wald, "Black hole entropy is the Noether charge," *Phys.Rev.* **D48** (1993) 3427–3431, arXiv:gr-qc/9307038 [gr-qc].

[64] V. Iyer and R. M. Wald, "Some properties of Noether charge and a proposal for dynamical black hole entropy," *Phys.Rev.* **D50** (1994) 846–864, arXiv:gr-qc/9403028 [gr-qc].

[65] T. Jacobson, G. Kang, and R. C. Myers, "On black hole entropy," *Phys.Rev.* **D49** (1994) 6587–6598, arXiv:gr-qc/9312023 [gr-qc].

[66] T. Jacobson, G. Kang, and R. C. Myers, "Black hole entropy in higher curvature gravity," arXiv:gr-qc/9502009 [gr-qc].

[67] M. Levin and X.-G. Wen, "Detecting Topological Order in a Ground State Wave Function," *Phys.Rev.Lett.* **96** (2006) 110405.

[68] A. Kitaev and J. Preskill, "Topological entanglement entropy," *Phys.Rev.Lett.* **96** (2006) 110404, arXiv:hep-th/0510092 [hep-th].

[69] B. Hsu, M. Mulligan, E. Fradkin, and E.-A. Kim, "Universal entanglement entropy in 2D conformal quantum critical points," *Physical Review B* (2008) , arXiv:0812.0203 [cond-mat.stat-mech].

[70] I. R. Klebanov, D. Kutasov, and A. Murugan, "Entanglement as a probe of confinement," *Nucl.Phys.* **B796** (2008) 274–293, arXiv:0709.2140 [hep-th].

[71] T. Nishioka and T. Takayanagi, "AdS Bubbles, Entropy and Closed String Tachyons," *JHEP* **0701** (2007) 090, arXiv:hep-th/0611035 [hep-th].

[72] N. Ogawa and T. Takayanagi, "Higher Derivative Corrections to Holographic Entanglement Entropy for AdS Solitons," *JHEP* **1110** (2011) 147, arXiv:1107.4363 [hep-th].

[73] A. Lewkowycz, "Holographic Entanglement Entropy and Confinement," *JHEP* **1205** (2012) 032, arXiv:1204.0588 [hep-th].

[74] M. Van Raamsdonk, "Comments on quantum gravity and entanglement," arXiv:0907.2939 [hep-th].

[75] M. Van Raamsdonk, "Building up spacetime with quantum entanglement," *Gen.Rel.Grav.* **42** (2010) 2323–2329, arXiv:1005.3035 [hep-th].

[76] V. E. Hubeny and M. Rangamani, "Causal Holographic Information," arXiv:1204.1698 [hep-th].

[77] B. Czech, J. L. Karczmarek, F. Nogueira, and M. Van Raamsdonk, "The Gravity Dual of a Density Matrix," arXiv:1204.1330 [hep-th].

[78] H. Casini and M. Huerta, "Universal terms for the entanglement entropy in 2+1 dimensions," *Nucl.Phys.* **B764** (2007) 183–201, arXiv:hep-th/0606256 [hep-th].

[79] E. Fradkin and J. E. Moore, "Entanglement entropy of 2D conformal quantum critical points: hearing the shape of a quantum drum," *Phys.Rev.Lett.* **97** (2006) 050404, arXiv:cond-mat/0605683 [cond-mat.str-el].

[80] H. Casini and M. Huerta, "A Finite entanglement entropy and the c-theorem," *Phys.Lett.* **B600** (2004) 142–150, arXiv:hep-th/0405111 [hep-th].

[81] H. Casini and M. Huerta, "A c-theorem for the entanglement entropy," *J.Phys.A* **A40** (2007) 7031–7036, arXiv:cond-mat/0610375 [cond-mat].

[82] P. Calabrese and J. L. Cardy, "Entanglement entropy and quantum field theory: A Non-technical introduction," *Int.J.Quant.Inf.* **4** (2006) 429, arXiv:quant-ph/0505193 [quant-ph].

[83] P. Calabrese and J. Cardy, "Entanglement entropy and conformal field theory," *J.Phys.A* **A42** (2009) 504005, arXiv:0905.4013 [cond-mat.stat-mech].

[84] D. Freedman, S. Gubser, K. Pilch, and N. Warner, "Renormalization group flows from holography supersymmetry and a c theorem," *Adv.Theor.Math.Phys.* **3** (1999) 363–417, arXiv:hep-th/9904017 [hep-th].

[85] L. Girardello, M. Petrini, M. Porrati, and A. Zaffaroni, "Novel local CFT and exact results on perturbations of N=4 superYang Mills from AdS dynamics," *JHEP* **9812** (1998) 022, arXiv:hep-th/9810126 [hep-th].

[86] L. Girardello, M. Petrini, M. Porrati, and A. Zaffaroni, "The Supergravity dual of N=1 superYang-Mills theory," *Nucl.Phys.* **B569** (2000) 451–469, arXiv:hep-th/9909047 [hep-th].

[87] R. C. Myers and A. Sinha, "Holographic c-theorems in arbitrary dimensions," *JHEP* **1101** (2011) 125, arXiv:1011.5819 [hep-th].

[88] R. C. Myers and A. Sinha, "Seeing a c-theorem with holography," *Phys.Rev.* **D82** (2010) 046006, arXiv:1006.1263 [hep-th].

[89] D. L. Jafferis, "The Exact Superconformal R-Symmetry Extremizes Z," *JHEP* **1205** (2012) 159, arXiv:1012.3210 [hep-th].

[90] D. L. Jafferis, I. R. Klebanov, S. S. Pufu, and B. R. Safdi, "Towards the F-Theorem: N=2 Field Theories on the Three-Sphere," *JHEP* **1106** (2011) 102, arXiv:1103.1181 [hep-th].

[91] I. R. Klebanov, S. S. Pufu, and B. R. Safdi, "F-Theorem without Supersymmetry," *JHEP* **1110** (2011) 038, arXiv:1105.4598 [hep-th].

[92] I. R. Klebanov, S. S. Pufu, S. Sachdev, and B. R. Safdi, "Entanglement Entropy of 3-d Conformal Gauge Theories with Many Flavors," *JHEP* **1205** (2012) 036, arXiv:1112.5342 [hep-th].

[93] T. Albash and C. V. Johnson, "Holographic Entanglement Entropy and Renormalization Group Flow," *JHEP* **1202** (2012) 095, arXiv:1110.1074 [hep-th].

[94] S. Hawking and G. Ellis, "The Large scale structure of space-time,".

[95] C. Fefferman and C. Graham, "Conformal invariants," *The mathematical heritage of lie Cartan (Lyon, 1984). Astrisque, Numero Hors Serie* (1985) 95–116.

[96] C. Fefferman and C. R. Graham, "The ambient metric," *ArXiv e-prints* (2007) , arXiv:0710.0919 [math.DG].

[97] M. Henningson and K. Skenderis, "The Holographic Weyl anomaly," *JHEP* **9807** (1998) 023, arXiv:hep-th/9806087 [hep-th].

[98] M. Henningson and K. Skenderis, "Holography and the Weyl anomaly," *Fortsch.Phys.* **48** (2000) 125–128, arXiv:hep-th/9812032 [hep-th].

[99] S. Nojiri and S. D. Odintsov, "On the conformal anomaly from higher derivative gravity in AdS/CFT correspondence," *Int.J.Mod.Phys.* **A15** (2000) 413–428, arXiv:hep-th/9903033 [hep-th].

[100] M. Blau, K. Narain, and E. Gava, "On subleading contributions to the AdS/CFT trace anomaly," *JHEP* **9909** (1999) 018, arXiv:hep-th/9904179 [hep-th].

[101] M. Brigante, H. Liu, R. C. Myers, S. Shenker, and S. Yaida, "Viscosity Bound Violation in Higher Derivative Gravity," *Phys.Rev.* **D77** (2008) 126006, arXiv:0712.0805 [hep-th].

[102] M. Brigante, H. Liu, R. C. Myers, S. Shenker, and S. Yaida, "The Viscosity Bound and Causality Violation," *Phys.Rev.Lett.* **100** (2008) 191601, arXiv:0802.3318 [hep-th].

[103] A. Buchel and R. C. Myers, "Causality of Holographic Hydrodynamics," *JHEP* **0908** (2009) 016, arXiv:0906.2922 [hep-th].

[104] D. M. Hofman, "Higher Derivative Gravity, Causality and Positivity of Energy in a UV complete QFT," *Nucl.Phys.* **B823** (2009) 174–194, arXiv:0907.1625 [hep-th].

[105] X.-H. Ge and S.-J. Sin, "Shear viscosity, instability and the upper bound of the Gauss-Bonnet coupling constant," *JHEP* **0905** (2009) 051, arXiv:0903.2527 [hep-th].

[106] R.-G. Cai, Z.-Y. Nie, and Y.-W. Sun, "Shear Viscosity from Effective Couplings of Gravitons," *Phys.Rev.* **D78** (2008) 126007, arXiv:0811.1665 [hep-th].

[107] R.-G. Cai, Z.-Y. Nie, N. Ohta, and Y.-W. Sun, "Shear Viscosity from Gauss-Bonnet Gravity with a Dilaton Coupling," *Phys.Rev.* **D79** (2009) 066004, arXiv:0901.1421 [hep-th].

[108] J. de Boer, M. Kulaxizi, and A. Parnachev, "AdS(7)/CFT(6), Gauss-Bonnet Gravity, and Viscosity Bound," *JHEP* **1003** (2010) 087, arXiv:0910.5347 [hep-th].

[109] X. O. Camanho and J. D. Edelstein, "Causality constraints in AdS/CFT from conformal collider physics and Gauss-Bonnet gravity," *JHEP* **1004** (2010) 007, arXiv:0911.3160 [hep-th].

[110] D. G. Boulware and S. Deser, "String Generated Gravity Models," *Phys.Rev.Lett.* **55** (1985) 2656.

[111] R. C. Myers and B. Robinson, "Black Holes in Quasi-topological Gravity," *JHEP* **1008** (2010) 067, arXiv:1003.5357 [gr-qc].

[112] R. C. Myers, M. F. Paulos, and A. Sinha, "Holographic studies of quasi-topological gravity," *JHEP* **1008** (2010) 035, arXiv:1004.2055 [hep-th].

[113] A. Buchel, J. Escobedo, R. C. Myers, M. F. Paulos, A. Sinha, *et al.*, "Holographic GB gravity in arbitrary dimensions," *JHEP* **1003** (2010) 111, arXiv:0911.4257 [hep-th].

[114] L.-Y. Hung, R. C. Myers, M. Smolkin, and A. Yale, "Holographic Calculations of Renyi Entropy," *JHEP* **1112** (2011) 047, arXiv:1110.1084 [hep-th].

[115] C. Imbimbo, A. Schwimmer, S. Theisen, and S. Yankielowicz, "Diffeomorphisms and holographic anomalies," *Class.Quant.Grav.* **17** (2000) 1129–1138, arXiv:hep-th/9910267 [hep-th].

[116] A. Schwimmer and S. Theisen, "Entanglement Entropy, Trace Anomalies and Holography," *Nucl.Phys.* **B801** (2008) 1–24, arXiv:0802.1017 [hep-th].

[117] A. Sinha, "On higher derivative gravity, c-theorems and cosmology," *Class.Quant.Grav.* **28** (2011) 085002, arXiv:1008.4315 [hep-th].

[118] J. T. Liu, W. Sabra, and Z. Zhao, "Holographic c-theorems and higher derivative gravity," arXiv:1012.3382 [hep-th].

[119] M. F. Paulos, "Holographic phase space: c-functions and black holes as renormalization group flows," *JHEP* **1105** (2011) 043, arXiv:1101.5993 [hep-th].

[120] A. Allais, "Double-trace deformations, holography and the c-conjecture," *JHEP* **1011** (2010) 040, arXiv:1007.2047 [hep-th].

[121] R. V. Buniy, S. D. Hsu, and B. M. Murray, "The Null energy condition and instability," *Phys.Rev.* **D74** (2006) 063518, arXiv:hep-th/0606091 [hep-th].

[122] S. Dubovsky, T. Gregoire, A. Nicolis, and R. Rattazzi, "Null energy condition and superluminal propagation," *JHEP* **0603** (2006) 025, arXiv:hep-th/0512260 [hep-th].

[123] E. Witten, "Anti-de Sitter space, thermal phase transition, and confinement in gauge theories," *Adv.Theor.Math.Phys.* **2** (1998) 505–532, arXiv:hep-th/9803131 [hep-th].

[124] A. Chamblin, R. Emparan, C. V. Johnson, and R. C. Myers, "Charged AdS black holes and catastrophic holography," *Phys.Rev.* **D60** (1999) 064018, arXiv:hep-th/9902170 [hep-th].

[125] D. Mateos, R. C. Myers, and R. M. Thomson, "Holographic phase transitions with fundamental matter," *Phys.Rev.Lett.* **97** (2006) 091601, arXiv:hep-th/0605046 [hep-th].

[126] A. Pakman and A. Parnachev, "Topological Entanglement Entropy and Holography," *JHEP* **0807** (2008) 097, arXiv:0805.1891 [hep-th].

[127] T. Albash and C. V. Johnson, "Holographic Studies of Entanglement Entropy in Superconductors," *JHEP* **1205** (2012) 079, arXiv:1202.2605 [hep-th].

[128] T. Albash and C. V. Johnson, "Evolution of Holographic Entanglement Entropy after Thermal and Electromagnetic Quenches," *New J.Phys.* **13** (2011) 045017, arXiv:1008.3027 [hep-th].

[129] A. Sinha, "On the new massive gravity and AdS/CFT," *JHEP* **1006** (2010) 061, arXiv:1003.0683 [hep-th].

[130] M. F. Paulos, "New massive gravity extended with an arbitrary number of curvature corrections," *Phys.Rev.* **D82** (2010) 084042, arXiv:1005.1646 [hep-th].

[131] I. Gullu, T. C. Sisman, and B. Tekin, "c-functions in the Born-Infeld extended New Massive Gravity," *Phys.Rev.* **D82** (2010) 024032, arXiv:1005.3214 [hep-th].

[132] I. Low and A. Zee, "Naked singularity and Gauss-Bonnet term in brane world scenarios," *Nucl.Phys.* **B585** (2000) 395–404, arXiv:hep-th/0004124 [hep-th].

[133] U. Camara and G. Sotkov, "New Massive Gravity Domain Walls," *Phys.Lett.* **B694** (2010) 94–99, arXiv:1008.2553 [hep-th].

[134] E. Gava, P. Karndumri, and K. Narain, "AdS_3 vacua and RG flows in three dimensional gauged supergravities," *JHEP* **1004** (2010) 117, arXiv:1002.3760 [hep-th].

[135] D. M. Hofman and J. Maldacena, "Conformal collider physics: Energy and charge correlations," *JHEP* **0805** (2008) 012, arXiv:0803.1467 [hep-th].

[136] R. Rattazzi, V. S. Rychkov, E. Tonni, and A. Vichi, "Bounding scalar operator dimensions in 4D CFT," *JHEP* **0812** (2008) 031, arXiv:0807.0004 [hep-th].

[137] S. Hellerman, "A Universal Inequality for CFT and Quantum Gravity," *JHEP* **1108** (2011) 130, arXiv:0902.2790 [hep-th].

[138] V. S. Rychkov and A. Vichi, "Universal Constraints on Conformal Operator Dimensions," *Phys.Rev.* **D80** (2009) 045006, arXiv:0905.2211 [hep-th].

[139] D. Poland and D. Simmons-Duffin, "Bounds on 4D Conformal and Superconformal Field Theories," *JHEP* **1105** (2011) 017, arXiv:1009.2087 [hep-th].

[140] T. Grover, A. M. Turner, and A. Vishwanath, "Entanglement Entropy of Gapped Phases and Topological Order in Three dimensions," *Phys.Rev.* **B84** (2011) 195120, arXiv:1108.4038 [cond-mat.str-el].

[141] M. P. Hertzberg and F. Wilczek, "Some Calculable Contributions to Entanglement Entropy," *Phys.Rev.Lett.* **106** (2011) 050404, arXiv:1007.0993 [hep-th].

[142] I. R. Klebanov, T. Nishioka, S. S. Pufu, and B. R. Safdi, "On Shape Dependence and RG Flow of Entanglement Entropy," arXiv:1204.4160 [hep-th].

[143] C. Holzhey, F. Larsen, and F. Wilczek, "Geometric and renormalized entropy in conformal field theory," *Nucl.Phys.* **B424** (1994) 443–467, arXiv:hep-th/9403108 [hep-th].

[144] R. C. Myers and A. Singh, "Comments on Holographic Entanglement Entropy and RG Flows," *JHEP* **1204** (2012) 122, arXiv:1202.2068 [hep-th].

[145] H. Casini and M. Huerta, "On the RG running of the entanglement entropy of a circle," arXiv:1202.5650 [hep-th].

[146] R. C. Myers and M. Smolkin, "Some Relevant Contributions to Entanglement Entropy," *in preparation.* .

[147] Private communications with Brian Swingle.

[148] D. Correa, J. Maldacena, and A. Sever, "The quark anti-quark potential and the cusp anomalous dimension from a TBA equation," arXiv:1203.1913 [hep-th].

[149] N. Drukker, D. J. Gross, and H. Ooguri, "Wilson loops and minimal surfaces," *Phys.Rev.* **D60** (1999) 125006, arXiv:hep-th/9904191 [hep-th].

[150] D. E. Berenstein, R. Corrado, W. Fischler, and J. M. Maldacena, "The Operator product expansion for Wilson loops and surfaces in the large N limit," *Phys.Rev.* **D59** (1999) 105023, arXiv:hep-th/9809188 [hep-th].

[151] H. Elvang, D. Z. Freedman, L.-Y. Hung, M. Kiermaier, R. C. Myers, *et al.*, "On renormalization group flows and the a-theorem in 6d," arXiv:1205.3994 [hep-th].